Adjustment of hydraulic, anatomical and leaf traits in *Fagus sylvatica* (L.) towards drier conditions.

A study in mature stands.

Dissertation

zur Erlangung des mathematisch-naturwissenschaftlichen Doktorgrades

„Doctor rerum naturalium"

der Georg-August-Universität Göttingen

im Promotionsprogramm

Biodiversity and Ecology

der Georg-August University School of Science (GAUSS)

vorgelegt von

Greta Carolin Weithmann

aus

Ravensburg

Göttingen, Juli 2021

Betreuungsausschuss:

- Prof. Dr. Christoph Leuschner, Abteilung Pflanzenökologie und Ökosystemforschung, Georg-August-Universität Göttingen
- Prof. Dr. Dirk Hölscher, Abteilung Waldbau und Waldökologie der Tropen, Georg-August-Universität Göttingen
- Prof. Dr. Bernhard Schuldt, Lehrstuhl für Ökophysiologie und Vegetationsökologie, Julius-Maximilians-Universität Würzburg

Mitglieder der Prüfungskommission:

- *Referent:* Prof. Dr. Christoph Leuschner, Abteilung Pflanzenökologie und Ökosystemforschung, Georg-August-Universität Göttingen
- *Korreferent:* Prof. Dr. Dirk Hölscher, Abteilung Waldbau und Waldökologie der Tropen, Georg-August-Universität Göttingen
- *Weitere Mitglieder der Prüfungskommission:*
    - Prof. Dr. Christian Ammer, Abteilung Waldbau und Waldökologie der gemäßigten Zonen, Georg-August-Universität Göttingen
    - Prof. Dr. Hermann Behling, Abteilung Palynologie und Paläoökologie, Georg-August-Universität Göttingen
    - Prof. Dr. Holger Kreft, Abteilung Biodiversität, Makroökologie und Biogeographie, Georg-August-Universität Göttingen
    - Prof. Dr. Bernhard Schuldt, Lehrstuhl für Ökophysiologie und Vegetationsökologie, Julius-Maximilians-Universität Würzburg

Tag der mündlichen Prüfung: 13.09.2021

SUMMARY

Hydraulic traits are closely linked to the ability of tree species to survive droughts and were therefore used to predict the disposition of trees to suffer from hydraulic failure in the face of climate change. While most studies focus on inter-specific differences in functional traits, less is known about the variability within tree species as well as within populations and about the factors influencing this variability. The species investigated in the presented thesis, European beech (*F. sylvatica*) is the most abundant tree species of Central Europe's natural forest vegetation and an important timber species for many countries. Despite its wide distribution range and the tolerance of a broad variety of climatic and edaphic growth conditions, European beech is known to be relatively drought sensitive. However, a high capacity to adapt to changing climatic conditions was suggested for this species due to a high intra-specific variability in hydraulic traits.

To assess the species' adaptive and acclimative potential to drier conditions and to support the identification of potentially drought-hardier provenances, this study provides a large dataset on xylem hydraulic, anatomical and leaf traits of upper-canopy branches collected from 300 beech trees growing on 30 different sites in the lowlands of northern Germany between the North Sea coast and the Polish border. A comprehensive approach to describe the water availability across the gradient was used by including the climatic water balance (CWB) or 60-year mean annual precipitation (MAP, in case of leaf traits), as well as the plant-available water capacity of the soils (AWC) and competition between neighbouring trees (CI) in the analyses. Furthermore, the effect of branch age on xylem hydraulic and anatomical traits and the effect of tree height on anatomy were considered. As sampling was conducted in the summers of 2018 and 2019, data on leaf traits were analysed for the two years separately and results were compared between the two years. The portion of trait variation attributed to the above-mentioned variables as well as the degree of between- and within- population variability were quantified.

The effect of water availability on xylem traits was rather low. Embolism resistance and vessel density were significantly related to AWC, while vessel diameter, lumen-to-sapwood area ratio and potential conductivity decreased significantly with decreasing CWB. Xylem-specific hydraulic conductivity was not affected by water availability. In contrast to the xylem traits, leaf traits showed considerable plasticity in response to climatic and edaphic aridity, with differing effects of water availability between the sampling years 2018 and 2019. For the 2018 data set, an increase in mean leaf size (LS) and a decrease in the sapwood-

to-leaf area ratio (Huber value, HV) towards drier conditions was observed, indicating that water supply to the sun canopy foliage is not improved upon precipitation reduction. However, this relationship was not pronounced in the 2019 data set, instead, specific leaf area (SLA) and water potential at turgor loss point (P_{tlp}) were adjusted towards drier sites. Furthermore, carbon isotope signature and P_{tlp} were modified in response to short-term CWB. While xylem traits were not related to tree height, branch age, which varied considerably by 20 years in branches of comparable diameter, had a major influence on most of the xylem traits. Embolism resistance and vessel diameter significantly decreased, whereas vessel density increased with increasing branch age. Vessel diameter was not significantly related to embolism resistance, but vessel grouping index and the lumen-to-sapwood area ratio showed a weak but significant relation. Within-population variability was larger than between-population variability for all investigated traits except for SLA and P_{tlp} of the 2019 data set.

Our results suggest that (1) anatomical modifications in response to water availability are rather a growth consequence of water limitation than an active acclimative response in order to increase hydraulic safety, and that (2) these modifications in terminal branches are independent of tree height. The rather small influence of water availability on embolism resistance and the high portion of unexplained variability suggest a minor acclimative capacity in this trait and indicate that embolism resistance might not be a promising trait for the identification of drought-resistant provenances. Overall, leaf traits appear to be under stronger environmental control than xylem traits. The increase in LS and decrease in HV with decreasing precipitation enhances the drought stress exposure of sun foliage at drier sites. Yet, under water shortage, osmotic adjustment to local water availability might be an important acclimative response in European beech.

CONTENT

CHAPTER

1

General Introduction

1.1 Forest ecosystems in a changing climate

Forests worldwide are of ecological, economic and social importance, as they are sources for food, timber and medically relevant substances and play a fundamental role in conservation of biodiversity (Morales-Hidalgo *et al.*, 2015). Additionally, forest ecosystems provide a wide range of ecological services, including regulation of water fluxes, reduction of drought-risks, decrease of erosion and soil protection, and cultural services ranging from benefits for the mental and physical health by improving the air quality and providing recreation opportunities to spiritual experiences, education and aesthetics (Nesbitt *et al.*, 2017; Watson *et al.*, 2018; Funk *et al.*, 2019). Moreover, forests play a prominent role in mitigating climate change (Bonan, 2008; Whitehead, 2011).

The human influence on the earth's climate is obvious. Temperature increased by approximately 1.0°C compared to pre-industrial levels and trends in intensity and frequency of some climate and weather extremes were observed (IPCC 2018). Global warming is predicted to reach 1.5°C between 2030 and 2052 if the increase continues at the current rate, and frequency and duration of heat waves will further increase, whereas cold winter extremes will continue to occur (IPCC 2014, Dosio *et al.*, 2018). One major opportunity to offset the anthropogenic greenhouse gas emissions and therefore mitigate the pace of global warming is the establishment, protection and management of forests (Sterck & Scholz, 2006; Houghton & Nassikas, 2018; Lutz *et al.*, 2018). Besides the large amount of annual carbon sequestration, forests cool the climate through feedbacks of evaporation with clouds and precipitation (Bonan, 2008).

Conversely, climate change is affecting forests around the globe (McDowell *et al.*, 2020). The long life-span of trees and the limited ability to migrate away from stress does not allow for rapid responses to changing environmental conditions. Therefore, forests are particularly sensitive to climate change, including positive and negative feedbacks (Lindner *et al.*, 2010). Increasing atmospheric concentrations of carbon dioxide, nitrogen inputs to ecosystems and prolonged growing seasons in the Northern Hemisphere may enhance plant growth (Peñuelas & Filella, 2001; Galloway *et al.*, 2008; Ballantyne *et al.*, 2012). However, fertilization effects may slow down in the future and negative impacts of climate change will increase (Peñuelas *et al.*, 2017). Satellite-based models revealed a widespread decrease of terrestrial gross primary production in response to a sharp increase in atmospheric vapour pressure deficit after the late 1990s (Yuan *et al.*, 2019) and over the past decades, drought-induced tree mortality rates increased over different forest types and climates (Allen *et al.*,

2010; Carnicer *et al.*, 2011; Breshears *et al.*, 2018; Senf *et al.*, 2018; Senf *et al.*, 2020a; Andrus *et al.*, 2021). Climate change facilitates disturbance occurrences, such as fire, drought, wind and insect disturbances, possibly resulting in altered forest ecosystems or shifts to non-forest ecosystems (Seidl *et al.*, 2017; McDowell *et al.*, 2020). Particularly, a combination of drought and warmer temperatures, so-called "hotter droughts" might have severe impacts on forest vegetation (Allen *et al.*, 2015). This co-occurrence of heat and drought is classified as compound event and hotter droughts are projected to increase in many regions (Zscheischler & Seneviratne, 2017; Zscheischler *et al.*, 2018).

Within Europe, the hotter drought of 2018 can be seen as a yet unprecedented event in this context (Buras *et al.*, 2020). The highest canopy mortality rate of the past 34 years was observed in 2018 (Senf *et al.*, 2020b), and also drought legacy effects were unexpectedly high in 2019 (Scharnweber *et al.*, 2020; Schuldt *et al.*, 2020; Walthert *et al.*, 2021). Nevertheless, the dieback of a particular tree species may allow the establishment of other yet absent species and significant changes in European forest species compositions can be expected (Buras & Menzel, 2019).

An anticipatory silvicultural management may mitigate the expected severe impacts on forest ecosystems. Thus, predicting tree mortality events in the context of these for trees abrupt changes in growing conditions is of major importance and a challenge for ecologists. Generally, species have different opportunities to react to changing environmental conditions, which can be divided into three strategies, i.e. phenotypic plasticity (acclimation), genotypic evolution (adaptation) and distributional shifts (migration; Anderson *et al.*, 2012). As trees are not able to migrate within short time periods, the ability of a species to acclimate to rapid climate change mainly depends on the degree of phenotypic plasticity and genetic diversity within a population, but few data are available on intra-specific trait variability in trees (Choat *et al.*, 2018). Therefore, understanding the variability of traits related to drought resistance in a dominating European tree species, i.e. *Fagus sylvatica* L., can be crucial for the development of precise ecological predictions.

1.2 Hydraulic system and drought vulnerability

A mature tree can lift hundreds of litres of water each day from the soil to the leaves up to more than 100 m, but less than one percent of the water absorbed is retained in biomass; the remainder is lost through transpiration as an inevitable consequence of carbon dioxide

assimilation (Lambers & Oliveira, 2019). Water is crucial for most biochemical processes, mass transport and plant structure. To satisfy the water demand required for transpiration, trees need an efficient long-distance transport pathway (Tyree, 2003). The water moves through a network of dead conduit cells of the xylem tissue (wood), which – besides the transport function - also provides mechanical support and serves as storage (Zimmermann, 1983). According to the so-called Cohesion-Tension theory, water is transported under large negative pressure, but whether the high degree of negative pressure in sap really exists has been questioned from the time it was first proposed (Brown, 2013). Yet, there is plenty of circumstantial evidence for large negative pressures in plants (Schenk *et al.*, 2017).

To mitigate water loss during drought, trees use several morphological, anatomical and physiological traits. Figure 1.1 shows important traits that are associated with drought-induced mortality of trees (Choat *et al.*, 2018) and gives a first overview of the traits investigated in the present study (investigated traits are highlighted).

A key mechanism involved in drought-induced tree mortality is the damage of the hydraulic system (McDowell *et al.*, 2008; Adams *et al.*, 2017; Brodribb *et al.*, 2020). Even though a number of co-contributing factors, such as the depletion of carbohydrate reserves and increased vulnerability to pests and insect also play a role in tree mortality, traits related to the hydraulic system are key predictors of tree death (Choat *et al.*, 2018).
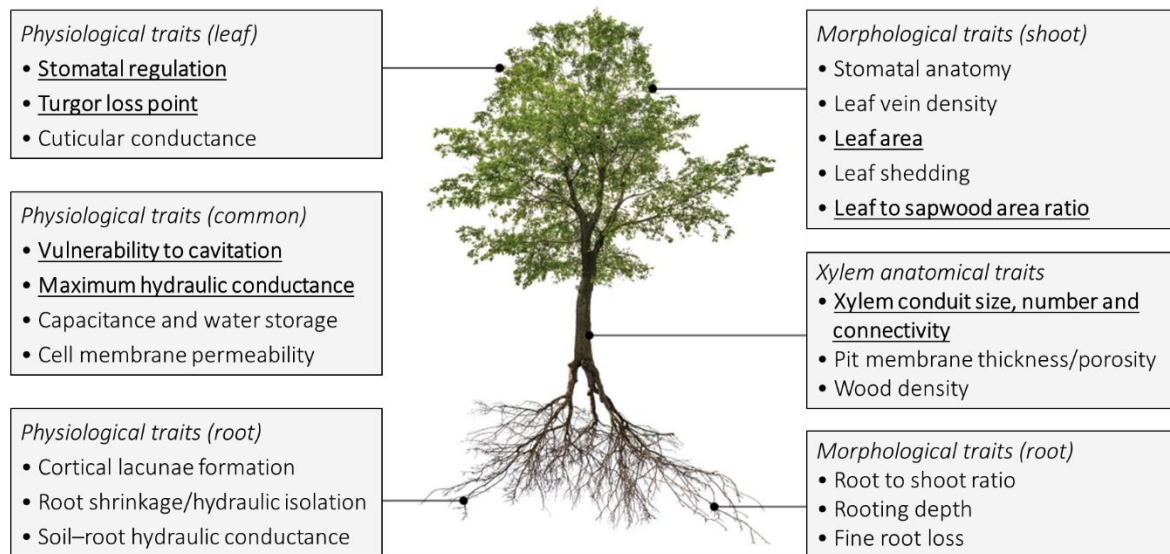

Figure 1.1: Tree physiological, morphological and anatomical traits associated with drought-induced mortality. Traits investigated in this study are in bold and underlined. The figure does not represent an exhaustive list of traits relevant to the response of trees to drought and drought-induced mortality. (source: Choat *et al.*, 2018, modified).

1.2.1   Embolism resistance and hydraulic conductivity

The xylem transport relies on a mechanism where liquid water is held under tension (Tyree, 2003). During drought, soil moisture declines, often accompanied by elevated temperatures and higher evaporative demand of the atmosphere. These factors induce water stress in plants, which is expressed as an elevated tension in the xylem sap, which in turn increases the risk of embolism formation (Choat *et al.*, 2018). These drought-induced embolisms block water flow through the xylem, resulting in a lower hydraulic conductivity and reduced delivery to the water demanding canopy. Ongoing drought increases the probability of embolism spread throughout the hydraulic network causing systemic vascular dysfunction (Knipfer *et al.*, 2015). Commonly, a trade-off between hydraulic safety (defined as the xylem water potential at which a meaningful percentage of maximum efficiency is lost) and hydraulic efficiency (i.e. the xylem-specific hydraulic conductivity) is assumed. As hydraulic safety is mainly determined by pit membrane properties (Jansen *et al.*, 2009; Lens *et al.*, 2011; Li *et al.*, 2016), one hypothesis linking efficiency and safety suggests that greater safety is reached by less porous pit membranes with higher flow resistance and therefore lower efficiency, but to date this hypothesis could not be confirmed (Wheeler *et al.*, 2005). A recent study revealed that embolism resistance is to a lesser extent related to the number of pits per vessel, but rather determined by the size of pore constrictions in pit membranes, suggesting that hydraulic safety might be uncoupled from hydraulic efficiency (Kaack *et al.*, 2021). Vulnerability to drought-induced embolism is frequently quantified as the xylem water potential inducing 50% loss of hydraulic conductance (P_{50}, Bréda *et al.*, 2006). Across species, embolism resistance increases with climatic aridity (Maherali *et al.*, 2004; Choat *et al.*, 2007; Larter *et al.*, 2017; Li *et al.*, 2018), and increased values of P_{50} were associated with decreasing tolerance to water stress (Nardini *et al.*, 2013; Correia *et al.*, 2019). Yet, less is known about the drivers of intra-specific variability in this trait and studies investigating the effect of climate on embolism resistance in *F. sylvatica* revealed ambiguous results (Herbette *et al.*, 2010; Wortemann *et al.*, 2011; Schuldt *et al.*, 2016; Stojnic *et al.*, 2017; Rosas *et al.*, 2019). As embolism resistance has been identified as an important trait related to tree mortality after drought events in many regions (Anderegg *et al.*, 2016; Correia *et al.*, 2019; Powers *et al.*, 2020), deeper knowledge on the drivers of intra-specific variability in embolism resistance is of major importance.

1.2.2 Xylem anatomical traits

The water transport capability of the xylem is one of the traits defining the drought tolerance of a species (Hacke *et al.*, 2000). Different cell types are characteristic for the xylem: the tracheids and the vessels (the latter only in angiosperms) form conduits of pipe-like structure for transport of water. To withstand the compression caused by negative pressure, the walls of these dead cells are reinforced by a deposit of lignin and include a thick secondary layer. In vessels, the end walls of the cells are partly or completely dissolved, thus very long conduits can be formed (Cochard, 2006). Length and diameter of conduits are strongly related to the hydraulic conductivity of the xylem, as lumen conductivity increases with the fourth power of lumen diameter (Sperry *et al.*, 2006). Furthermore, vessel diameter strongly influences the degree of vulnerability to freezing-induced embolism and can also be related to drought-induced embolism (Hacke *et al.*, 2017). Variation in vessel diameter is therefore an important parameter when evaluating plant water relations. Xylem anatomical traits, i.e. vessel size, vessel density, vessel grouping or lumen-to-sapwood area ratio are influenced by different plant-internal and abiotic factors. In this context, water and nutrient availability, cambial age and flow path length can be important (Leal *et al.*, 2007; Borghetti *et al.*, 2017; Gleason *et al.*, 2018; Li *et al.*, 2019). Even though anatomical traits have been studied for a long time, there are still fundamental gaps in the understanding of vessel development in trees, and the variation in vessel diameter in response to environmental factors is complex (Hacke *et al.*, 2017).

1.2.3 Leaf traits

The leaf area represents the surface for photosynthetic gas exchange and transpiration, thus the relation between leaf area and the water balance of a site is obvious (Grier & Running, 1977). Especially when water availability is limited, the cooling of leaves by transpirational loss is particularly critical for large leaves, which face greater risk of heat damage (Gates, 1968). Generally, leaf size is predicted to decrease towards drier and hotter conditions, but a global analysis of leaf size revealed a decrease of leaf size with increasing temperature only for dry sites, while across wetter sites leaf size increased with the temperature of the warmest month (Wright *et al.*, 2017). Furthermore, trees can adjust their hydraulic system in response to drought by changes in the allocation pattern of water-absorbing, -conducting and -transpiring tissues (Mencuccini & Grace, 1995). To maintain a greater transport capacity and to prevent a drop in water potential under dry conditions, the leaf area-to-sapwood area ratio and shoot-to-root ratio may be reduced (Choat *et al.*, 2018).

Stomatal pores on the leaf surfaces play an important role by regulating the leaf gas exchange. Even though stomatal closure in response to water deficit represents a primary limitation to photosynthesis, it can prevent the water demand of the leaves to exceed water supply capacity, which would result in embolism formation and desiccation of the plant (Martin-StPaul *et al.*, 2017). Whether stomatal closure precedes embolism formation or is co-occurring has been disputed, but recent studies indicate that trees usually close their stomata before reaching the threshold of water potential inducing significant embolism formation (Hochberg *et al.*, 2017; Martin-StPaul *et al.*, 2017). However, stomatal closure induces negative consequences, including the loss of canopy evaporative cooling through transpiration involving a greater probability of photodamage, and the depletion of non-structural carbohydrate pools (Choat *et al.*, 2018).

The leaf water potential at turgor loss point (P_{tlp}) is a meaningful trait to derive the drought response of a species and is linked to species distribution across moisture gradients (Bartlett *et al.*, 2012b; Maréchaux *et al.*, 2015; Zhu *et al.*, 2018; Rosas *et al.*, 2019). Physiologically, P_{tlp} is the leaf water potential at which average cell turgor pressure is lost and the water potential therefore equals the osmotic potential (Bartlett *et al.*, 2012a). As for the other traits, less studies focus on the intra-specific differences in P_{tlp} compared to adjustments across species, but significant declines of P_{tlp} towards drier conditions were observed for *Castanopsis fargesii* Franch. and *Eucalyptus obliqua* L'Hér. (Liang *et al.*, 2019; Pritzkow *et al.*, 2020). For a better understanding and to improve predictions of species responses to climate change, it is essential to investigate intraspecific variation in hydraulic architecture across climatic gradients.

1.3 The investigated species: *Fagus sylvatica* (L.)

1.3.1 Ecology and distribution of European beech

European beech is the dominating species in deciduous forests in Central Europe and important for timber production. The species can survive over a wide range of soil conditions, expositions and soil depths. Beech forests can therefore be found on almost all terrestrial soil types. Due to its high shade tolerance in the juvenile and adult life stage, *F. sylvatica* can outcompete all other Central European tree species under a variety of conditions (Leuschner & Ellenberg, 2017). Nevertheless, beech is sensitive to flooding and often absent in waterlogged depressions (Kreuzwieser *et al.*, 2002).

The potential natural area of beech forests covers 9% of the area of Europe and in Germany, the centre of the natural distribution area, two thirds of the land surface is potentially covered by beech forests (Bohn & Gollub, 2007). Since the 19th century, native beech has been replaced by fast-growing coniferous tree species, such as Norway spruce (*Picea abies*) in many parts of Europe (Leuschner & Ellenberg, 2017). As *P. abies* is highly vulnerable to biotic and abiotic stress factors and mixed forests may enhance biodiversity as well as create ecologically stable ecosystems, forest conversion of Norway spruce plantations back to native broadleaved forests has become an important topic (e.g. Elmer *et al.*, 2004; Ammer *et al.*, 2008; Verstraeten *et al.*, 2013; Heine *et al.*, 2019). Consequently, the portion of European beech within German forests has increased in the last decades (BMEL 2014).

The distribution area of *F. sylvatica* (Figure 1.2) comprises a large spectrum of climatic and edaphic conditions. The requirements for the presence of *F. sylvatica* are sufficient moisture (> 500 mm yr^{-1}), moderate summer temperatures (mean July temperature $< 19°C$) and mild winters as well as the absence of extreme drought and heat, winter frosts ($< -35°C$) and severe late frosts (review in Bolte *et al.*, 2007). Furthermore, the sensitivity of the species to reductions in air humidity, may restrict its occurrence to the cloudy montane belt in the continental and southern parts of the distribution range (Leuschner, 2020). Nevertheless, it is considered as difficult by Bolte *et al.* (2007) to determine correlations of distribution margins with single climatic factors, also because of the variance in drought and frost adaptation between different beech populations. For instance, at the cold distribution margin, tree growth is more affected by drought than by cold events in winter and spring, while the adaption to drought seems to be higher at the dry distribution margin (Muffler *et al.*, 2020).
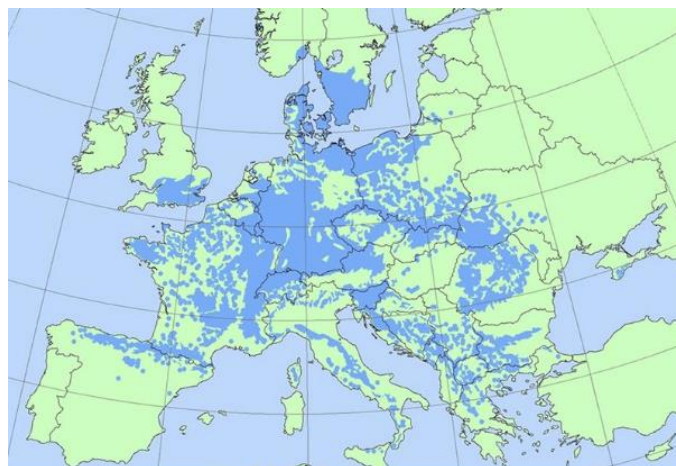

Figure 1.2: Distribution map of *Fagus sylvatica* (www.euforgen.org)

1.3.2   Drought response of *F. sylvatica*

Many studies focus on the drought sensitivity of European beech, but uncertainties about the vulnerability of this species remain. Despite the large leaf area of European beech trees, the species has a relatively conservative water use, probably due to a moderate maximum leaf conductance (Leuschner, 2020). Leaf conductance is reduced when water availability drops below a certain threshold (Granier *et al.*, 2007; Walthert *et al.*, 2021) and beech saplings showed an increase in the $\delta^{13}C$-signature of leaf mass under drought, indicating partial stomatal closure (Knutzen *et al.*, 2015; Pflug *et al.*, 2018). The species resembles more an anisohydric species in view of the large diurnal amplitude in leaf water potential (Leuschner, 2020). The capability for leaf osmotic adjustment, a trait quantifying the "drought tolerance" rather than "drought avoidance", seems to be limited in European beech, as only some studies observed a reduction of the water potential at turgor loss point after drought exposure (Tomasella *et al.*, 2018; 2019), while others did not (Knutzen *et al.*, 2015; Lübbe *et al.*, 2017). Moreover, the leaf expansion taking place at the beginning of the growing season, which is triggered by spring moisture (Meier & Leuschner, 2008b) and the missing adaption in leaf-to-sapwood area ratio towards drier sites (Schuldt *et al.*, 2016), can lead to a mismatch between evaporative demand and water availability during dry summers resulting in pre-senescent leaf shedding (Leuschner, 2020). During the 2018-drought, widespread early discoloration and pre-senescent leaf abscission in *F. sylvatica* was a prominent stress response (Braun *et al.*, 2020; Schuldt *et al.*, 2020; Walthert *et al.*, 2021). Defoliation occurs rather as a consequence of embolism than preventing it and can be a predictor for irrecoverable crown dieback (Walthert *et al.*, 2021).

Regarding the rooting system, about two third of European beech's fine root biomass was found to be located in the organic layer and upper $0 - 30$ cm of the mineral soil (Meier *et al.*, 2018) and morphological plasticity of fine roots was rather low (Hertel *et al.*, 2013). Summer drought may increase fine root mortality and reduce the root biomass, but compensatory fine root production may occur in drought-exposed stands (Meier & Leuschner, 2008a). Furthermore, only minor adaptive modifications with respect to the size and structure of the rooting system in response to a decline in long-term precipitation were observed (Meier *et al.*, 2018). So, on the whole tree-level, *F. sylvatica* was defined as a drought and heat sensitive species (Leuschner, 2020).

1.3.3 European beech in the context of global warming

Climate trends for Central Europe predict an increase in summer temperatures of 1.3 – 2.7°C and a decrease in summer precipitation of up to 25% for the period 2051 – 2080 compared to 1951 – 2000 (Lindner *et al.*, 2014). The risks of European beech under changing climatic conditions have been a matter of debate for many years (Rennenberg *et al.*, 2004; Ammer *et al.*, 2005; Bolte, 2005). On the one hand, a high acclimation potential and regeneration ability of this species was anticipated due to the observed high intra-specific variability in drought response-related traits (Kölling *et al.*, 2005; Bresson *et al.*, 2011; Stojnic *et al.*, 2017) and some studies showed a low vulnerability of this species under drought (Pflug *et al.*, 2018; Dietrich *et al.*, 2019). On the other hand, dendroecological studies showed a recent growth decline not only at the southern and eastern limits of the beech range, but also in the centre of the distribution area (Jump *et al.*, 2006; Weber *et al.*, 2013; Knutzen *et al.*, 2017) and it remains unclear whether the anticipated acclimation capacity will be sufficient to cope with increasing aridity. A recent study of Zimmermann *et al.* (2021) found that *F. sylvatica* was the only species out of five temperate broad-leaved tree species showing a significant long-term decline in hydraulically-weighted vessel diameter, accompanied by a constant decline in tree-ring width, supporting the assumed drought-sensitivity of this species.

The severe impact of the 2018/2019 drought on beech trees might give an outlook on the future risks, European forests will be exposed to. Within forests of Austria, Germany and Switzerland, the most affected tree species were Norway spruce and European beech and especially for *F. sylvatica*, a partial or complete canopy dieback in various stands, often followed by the death of these trees in 2019, was unexpected (Schuldt *et al.*, 2020). Particularly the insufficient recharge of soil water in the winter 2018/2019 and the warmer and drier spring/summer 2019 (compared to the long-term average) caused the high drought severity in 2019 and resulted in strong growth reductions in *F. sylvatica*, but also in other broadleaved species, e.g. *Quercus robur* L., *Acer pseudoplatanus* L. and *Carpinus betulus* L. in Northern Germany (Scharnweber *et al.*, 2020). Therefore, the identification of more drought-resistant populations among native species can be an approach for a sustainable forest management, and information about the degree of intra-specific adjustments in European beech to drier conditions may help to provide suggestions on the regional scale for the cultivation of this important species.

1.4 Study design and site description

The study was conducted on mature *F. sylvatica* trees growing in 30 different stands located in the lowlands of northern Germany (19 – 159 m a.s.l.) between the North Sea coast and the Polish border in the centre of the species' distribution range (Figure 1.3 A). All stands are stocking on deep, mostly nutrient-poor sandy soils developed from deposits of the penultimate (Saalian) and last glacial (Weichselian). The stands are monospecific, have a cohort-like age structure and most of them are managed for silvicultural purposes, but no recent thinnings have occurred. Secondary canopy or shrub layers were mostly absent and canopy closure was high (> 90%).

The climate of the study area is cool-temperate oceanic to sub-continental with a gradient in 60-year mean annual precipitation (MAP) decreasing from northwest to southeast from 867 to 496 mm yr^{-1} and mean annual temperature ranging from 8.5 to 9.7 °C across the stands. Fluctuations in annual precipitation and mean temperature over the 60 years before sample collection run relatively parallel for the different sites, indicating that long-term means reflect the relative differences in precipitation and temperature between the sites (Figure 1.3 B). To combine the effects of precipitation and temperature, we included the climatic water balance (CWB), which is calculated as the difference between precipitation and potential evapotranspiration (which depends on temperature), as explanatory variable for xylem traits. As mean early growing-season precipitation and mean growing season precipitation were highly correlated with MAP, we decided to include the full-year means of the climatic variables in our analyses. The water available for a tree not only depends on climatic factors but also on the soil conditions. We therefore included the plant-available water capacity of the soil (AWC) and further a measure of competition intensity in the neighbourhood of the target tree (CI), which may also affect the water content of the soil, as variables to describe water availability. As trees differed in height and branch age of the collected branches varied, the influence of these two variables on xylem traits was also considered.

The studied traits were determined in branch and leaf samples of ten trees per stand, collected between June and August in 2018 and 2019, respectively. The investigated branch samples were first-order side branches of a collected main branch from the uppermost sun-exposed crown. Foliar traits were analysed in leaves of three branches per tree (n = 900) and xylem traits (embolism resistance, xylem-specific hydraulic conductivity and xylem anatomy) in one branch sample per tree (n = 300). The short branch segments for the anatomical analyses were cut from the basipetal end of the branches used for the conductivity measurements and the subsequent construction of vulnerability curves.
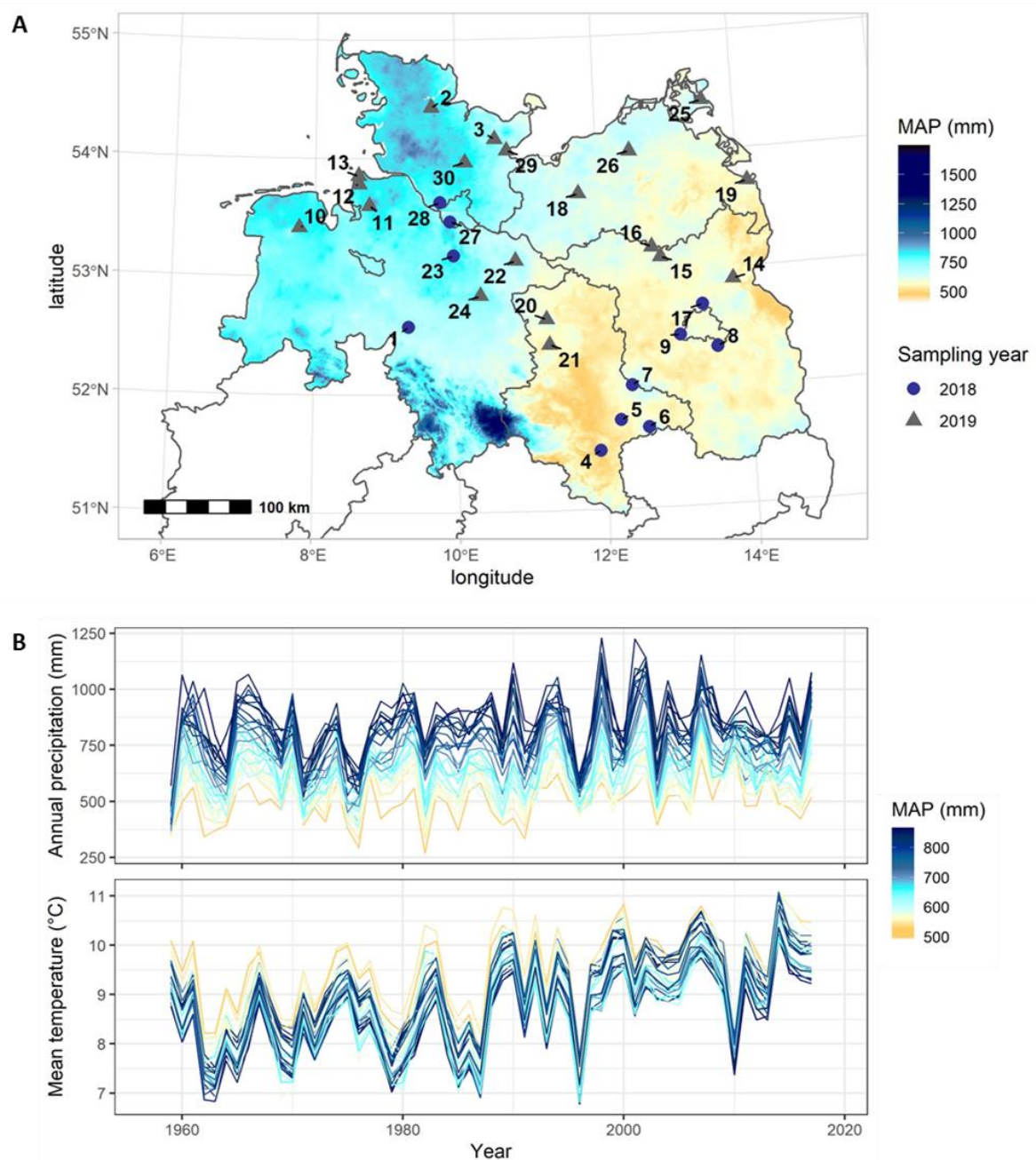
Figure 1.3: Map of the northern part of Germany with federal states and the location of the 30 investigated beech stands. Colours and shape of the stand-symbols show the sampling year (2018 or 2019) and mean annual precipitation (MAP, 1958-2017, data provided by DWD) across the region is shown (A). Long-term trends in annual precipitation (top) and mean annual temperature (bottom) of the 30 study sites. Line colours indicate the 60-year MAP for the different sites (B).

1.5 General study objectives

With the overall aim to gain further information about the potential of European beech to adapt or acclimate to drier conditions, this study focuses on functional traits related to the drought vulnerability of trees, which were investigated across a precipitation gradient. Besides climatic variables, the plant-available soil water capacity was considered as an important factor to describe water availability across the gradient.

The present PhD thesis is subdivided into three studies focusing on different traits, i.e. xylem embolism resistance and xylem-specific hydraulic conductivity (Chapter 2), xylem anatomical traits (Chapter 3) and leaf traits (Chapter 4), with the aim to identify the drivers of the variability in these traits.

The main study objectives can be summarized as follows:

    i)   to determine the effect of water availability on the investigated traits. Variables attributed to long-term water availability were
- climatic water balance or mean annual precipitation,
- plant-available water capacity of the soil,
- and competition intensity between neighbouring trees.

            Further, the effects of branch age and tree height on xylem traits were considered.

    ii)   to quantify the degree of trait variation explained by the above-mentioned variables and measure the degree of between- and within-population variability.

    iii)   to quantify the differences in leaf traits between samples harvested in different years and to identify the influence of short-term water availability on leaf traits.

The overarching hypothesis of this study was that traits commonly assigned to the drought vulnerability of trees are adjusted towards drier conditions, i.e. embolism resistance and sapwood-to-leaf area ratio increase, whereas the leaf water potential at turgor loss point and vessel diameter decrease with a reduction in water availability.

References

Adams HD, Zeppel MJB, Anderegg WRL, Hartmann H, Landhäusser SM, Tissue DT, Huxman TE, Hudson PJ, Franz TE, Allen CD *et al.* 2017. A multi-species synthesis of physiological mechanisms in drought-induced tree mortality. *Nature Ecology & Evolution* **1**: 1285–1291.

Allen CD, Breshears DD, McDowell NG. 2015. On underestimation of global vulnerability to tree mortality and forest die-off from hotter drought in the Anthropocene. *Ecosphere* **6**: art129.

Allen CD, Macalady AK, Chenchouni H, Bachelet D, McDowell N, Vennetier M, Kitzberger T, Rigling A, Breshears DD, Hogg EH *et al.* 2010. A global overview of drought and heat-induced tree mortality reveals emerging climate change risks for forests. *Forest Ecology and Management* **259**: 660–684.

Ammer C, Albrecht L, Borchert H, Brosinger F, Stimm B. 2005. Zur Zukunft der Buche (*Fagus sylvatica* L.) in Mitteleuropa – kritische Anmerkungen zu einem Beitrag von Rennenberg et al. (2004). *Allgemeine Forst und Jagdzeitung* **176**: 60–67.

Ammer C, Bickel E, Kölling C. 2008. Converting Norway spruce stands with beech - A review of arguments and techniques. *Austrian Journal of Forest Science* **125**: 3–26.

Anderegg WRL, Klein T, Bartlett M, Sack L, Pellegrini AFA, Choat B, Jansen S. 2016. Meta-analysis reveals that hydraulic traits explain cross-species patterns of drought-induced tree mortality across the globe. *PNAS* **113**: 5024–5029.

Anderson JT, Panetta AM, Mitchell-Olds T. 2012. Evolutionary and ecological responses to anthropogenic climate change: update on anthropogenic climate change. *Plant Physiology* **160**: 1728–1740.

Andrus RA, Chai RK, Harvey BJ, Rodman KC, Veblen TT. 2021. Increasing rates of subalpine tree mortality linked to warmer and drier summers. *Journal of Ecology*. doi: 10.1111/1365-2745.13634.

Ballantyne AP, Alden CB, Miller JB, Tans PP, White JWC. 2012. Increase in observed net carbon dioxide uptake by land and oceans during the past 50 years. *Nature* **488**: 70–72.

Bartlett MK, Scoffoni C, Ardy R, Zhang Y, Sun S, Cao K, Sack L. 2012a. Rapid determination of comparative drought tolerance traits: using an osmometer to predict turgor loss point. *Methods in Ecology and Evolution* **3**: 880–888.

Bartlett MK, Scoffoni C, Sack L. 2012b. The determinants of leaf turgor loss point and prediction of drought tolerance of species and biomes: a global meta-analysis. *Ecology letters* **15**: 393–405.

BMEL (Bundesministerium für Ernährung und Landwirtschaft). 2014. Der Wald in Deutschland. Ausgewählte Ergebnisse der dritten Bundeswaldinventur. https://www.bmel.de/DE/themen/wald/wald-in-deutschland/bundeswaldinventur.html.

Bohn U, Gollub G. 2007. Buchenwälder als natürliche Vegetation in Europa. Beech forests as natural vegetation in Europe. *Natur und Landschaft*: 391–397.

Bolte A. 2005. Zur Zukunft der Buche in Mitteleuropa. *AFZ-DerWald*.

Bolte A, Czajkowski T, Kompa T. 2007. The north-eastern distribution range of European beech - a review. *Forestry: An International Journal of Forest Research* **80**: 413–429.

Bonan GB. 2008. Forests and climate change: forcings, feedbacks, and the climate benefits of forests. *Science* **320**: 1444–1449.

Borghetti M, Gentilesca T, Leonardi S, van Noije T, Rita A, Mencuccini M. 2017. Long-term temporal relationships between environmental conditions and xylem functional traits: a meta-analysis across a range of woody species along climatic and nitrogen deposition gradients. *Tree Physiology* **37**: 4–17.

Braun S, Witte LC de, **Hopf SE. 2020.** Auswirkungen des Trockensommers 2018 auf Flächen der Interkantonalen Walddauerbeobachtung. *Schweizerische Zeitschrift für Forstwesen* **171**: 270–280.

Bréda N, Huc R, Granier A, Dreyer E. 2006. Temperate forest trees and stands under severe drought: a review of ecophysiological responses, adaptation processes and long-term consequences. *Annals of Forest Science* **63**: 625–644.

Breshears DD, Carroll CJW, Redmond MD, Wion AP, Allen CD, Cobb NS, Meneses N, Field JP, Wilson LA, Law DJ *et al.* 2018. A dirty dozen ways to die: metrics and modifiers of mortality driven by drought and warming for a tree species. *Frontiers in Forests and Global Change* **1**: 4.

Bresson CC, Vitasse Y, Kremer A, Delzon S. 2011. To what extent is altitudinal variation of functional traits driven by genetic adaptation in European oak and beech? *Tree Physiology* **31**: 1164–1174.

Brodribb TJ, Powers J, Cochard H, Choat B. 2020. Hanging by a thread? Forests and drought. *Science* **368**: 261–266.

Brown HR. 2013. The theory of the rise of sap in trees: some historical and conceptual remarks. *Physics in Perspective* **15**: 320–358.

Buras A, Menzel A. 2019. Projecting tree species composition changes of european forests for 2061-2090 under RCP 4.5 and RCP 8.5 scenarios. *Frontiers in Plant Science*. doi: 10.3389/fpls.2018.01986.

Buras A, Rammig A, Zang CS. 2020. Quantifying impacts of the 2018 drought on European ecosystems in comparison to 2003. *Biogeosciences* **17**: 1655–1672.

Carnicer J, Coll M, Ninyerola M, Pons X, Sánchez G, Peñuelas J. 2011. Widespread crown condition decline, food web disruption, and amplified tree mortality with increased climate change-type drought. *PNAS* **108**: 1474–1478.

Choat B, Brodribb TJ, Brodersen CR, Duursma RA, López R, Medlyn BE. 2018. Triggers of tree mortality under drought. *Nature* **558**: 531–539.

Choat B, Sack L, Holbrook NM. 2007. Diversity of hydraulic traits in nine *Cordia* species growing in tropical forests with contrasting precipitation. *New Phytologist* **175**: 686–698.

Cochard H. 2006. Cavitation in trees. *Comptes Rendus Physique* **7**: 1018–1026.

Correia DLP, Bouchard M, Filotas É, Raulier F. 2019. Disentangling the effect of drought on stand mortality and productivity in northern temperate and boreal forests. *Journal of Applied Ecology* **56**: 758–768.

Dietrich L, Delzon S, Hoch G, Kahmen A. 2019. No role for xylem embolism or carbohydrate shortage in temperate trees during the severe 2015 drought. *Journal of Ecology* **107**: 334–349.

Dosio A, Mentaschi L, Fischer EM, Wyser K. 2018. Extreme heat waves under 1.5 °C and 2 °C global warming. *Environmental Research Letters* **13**: 54006.

Elmer M, La France M, Förster G, Roth M. 2004. Changes in the decomposer community when converting spruce monocultures to mixed spruce/beech stands. *Plant and Soil* **264**: 97–109.

Funk JM, Aguilar-Amuchastegui N, Baldwin-Cantello W, Busch J, Chuvasov E, Evans T, Griffin B, Harris N, Ferreira MN, Petersen K *et al.* 2019. Securing the climate benefits of stable forests. *Climate Policy* **19**: 845–860.

Galloway JN, Townsend AR, Erisman JW, Bekunda M, Cai Z, Freney JR, Martinelli LA, Seitzinger SP, Sutton MA. 2008. Transformation of the nitrogen cycle: recent trends, questions, and potential solutions. *Science* **320**: 889–892.

Gates DM. 1968. Transpiration and leaf temperature. *Annual Review of Plant Physiology* **19**: 211–238.

Gleason SM, Blackman CJ, Gleason ST, McCulloh KA, Ocheltree TW, Westoby M. 2018. Vessel scaling in evergreen angiosperm leaves conforms with Murray's law and area-filling assumptions: implications for plant size, leaf size and cold tolerance. *New Phytologist* **218**: 1360–1370.

Granier A, Reichstein M, Bréda N, Janssens IA, Falge E, Ciais P, Grünwald T, Aubinet M, Berbigier P, Bernhofer C *et al.* 2007. Evidence for soil water control on carbon and water dynamics in European forests during the extremely dry year: 2003. *Agricultural and Forest Meteorology* **143**: 123–145.

Grier CG, Running SW. 1977. Leaf area of mature northwestern coniferous forests: relation to site water balance. *Ecology* **58**: 893–899.

Hacke UG, Sperry JS, Pittermann J. 2000. Drought experience and cavitation resistance in six shrubs from the Great Basin, Utah. *Basic and Applied Ecology* **1**: 31–41.

Hacke UG, Spicer R, Schreiber SG, Plavcová L. 2017. An ecophysiological and developmental perspective on variation in vessel diameter. *Plant, Cell & Environment* **40**: 831–845.

Heine P, Hausen J, Ottermanns R, Schäffer A, Roß-Nickoll M. 2019. Forest conversion from Norway spruce to European beech increases species richness and functional structure of aboveground macrofungal communities. *Forest Ecology and Management* **432**: 522–533.

Herbette S, Wortemann R, Awad H, Huc R, Cochard H, Barigah TS. 2010. Insights into xylem vulnerability to cavitation in *Fagus sylvatica* L.: phenotypic and environmental sources of variability. *Tree Physiology* **30**: 1448–1455.

Hertel D, Strecker T, Müller-Haubold H, Leuschner C. 2013. Fine root biomass and dynamics in beech forests across a precipitation gradient - is optimal resource partitioning theory applicable to water-limited mature trees? *Journal of Ecology* **101**: 1183–1200.

Hochberg U, Windt CW, Ponomarenko A, Zhang Y-J, Gersony J, Rockwell FE, Holbrook NM. 2017. Stomatal closure, basal leaf embolism, and shedding protect the hydraulic integrity of grape stems. *Plant Physiology* **174**: 764–775.

Houghton RA, Nassikas AA. 2018. Negative emissions from stopping deforestation and forest degradation, globally. *Global Change Biology* **24**: 350–359.

IPCC 2014: Climate Change 2014: Synthesis Report. Contribution of Working Groups I, II and III to the Fifth Assessment Report of the Intergovernmental Panel on Climate Change. Core Writing Team, R.K. Pachauri and L.A. Meyer (eds.). IPCC, Geneva, Switzerland.

IPCC 2018: Global Warming of 1.5°C. An IPCC Special Report on the impacts of global warming of 1.5°C above pre-industrial levels and related global greenhouse gas emission pathways, in the context of strengthening the global response to the threat of climate change, sustainable development, and efforts to eradicate poverty. Masson-Delmotte, V., P. Zhai, H.-O. Pörtner, D. Roberts, J. Skea, P.R. Shukla, A. Pirani, W. Moufouma-Okia, C. Péan, R. Pidcock, S. Connors, J.B.R. Matthews, Y. Chen, X. Zhou, M.I. Gomis, E. Lonnoy, T. Maycock, M. Tignor, and T. Waterfield (eds.). In Press.

Jansen S, Choat B, Pletsers A. 2009. Morphological variation of intervessel pit membranes and implications to xylem function in angiosperms. *American Journal of Botany* **96**: 409–419.

Jump AS, Hunt JM, Peñuelas J. 2006. Rapid climate change-related growth decline at the southern range edge of *Fagus sylvatica*. *Global Change Biology* **12**: 2163–2174.

Kaack L, Weber M, Isasa E, Karimi Z, Li S, Pereira L, Trabi CL, Zhang Y, Schenk HJ, Schuldt B et al. 2021. Pore constrictions in intervessel pit membranes provide a mechanistic explanation for xylem embolism resistance in angiosperms. *New Phytologist* **230**: 1829–1843.

Knipfer T, Brodersen CR, Zedan A, Kluepfel DA, McElrone AJ. 2015. Patterns of drought-induced embolism formation and spread in living walnut saplings visualized using X-ray microtomography. *Tree Physiology* **35**: 744–755.

Knutzen F, Dulamsuren C, Meier IC, Leuschner C. 2017. Recent climate warming-related growth decline impairs European beech in the center of its distribution range. *Ecosystems* **20**: 1494–1511.

Knutzen F, Meier IC, Leuschner C. 2015. Does reduced precipitation trigger physiological and morphological drought adaptations in European beech (*Fagus sylvatica* L.)? Comparing provenances across a precipitation gradient. *Tree Physiology* **35**: 949–963.

Kölling C, Walentowski H, Borchert H. 2005. Die Buche in Mitteleuropa. Eine Waldbaumart mit grandioser Vergangenheit und sicherer Zukunft. *AFZ-DerWald*.

Kreuzwieser J, Fürniss S, Rennenberg H. 2002. Impact of waterlogging on the N-metabolism of flood tolerant and non-tolerant tree species. *Plant, Cell & Environment* **25**: 1039–1049.

Lambers H, Oliveira RS. 2019. Plant Physiological Ecology. Cham: Springer Nature Switzerland AG.

Larter M, Pfautsch S, Domec J-C, Trueba S, Nagalingum N, Delzon S. 2017. Aridity drove the evolution of extreme embolism resistance and the radiation of conifer genus *Callitris*. *New Phytologist* **215**: 97–112.

Leal S, Sousa VB, Pereira H. 2007. Radial variation of vessel size and distribution in cork oak wood (*Quercus suber* L.). *Wood Science and Technology* **41**: 339–350.

Lens F, Sperry JS, Christman MA, Choat B, Rabaey D, Jansen S. 2011. Testing hypotheses that link wood anatomy to cavitation resistance and hydraulic conductivity in the genus *Acer*. *New Phytologist* **190**: 709–723.

Leuschner C 2009. Die Trockenheitsempfindlichkeit der Rotbuche vor dem Hintergrund des prognostizierten Klimawandels. Jahrbuch der Akademie der Wissenschaften zu Göttingen. Walter de Gruyter, Berlin. 281–296.

Leuschner C. 2020. Drought response of European beech (*Fagus sylvatica* L.) - A review. *Perspectives in Plant Ecology, Evolution and Systematics* **47**: 125576.

Leuschner C, Ellenberg H. 2017. Ecology of Central European Forests. Cham: Springer.

Li S, Lens F, Espino S, Karimi Z, Klepsch M, Schenk HJ, Schmitt M, Schuldt B, Jansen S. 2016. Intervessel pit membrane thickness as a key determinant of embolism resistance in angiosperm xylem. *IAWA Journal* **37**: 152–171.

Li S, Li X, Link R, Li R, Deng L, Schuldt B, Jiang X, Zhao R, Zheng J, Li S et al. 2019. Influence of cambial age and axial height on the spatial patterns of xylem traits in *Catalpa bungei*, a ring-porous tree species native to China. *Forests* **10**: 662.

Li X, Blackman CJ, Choat B, Duursma RA, Rymer PD, Medlyn BE, Tissue DT. 2018. Tree hydraulic traits are coordinated and strongly linked to climate-of-origin across a rainfall gradient. *Plant, Cell & Environment* **41**: 646–660.

Liang X, He P, Liu H, Zhu S, Uyehara IK, Hou H, Wu G, Zhang H, You Z, Xiao Y *et al.* 2019. Precipitation has dominant influences on the variation of plant hydraulics of the native *Castanopsis fargesii* (Fagaceae) in subtropical China. *Agricultural and Forest Meteorology* **271**: 83–91.

Lindner M, Fitzgerald JB, Zimmermann NE, Reyer C, Delzon S, van der Maaten E, Schelhaas M-J, Lasch P, Eggers J, van der Maaten-Theunissen M *et al.* 2014. Climate change and European forests: what do we know, what are the uncertainties, and what are the implications for forest management? *Journal of Environmental Management* **146**: 69–83.

Lindner M, Maroschek M, Netherer S, Kremer A, Barbati A, Garcia-Gonzalo J, Seidl R, Delzon S, Corona P, Kolström M *et al.* 2010. Climate change impacts, adaptive capacity, and vulnerability of European forest ecosystems. *Forest Ecology and Management* **259**: 698–709.

Lübbe T, Schuldt B, Leuschner C. 2017. Acclimation of leaf water status and stem hydraulics to drought and tree neighbourhood: alternative strategies among the saplings of five temperate deciduous tree species. *Tree Physiology* **37**: 456–468.

Lutz JA, Furniss TJ, Johnson DJ, Davies SJ, Allen D, Alonso A, Anderson-Teixeira KJ, Andrade A, Baltzer J, Becker KML *et al.* 2018. Global importance of large-diameter trees. *Global Ecology and Biogeography* **27**: 849–864.

Maherali H, Pockman WT, Jackson RB. 2004. Adaptive variation in the vulnerability of woody plants to xylem cavitation. *Ecology* **85**: 2184–2199.

Maréchaux I, Bartlett MK, Sack L, Baraloto C, Engel J, Joetzjer E, Chave J. 2015. Drought tolerance as predicted by leaf water potential at turgor loss point varies strongly across species within an Amazonian forest. *Functional Ecology* **29**: 1268–1277.

Martin-StPaul N, Delzon S, Cochard H. 2017. Plant resistance to drought depends on timely stomatal closure. *Ecology Letters* **20**: 1437–1447.

McDowell N, Pockman WT, Allen CD, Breshears DD, Cobb N, Kolb T, Plaut J, Sperry J, West A, Williams DG *et al.* 2008. Mechanisms of plant survival and mortality during drought: why do some plants survive while others succumb to drought? *New Phytologist* **178**: 719–739.

McDowell NG, Allen CD, Anderson-Teixeira K, Aukema BH, Bond-Lamberty B, Chini L, Clark JS, Dietze M, Grossiord C, Hanbury-Brown A *et al.* 2020. Pervasive shifts in forest dynamics in a changing world. *Science* **368**. eaaz9463.

Meier IC, Knutzen F, Eder LM, Müller-Haubold H, Goebel M-O, Bachmann J, Hertel D, Leuschner C. 2018. The deep root system of *Fagus sylvatica* on sandy soil: structure and variation across a precipitation gradient. *Ecosystems* **21**: 280–296.

Meier IC, Leuschner C. 2008a. Belowground drought response of European beech: fine root biomass and carbon partitioning in 14 mature stands across a precipitation gradient. *Global Change Biology* **14**: 2081–2095.

Meier IC, Leuschner C. 2008b. Leaf size and leaf area index in *Fagus sylvatica* forests: competing effects of precipitation, temperature, and nitrogen availability. *Ecosystems* **11**: 655–669.

Mencuccini M, Grace J. 1995. Climate influences the leaf area/sapwood area ratio in Scots pine. *Tree Physiology* **15**: 1–10.

Morales-Hidalgo D, Oswalt SN, Somanathan E. 2015. Status and trends in global primary forest, protected areas, and areas designated for conservation of biodiversity from the Global Forest Resources Assessment 2015. *Forest Ecology and Management* **352**: 68–77.

Muffler L, Weigel R, Hacket-Pain AJ, Klisz M, Maaten E, Wilmking M, Kreyling J, Maaten-Theunissen M. 2020. Lowest drought sensitivity and decreasing growth synchrony towards the dry distribution margin of European beech. *Journal of Biogeography* **47**: 1910–1921.

Nardini A, Battistuzzo M, Savi T. 2013. Shoot desiccation and hydraulic failure in temperate woody angiosperms during an extreme summer drought. *New Phytologist* **200**: 322–329.

Nesbitt L, Hotte N, Barron S, Cowan J, Sheppard SRJ. 2017. The social and economic value of cultural ecosystem services provided by urban forests in North America: A review and suggestions for future research. *Urban Forestry & Urban Greening* **25**: 103–111.

Peñuelas J, Ciais P, Canadell JG, Janssens IA, Fernández-Martínez M, Carnicer J, Obersteiner M, Piao S, Vautard R, Sardans J. 2017. Shifting from a fertilization-dominated to a warming-dominated period. *Nature Ecology & Evolution* **1**: 1438–1445.

Peñuelas J, Filella I. 2001. Phenology. Responses to a warming world. *Science* **294**: 793–795.

Pflug EE, Buchmann N, Siegwolf RTW, Schaub M, Rigling A, Arend M. 2018. Resilient leaf physiological response of European beech (*Fagus sylvatica* L.) to summer drought and drought release. *Frontiers in Plant Science* **9**: 187.

Powers JS, Vargas G G, Brodribb TJ, Schwartz NB, Pérez-Aviles D, Smith-Martin CM, Becknell JM, Aureli F, Blanco R, Calderón-Morales E *et al.* 2020. A catastrophic tropical drought kills hydraulically vulnerable tree species. *Global Change Biology* **26**: 3122–3133.

Pritzkow C, Williamson V, Szota C, Trouvé R, Arndt SK. 2020. Phenotypic plasticity and genetic adaptation of functional traits influences intra-specific variation in hydraulic efficiency and safety. *Tree Physiology* **40**: 215–229.

Rennenberg H, Seiler W, Matyssek R, Gessler A, Kreuzwieser J. 2004. Die Buche (*Fagus sylvatica* L.) - ein Waldbaum ohne Zukunft im südlichen Mitteleuropa? *Allgemeine Forst- und Jagdzeitung* **175**: 210.

Rosas T, Mencuccini M, Barba J, Cochard H, Saura-Mas S, Martínez-Vilalta J. 2019. Adjustments and coordination of hydraulic, leaf and stem traits along a water availability gradient. *New Phytologist* **223**: 632–646.

Scharnweber T, Smiljanic M, Cruz-García R, Manthey M, Wilmking M. 2020. Tree growth at the end of the 21st century - the extreme years 2018/19 as template for future growth conditions. *Environmental Research Letters* **15**: 74022.

Schenk HJ, Espino S, Romo DM, Nima N, Do AYT, Michaud JM, Papahadjopoulos-Sternberg B, Yang J, Zuo YY, Steppe K *et al.* 2017. Xylem surfactants introduce a new element to the Cohesion-Tension theory. *Plant Physiology* **173**: 1177–1196.

Schuldt B, Buras A, Arend M, Vitasse Y, Beierkuhnlein C, Damm A, Gharun M, Grams TEE, Hauck M, Hajek P *et al.* 2020. A first assessment of the impact of the extreme 2018 summer drought on Central European forests. *Basic and Applied Ecology* **45**: 86–103.

Schuldt B, Knutzen F, Delzon S, Jansen S, Müller-Haubold H, Burlett R, Clough Y, Leuschner C. 2016. How adaptable is the hydraulic system of European beech in the face of climate change-related precipitation reduction? *New Phytologist* **210**: 443–458.

Seidl R, Thom D, Kautz M, Martin-Benito D, Peltoniemi M, Vacchiano G, Wild J, Ascoli D, Petr M, Honkaniemi J *et al.* 2017. Forest disturbances under climate change. *Nature Climate Change* **7**: 395–402.

Senf C, Buras A, Zang CS, Rammig A, Seidl R. 2020a. Excess forest mortality is consistently linked to drought across Europe. *Nature Communications* **11**: 6200.

Senf C, Pflugmacher D, Zhiqiang Y, Sebald J, Knorn J, Neumann M, Hostert P, Seidl R. 2018. Canopy mortality has doubled in Europe's temperate forests over the last three decades. *Nature Communications* **9**: 4978.

Senf C, Sebald J, Seidl R. 2020b. Increases in canopy mortality and their impact on the demographic structure of Europe's forests. *bioRxiv.* doi: 10.1101/2020.03.30.015818.

Sperry JS, Hacke UG, Pittermann J. 2006. Size and function in conifer tracheids and angiosperm vessels. *American Journal of Botany* **93**: 1490–1500.

Sterck C, Scholz SM. 2006. The role of forests in global climate change: whence we come and where we go. *International Affairs* **82**: 861–879.

Stojnic S, Suchocka M, Benito-Garzón M, Torres-Ruiz JM, Cochard H, Bolte A, Cocozza C, Cvjetkovic B, Luis M de, **Martinez-Vilalta J** *et al.* **2017.** Variation in xylem vulnerability to embolism in European beech from geographically marginal populations. *Tree Physiology* **38**: 173–185.

Tomasella M, Beikircher B, Häberle K-H, Hesse B, Kallenbach C, Matyssek R, Mayr S. 2018. Acclimation of branch and leaf hydraulics in adult *Fagus sylvatica* and *Picea abies* in a forest through-fall exclusion experiment. *Tree Physiology* **38**: 198–211.

Tomasella M, Nardini A, Hesse BD, Machlet A, Matyssek R, Häberle K-H. 2019. Close to the edge: effects of repeated severe drought on stem hydraulics and non-structural carbohydrates in European beech saplings. *Tree Physiology* **39**: 717–728.

Tyree MT. 2003. Plant hydraulics: the ascent of water. *Nature* **423**: 923.

Verstraeten G, Baeten L, Frenne P de, **Vanhellemont M, Thomaes A, Boonen W, Muys B, Verheyen K. 2013.** Understorey vegetation shifts following the conversion of temperate deciduous forest to spruce plantation. *Forest Ecology and Management* **289**: 363–370.

Walthert L, Ganthaler A, Mayr S, Saurer M, Waldner P, Walser M, Zweifel R, Arx G von. **2021.** From the comfort zone to crown dieback: Sequence of physiological stress thresholds in mature European beech trees across progressive drought. *Science of the Total Environment* **753**: 141792.

Watson JEM, Evans T, Venter O, Williams B, Tulloch A, Stewart C, Thompson I, Ray JC, Murray K, Salazar A *et al.* **2018.** The exceptional value of intact forest ecosystems. *Nature Ecology & Evolution* **2**: 599–610.

Weber P, Bugmann H, Pluess AR, Walthert L, Rigling A. 2013. Drought response and changing mean sensitivity of European beech close to the dry distribution limit. *Trees* **27**: 171–181.

Wheeler JK, Sperry JS, Hacke UG, Hoang ND. 2005. Inter-vessel pitting and cavitation in woody Rosaceae and other vesselled plants: a basis for a safety versus efficiency trade-off in xylem transport. *Plant;Cell & Environment* **28**: 800–812.

Whitehead D. 2011. Forests as carbon sinks—benefits and consequences. *Tree Physiology* **31**: 893–902.

Wortemann R, Herbette S, Barigah TS, Fumanal B, Alia R, Ducousso A, Gomory D, Roeckel-Drevet P, Cochard H. 2011. Genotypic variability and phenotypic plasticity of cavitation resistance in *Fagus sylvatica* L. across Europe. *Tree Physiology* **31**: 1175–1182.

Wright IJ, Dong N, Maire V, Prentice IC, Westoby M, Díaz S, Gallagher RV, Jacobs BF, Kooyman R, Law EA *et al.* **2017.** Global climatic drivers of leaf size. *Science* **357**: 917–921.

Yuan W, Zheng Y, Piao S, Ciais P, Lombardozzi D, Wang Y, Ryu Y, Chen G, Dong W, Hu Z *et al.* 2019. Increased atmospheric vapor pressure deficit reduces global vegetation growth. *Science advances* **5**: eaax1396.

Zhu S-D, Chen Y-J, Ye Q, He P-C, Liu H, Li R-H, Fu P-L, Jiang G-F, Cao K-F. 2018. Leaf turgor loss point is correlated with drought tolerance and leaf carbon economics traits. *Tree Physiology* **38**: 658–663.

Zimmermann J, Link RM, Hauck M, Leuschner C, Schuldt B. 2021. 60-year record of stem xylem anatomy and related hydraulic modification under increased summer drought in ring- and diffuse-porous temperate broad-leaved tree species. *Trees* **35**: 919–937.

Zimmermann MH. 1983. Xylem structure and the ascent of sap. Berlin, Heidelberg: Springer Berlin Heidelberg.

Zscheischler J, Seneviratne SI. 2017. Dependence of drivers affects risks associated with compound events. *Science advances* **3**: e1700263.

Zscheischler J, Westra S, van den Hurk BJJM, Seneviratne SI, Ward PJ, Pitman A, AghaKouchak A, Bresch DN, Leonard M, Wahl T *et al.* 2018. Future climate risk from compound events. *Nature Climate Change* **8**: 469–477.

CHAPTER 2

Soil water availability and branch age explain variability in xylem safety of European beech in Central Europe

Greta Weithmann, Christoph Leuschner, Roman M. Link, Bat-Enerel Banzragch, Laura Würzberg, Bernhard Schuldt

2.1 Abstract

Xylem embolism resistance has been identified as a key trait with a causal relation to drought-induced tree mortality, but not much is known about its intra-specific trait variability (ITV) in dependence on environmental variation.

We measured xylem safety and efficiency in 300 European beech (F*agus sylvatica* L.) trees across 30 sites in Central Europe, covering a precipitation reduction from 886 to 522 mm yr^{-1}. A broad range of variables that might affect embolism resistance in mature trees, including climatic and soil water availability, competition, and branch age, were examined.

The average P_{50}-value varied by up to 1 MPa between sites. Neither climatic aridity nor structural variables had a significant influence on P_{50}. However, P_{50} was less negative for trees with a higher soil water storage capacity, and positively related to branch age, while specific conductivity (K_s) was not. The greatest part of the ITV for xylem safety and efficiency was attributed to random variability within populations.

We conclude that the influence of site water availability on P_{50} and K_s is low in European beech, and that the high degree of within-population variability for P_{50}, partly due to variation in branch age, hampers the identification of a clear environmental signal.

Keywords: Available soil water capacity, climatic water balance, embolism resistance, Hegyi competition index, hydraulic conductivity, hydraulic plasticity, precipitation gradient, xylem vulnerability curve.

2.2 Introduction

Drought-induced tree mortality has been documented worldwide (Allen *et al.,* 2010; Allen *et al.,* 2015; Hartmann *et al.,* 2018), including European temperate forests (Braun *et al.,* 2020; Schuldt *et al.,* 2020). The capability of different tree species to survive extreme drought intensities varies, but reliable trait-based predictions of future climate warming-related vitality reductions and forest community changes do rarely exist due to insufficient knowledge of plant trait variability (cf. Berzaghi *et al.,* 2020). Because natural selection acts on heritable variation, knowledge of the degree of within-population trait variability is essential in order to evaluate the capacity of a species to cope with climate change (Nicotra *et al.,* 2010). However, although growing in numbers, to date relatively few field studies have quantified the variability in plant hydraulic traits across a species' range (e.g. Martinez-Vilalta *et al.,* 2009; Schuldt *et al.,* 2016; Stojnic *et al.,* 2018; Rosas *et al.,* 2019; Fajardo *et al.,* 2020; Fuchs *et al.,* 2021).

In Central Europe, European beech (*Fagus sylvatica* L.) is the dominant species of natural forest vegetation and occurs under widely different precipitation regimes (Leuschner & Ellenberg, 2017). For colonizing such a wide spectrum of habitats, a high degree of intra-specific trait variability is a likely prerequisite. In the recent past, however, mass mortality of European beech after extreme drought events has been reported not only from locations at the range edge (e.g. Lakatos & Molnár, 2009) but also from the centre of its distribution range (Braun *et al.,* 2020; Leuschner, 2020; Schuldt *et al.,* 2020). This matches earlier findings from physiological studies on the species' drought sensitivity showing low water potentials, reduced nitrogen uptake and a high water use efficiency under dry conditions (Rennenberg *et al.,* 2004; Geßler *et al.,* 2006) and dendroecological evidence of long-term growth declines in various Central European beech forest regions (review in Leuschner, 2020). It therefore remains questionable whether the intra-specific variability in plant hydraulic traits observed across marginal populations (Stojnic *et al.,* 2018) is likewise present in the centre of the species' distribution range.

While the processes causing drought-induced tree mortality are complex, one key mechanism involved in tree mortality upon drought is the partial or complete loss of xylem functionality due to embolism formation (Adams *et al.,* 2017; Choat *et al.,* 2018; Brodribb *et al.,* 2020). Even though a number of co-occurring risk factors have been identified, plant hydraulic traits, foremost xylem embolism resistance, have been related to the survival success of trees after severe droughts in various forest regions (Rowland *et al.,* 2015; Anderegg *et al.,* 2016; Adams *et al.,* 2017; Tai *et al.,* 2017; Correia *et al.,* 2019; Hajek *et al.,*

2020; Li *et al.,* 2020; Powers *et al.,* 2020). Upon drought stress, the tension in the water conducting conduits increases and may cause embolism in the xylem and eventually lead to the collapse of the hydraulic system (Tyree & Sperry, 1989). Hence, maintaining the continuity of the water column in the conduit system is essential for vascular plants (Hacke *et al.,* 2017). Species comparisons have revealed that embolism resistance generally increases with climatic aridity (Maherali *et al.,* 2004; Choat *et al.,* 2007; Larter *et al.,* 2017; Li *et al.,* 2018; Skelton *et al.,* 2021). For temperate broadleaved species and at the intra-specific level, however, results are mixed (e.g., Schuldt *et al.,* 2016; Rosas *et al.,* 2019; Fuchs *et al.,* 2021).

The capacity of European beech to form productive forests in various regions of Western, Central and Eastern Europe with oceanic to continental climates suggests considerable phenotypic plasticity, i.e. the ability to acclimate to different environmental conditions, or high genotypic variation in its distribution range (Bolte *et al.,* 2007; Meier & Leuschner, 2008; Bresson *et al.,* 2011). Because natural selection always involves the inheritance of genetic information, however, it is a logical consequence to address the amplitude of phenotypic-plastic responses in ecological studies (Olson, 2019). Population genetic studies have shown that within-population genetic variance is usually larger than genetic differences between European beech populations, at least in the centre of its distribution range (Buiteveld *et al.,* 2007; Carsjens *et al.,* 2014). In correspondence, earlier studies revealed a high intra-population variability of embolism resistance in European beech stands (Herbette *et al.,* 2010; Wortemann *et al.,* 2011; Aranda *et al.,* 2015; Hajek *et al.,* 2016). Significant differences in embolism resistance between populations, on the other hand, were only observed for marginal populations (Stojnic *et al.,* 2018), and in one study comparing stands of similar age and structure on similar soils in Germany (Schuldt *et al.,* 2016), which differed only little in their genetic structure (Carsjens *et al.,* 2014). This leads to the hypothesis that differences in embolism resistance in European beech are largely caused by the selective force of the local environment that leads to adaptive modifications in the traits of the individuals (Schuldt *et al.,* 2016; Stojnic *et al.,* 2018), but it remains speculative why others did not observe a clear climatic signal (Herbette *et al.,* 2010; Wortemann *et al.,* 2011; Rosas *et al.,* 2019). One reason for the contradicting results might be the selection of different explanatory variables. Most field studies along climatic gradients did neither include soil texture and soil water storage capacity, nor branch age in the analysis. This is surprising, as all of these variables have been found to influence xylem hydraulic properties, at least in certain species (Schuldt *et al.,* 2016; Waite *et al.,* 2019).

Soil physical properties are important as determinants of soil water storage capacity that directly impact the supply of water and nutrients to the plant. Across all climatic zones, soil depth and texture are important variables in attempts to predict drought-induced tree mortality (O'Brien *et al.,* 2017). This has been confirmed, for example, in Norway spruce, where the risk of mortality seems to depend on soil conditions (Rehschuh *et al.,* 2017), and the inclusion of soil characteristics in models of tree and shrub mortality improved their predictions (Tai *et al.,* 2017; Renne *et al.,* 2019). Furthermore, there is evidence that xylem safety closely correlates with local soil water conditions (Beikircher & Mayr, 2009; Awad *et al.,* 2010).

Water availability depends not only on climatic and edaphic conditions, but also on competition between neighbouring trees, which therefore may affect the mortality of trees in forest stands (Das *et al.,* 2011; Ruiz-Benito *et al.,* 2013; Young *et al.,* 2017; Hajek *et al.,* 2020). In European beech*,* intra-specific competition between neighbouring trees was found to influence the drought response, leading for example to reduced stomatal conductance when exposed to competition at dry sites (Baudis *et al.,* 2014). Further, it has been hypothesized that differences in belowground competition might mask the effect of environmental drivers of xylem safety (Fuchs *et al.,* 2021).

On the individual level, tree height (or flow path length) influences xylem architecture through an increasing conduit size towards the stem base (Anfodillo *et al.,* 2013; Olson *et al.,* 2014, 2021; Fajardo *et al.,* 2020). With increasing height and flow path length, the water potential gradient necessary to maintain a given flow rate increases due to the influence of both gravitational force and friction (Koch *et al.,* 2004; Woodruff *et al.,* 2004; Ishii *et al.,* 2008; Ambrose *et al.,* 2016). Consequently, it would be advantageous for the tree to increase embolism resistance with increasing height. Indeed, studies comparing branches at different heights within a tree indicate that xylem safety is positively associated with height (Burgess *et al.,* 2006; Woodruff *et al.,* 2008). This contradicts findings, foremost from the tropics, that taller trees are less embolism resistant than smaller ones, both at the intra- and inter-specific level (Rowland *et al.,* 2015; Olson *et al.,* 2018; Liu *et al.,* 2019; but see Bittencourt *et al.,* 2020). Most likely, the latter can be attributed to a higher transpirational demand of taller trees exposed to a drier atmosphere in environments where water availability is commonly not limiting (cf. Olson *et al.,* 2020).

Another important factor potentially influencing embolism resistance is hydraulic efficiency, which is typically assumed to scale positively with conduit size (Tyree *et al.,* 1994; Gleason *et al.,* 2016). Generally, narrow xylem conduits are considered to be safer than wider ones,

leading to the paradigm that there is a safety-efficiency trade-off (Hacke *et al.,* 2017). In branches of European beech, however, no trade-off between xylem safety and hydraulic efficiency was observed (Cochard *et al.,* 1999; Hajek *et al.,* 2016). Yet, branch age was found to correlate positively with the xylem pressure at 50% loss of hydraulic conductance (P_{50}), i.e. younger branches were found to be more resistant than older branches of comparable diameter (Schuldt *et al.,* 2016). Thus, neither the effects of soil hydrology nor those of stand structure on embolism resistance are well understood.

In the present study, we measured branch xylem safety and hydraulic efficiency in 300 mature European beech trees from 30 stands across a climatic gradient from oceanic to sub-continental, mirrored in a reduction in mean annual precipitation (MAP) by 364 mm yr^{-1}. We hypothesized that embolism resistance of European beech populations is influenced by (i) site water availability, as determined jointly by climatic and edaphic factors, (ii) competition between neighbouring trees, and (iii) branch age. From the existing reports, we expected a higher embolism resistance for drier sites, competitively inferior trees, and for younger branches of a given size.

2.3 Materials and Methods

2.3.1 Study sites and climatic conditions

The study was carried out at 30 mature European beech (*Fagus sylvatica* L.) stands in the centre of the species distribution range across a gradient from a cool-temperate oceanic to sub-continental climate in the lowlands of northern Germany between the North Sea coast and the Polish border (Figure 2.1). The stands were monospecific and grew at elevations of 19 to 159 m a.s.l. on predominantly nutrient-poor sandy pleistocene soils with a soil depth >120 cm. Mean annual precipitation (MAP) decreased from West to East from 886 to 522 mm yr^{-1}, while mean annual temperature (MAT) increased from 9.0 to 10.0°C. All stands have a cohort-like age structure and are managed for silvicultural purposes, but the last thinning occurred at least seven years ago, and canopy closure was > 90 % in all cases. The values for monthly precipitation, air temperature and potential evapotranspiration were extracted for the period from 1991-2018 from the Climate Data Centre (CDC) of the German Weather Service (DWD, Deutscher Wetterdienst, Offenbach, https://opendata.dwd.de/, accessed 2019-11-14) using the R package rdwd v. 1.2.0 (Boessenkool, 2020). The climate variables for the 30 sites were calculated from extrapolated 1 km-gridded data. The extracted precipitation and potential evapotranspiration data were then used to calculate the monthly

cumulative water balance (CWB, mm) as the difference between precipitation and potential evapotranspiration. As mean early growing-season precipitation (April-June, MSP) and mean growing season precipitation (MGSP) were highly correlated with mean annual precipitation (MAP; Figure S2.1), we decided to include the full-year means of the climatic variables in our analyses.
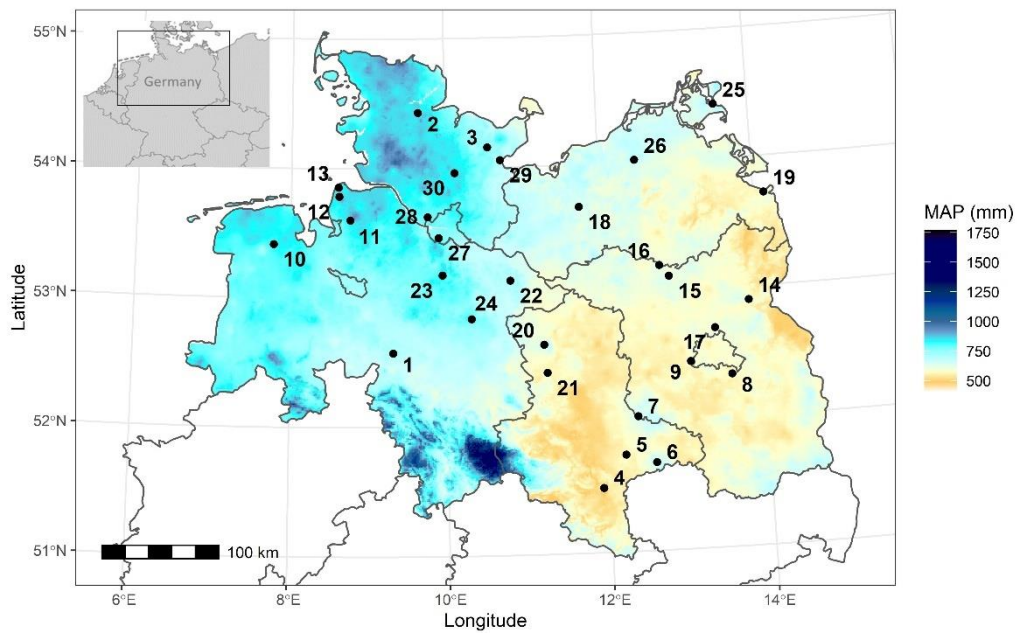

Figure 2.1: Map of the northern part of Germany with federal states and the location of the 30 investigated beech stands. Colours indicate mean annual precipitation (MAP, 1991-2018, data provided by DWD). For site codes and more physiographic information, see Table 2.1 and Table S2.1.

Table 2.1: Stand characteristics of the 30 investigated European beech (*Fagus sylvatica* L.) forests. Given are site number (see Figure 2.1), location name, elevation (m a.s.l.), mean annual precipitation (MAP, mm yr^{-1}), mean early growing-season precipitation (April – June; MSP, mm), mean climatic water balance (CWB, mm month^{-1}), and mean annual temperature (MAT, °C) for the period 1991 – 2018, plant-available water capacity (AWC, mm), tree age, diameter at breast height (DBH, cm), tree height (Height, m), and the Hegyi competition index (CI). Climate data were retrieved from the Climate Data Centre of the German Weather Service (DWD, Offenbach). For data on tree level, means per site ± SE are given.

Site	Name	Elevation	MAP	MSP	CWB	MAT	AWC	Tree age	DBH	Height	CI
1	Grinderwald	85	720.7	162.1	10.19	9.9	301.0	88.5 ± 4.7	44.9 ± 1.0	26.6 ± 0.6	0.49 ± 0.04
2	Brekendorf	99	878.3	179.0	25.56	9.0	226.8	110.5 ± 1.4	45.6 ± 2.3	27.1 ± 0.5	0.59 ± 0.08
3	Malente	77	752.8	165.4	14.93	9.1	252.5	108.0 ± 3.7	58.2 ± 2.8	30.0 ± 0.4	0.44 ± 0.05
4	Halle	124	522.0	137.6	-10.82	10.0	286.4	87.0 ± 1.7	45.1 ± 0.5	25.2 ± 0.7	0.49 ± 0.03
5	Mosigkauer Heide	80	565.8	142.9	-7.31	10.0	177.8	93.6 ± 0.8	44.5 ± 1.2	28.1 ± 0.5	0.53 ± 0.05
6	Dübener Heide	159	673.3	157.4	3.12	9.5	90.7	86.2 ± 1.9	42.0 ± 2.2	26.8 ± 0.5	0.64 ± 0.08
7	Medewitz	142	653.1	154.8	1.87	9.5	126.0	95.3 ± 2.1	47.9 ± 2.5	28.8 ± 0.5	0.54 ± 0.04
8	Zeuthen	47	575.7	145.8	-7.32	9.7	169.4	80.5 ± 1.1	40.2 ± 0.8	28.1 ± 0.6	0.60 ± 0.06
9	Potsdam	45	582.3	144.3	-6.14	9.9	197.6	94.5 ± 2.3	35.7 ± 1.1	21.1 ± 0.3	0.58 ± 0.08
10	Wiesmoor	19	819.7	172.5	19.01	9.7	57.7	84.3 ± 2.4	43.2 ± 1.6	27.1 ± 0.4	0.51 ± 0.03
11	Drangstedt	30	858.4	181.3	22.59	9.6	203.0	98.9 ± 2.2	53.7 ± 2.7	34.4 ± 0.8	0.44 ± 0.04
12	Nordholz	33	886.2	185.7	25.23	9.6	103.7	84.7 ± 1.8	44.5 ± 1.4	30.6 ± 0.3	0.51 ± 0.09
13	Sahlenburg	23	849.0	177.7	22.23	9.7	75.7	91.9 ± 1.3	42.3 ± 1.9	26.1 ± 0.6	0.57 ± 0.06
14	Chorin	64	571.4	142.1	-6.02	9.6	118.6	91.4 ± 2.8	49.6 ± 2.4	30.9 ± 0.6	0.46 ± 0.04
15	Warenthin	81	610.7	149.5	-0.60	9.2	146.6	139.9 ± 6.2	46.2 ± 1.6	29.2 ± 0.5	0.44 ± 0.05
16	Zempow	109	627.8	153.0	2.19	9.0	188.7	102.3 ± 4.4	40.5 ± 1.4	28.8 ± 0.4	0.41 ± 0.03
17	Summt	58	601.9	145.1	-3.49	9.8	43.4	89.9 ± 2.1	45.1 ± 1.5	27.5 ± 0.4	0.52 ± 0.05
18	Kaarzer Holz	70	655.3	156.2	5.64	9.2	78.9	94.7 ± 4.7	45.4 ± 1.6	28.3 ± 0.7	0.40 ± 0.03
19	Eggesiner Forst	32	584.5	149.4	-1.71	9.1	130.4	112.3 ± 5.3	44.0 ± 1.5	27.2 ± 0.5	0.39 ± 0.07
20	Klötze	116	648.4	153.0	2.74	9.4	260.2	131.4 ± 4.4	47.9 ± 1.5	33.9 ± 1.0	0.61 ± 0.06
21	Calvörde	87	572.8	139.9	-4.65	9.7	159.5	106.8 ± 3.8	42.0 ± 1.1	26.5 ± 0.4	0.59 ± 0.06
22	Göhrde	94	718.7	164.2	10.48	9.2	172.1	164.6 ± 10.2	46.1 ± 2.5	26.7 ± 0.6	0.49 ± 0.03
23	Sellhorn	144	863.2	192.3	24.32	9.0	161.3	121.0 ± 4.9	43.0 ± 1.1	30.1 ± 0.7	0.62 ± 0.04
24	Unterlüß	141	804.7	174.5	17.93	9.1	127.1	110.6 ± 3.4	46.3 ± 1.5	28.9 ± 0.6	0.43 ± 0.04
25	Prora	37	646.3	152.4	5.87	9.1	218.3	122.1 ± 5.7	48.1 ± 1.9	28.0 ± 0.4	0.56 ± 0.05
26	Tessin	49	663.3	158.8	6.40	9.0	166.2	85.1 ± 1.5	43.3 ± 1.4	30.7 ± 0.5	0.62 ± 0.05
27	Haake	72	798.0	179.3	17.45	9.7	88.4	153.7 ± 6.6	47.1 ± 2.0	28.4 ± 0.6	0.59 ± 0.06
28	Klövensteen	34	799.0	175.3	17.48	9.6	158.2	119.0 ± 2.7	46.5 ± 1.5	31.1 ± 0.6	0.46 ± 0.01
29	Haffkrug	51	707.8	157.3	10.81	9.2	256.4	62.4 ± 1.4	42.2 ± 1.9	27.9 ± 0.6	0.48 ± 0.05
30	Heidmühlen	68	851.5	179.8	22.69	9.2	164.2	138.2 ± 5.4	44.3 ± 1.3	27.5 ± 0.5	0.73 ± 0.09

2.3.2 Soil characteristics

To estimate plant-available soil water capacity (AWC, mm) at the 30 sites and to characterize the soil chemical regime, soil samples were taken from three different depth layers (0 – 10 cm, 10 – 30 cm and 30 – 60 cm) in each two soil pits dug in every stand. We determined the soil organic carbon to nitrogen ratio (C_{org}/N_t), total phosphorus content and soil pH. Subsequently, the stone content (>2 mm) was determined by sieving a soil volume of 45,000 cm^3 that was excavated in one pit per stand. Soil bulk density and soil particle size

distribution, i.e. the relative proportion of sand- (63 – 2000 µm), silt- (2.0 – 63 µm), and clay-sized (< 2.0 µm) particles, were also determined for three soil depths per stand within one soil pit. The sand fraction was determined by sieving, while the silt and clay fractions were measured by differential sedimentation (PARIO Soil Particle Analyser, METER Group AG, Munich, Germany) (Table S2.1). From particle size distribution and soil bulk density, soil hydraulic properties (the van Genuchten (1980) parameters) were derived by deploying pedotransfer functions according to Schaap *et al.,* (2001), using the module "Rosetta light", implemented in the Software RETC (version 6.02, van Genuchten *et al.,* 1991). The volumetric water contents at permanent wilting point and field capacity were then retrieved from the estimated retention curves using the conventional water potentials of -1.5 MPa (pF 4.2) and -60 hPa (pF 1.8). Soil AWC, defined as the water content between field capacity and permanent wilting point, was then calculated for the three depth layers to 60 cm and extrapolated to a standard depth of 100 cm, assuming a homogenous soil particle composition in the 30 – 100 cm layer. None of the sites had shallow soils, and soil depth exceeded 100 cm in all cases.

2.3.3   Tree dimensions, competition intensity and collection of branch samples

Within each stand, ten mature European beech trees of similar size and canopy position were selected. Tree age ranged from 62 to 164 years, diameter at breast height (DBH) from 36 to 58 cm and tree height from 21 to 34 m across the 30 sites (Table 2.1). All sample trees were dominant individuals in the upper canopy layer. For estimating competition intensity in the direct neighbourhood of our sample trees, we calculated the Hegyi competition index (CI; Hegyi, 1974) for each tree i from the distance and height of the three nearest neighbouring trees j as:

$$CI_i = \sum_{j=1}^{n} \frac{d_j/d_i}{Dist_{ij}},$$

where d_i is the diameter at breast height of the sampled tree i (cm), d_j the diameter at breast height of the competitor j (cm), $Dist_{ij}$ the distance between target tree and competitor (m), and n the number of directly neighbouring trees taken into account (= 3).

Long branch samples were collected in the summers 2018 and 2019 (June – August) from the uppermost sun-exposed crown by professional tree climbers. On the ground, three lateral branches with maximum 1 m length were cut, one of them was selected for hydraulic measurements later. Distance to the branch tip from the basipetal ends of the branch samples was estimated from diameter - length measurements of 85 upper-canopy beech branches

(Hajek *et al.,* 2015) and ranged from 37 to 91 cm with an average of 60.08 ± 0.55 cm (see Weithmann et al. in review for details). The air-cut ends of the branches were immediately transferred into a water-filled bucket and recut under water to release xylem tension. After ~20 min, small side-branches were shortened to a length of ca. 1 cm, branch segments wrapped in wet towels, sealed in plastic bags, and stored at a temperature of 7°C until further processing within 2 weeks.

2.3.4   Hydraulic measurements

In the laboratory, one sample per tree was selected for the hydraulic measurements. The branches of 8.97 ± 0.06 mm (mean ± SE) basipetal diameter were shortened to a length of 34.16 ± 0.11 cm (mean ± SE).

lateral branches cut-off and sealed with quick-drying instant glue (Loctite 431, Henkel, Düsseldorf, Germany), the bark removed at the basipetal end, and segments connected to a Xyl'em embolism meter (Bronkhorst France, Montigny les Cormeilles, France). After measuring the initial hydraulic conductivity (K_h, kg m MPa^{-1} s^{-1}) at low pressure (6 kPa), samples were flushed up to four times at high pressure (120 kPa) for ten minutes with filtered, degassed and demineralized water containing 10 mM KCl and 1 mM $CaCl_2$ until no further increase in K_h was observed. Specific conductivity (K_s, kg m^{-1} MPa^{-1} s^{-1}) was calculated by dividing maximum K_h obtained from the Xyl'em measurements after the flushing procedure by the xylem cross-sectional area without pith and bark (A_{xylem}), which was estimated from the branch cross-sectional area (A_{cross}) as $A_{xylem} = -3.715 + 0.770 * A_{cross}$ (Schuldt *et al.,* 2016). Subsequently, the same branch segments were shortened to 27.5 cm, the bark was removed at both ends and xylem vulnerability curves were constructed with the flow-centrifuge technique (Cavitron; Cochard *et al.,* 2005). In European beech, an average maximum vessel length of 19.3 ± 2.6 cm has been reported (Lübbe *et al.,* 2022), which makes this species suited for flow-centrifuge measurements with a 30 cm-rotor. Segments were inserted into a custom-made honey-comb rotor attached to a Sorvall RC-5C centrifuge (Thermo Fisher Scientific, Waltham, MA, USA). While spinning, conductivity was calculated continuously by the software CaviSoft (version 4.0, University of Bordeaux, France). Measurements started at a pressure of -0.37 MPa, which was raised stepwise until 90% loss of hydraulic conductivity was reached.

Analogous to Ogle *et al.,* (2009), we estimated the parameters of the vulnerability curves based on K_s instead of converting measured conductivities into percent loss of conductivity.

To do so, we reformulated the sigmoidal model of Pammenter & Vander Willigen (1998) to obtain the following equation for the expected value of K_s for observation i of sample j:

$$K_{s_{ij}} = K_{max_j}\left(1 - \frac{1}{1 + exp\left(-s_j\left(\Psi_i - P_{50_j}\right)\right)}\right)$$

where Ψ_i is the pressure induced by the rotation of the rotor (corresponding to xylem water potential), K_{max} the estimated maximum conductivity, P_{50} the water potential at 50% loss of conductance, and s the slope of the regression line on the logit scale. The xylem pressures at 12% and 88% loss of conductance (P_{12} and P_{88}, respectively) were calculated by inserting the desired quantiles of loss of conductance into the model equation of Pammenter & Vander Willigen (1998) and solving for the corresponding water potential.

To assess a potential effect of the flushing procedure on results of the flow-centrifuge measurements, P_{50}-values of non-flushed branches of 13 trees were compared to flushed branches of the same trees. 20 branches were harvested from site number 28 in August 2018 at the end of the sampling campaign, and six were collected from three other sites end of July in 2018.

2.3.5   Branch age

From the basipetal and acropetal end of the branch samples used for hydraulic measurements, semi-thin transverse sections were cut with a sliding microtome (G.S.L.1; Schenkung Dapples, Zurich, Switzerland) and growth rings counted at ×100 magnification under a stereomicroscope (SteREOV20; Carl Zeiss MicroImaging GmbH, Göttingen, Germany) for estimating the age of the branch at both ends. For all subsequent analyses, we estimated the mean of the basipetal and acropetal branch age.

2.3.6   Statistical analyses

All statistical analyses were performed with the R version 3.6.2 (R. Core Team, 2019) in the framework of the tidyverse package (Wickham *et al.,* 2019). Five separate linear mixed effects models were fitted with the R package lme4 v. 1.1-23 (Bates *et al.,* 2015) using Restricted Maximum Likelihood with P_{50}, P_{12}, P_{88}, slope and K_s as responses, fixed effects for CWB, AWC, CI, tree height and branch age, and random intercepts for sites.

As precipitation averages over different timescales were highly correlated and as mentioned above, spring and growing season precipitation were tightly associated with full-year precipitation (Fig. S1), and data for potential evapotranspiration, which are needed for

calculating CWB, are only provided from 1991 onwards, mean annual CWB of the period 1991 – 2018 was included in the models as the sole climate variable. As temperature directly influences potential evapotranspiration, it enters the model through CWB.

Data on branch age and slope of the vulnerability curves were log transformed, and all numeric predictor variables were scaled by their standard deviations and centred around zero. Inference was based on Wald *t*-tests with Satterthwaite's approximation to the degrees of freedom using R package `lmerTest` v. 3.1-2 (Kuznetsova *et al.,* 2017). The marginal and conditional R^2 (Nakagawa *et al.,* 2017) was computed based on R package `MuMIn` v. 1.43.17 (Bartón, 2020).

To illustrate pairwise linear associations between variables, Pearson correlation analyses were carried out using the R package `corrmorant` v. 0.0.0.9007 (Link, 2020). No problematic level of multi-collinearity was detected in the explanatory variables of the model, with all pairwise correlations being well below 0.7 (Figure S2.3; cf. Dormann *et al.,* 2013).

To exclude a possible relationship between the mean and total leaf area or tree height and branch age, linear regression analyses were conducted using the `lm`-function. All leaves distal to the basal end of the segment used for hydraulic measurements were removed, a sub-sample was scanned and the whole leaf area supported by the branch was calculated from the dry mass and area of the scanned leaves (for details, see Weithmann *et al.,* 2022).

2.4 Results

2.4.1 Embolism resistance and hydraulic conductivity across trees and sites

The measured P_{50}-values of the branch xylem varied markedly between the different sites and also between trees within the same site (Figure 2.2a). The average P_{50} of the 300 studied European beech branches was -3.38 ± 0.02 MPa (mean ± SE), with site means ranging from -3.84 ± 0.10 MPa to -2.82 ± 0.09 MPa (Table S2.2). The maximal difference between P_{50}-values among the ten trees per stand was 1.32 MPa. Mean P_{12} of the different sites ranged from -3.03 ± 0.09 MPa to -1.85 ± 0.09 MPa, and mean P_{88} from -4.75 ± 0.09 MPa to -3.69 ± 0.07 MPa, respectively. Specific conductivity (K_s) of the branch xylem ranged from 0.12 to 3.12 kg m^{-1} MPa^{-1} s^{-1} with site means varying between 1.14 ± 0.15 kg m^{-1} MPa^{-1} s^{-1} and 1.95 ± 0.14 kg m^{-1} MPa^{-1} s^{-1} (Figure 2.2b, Table S2.2).
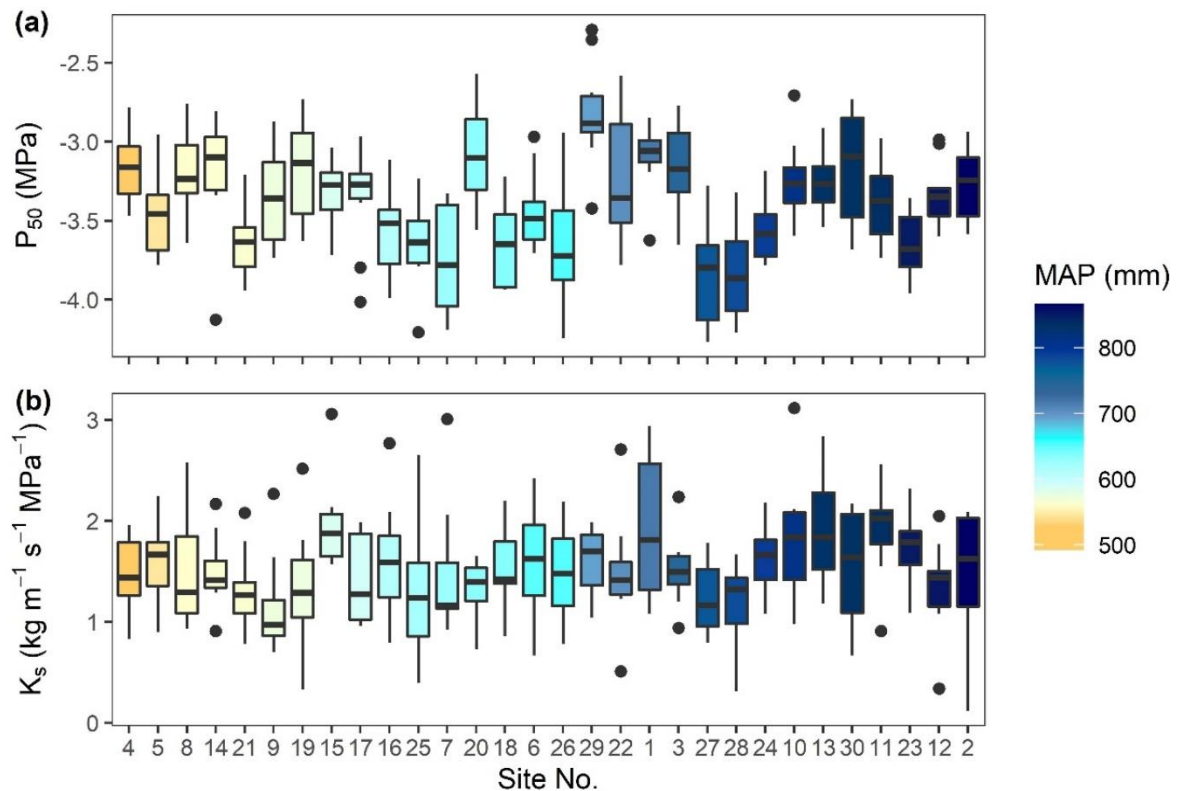
Figure 2.2: Box plots visualizing P_{50} values (a) and specific conductivity (K_s, b) of branch segments of European beech in the 30 stands (10 trees per stand). Colours indicate mean annual precipitation (MAP, 1991-2018, data provided by DWD) of the different sites (see Figure 2.1).

2.4.2   Effect of climatic and soil variables on hydraulic safety and efficiency

According to the linear mixed effects (LME) models, the climatic water balance (CWB) as a measure of the climatic water availability was unrelated to any of the variables related to hydraulic safety or efficiency (P_{12}, P_{50}, P_{88}, *slope*, K_s, Table 2.2; see Table S2.3 for standard errors, degrees of freedom and test statistics). The linear regression analyses that were carried out for visualization showed no significant relation of mean annual precipitation (MAP) or CWB and P_{50} in support of the LME results (Figure 2.3, a and b). However, we found a significant effect of the plant-available water capacity of the soil (AWC) on P_{50} (Table 2.2), a variable that introduces soil physics into the model and represents the soil water availability. Trees growing on sites with lower AWC developed a more negative P_{50}-value (Figure 2.3c), but both P_{12} and P_{88} as well as K_s were unaffected (Table 2.2). Mean annual temperature (MAT) and soil chemical properties, which were not included as model parameters, were not associated with P_{50} or K_s (Figure S2.2).

Table 2.2: Results from the linear mixed effects model examining the influence of climatic water balance (CWB), plant-available water capacity (AWC), tree height, branch age (log transformed) and Hegyi competition index (CI) as fixed variables and random intercept for site on the xylem pressures at 50%, 12% and 88% loss of conductivity (P_{50}, P_{12} and P_{88}, respectively), the slope at the water potential at 50% loss of conductance (log-transformed) and specific conductivity (K_s; n = 298). See Table S2.3 for standard errors, test statistics, and degrees of freedom.

Fixed parts	P_{12} Est.	P_{12} p	P_{50} Est.	P_{50} p	P_{88} Est.	P_{88} p	slope (log) Est.	slope (log) p	K_s Est.	K_s p
(Intercept)	-2.655	**<0.001**	-3.381	**<0.001**	-4.107	**<0.001**	1.049	**<0.001**	1.553	**<0.001**
CWB	0.031	0.497	0.004	0.929	-0.023	0.617	-0.040	0.149	0.026	0.576
AWC	0.089	0.053	0.086	**0.041**	0.083	0.078	0.000	0.991	0.046	0.321
Tr. height	0.010	0.773	0.000	0.988	-0.011	0.697	-0.024	0.267	-0.009	0.823
Br. age (log)	0.080	**0.002**	0.088	**<0.001**	0.097	**<0.001**	0.015	0.385	-0.048	0.160
CI	-0.024	0.340	-0.011	0.541	0.003	0.893	0.016	0.347	0.022	0.510
Random part										
Sd (Intercept)	0.205		0.199		0.228		0.118		0.175	
Sd (Obs.)	0.381		0.279		0.280		0.258		0.535	
Marginal R²	0.082		0.128		0.135		0.041		0.016	
Cond. R²	0.289		0.421		0.480		0.208		0.111	
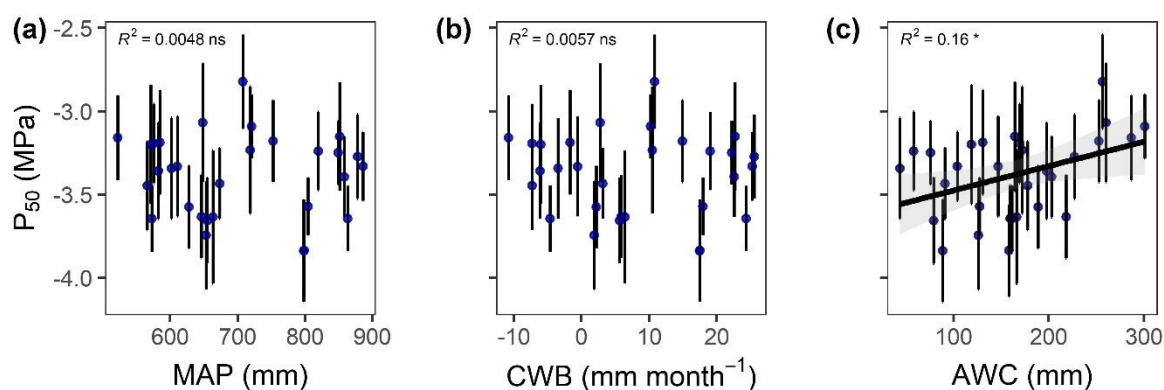
Figure 2.3: (a) Mean annual precipitation (MAP), (b) climatic water balance (CWB) and (c) available water capacity of the soil (AWC) in relation to the xylem pressure at 50% loss of hydraulic conductance (P_{50}). Given values are means ± SE per site; asterisks indicate the level of significance and R^2 values the explained variance of the linear regression through the plot averages (*, $p < 0.05$; ns, non-significant relationship). For significant relationship, the linear regression line with its 95% confidence intervals is shown.

2.4.3   Influence of branch age and competition on embolism resistance

We observed a highly significant effect of branch age on all three measures of embolism resistance (P_{12}, P_{50} and P_{88}). In contrast, branch age affected neither the slope of the vulnerability curve at the water potential at 50% loss of hydraulic conductance (*slope*) nor K_s (Table 2.2). The mean age of the studied branch samples (averaged between basipetal and acropetal end) ranged from 1.5 to 20.5 years (mean ± SE: 6.0 ± 0.2 years), even though

branch diameter was roughly similar (Figure 2.4a). Across the gradient, no effect of water availability on branch age was observed (Figure S2.6), and neither CWB nor AWC had a significant effect on branch age according to a linear mixed effects model (data not shown). Despite considerable variability within the younger branch age classes, older branches showed higher P_{50}-values and were less embolism resistant (Figure 2.4b, c). In a subsample of 13 trees, we could confirm that the observed age effect was not a consequence of the flushing procedure. The constructed vulnerability curves of flushed and non-flushed samples were comparable in their shape (Figure 2.5a), and the estimated slope and P_{50}-value did not differ between both treatments (Figure 2.5b). Interestingly, no significant relationship between branch age and branch diameter or the degree of branch tapering (difference between basipetal and acropetal branch diameter) was found (R^2 = 0.006 and 0.004, respectively; data not shown). Branch age at the basipetal end of the segments was significantly related to the age at the acropetal end, and mean branch age was significantly related to the difference between the age of the basipetal and acropetal end (Figure S2.4). No relationship between branch age and mean or total leaf area of the corresponding branch was observed, and branch age was not related to tree height (Figure S2.5). Neither the Hegyi competition index (CI) nor tree height showed a significant effect on xylem safety or efficiency (Table 2.2).
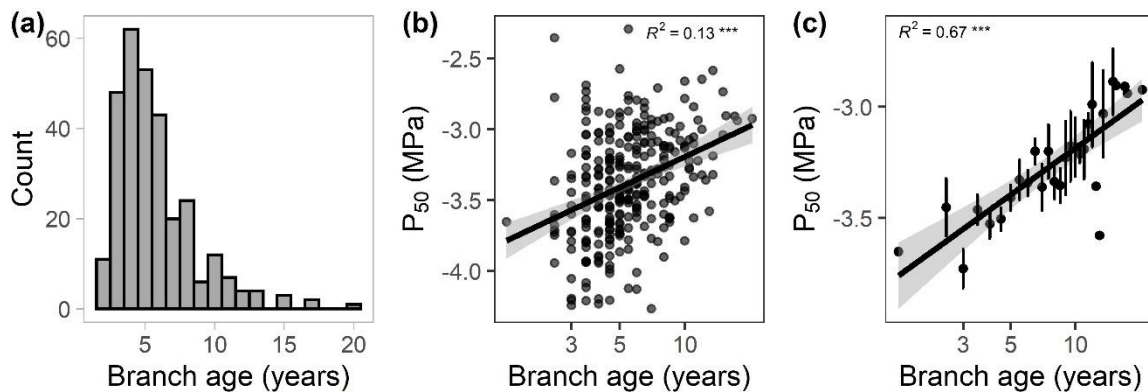
Figure 2.4: (a) Histagramm showing the frequency of branch ages for the 300 samples, (b) linear regression of mean branch age (log10-scaled) on P_{50} at tree level, (c) and linear regression of mean branch age (log10-scaled) on P_{50}. (c) Given are the means per given age ± SE, i.e. averaged values per corresponding growth ring, asterisks in (b) and (c) indicate the level of significance and R^2 values the explained variance of the corresponding linear regression line (***, $p < 0.001$).
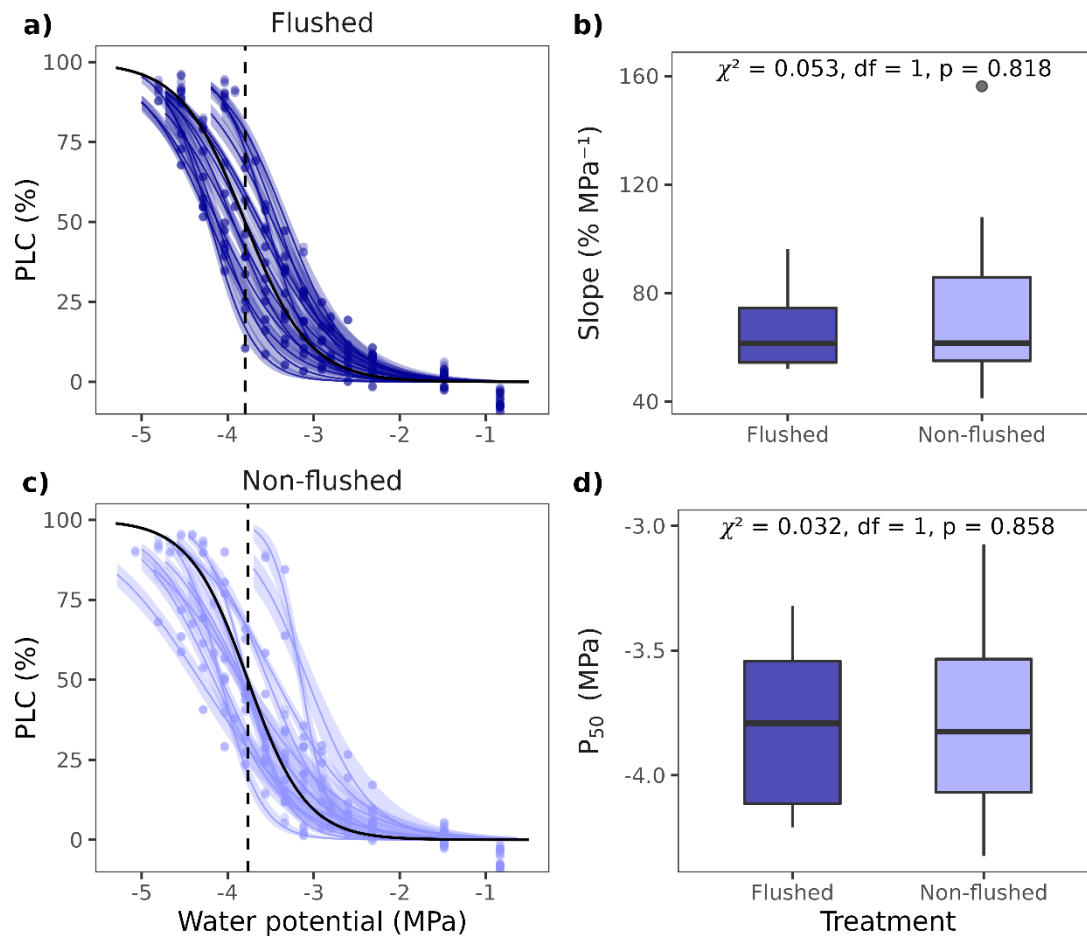
Figure 2.5: (a) Measured vulnerability curves of flushed vs. non-flushed samples. Shown are observed PLC and the predicted vulnerability curves with their bootstrapped 95% confidence intervals overlaid with the average vulnerability curve (black) and the mean P_{50} (black dashed line). (b) Further given are the estimated slope (above) and P_{50} (below) for the two treatments with the *p*-values and summary statistics from a Kruskal-Wallis test comparing the two treatments.

2.4.4 Variance decomposition

According to the results of the LME models, the explained variance of the fixed effects (CWB, AWC, CI, tree height and branch age) was low (~13% for P_{50}, Figure 2.6). Differences between sites that were not attributed to the fixed effects accounted for 29% of the variance in P_{50}, while 58% of the variance resulted from differences between trees in a stand. The fraction of variance explained by the fixed effects and the random site effect increased from P_{12} and P_{50} to P_{88} from 8% to 13%, and from 21% to 35%, respectively, whereas differences in *slope* and K_s were mainly attributable to unexplained differences between individual trees (79% and 89%, respectively).

2.4.5   No trade-off between safety and efficiency

Pairwise linear correlations of the variables included in the models showed no relationship between P_{50} and K_s at the branch level despite considerable variation in P_{50} of 1 MPa ($r = 0.06$, Figure S2.3).
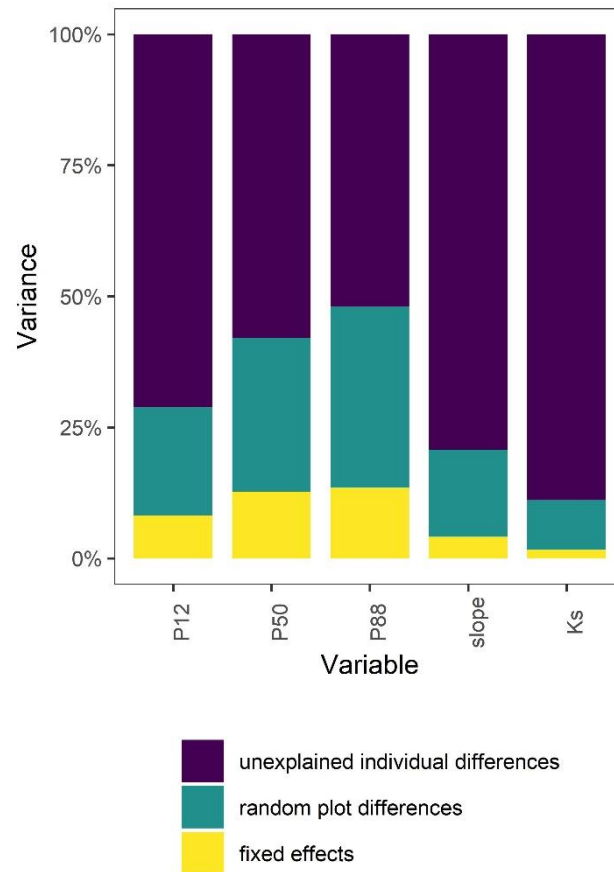

Figure 2.6: Variance components of the linear mixed effects models for P_{12}, P_{50}, P_{88}, slope of the vulnerability curve at P_{50}, and K_s with climatic water balance (CWB), plant-available water capacity (AWC), tree height branch age and Hegyi competition index (CI), as fixed effects and random site effects and residual variability between individuals (see Table 2.2).

2.5 Discussion

2.5.1   Influence of climatic aridity and soil water availability on xylem safety and efficiency

We observed a high degree of intra-specific variability in the xylem pressure at 50% loss of hydraulic conductance (P_{50}) of sun-canopy branches in mature European beech forests. Across the 30 studied sites in Central Europe, mean P_{50} varied from -2.82 to -3.84 MPa, which is similar to the range reported in earlier field studies (Herbette *et al.,* 2010; Stojnic

et al., 2018). Xylem specific conductivity (K_s) likewise revealed a considerable intra-specific variability, with site means ranging from 1.1 to 2.0 kg m^{-1} MPa^{-1} s^{-1}. Despite these pronounced differences in xylem safety and efficiency across sites, observed trait variability could neither be attributed to climatic water availability nor tree and stand structural variables, and the highest proportion of variance was caused by between-tree differences, especially in case of K_s. Although the fixed effects only explained 13% of the total variance in P_{50}, we observed a significant influence of the plant-available water storage capacity (AWC) of the soil, i.e. soil physical properties that determine soil water availability in rainless periods and the flow resistance experienced by water-absorbing roots in drying soil. Based on earlier research that showed a more embolism-resistant xylem in European beech trees with higher drought exposure (Schuldt *et al.,* 2016; Stojnic *et al.,* 2018), we expected that embolism resistance is influenced by both climatic and edaphic measures of water availability (CWB and AWC). This is also suggested by the studies of Wortemann *et al.* (2011) and Lübbe *et al.* (2017), who documented effects of water availability on embolism resistance in European beech, and by other work showing a high degree of hydraulic plasticity in this species (Herbette *et al.,* 2010; 2020; Aranda *et al.,* 2015; 2017; Nguyen *et al.,* 2017; Noyer *et al.,* 2017). To date, however, the existing evidence for an intra-specific increase in xylem safety with increasing climatic aridity in European beech is scarce (e.g. Schuldt *et al.,* 2016; Stojnic *et al.,* 2018). In fact, most field studies on mature trees failed to detect the anticipated adaption of xylem safety to water availability at the intra-specific level in coniferous and broad-leaved (diffuse- or ring-porous) temperate tree species (e.g. Martínez-Vilalta *et al.,* 2009; Martin-StPaul *et al.,* 2013; Lamy *et al.,* 2014; González-Muñoz *et al.,* 2018; Rosas *et al.,* 2019). However, embolism resistance likely depends not only on the precipitation regime, but also on stand structural and edaphic properties. We originally assumed that Schuldt *et al.* (2016) found a clear climatic effect on P_{50} mainly because soil and stand structure were well comparable across their rather local precipitation gradient (cf. Hertel *et al.,* 2013; Müller-Haubold *et al.,* 2013). Because this is usually not the case when larger regions are studied, we additionally included competition index (CI) and soil available water capacity (AWC) as fixed effects in the mixed models. In contrast to Schuldt *et al.* (2016), the precipitation gradient was steeper in our study (364 mm yr^{-1} versus 261 mm yr^{-1}, respectively) and the P_{50} variation across sites was consequently larger (1.02 MPa versus 0.33 MPa, respectively). As we did not find convincing evidence of a significant effect of climatic aridity, expressed through CWB, on embolism resistance, we conclude that soil physical properties that determine water storage capacity must be more

important drivers for European beech. This seems plausible in regions where site differences in soil grain size distribution or soil depth cause considerable variance in soil water storage, which may outweigh gradients in summer precipitation. In our study, only beech stands on deep and predominantly sandy soils were included. A greater effect of AWC might be observed when stands on deep and shallow soils are compared, or sites that differ strongly in soil physical properties. However, our results are supportive for the assumption of Carminati & Javaux (2020) that the hydraulic conductivity of the rhizosphere may be the primary driver of stomatal closure during drought. This would require a close coordination between root and rhizosphere conductance and xylem safety of sun-canopy branches.

2.5.2   Effects of neighbourhood composition and branch age on embolism resistance

Root competition between neighbouring trees may have a large effect on soil water availability, especially in periods with water deficits, as is visible in thinning experiments in forests (McDowell *et al.,* 2006; Moreno & Cubera, 2008). We therefore included Hegyi's competition index as a fixed effect in the models in order to account for the social status of the individual in the stand, but an effect on embolism resistance did not appear. Tree height was another variable included in the analysis in order to account for the increase in gravitational force and friction with height in accordance with the hydraulic limitation hypothesis (Ryan *et al.,* 2006), which predicts a vertical decline in P_{50} (cf. Burgess *et al.,* 2006; Woodruff *et al.,* 2008; Ambrose *et al.,* 2009). In our study, tree height was largely comparable among the trees of a stand, but mean tree height varied by up to 13.3 m between sites. Yet, tree height was unrelated to P_{50}, and also unaffected by the climatic and edaphic variability among the sites. A study on the xylem anatomy of the branches used for the hydraulic measurements revealed neither an effect of tree height on vessel diameter nor a relation between vessel diameter and P_{50} across our gradient (Weithmann *et al.*, in review). Furthermore, mean leaf area, which is related to vessel diameter at the petiole base (Olson *et al.,* 2021), did not affect embolism resistance or K_s (results not shown).

As suggested by Schuldt *et al.* (2016), we further considered branch age as a fixed factor to explain P_{50}. The authors observed a highly significant positive effect of branch age on P_{50} in European beech, i.e. older branches were found to be less resistant. In European beech, an annual length increment in upper-canopy branches of 17 cm yr^{-1} has been reported (Hajek *et al.,* 2015). This highlights the need for multi-aged branches for the construction of xylem vulnerability curves with the flow centrifuge technique. In our study, the age of our similar-sized branches (mean ± SE: 8.9 ± 0.1 mm) ranged from 1.5 to 20.5 years (mean ± SE:

6.0 ± 0.2 years) and was the most influential factor affecting embolism resistance (P_{12}, P_{50} and P_{88}). The large variability in annual growth rate is likely driven by the specific microclimatic conditions at the position of the branch in the uppermost canopy. This assumption is supported by the fact that branch age was unrelated to water availability, tree height and mean or total leaf area per branch. Nevertheless, branch age significantly affected vessel diameter variation, with smaller vessel diameters found in older branches (Weithmann *et al.,* in review). As older branches had smaller vessels and a lower embolism resistance, we can exclude an indirect effect of vessel diameter variation on P_{50}. We speculate that the observed age effect results from a "fatigue mechanism", i.e. physical damage of the pit membranes due to embolisms occurring either after drought (cavitation fatigue) or frost events (frost fatigue) (Hacke *et al.,* 2001; Christensen-Dalsgaard & Tyree, 2014; Zhang *et al.,* 2018; Dai *et al.,* 2020). In older branches, but of similar diameter, a higher portion of conduits has experienced frost or drought events during their lifetime. As a consequence of fatigue, however, we would have expected steeper vulnerability curves for older branches, but no relation of branch age to the slope of the vulnerability curves was observed. In order to ensure that vulnerability curves included all potentially functional xylem conduits rather than just the portion that was functional at the time of collection, we flushed all samples prior to the construction of vulnerability curves as recommended by Hacke & Sperry (2001). This procedure should increase the comparability of branches harvested under different climatic conditions. However, to date no widely accepted protocol exists as to whether xylem vulnerability curves should be constructed with flushed or non-flushed samples. In order to test whether flushing is affecting the results of vulnerability measurements with a flow centrifuge, we investigated the effect of flushing in 80 multi-aged branches of four temperate diffuse-porous tree species. Although flushed samples had a significantly higher hydraulic conductivity, vulnerability curve parameters were unaffected by this treatment (Weithmann *et al.,* unpublished). Similarly, we could not detect an effect of the flushing procedure on the estimated slope of the curve or the P_{50}-value in 13 trees studied at one of our sites (Figure 2.5). The flushing effect is hence unlikely to be the primary cause of the highly significant influence of branch age on embolism resistance. Rather, novel visualization techniques of in-situ embolism formation indicate that vessels in older annual rings embolize first during desiccation (Fukuda *et al.,* 2015; Knipfer *et al.,* 2019; Lemaire *et al.,* 2020; Meixner *et al.,* 2020). Because all vessels were hydraulically functional in these studies, it remains unclear why older vessels are more vulnerable than younger ones. Possible explanations include

frost-fatigue or the potential coating of pit membranes by xylem sap surfactants (Schenk *et al.,* 2021).

2.5.3 Intra-specific trait variability

Consistent with previous studies, we observed a high degree of intra-population variability in xylem safety, which is unlikely to be caused by small-scale soil moisture variation and/or competition between neighbouring trees. European beech is known for a high degree of intra-population genetic variability (Wortemann *et al.,* 2011; Aranda *et al.,* 2015; Hajek *et al.,* 2016) and a high degree of within-crown plasticity of P_{50} has been reported for European beech (Cochard *et al.,* 1999; Lemoine *et al.,* 2002; Herbette *et al.,* 2010; Schuldt *et al.,* 2016). We speculate that differences in light intensity and VPD within the crown of single trees experienced by given branches during their lifetime, as well as the observed correlation between branch age and P_{50} can well explain this heterogeneity. In field studies, it is hardly possible to control for these potentially influential factors. In our study, only similar-sized branches with a comparable number of lateral twigs (mean ± SE: 6.3 ± 0.1 n) were sampled in the 30 stands. However, we observed neither a relationship between branch age and branch diameter nor the degree of branch tapering (difference between basipetal and acropetal segment diameter). This made it impossible to exclude older branches during sampling. Furthermore, the growth conditions during the lifespan of branches are difficult to compare. The only option to reduce the high degree of intra-tree variability in embolism resistance is to sample a large number of replicates from each tree, which reduces the number of stands that can be investigated and results in an additional nesting level and corresponding issues with pseudoreplication. Our study with 300 climbed trees on 30 sites reached the limits of field studies in terms of labour effort. Future studies on within-crown variation, within-population variability and ontogenetic change in P_{50} would help to assess the results of provenance and environmental gradient studies of embolism resistance in a broader context. Besides the high intra-population variability, we also observed considerable between-population variability that was explained by the fixed effects. For P_{50}, 29% of the variance was attributed to random differences between sites, which might be attributed to unobserved environmental variables, small-scale climatic deviations from long-term trends, or phylogenetic differences between populations. As we included a broad range of climatic and edaphic variables, it is unlikely that all of the unexplained between-population variance is driven by unobserved environmental variables. However, the observed rapid response of beech vessel properties to extreme climate conditions (Zimmermann *et al.,* 2021) suggests

that small-scale climate fluctuations may precipitate transient changes in embolism resistance at some sites. In either case, the magnitude of the unobserved between-population variability is indicative for a possible phylogenetic signal in embolism resistance and may thus indicate a potential for the selection of more drought-resistant genotypes.

2.5.4   Trade-off between xylem safety and efficiency

Previous studies failed to detect any relationship between xylem safety and efficiency in European beech (Cochard *et al.,* 1999; Hajek *et al.,* 2016; Schuldt *et al.,* 2016). In accordance with these results, we did not find a relationship between P_{50} and K_s at the intra-specific level (see Fig. S3). At the inter-specific level, however, this trade-off has repeatedly been reported (e.g. Wheeler *et al.,* 2005; Maherali *et al.,* 2006; Schumann *et al.,* 2019; van der Sande *et al.,* 2019). It is not yet understood why intra-specific studies commonly fail to detect this anticipated relationship (cf. Tyree *et al.,* 1994), while inter-specific studies often confirm it. One may speculate that due to the restricted range in vessel diameter variation and embolism resistance found in intra-specific studies, they often lack the power to detect such a relation. Furthermore, vessel diameter is only indirectly related to embolism resistance through its relatedness to inter-vessel pit membrane thickness (Isasa *et al.,* unpublished). As shown by a modelling approach, this ultra-structural wood trait, in combination with the number of pits per vessel, is directly affecting xylem embolism resistance (Kaack *et al.,* 2021). In either case, when comparing relationships at the within- and between-species level, there is a risk of succumbing to ecological fallacies, i.e. using conclusions from between-group relationships to draw inferences on within-group relationships or vice versa. The driving forces for differences on the two levels of aggregation are likely very different, with between-species differences being driven by natural selection for trait combinations associated with different drought resistance strategies, and within-species differences to a large degree mirroring ontogenetic changes that often reflect relatively static allometric scaling rules. Accordingly, the existence of an interspecific trade-off thus does not necessarily imply the existence of a within-species relationship.

2.5.5   Conclusion

To our knowledge, this study provides the largest intra-specific dataset on the xylem safety and efficiency of a tree species across a climatic gradient available so far. European beech, the most important tree species of Central Europe's natural forest vegetation and an important timber species, seems to be vulnerable to climate warming-related drought and

heat events. This became widely evident during the extreme 2018/19 drought event, when exceptionally low foliar water potentials crossing the threshold for xylem hydraulic failure were observed at various sites in Central Europe (Schuldt *et al.*, 2020; Walthert *et al.*, 2021). Understanding to what extent European beech is capable of acclimating its branch hydraulic system to achieve greater drought tolerance is therefore of high importance.

Our gradient study showed that P_{50} differed by 1 MPa across the sites, but this intra-specific trait variability was neither related to changes in the climatic water balance nor to tree height or neighbourhood composition. Instead, soil water availability as approximated by the soil capacity for plant-available water was the most important determinant, even though the explained variance was small. The expected increase in embolism resistance towards drier sites as a result of adaptation or acclimation to drought could therefore only partly be confirmed. Branch age was, however, the by far most important single factor influencing xylem embolism resistance, which is unrelated to any site or stand attribute. A much greater proportion of variance in P_{50} is attributable to phenotypic or genotypic variation between tree individuals and assumable to variation across the crown. Certainly, the considerable hydraulic plasticity within European beech populations may represent a solid basis for selection processes. However, the weak influence of water availability on xylem safety indicates that the relevant xylem anatomical traits may be more controlled by factors other than drought, and xylem safety might not be a promising factor for identifying more drought-resistant provenances.

Acknowledgements

2.6 Supplementary information

Table S2.1: Soil characteristics and coordinates of the 30 investigated beech (*Fagus sylvatica*) forests. Soil properties refer to the upper 60 cm of mineral soil. Given are the bulk density (g cm^{-3}), ratios of sand, silt and clay (expressed in % of soil mass without stone content), pH value (H$_2$O) of mineral soil, carbon/nitrogen ratio of mineral soil (C$_{org}$/N$_t$, g g^{-1}), and phosphor concentration of mineral soil (P, µg g^{-1}).

Site	Name	Latitude	Longitude	Bulk density	Sand	Silt	Clay	pH	C$_{org}$/N$_t$	P
1	Grinderwald	52.5723	9.3145	1.1	64.9	32.3	2.8	4.2	21	1.85
2	Brekendorf	54.4287	9.6530	1.2	75	25	0	4.1	14.4	1.97
3	Malente	54.1547	10.5594	1.1	72.4	25.4	2.2	4.3	16.7	3.31
4	Halle	51.4997	11.9165	1.2	51.4	24.8	23.8	4.3	18.8	1.89
5	Mosigkauer Heide	51.7496	12.2095	1.4	64.8	34.3	1	4.6	12.8	1.35
6	Dübener Heide	51.6811	12.5857	1.3	90.6	9.1	0.3	4.3	20.1	1.96
7	Medewitz	52.0416	12.3792	1.3	87.1	10.9	2	4.2	19.2	5.94
8	Zeuthen	52.3322	13.5853	1.4	77.7	18.2	4.1	4.2	17.3	6.46
9	Potsdam	52.4461	13.0745	1.3	74.7	11.7	13.6	4.2	24.8	6.07
10	Wiesmoor	53.4128	7.7775	0.9	63.3	2.5	0.9	3.9	31.5	1.95
11	Drangstedt	53.5998	8.7668	1.3	71.5	26.5	2.1	4.1	25.7	1.41
12	Nordholz	53.7829	8.6215	1.3	87.7	11.3	1	4.5	31.6	1.93
13	Sahlenburg	53.8530	8.6120	1.3	93.3	6.7	0	4.3	31.9	0.64
14	Chorin	52.8964	13.8539	1.3	88	10.3	1.7	4.4	22.3	18.74
15	Warenthin	53.1133	12.8536	1.2	86.8	13.1	0.1	4.7	24.6	12.64
16	Zempow	53.1996	12.7374	1.1	87	7.8	5.2	4.5	23.5	2.27
17	Summt	52.6960	13.4046	0.9	64.1	2.2	0.4	4.5	24.8	32.78
18	Kaarzer Holz	53.6747	11.7339	1.3	94.1	4.5	1.3	4.8	15.6	9.98
19	Eggesiner Forst	53.7150	14.1382	1.3	85.2	12.9	2	4.5	22.8	4.53
20	Klötze	52.6207	11.2298	1.0	81.7	16.2	2.1	4.3	14.7	1.96
21	Calvörde	52.4039	11.2606	1.4	77.8	22.2	0	4.4	14.5	5.89
22	Göhrde	53.1226	10.8196	1.2	81.2	17.4	1.4	4.7	24	1.09
23	Sellhorn	53.1722	9.9528	1.2	87.9	9.7	2.5	4.2	25.1	1.07
24	Unterlüß	52.8312	10.3170	1.2	87.8	11.1	1	4.5	24	1.33
25	Prora	54.4167	13.5552	1.2	72.8	23.9	3.3	4.2	19	5.29
26	Tessin	54.0201	12.4801	1.3	80.7	15.8	3.5	4.1	19.5	4.47
27	Haake	53.4612	9.9075	1.2	91.1	8.9	0	4.2	27.2	7.7
28	Klövensteen	53.6233	9.7681	1.1	86.5	13.5	0	4	28.5	3.01
29	Haffkrug	54.0554	10.7229	1.1	72.2	25	2.7	4.3	16.3	3.94
30	Heidmühlen	53.9619	10.1255	1.1	86.2	13	0.7	4.1	30.3	1.56

Table S2.2: Summary of all major variables explored. Given are means ± SE per site of the xylem pressures at 12%, 50% and 88% loss of hydraulic conductance (P_{12}, P_{50} and P_{88}, respectively), the slope at P_{50}, and specific conductivity (K_s).

Site	Name	P_{12}	P_{50}	P_{88}	slope	K_s
1	Grinderwald	-2.49 ± 0.06	-3.09 ± 0.06	-3.69 ± 0.07	2.85 ± 0.09	1.94 ± 0.23
2	Brekendorf	-2.54 ± 0.11	-3.27 ± 0.08	-4.00 ± 0.07	2.27 ± 0.12	1.49 ± 0.20
3	Malente	-2.41 ± 0.09	-3.18 ± 0.08	-3.94 ± 0.07	2.29 ± 0.06	1.51 ± 0.11
4	Halle	-2.58 ± 0.12	-3.16 ± 0.08	-3.74 ± 0.05	2.89 ± 0.15	1.45 ± 0.15
5	Mosigkauer Heide	-2.64 ± 0.10	-3.45 ± 0.08	-4.25 ± 0.07	2.14 ± 0.06	1.63 ± 0.13
6	Dübener Heide	-2.58 ± 0.08	-3.43 ± 0.07	-4.29 ± 0.08	2.16 ± 0.09	1.60 ± 0.16
7	Medewitz	-2.91 ± 0.12	-3.74 ± 0.10	-4.58 ± 0.10	1.93 ± 0.06	1.47 ± 0.20
8	Zeuthen	-2.60 ± 0.08	-3.19 ± 0.07	-3.78 ± 0.07	2.86 ± 0.08	1.55 ± 0.20
9	Potsdam	-2.78 ± 0.09	-3.36 ± 0.09	-3.93 ± 0.10	2.76 ± 0.11	1.14 ± 0.15
10	Wiesmoor	-2.55 ± 0.07	-3.24 ± 0.07	-3.92 ± 0.08	2.61 ± 0.04	1.84 ± 0.19
11	Drangstedt	-2.74 ± 0.09	-3.39 ± 0.08	-4.04 ± 0.07	2.70 ± 0.06	1.92 ± 0.14
12	Nordholz	-2.65 ± 0.08	-3.33 ± 0.07	-4.01 ± 0.06	2.49 ± 0.07	1.36 ± 0.14
13	Sahlenburg	-2.62 ± 0.08	-3.25 ± 0.06	-3.87 ± 0.05	2.80 ± 0.12	1.91 ± 0.17
14	Chorin	-2.45 ± 0.14	-3.20 ± 0.11	-3.95 ± 0.09	2.37 ± 0.11	1.50 ± 0.11
15	Warenthin	-2.63 ± 0.15	-3.33 ± 0.09	-4.04 ± 0.06	2.22 ± 0.11	1.95 ± 0.14
16	Zempow	-2.90 ± 0.10	-3.57 ± 0.08	-4.25 ± 0.07	2.52 ± 0.11	1.61 ± 0.18
17	Summt	-2.74 ± 0.10	-3.34 ± 0.10	-3.95 ± 0.10	2.90 ± 0.09	1.40 ± 0.14
18	Kaarzer Holz	-2.94 ± 0.13	-3.66 ± 0.08	-4.37 ± 0.07	2.29 ± 0.14	1.52 ± 0.13
19	Eggesiner Forst	-2.53 ± 0.11	-3.19 ± 0.10	-3.84 ± 0.09	2.58 ± 0.05	1.34 ± 0.18
20	Klötze	-2.32 ± 0.15	-3.07 ± 0.11	-3.82 ± 0.08	2.25 ± 0.10	1.32 ± 0.09
21	Calvörde	-3.01 ± 0.08	-3.64 ± 0.06	-4.27 ± 0.06	2.66 ± 0.10	1.30 ± 0.13
22	Göhrde	-2.47 ± 0.12	-3.23 ± 0.12	-4.00 ± 0.13	2.29 ± 0.10	1.49 ± 0.18
23	Sellhorn	-2.90 ± 0.06	-3.64 ± 0.06	-4.39 ± 0.07	2.18 ± 0.08	1.75 ± 0.11
24	Unterlüß	-2.84 ± 0.06	-3.57 ± 0.05	-4.30 ± 0.07	2.22 ± 0.09	1.61 ± 0.11
25	Prora	-2.76 ± 0.14	-3.63 ± 0.08	-4.50 ± 0.07	1.86 ± 0.11	1.30 ± 0.20
26	Tessin	-2.99 ± 0.15	-3.63 ± 0.13	-4.28 ± 0.11	2.53 ± 0.11	1.51 ± 0.15
27	Haake	-2.92 ± 0.13	-3.84 ± 0.10	-4.75 ± 0.09	1.88 ± 0.09	1.23 ± 0.11
28	Klövensteen	-3.03 ± 0.09	-3.84 ± 0.09	-4.64 ± 0.09	2.08 ± 0.07	1.19 ± 0.14
29	Haffkrug	-1.85 ± 0.09	-2.82 ± 0.09	-3.80 ± 0.10	2.06 ± 0.07	1.59 ± 0.11
30	Heidmühlen	-2.25 ± 0.12	-3.15 ± 0.10	-4.05 ± 0.10	2.00 ± 0.08	1.56 ± 0.18

Table S2.3: Standard errors (*SE*), degrees of freedom (*df*) and test statistics (*t - val.*) of linear mixed effects models examining the influence of climatic water balance (CWB), plant-available water capacity (AWC), tree height, branch age (log transformed) and the Hegyi competition index (CI) as fixed variables and site as random variable on P_{12}, P_{50}, P_{88}, slope (log-transformed) and K_s (n = 298, except for K_s: n = 296).

Fixed parts	P_{12}			P_{50}			P_{88}			slope (log)			K_s		
	SE	df	t - val.	SE	df	t - val.	SE	df	t - val.	SE	df	t - val.	SE	df	t - val.
(Intercept)	0.044	26.375	-60.995	0.040	26.183	-85.189	0.045	26.191	-91.857	0.026	26.465	40.020	0.045	26.428	34.876
CWB	0.045	28.030	0.689	0.041	27.550	0.090	0.046	27.396	-0.505	0.027	28.236	-1.483	0.046	28.305	0.566
AWC	0.044	26.651	2.028	0.040	26.381	2.146	0.045	26.355	1.832	0.026	26.787	0.011	0.045	26.836	1.012
Tr. height	0.034	160.694	0.289	0.026	217.058	0.015	0.027	244.401	-0.390	0.022	133.899	-1.115	0.041	96.674	-0.225
Br. age (log)	0.025	291.999	3.155	0.019	288.838	4.678	0.019	285.830	5.131	0.017	290.433	0.870	0.034	277.192	-1.410
CI	0.025	291.026	-0.955	0.019	286.680	-0.611	0.019	283.898	0.135	0.017	291.986	0.942	0.034	288.992	0.659
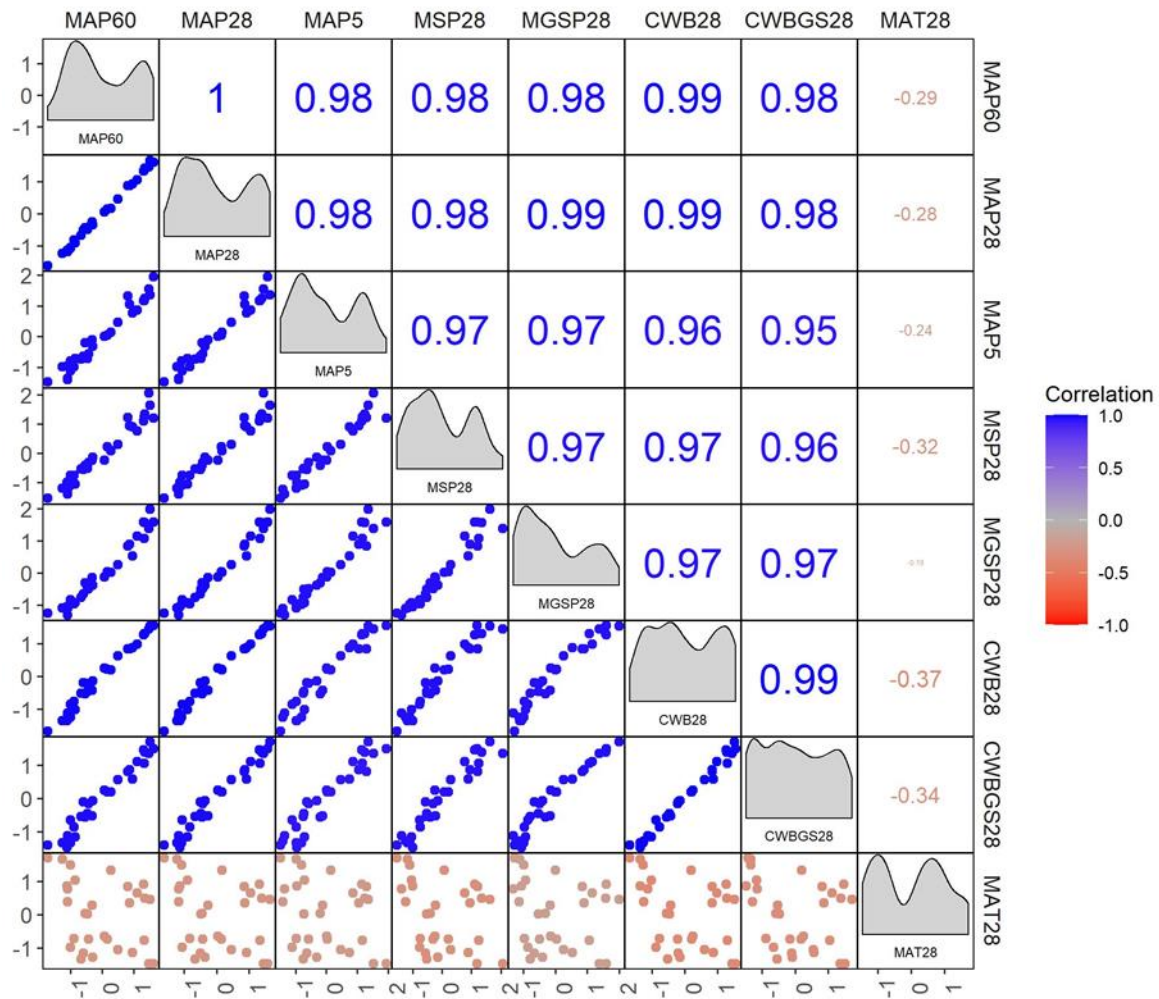
Figure S2.1: Correlation matrix on site level of climatic variables. Mean annual precipitation for the period 1959 – 2018 (MAP60), for the period 1991 – 2018 (MAP28) and for a time period of 5 years before date of harvest (MAP5), mean early growing season precipitation (April – June, MSP28), mean growing season precipitation (April – September, MGSP28), mean climatic water balance (precipitation - potential evapotranspiration, CWB28), mean growing season climatic water balance (April – September, CWBGS28) and mean annual temperature. Unless otherwise noted means refer to a time period of 1991 – 2018, data were provided by DWD. The lower triangle depicts the variables from x- and y-axis in relation, the upper triangle shows the correlation strength (Pearson's *r*) and the plot diagonal shows density plots of the corresponding variables.
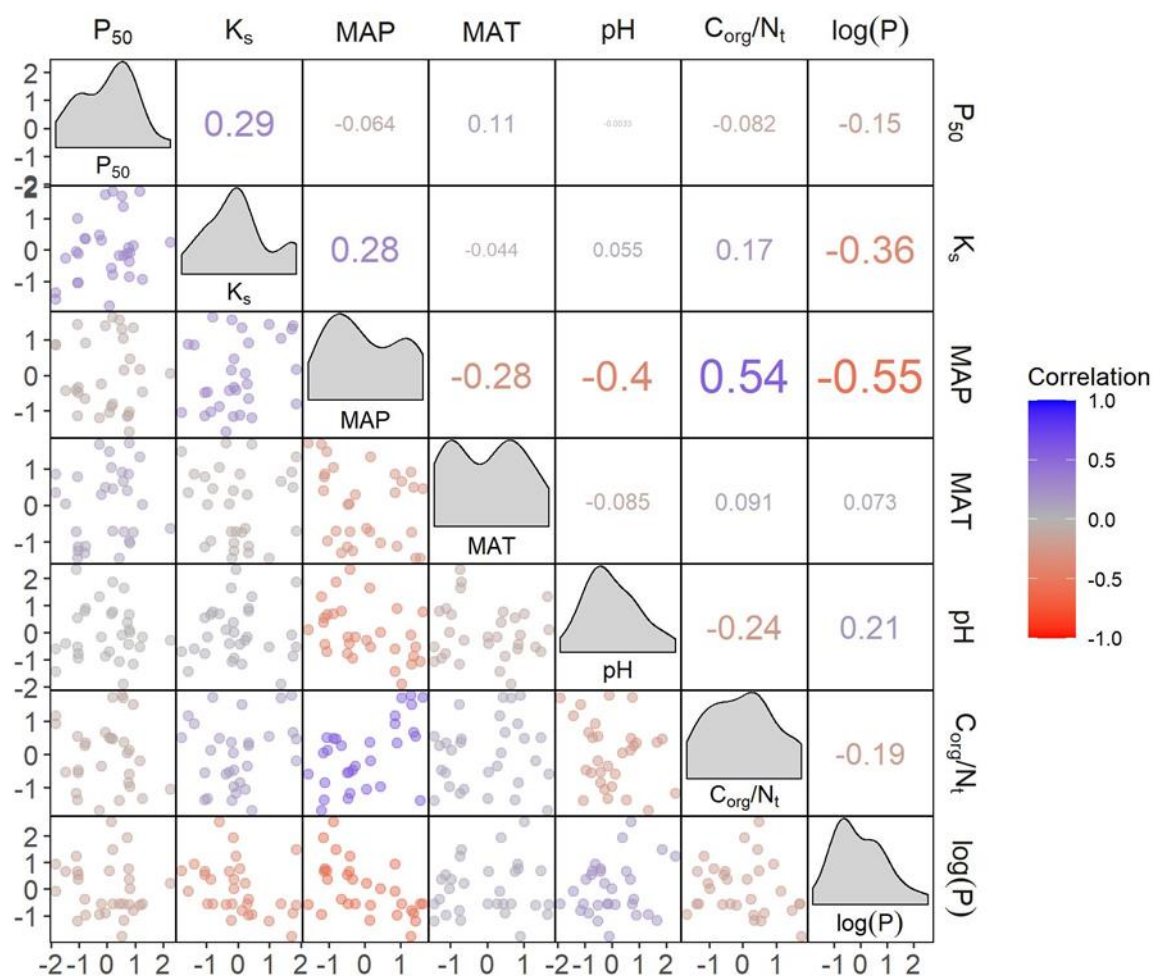
Figure S2.2: Correlation matrix on site level (n = 30) of mean P_{50} values and mean K_s values of European beech branch segments, climatic variables (mean annual precipitation (MAP, 1991-2018) and mean annual temperature (MAT, 1991 – 2018)) and soil variables (pH value, organic carbon to total nitrogen ratio (C_{org}/N_t), and phosphor content (P, log-transformed)). Values are scaled by the standard deviation and centred around zero. The lower triangle depicts the variables from x- and y-axis in relation, the upper triangle shows the correlation strength (Pearson's *r*) and the plot diagonal shows density plots of the corresponding variables.
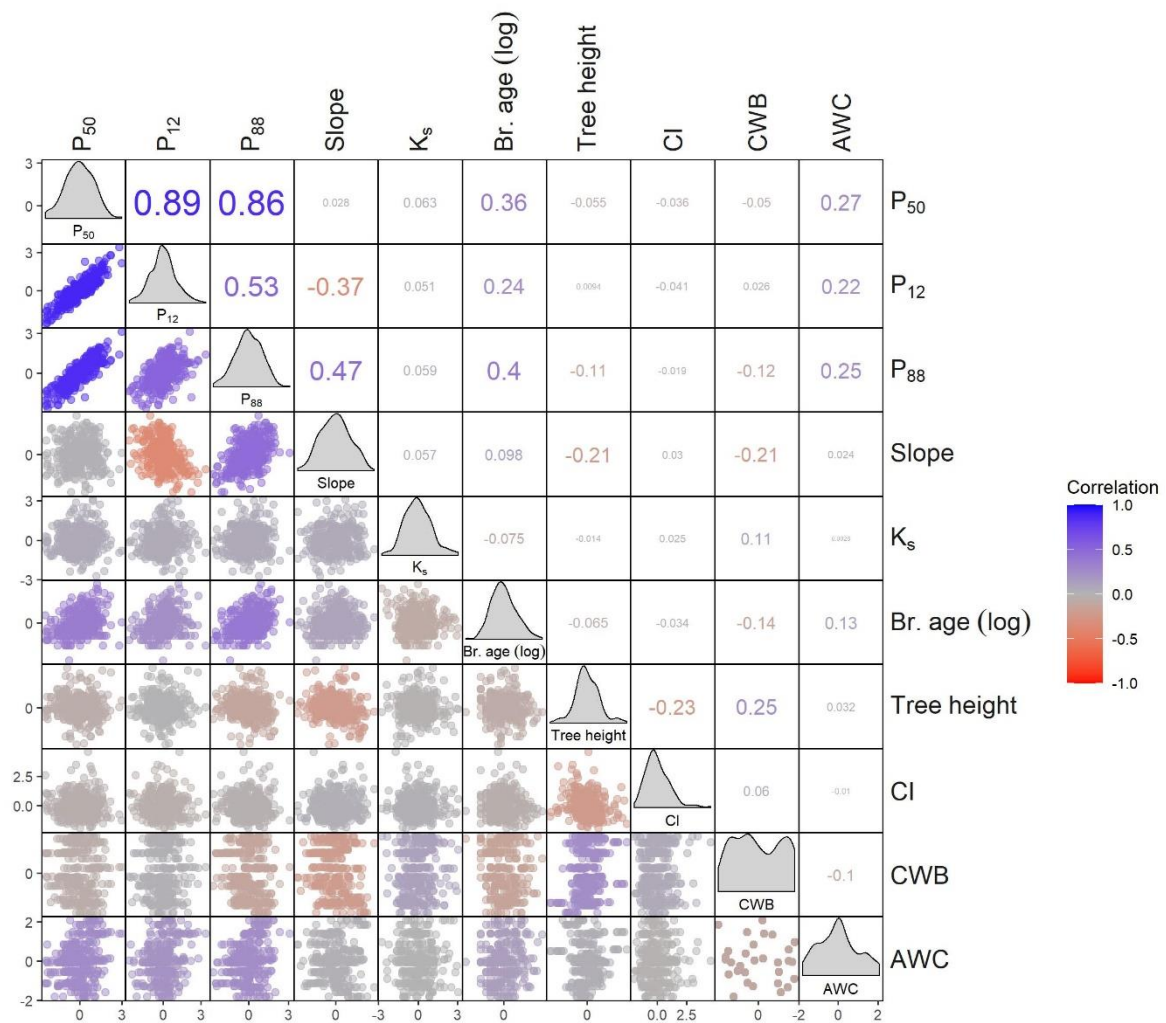
Figure S2.3: Correlation matrix of P_{50}-, P_{12}-, P_{88}-values, slope of the vulnerability curves, hydraulic conductivity (K_s) age of branch segment (Br. age; log transformed), tree height, Hegyi competition index (CI), climatic water balance (CWB) and plant-available soil water capacity (AWC). For data on tree level: n = 300, except for CI: n = 298 and for data on site level: n = 30. Values are scaled by the standard deviation and centred around zero. The lower triangle depicts the variables from x- and y-axis in relation, the upper triangle shows the correlation strength (Pearson's r) and the plot diagonal shows density plots of the corresponding variables.
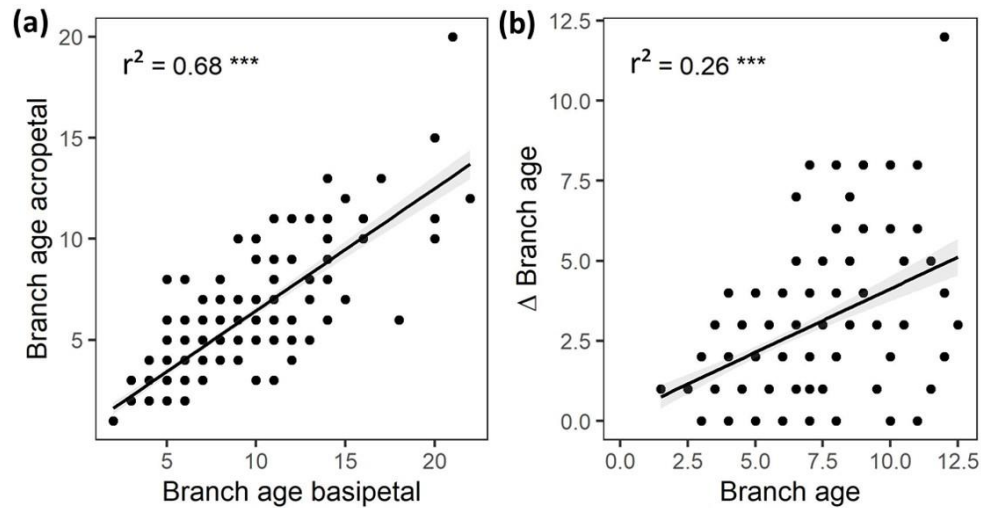
Figure S2.4: (a) Linear regressions of the branch age (years) at the basipetal end on the branch age of the acropetal end and (b) of the mean branch age (mean of acropetal and basipetal age) on the difference of the age between the two ends. The linear regression line with its 95% confidence intervals is shown. Asterisks indicate the level of significance (***, $p < 0.001$).
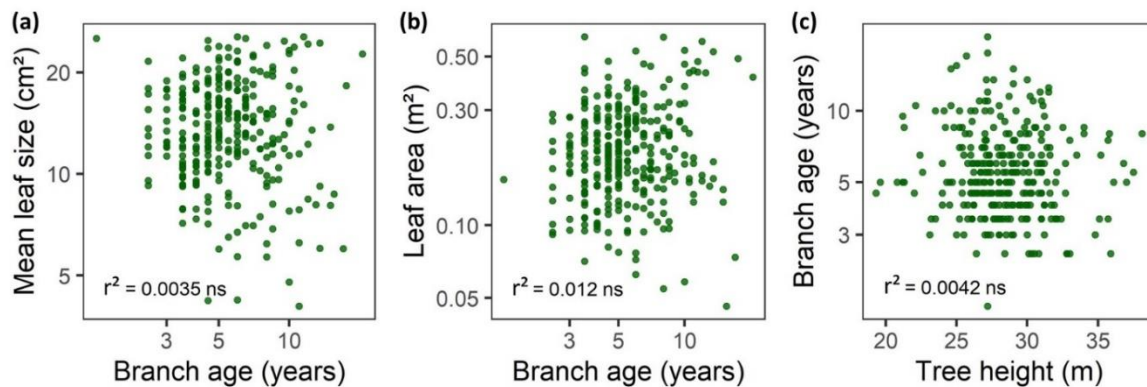
Figure S2.5: (a) Linear regressions of mean branch age on mean leaf size of the corresponding branch or (b) leaf area of the corresponding branch and (c) linear regression of tree height on branch age. Given are R^2-values and level of significance (ns = non-significant relationship).
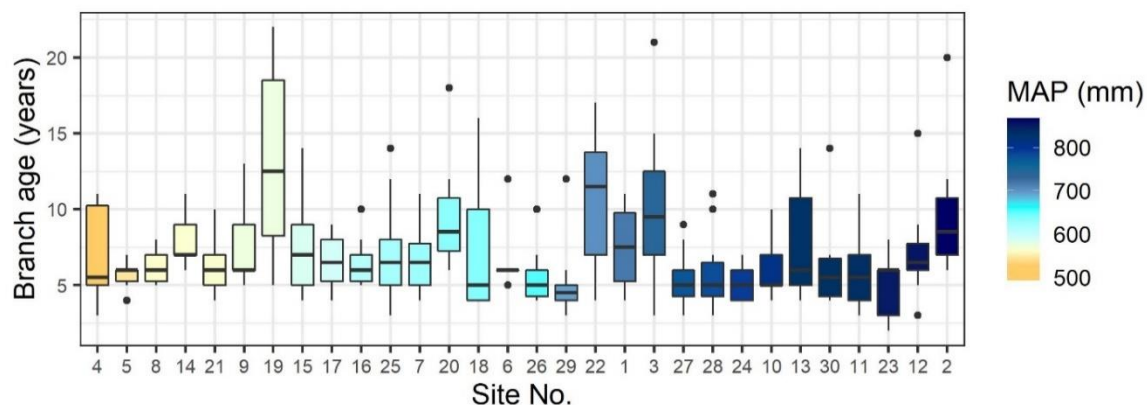
Figure S2.6: Box plots visualizing the age of the investigated branch segments of European beech in the 30 stands (10 trees per stand). Colours indicate mean annual precipitation (MAP, 1991-2018, data provided by DWD) of the different sites (see Figure 2.1).

References

Adams HD, Zeppel MJB, Anderegg WRL, Hartmann H, Landhäusser SM, Tissue DT, Huxman TE, Hudson PJ, Franz TE, Allen CD *et al.* 2017. A multi-species synthesis of physiological mechanisms in drought-induced tree mortality. *Nature Ecology & Evolution* **1**: 1285–1291.

Allen CD, Breshears DD, McDowell NG. 2015. On underestimation of global vulnerability to tree mortality and forest die-off from hotter drought in the Anthropocene. *Ecosphere* **6**: art129.

Allen CD, Macalady AK, Chenchouni H, Bachelet D, McDowell N, Vennetier M, Kitzberger T, Rigling A, Breshears DD, Hogg EH *et al.* 2010. A global overview of drought and heat-induced tree mortality reveals emerging climate change risks for forests. *Forest Ecology and Management* **259**: 660–684.

Ambrose AR, Baxter WL, Wong CS, Burgess SS, Williams CB, Næsborg RR, Koch GW, Dawson TE. 2016. Hydraulic constraints modify optimal photosynthetic profiles in giant sequoia trees. *Oecologia* **182**:713–730.

Ambrose AR, Sillett SC, Dawson TE. 2009. Effects of tree height on branch hydraulics, leaf structure and gas exchange in California redwoods. *Plant, Cell & Environment* **32**:743–757.

Anderegg WRL, Klein T, Bartlett M, Sack L, Pellegrini AFA, Choat B, Jansen S. 2016. Meta-analysis reveals that hydraulic traits explain cross-species patterns of drought-induced tree mortality across the globe. *PNAS* **113**: 5024–5029.

Anfodillo T, Petit G, Crivellaro A. 2013. Axial conduit widening in woody species: a still neglected anatomical pattern. *IAWA Journal* **34**:352–364.

Aranda I, Bahamonde HA, Sánchez-Gómez D. 2017. Intra-population variability in the drought response of a beech (*Fagus sylvatica* L.) population in the southwest of Europe. *Tree Physiology* **37**: 938–949.

Aranda I, Cano FJ, Gascó A, Cochard H, Nardini A, Mancha JA, López R, Sánchez-Gómez D. 2015. Variation in photosynthetic performance and hydraulic architecture across European beech (*Fagus sylvatica* L.) populations supports the case for local adaptation to water stress. *Tree Physiology* **35**: 34–46.

Awad H, Barigah T, Badel E, Cochard H, Herbette S. 2010. Poplar vulnerability to xylem cavitation acclimates to drier soil conditions. *Physiologia Plantarum* **139**: 280–288.

Bartón K. 2020. MuMIn: Multi-Model Inference. https://CRAN.R-project.org/package=MuMIn.

Bates D, Mächler M, Bolker B, Walker S. 2015. Fitting linear mixed-effects models using lme4. *Journal of Statistical Software* **67**: 1–48.

Baudis M, Ellerbrock RH, Felsmann K, Gessler A, Gimbel K, Kayler Z, Puhlmann H, Ulrich A, Weiler M, Welk E *et al*. 2014. Intraspecific differences in responses to rainshelter-induced drought and competition of *Fagus sylvatica* L. across Germany. *Forest Ecology and Management* **330**: 283–293.

Beikircher B, Mayr S. 2009. Intraspecific differences in drought tolerance and acclimation in hydraulics of *Ligustrum vulgare* and *Viburnum lantana*. *Tree Physiology* **29**: 765–775.

Berzaghi F, Wright IJ, Kramer K, Oddou-Muratorio S, Bohn FJ, Reyer CPO, Sabaté S, Sanders TGM, Hartig F. 2020. Towards a new generation of trait-flexible vegetation models. *Trends in Ecology & Evolution* **35**: 191–205.

Bittencourt PR, Oliveira RS, da Costa AC, Giles AL, Coughlin I, Costa PB, Bartholomew DC, Ferreira LV, Vasconcelos SS, Barros FV *et al*. 2020. Amazonia trees have limited capacity to acclimate plant hydraulic properties in response to long-term drought. *Global Change Biology* **26**:3569–3584.

Boessenkool B. 2020. rdwd: Select and download climate data from 'DWD' (German Weather Service). https://CRAN.R-project.org/package=rdwd.

Bolte A, Czajkowski T, Kompa T. 2007. The north-eastern distribution range of European beech − A review. *Forestry* **80**: 413–429.

Braun S, Witte LC de, **Hopf SE. 2020.** Auswirkungen des Trockensommers 2018 auf Flächen der Interkantonalen Walddauerbeobachtung. *Schweizerische Zeitschrift für Forstwesen* **171**: 270–280.

Bresson CC, Vitasse Y, Kremer A, Delzon S. 2011. To what extent is altitudinal variation of functional traits driven by genetic adaptation in European oak and beech? *Tree Physiology* **31**: 1164–1174.

Brodribb TJ, Powers J, Cochard H, Choat B. 2020. Hanging by a thread? Forests and drought. *Science* **368**: 261–266.

Buiteveld J, Vendramin GG, Leonardi S, Kramer K, Geburek T. 2007. Genetic diversity and differentiation in European beech (*Fagus sylvatica* L.) stands differing in management history. *Forest Ecology and Management* **247**: 98–106.

Burgess SS, Pittermann J, Dawson TE. 2006. Hydraulic efficiency and safety of branch xylem increases with height in *Sequoia sempervirens* (D. Don) crowns. *Plant Cell & Environment* **29**:229–239.

Carminati A, Javaux M. 2020. Soil rather than xylem vulnerability controls stomatal response to drought. *Trends in Plant Science* **25**: 868–880.

Carsjens C, Ngoc QN, Guzy J, Knutzen F, Meier IC, Müller M, Finkeldey R, Leuschner C, Polle A. 2014. Intra-specific variations in expression of stress-related genes in beech progenies are stronger than drought-induced responses. *Tree Physiology* **34**: 1348–1361.

Choat B, Brodribb TJ, Brodersen CR, Duursma RA, López R, Medlyn BE. 2018. Triggers of tree mortality under drought. *Nature* **558**: 531–539.

Choat B, Sack L, Holbrook NM. 2007. Diversity of hydraulic traits in nine *Cordia* species growing in tropical forests with contrasting precipitation. *New Phytologist* **175**: 686–698.

Christensen-Dalsgaard KK, Tyree MT. 2014. Frost fatigue and spring recovery of xylem vessels in three diffuse-porous trees in situ. *Plant, Cell and Environment* **37**: 1074–1085.

Cochard H, Damour G, Bodet C, Tharwat I, Poirier M, Améglio T. 2005. Evaluation of a new centrifuge technique for rapid generation of xylem vulnerability curves. *Physiologia Plantarum* **124**: 410–418.

Cochard H, Lemoine D, Dreyer E. 1999. The effects of acclimation to sunlight on the xylem vulnerability to embolism in *Fagus sylvatica* L. *Plant, Cell & Environment* **22**: 101–108.

Correia DLP, Bouchard M, Filotas É, Raulier F. 2019. Disentangling the effect of drought on stand mortality and productivity in northern temperate and boreal forests. *Journal of Applied Ecology* **56**: 758–768.

Dai Y, Wang L, Wan X. 2020. Frost fatigue and its spring recovery of xylem conduits in ring-porous, diffuse-porous, and coniferous species in situ. *Plant Physiology and Biochemistry* **146**: 177–186.

Das A, Battles J, Stephenson NL, van Mantgem PJ. 2011. The contribution of competition to tree mortality in old-growth coniferous forests. *Forest Ecology and Management* **261**: 1203–1213.

Dormann CF, Elith J, Bacher S, Buchmann C, Carl G, Carré G, Marquéz JRG, Gruber B, Lafourcade B, Leitão PJ, et al. 2013. Collinearity: a review of methods to deal with it and a simulation study evaluating their performance. *Ecography* **36**: 27–46.

Fajardo A, Martínez-Pérez C, Cervantes-Alcayde MA, Olson ME. 2020. Stem length, not climate, controls vessel diameter in two trees species across a sharp precipitation gradient. *New Phytologist* **225**:2347–2355.

Fuchs S, Leuschner C, Link RM, Schuldt B. 2021. Hydraulic variability of three temperate broadleaf tree species along a water availability gradient in central Europe. *New Phytologist* **231**:1387–1400.

Fukuda K, Kawaguchi D, Aihara T, Ogasa MY, Miki NH, Haishi T, Umebayashi T. 2015. Vulnerability to cavitation differs between current-year and older xylem: non-destructive observation with a compact magnetic resonance imaging system of two deciduous diffuse-porous species. *Plant, Cell & Environment* **38**: 2508–2518.

Geßler A, Keitel C, Kreuzwieser J, Matyssek R, Seiler W, Rennenberg H. 2006. Potential risks for European beech (*Fagus sylvatica* L.) in a changing climate. *Trees* **21**: 1–11.

Gleason SM, Westoby M, Jansen S, Choat B, Hacke UG, Pratt RB, Bhaskar R, Brodribb TJ, Bucci SJ, Cao K-F *et al.* 2016. Weak tradeoff between xylem safety and xylem-specific hydraulic efficiency across the world's woody plant species. *New Phytologist* **209**: 123–136.

González-Muñoz N, Sterck F, Torres-Ruiz JM, Petit G, Cochard H, Arx G von, Lintunen A, Caldeira MC, Capdeville G, Copini P *et al.* 2018. Quantifying in situ phenotypic variability in the hydraulic properties of four tree species across their distribution range in Europe. *PLOS ONE* **13**: e0196075.

Hacke UG, Sperry JS. 2001. Functional and ecological xylem anatomy. *Perspectives in Plant Ecology, Evolution and Systematics* **4**: 97–115.

Hacke UG, Spicer R, Schreiber SG, Plavcová L. 2017. An ecophysiological and developmental perspective on variation in vessel diameter. *Plant, Cell and Environment* **40**: 831–845.

Hacke UG, Stiller V, Sperry JS, Pittermann J, McCulloh KA. 2001. Cavitation fatigue. Embolism and refilling cycles can weaken the cavitation resistance of xylem. *Plant Physiology* **125**: 779–786.

Hajek P, Kurjak D, Wühlisch G von, Delzon S, Schuldt B. 2016. Intraspecific variation in wood anatomical, hydraulic, and foliar traits in ten European beech provenances differing in growth yield. *Frontiers in Plant Science* **7**: 791.

Hajek P, Link RM, Nock C, Bauhus J, Gebauer T, Gessler A, Kovach K, Messier C, Paquette A, Saurer M *et al.* 2020. Mutually inclusive mechanisms of drought-induced tree mortality. *bioRxiv*: 2020.12.17.423038.

Hajek P, Seidel D, Leuschner C. **2015**. Mechanical abrasion, and not competition for light, is the dominant canopy interaction in a temperate mixed forest. *Forest Ecology and Management* **348**: 108–116.

Hartmann H, Moura CF, Anderegg WRL, Ruehr NK, Salmon Y, Allen CD, Arndt SK, Breshears DD, Davi H, Galbraith D *et al.* 2018. Research frontiers for improving our understanding of drought-induced tree and forest mortality. *New Phytologist* **218**: 15–28.

Hegyi F. 1974. A simulation model for managing jack pine stands. In: Fries J ed. *Growth models for tree and stand simulation.* Royal College of Forestry, Stockholm: 74–90.

Herbette S, Charrier O, Cochard H, Barigah TS. 2020. Delayed effect of drought on the xylem vulnerability to embolism in *Fagus sylvatica*. *Canadian Journal of Forest Research*. doi: 10.1139/cjfr-2020-0256.

Herbette S, Wortemann R, Awad H, Huc R, Cochard H, Barigah TS. 2010. Insights into xylem vulnerability to cavitation in *Fagus sylvatica* L.: phenotypic and environmental sources of variability. *Tree Physiology* **30**: 1448–1455.

Hertel D, Strecker T, Müller-Haubold H, Leuschner C. 2013. Fine root biomass and dynamics in beech forests across a precipitation gradient - is optimal resource partitioning theory applicable to water-limited mature trees? *Journal of Ecology* **101**: 1183–1200.

Kaack L, Weber M, Isasa E, Karimi Z, Li S, Pereira L, Trabi CL, Zhang Y, Schenk HJ, Schuldt B *et al.* 2021. Pore constrictions in intervessel pit membranes reduce the risk of embolism spreading in angiosperm xylem. *New Phytologist*, accepted. doi: 10.1111/nph.17282.

Knipfer T, Reyes C, Earles JM, Berry ZC, Johnson DM, Brodersen CR, McElrone AJ. 2019. Spatiotemporal coupling of vessel cavitation and discharge of stored xylem water in a tree sapling. *Plant Physiology* **179**: 1658–1668.

Koch GW, Sillett SC, Jennings GM, Davis SD. 2004. The limits to tree height. *Nature* **428**:851–854.

Kuznetsova A, Brockhoff PB, Christensen RHB. 2017. lmerTest package: tests in linear mixed effects models. *Journal of Statistical Software* **82**: 1–26.

Lakatos F, Molnár M. 2009. Mass mortality of beech (*Fagus sylvatica* L.) in South-West Hungary. *Acta Silvatica et Lignaria Hungarica*: 75–82.

Lamy J-B, Delzon S, Bouche PS, Alia R, Vendramin GG, Cochard H, Plomion C. 2014. Limited genetic variability and phenotypic plasticity detected for cavitation resistance in a Mediterranean pine. *New Phytologist* **201**: 874–886.

Larter M, Pfautsch S, Domec J-C, Trueba S, Nagalingum N, Delzon S. 2017. Aridity drove the evolution of extreme embolism resistance and the radiation of conifer genus *Callitris*. *New Phytologist* **215**: 97–112.

Lemaire C, Quilichini Y, Brunel-Michac N, Santini J, Berti L, Cartailler J, Conchon P, Badel É, Herbette S. 2020. Plasticity of the xylem vulnerability to embolism in poplar relies on quantitative pit properties rather than on pit structure. *bioRxiv*. doi: 10.1101/2020.05.14.096222.

Lemoine D, Cochard H, Granier A. 2002. Within crown variation in hydraulic architecture in beech (*Fagus sylvatica* L): evidence for a stomatal control of xylem embolism. *Annals of Forest Science* **59**: 19–27.

Leuschner C. 2020. Drought response of European beech (*Fagus sylvatica* L.)—A review. *Perspectives in Plant Ecology, Evolution and Systematics* **47**: 125576.

Leuschner C, Ellenberg H. **2017.** Ecology of Central European Forests. Cham: Springer.

Li Q, Zhao M, Wang N, Liu S, Wang J, Zhang W, Yang N, Fan P, Wang R, Wang H *et al.* 2020. Water use strategies and drought intensity define the relative contributions of hydraulic failure and carbohydrate depletion during seedling mortality. *Plant Physiology and Biochemistry* **153**: 106–118.

Li X, Blackman CJ, Choat B, Duursma RA, Rymer PD, Medlyn BE, Tissue DT. 2018. Tree hydraulic traits are coordinated and strongly linked to climate-of-origin across a rainfall gradient. *Plant, Cell & Environment* **41**: 646–660.

Link RM. 2020. corrmorant: Flexible correlation matrices based on 'ggplot2'. R package version 0.0.0.9007. http://github.com/r-link/corrmorant.

Liu H, Gleason SM, Hao G, Hua L, He P, Goldstein G, Ye Q. 2019. Hydraulic traits are coordinated with maximum plant height at the global scale. *Science Advances* **5**:eaav1332.

Lübbe T, Schuldt B, Leuschner C. 2017. Acclimation of leaf water status and stem hydraulics to drought and tree neighbourhood: alternative strategies among the saplings of five temperate deciduous tree species. *Tree Physiology* **37**: 456–468.

Lübbe T, Lamarque LL, Delzon S, Torres Ruiz JM, Burlett R, Leuschner C, Schuldt B. 2022. High variation in hydraulic efficiency but not xylem safety between roots and branches in four temperate broad-leaved tree species. *Functional Ecology*, accepted.

Maherali H, Moura CE, Caldeira MC, Willson CJ, Jackson RB. 2006. Functional coordination between leaf gas exchange and vulnerability to xylem cavitation in temperate forest trees. *Plant, Cell & Environment* **29**: 571–583.

Maherali H, Pockman WT, Jackson RB. 2004. Adaptive variation in the vulnerability of woody plants to xylem cavitation. *Ecology* **85**: 2184–2199.

Martínez-Vilalta J, Cochard H, Mencuccini M, Sterck F, Herrero A, Korhonen JFJ, Llorens P, Nikinmaa E, Nolè A, Poyatos R *et al.* 2009. Hydraulic adjustment of Scots pine across Europe. *New Phytologist* **184**: 353–364.

Martin-StPaul NK, Limousin J-M, Vogt-Schilb H, Rodríguez-Calcerrada J, Rambal S, Longepierre D, Misson L. 2013. The temporal response to drought in a Mediterranean evergreen tree: comparing a regional precipitation gradient and a throughfall exclusion experiment. *Global Change Biology* **19**: 2413–2426.

McDowell NG, Adams HD, Bailey JD, Hess M, Kolb TE. 2006. Homeostatic maintenance of Ponderosa pine gas exchange in response to stand density changes. *Ecological Applications* **16**: 1164–1182.

Meier IC, Leuschner C. 2008. Genotypic variation and phenotypic plasticity in the drought response of fine roots of European beech. *Tree Physiology* **28**: 297–309.

Meixner M, Tomasella M, Foerst P, Windt CW. 2020. A small-scale MRI scanner and complementary imaging method to visualize and quantify xylem embolism formation. *New Phytologist* **226**: 1517–1529.

Moreno G, Cubera E. 2008. Impact of stand density on water status and leaf gas exchange in *Quercus ilex*. *Forest Ecology and Management* **254**: 74–84.

Müller-Haubold H, Hertel D, Seidel D, Knutzen F, Leuschner C. 2013. Climate responses of aboveground productivity and allocation in *Fagus sylvatica*: A transect study in mature forests. *Ecosystems* **16**: 1498–1516.

Nakagawa S, Johnson PCD, Schielzeth H. 2017. The coefficient of determination R^2 and intra-class correlation coefficient from generalized linear mixed-effects models revisited and expanded. *Journal of the Royal Society* **14**. doi: 10.1098/rsif.2017.0213.

Nicotra AB, Atkin OK, Bonser SP, Davidson AM, Finnegan EJ, Mathesius U, Poot P, Purugganan MD, Richards CL, Valladares F, van Kleunen M. 2010. Plant phenotypic plasticity in a changing climate. *Trends in Plant Science* **15**:684–692.

Nguyen QN, Polle A, Pena R. 2017. Intraspecific variations in drought response and fitness traits of beech *(Fagus sylvatica* L.) seedlings from three provenances differing in annual precipitation. *Trees* **31**: 1215–1225.

Noyer E, Lachenbruch B, Dlouhá J, Collet C, Ruelle J, Ningre F, Fournier M. 2017. Xylem traits in European beech (*Fagus sylvatica* L.) display a large plasticity in response to canopy release. *Annals of Forest Science* **74**: 1–11.

O'Brien MJ, Engelbrecht BMJ, Joswig J, Pereyra G, Schuldt B, Jansen S, Kattge J, Landhäusser SM, Levick SR, Preisler Y *et al.* 2017. A synthesis of tree functional traits related to drought-induced mortality in forests across climatic zones. *Journal of Applied Ecology* **54**: 1669–1686.

Ogle K, Barber JJ, Willson C, Thompson B. 2009. Hierarchical statistical modeling of xylem vulnerability to cavitation. *New Phytologist* **182**: 541–554.

Olson ME. 2019. Plant evolutionary ecology in the age of the extended evolutionary synthesis. *Integrative and Comparative Biology* **59**:493–502.

Olson ME, Anfodillo T, Rosell JA, Martínez-Méndez N. 2020. Across climates and species, higher vapour pressure deficit is associated with wider vessels for plants of the same height. *Plant Cell & Environment* **43**:3068–3080.

Olson ME, Anfodillo T, Gleason SM, McCulloh KA. 2021. Tip-to-base xylem conduit widening as an adaptation: causes, consequences, and empirical priorities. *New Phytologist* **229**:1877–1893.

Olson ME, Anfodillo T, Rosell JA, Petit G, Crivellaro A, Isnard S, León-Gómez C, Alvarado-Cárdenas LO, Castorena M. 2014. Universal hydraulics of the flowering plants: vessel diameter scales with stem length across angiosperm lineages, habits and climates. *Ecology Letters* **17**:988–997.

Olson ME, Soriano D, Rosell JA, Anfodillo T, Donoghue MJ, Edwards EJ, León-Gómez C, Dawson T, Camarero Martínez JJ, Castorena M, Echeverría A, Espinosa CI, Fajardo A, Gazol A, Isnard S, Lima RS, Marcati CR, Méndez-Alonzo R. 2018. Plant height and hydraulic vulnerability to drought and cold. *PNAS* **115**:7551–7556

Pammenter NW, Vander Willigen C. 1998. A mathematical and statistical analysis of the curves illustrating vulnerability of xylem to cavitation. *Tree Physiology* **18**: 589–593.

Powers JS, Vargas G G, Brodribb TJ, Schwartz NB, Pérez-Aviles D, Smith-Martin CM, Becknell JM, Aureli F, Blanco R, Calderón-Morales E *et al.* 2020. A catastrophic tropical drought kills hydraulically vulnerable tree species. *Global Change Biology* **26**: 3122–3133.

R. Core Team. 2019. R: A language and environment for statistical computing. Vienna, Austria. https://www.R-project.org/.

Rehschuh R, Mette T, Menzel A, Buras A. 2017. Soil properties affect the drought susceptibility of Norway spruce. *Dendrochronologia* **45**: 81–89.

Renne RR, Schlaepfer DR, Palmquist KA, Bradford JB, Burke IC, Lauenroth WK. 2019. Soil and stand structure explain shrub mortality patterns following global change-type drought and extreme precipitation. *Ecology* **100**: e02889.

Rennenberg H, Seiler W, Matyssek R, Gessler A, Kreuzwieser J. 2004. Die Buche (*Fagus sylvatica* L.) - ein Waldbaum ohne Zukunft im südlichen Mitteleuropa? *Allgemeine Forst und Jagdzeitung* **175**: 210.

Rosas T, Mencuccini M, Barba J, Cochard H, Saura-Mas S, Martínez-Vilalta J. 2019. Adjustments and coordination of hydraulic, leaf and stem traits along a water availability gradient. *New Phytologist* **223**: 632–646.

Rowland L, da Costa ACL, Galbraith DR, Oliveira RS, Binks OJ, Oliveira AAR, Pullen AM, Doughty CE, Metcalfe DB, Vasconcelos SS *et al.* 2015. Death from drought in tropical forests is triggered by hydraulics not carbon starvation. *Nature* **528**: 119–122.

Ruiz-Benito P, Lines ER, Gómez-Aparicio L, Zavala MA, Coomes DA. 2013. Patterns and drivers of tree mortality in Iberian forests: climatic effects are modified by competition. *PLOS ONE* **8**: e56843.

Ryan MG, Phillips N, Bond BJ. 2006. The hydraulic limitation hypothesis revisited. *Plant Cell & Environment* **29**:367–381.

Schenk HJ, Espino S, Romo DM, Nima N, Do AYT, Michaud JM, Papahadjopoulos-Sternberg B, Yang J, Zuo YY, Steppe K *et al.* 2017. Xylem surfactants introduce a new element to the cohesion-tension theory. *Plant Physiology* **173**: 1177–1196.

Schenk HJ, Michaud JM, Mocko K, Espino S, Melendres T, Roth MR, Welti R, Kaack L, Jansen S. **2021**. Lipids in xylem sap of woody plants across the angiosperm phylogeny. *The Plant Journal* **105**: 1477–1494.

Schuldt B, Buras A, Arend M, Vitasse Y, Beierkuhnlein C, Damm A, Gharun M, Grams TEE, Hauck M, Hajek P *et al.* 2020. A first assessment of the impact of the extreme 2018 summer drought on Central European forests. *Basic and Applied Ecology* **45**: 86–103.

Schuldt B, Knutzen F, Delzon S, Jansen S, Müller-Haubold H, Burlett R, Clough Y, Leuschner C. 2016. How adaptable is the hydraulic system of European beech in the face of climate change-related precipitation reduction? *New Phytologist* **210**: 443–458.

Schumann K, Leuschner C, Schuldt B. 2019. Xylem hydraulic safety and efficiency in relation to leaf and wood traits in three temperate *Acer* species differing in habitat preferences. *Trees* **33**: 1475–1490.

Skelton RP, Anderegg LD, Diaz J, Kling MM, Papper P, Lamarque LJ, Delzon S, Dawson TE, Ackerly DD. 2021. Evolutionary relationships between drought-related traits and climate shape large hydraulic safety margins in western North American oaks. *PNAS* **118**, DOI: 10.1073/pnas.2008987118.

Stojnic S, Suchocka M, Benito-Garzón M, Torres-Ruiz JM, Cochard H, Bolte A, Cocozza C, Cvjetkovic B, Luis M de, Martinez-Vilalta J *et al.* 2018. Variation in xylem vulnerability to embolism in European beech from geographically marginal populations. *Tree Physiology* **38**: 173–185.

Tai X, Mackay DS, Anderegg WRL, Sperry JS, Brooks PD. 2017. Plant hydraulics improves and topography mediates prediction of aspen mortality in southwestern USA. *New Phytologist* **213**: 113–127.

Tyree MT, Davis SD, Cochard H. 1994. Biophysical perspectives of xylem evolution: is there a trade-off of hydraulic efficiency for vulnerability to dysfunction? *IAWA Journal* **15**: 335–360.

Tyree MT, Sperry JS. 1989. Vulnerability of xylem to cavitation and embolism. *Annual Review of Plant Physiology and Plant Molecular Biology* **40**: 19–36.

van der Sande MT, Poorter L, Schnitzer SA, Engelbrecht BMJ, Markesteijn L. 2019. The hydraulic efficiency-safety trade-off differs between lianas and trees. *Ecology* **100**: e02666.

van Genuchten MT. 1980. A closed-form equation for predicting the hydraulic conductivity of unsaturated soils. *Soil Science Society of America Journal* **44**: 892–898.

van Genuchten MT, Leij FJ, Yates SR. 1991. The RETC code for quantifying the hydraulic functions of unsaturated soils. Washington, D.C.: Environmental Protection Agency EPA/600/2-91/065.

Waite P-A, Schuldt B, Mathias Link R, Breidenbach N, Triadiati T, Hennings N, Saad A, Leuschner C. 2019. Soil moisture regime and palm height influence embolism resistance in oil palm. *Tree Physiology* **39**: 1696–1712.

Walthert L, Ganthaler A, Mayr S, Saurer M, Waldner P, Walser M, Zweifel R, von Arx G. 2021. From the comfort zone to crown dieback: sequence of physiological stress thresholds in mature European beech trees across progressive drought. *Science of The Total Environment* **753**: 141792.

Weithmann G, Schuldt B, Link RM, Heil D, Hoeber S, John H, Müller-Haubold H, Schüler L-M, Schumann K, Leuschner C. 2022. Leaf trait modification in European beech trees in response to climatic and edaphic drought. *Plant Biology*, in press, DOI: 10.1111/plb.13366.

Wheeler JK, Sperry JS, Hacke UG, Hoang N. 2005. Inter-vessel pitting and cavitation in woody Rosaceae and other vesselled plants: a basis for a safety versus efficiency trade-off in xylem transport. *Plant, Cell and Environment* **28**: 800–812.

Wickham H, Averick M, Bryan J, Chang W, McGowan LD'A, François R, Grolemund G, Hayes A, Henry L, Hester J *et al.* 2019. Welcome to the tidyverse. *Journal of Open Source Software* **4**: 1686.

Woodruff DR, Bond BJ, Meinzer FC. 2004. Does turgor limit growth in tall trees? *Plant Cell & Environment* **27**:229–236.

Woodruff DR, Meinzer FC, Lachenbruch B. 2008. Height-related trends in leaf xylem anatomy and shoot hydraulic characteristics in a tall conifer: safety versus efficiency in water transport. *New Phytologist* **180**:90–99.

Wortemann R, Herbette S, Barigah TS, Fumanal B, Alia R, Ducousso A, Gomory D, Roeckel-Drevet P, Cochard H. 2011. Genotypic variability and phenotypic plasticity of cavitation resistance in *Fagus sylvatica* L. across Europe. *Tree Physiology* **31**: 1175–1182.

Young DJN, Stevens JT, Earles JM, Moore J, Ellis A, Jirka AL, Latimer AM. 2017. Long-term climate and competition explain forest mortality patterns under extreme drought. *Ecology letters* **20**: 78–86.

Zhang W, Feng F, Tyree MT. 2018. Seasonality of cavitation and frost fatigue in *Acer mono* Maxim. *Plant, Cell and Environment* **41**: 1278–1286.

Zimmermann J, Link RM, Hauck M, Leuschner C, Schuldt B. 2021. 60-year record of stem xylem anatomy and related hydraulic modification under increased summer drought in ring- and diffuse-porous temperate broad-leaved tree species. *Trees*, in press. doi: 10.1007/s00468-021-02090-2.

CHAPTER 3

Branch xylem vascular adjustments in European beech in response to decreasing water availability across a precipitation gradient

Greta Weithmann, Sharath Shyamappa Paligi, Bernhard Schuldt, Christoph Leuschner

3.1 Abstract

Crucial for the climate adaptation of trees is a xylem anatomical structure capable of adjusting to changing water regimes. While species comparisons across climate zones have demonstrated anatomical change in response to altered water availability and tree height, less is known about the adaptability of tree vascular systems to increasing water deficits at the intraspecific level. Information on the between-population and within-population variability of xylem traits helps assessing a species' ability to cope with climate change.

We investigated the variability of wood anatomical and related hydraulic traits in terminal branches of European beech (*Fagus sylvatica* L.) trees across a precipitation gradient (520 – 890 mm yr^{-1}) and examined the influence of climatic water balance (CWB), soil water capacity (AWC), neighbourhood competition (CI), tree height, and branch age on these traits. Further, the relationship between xylem anatomical traits and embolism resistance (P_{50}) was tested.

Within-population trait variation was larger than between-population variation. Vessel diameter, lumen-to-sapwood area ratio and potential conductivity of terminal branches decreased with decreasing CWB, but these traits were not affected by AWC, while vessel density increased with an AWC decrease. In contrast, none of the studied anatomical traits were influenced by variation in tree height (21 – 34 m) or CI. Branch age was highly variable (2 – 22 years) despite equal diameter and position in the flow path, suggesting different growth trajectories in the past. Vessel diameter decreased, and vessel density increased, with increasing branch age, reflecting negative annual radial growth trends. While vessel diameter was not related to P_{50}, vessel grouping index and lumen-to-sapwood area ratio showed a weak, though highly significant, positive relationship to P_{50}.

We conclude that the xylem anatomy of terminal tree-top branches in European beech is modified in response to increasing climatic aridity and/or decreasing soil water availability, independent of a tree height effect.

Keywords: branch age, drought acclimation, hydraulic conductivity, precipitation, soil moisture, tree height, vessel diameter.

3.2 Introduction

Water moves from roots to leaves in a network of dead conduit cells in the xylem, which also provides mechanical support and fulfils storage functions (Zimmermann, 1983). The xylem conduit dimensions and the structure of pit membranes determine both hydraulic efficiency and xylem safety and thus are key for understanding the functioning of the hydraulic system. Given current and predicted climatic change, understanding adjustments in the hydraulic architecture across environmental gradients can help to assess the adaptive potential of a species', and information about the degree of intraspecific plasticity is crucial for trait-based modelling approaches.

The anatomical structure of the xylem varies along the flow path from the root to the leaf, it differs between plants of contrasting phylogenetic position, and it may change in response to environmental changes (Wheeler & Baas, 1993; Chenlemuge *et al.,* 2015; Schreiber *et al.,* 2015). Various plant-internal and abiotic factors are influencing xylem anatomy, among them water and nutrient availability, cambial age and flow path length (Maherali *et al.,* 2004; Leal *et al.,* 2007; Lens *et al.,* 2001; Borghetti *et al.,* 2017; Gleason *et al.,* 2018; Li *et al.,* 2019). A major research focus has been the influence of climate and water availability on xylem anatomy, both at the inter-specific and intra-specific levels. A decline in water availability has traditionally been associated with the formation of smaller vessels and higher vessel densities (Carlquist 1977; Baas *et al.,* 1983; Wiemann *et al.,* 1998). Whether this relation can be generalized and holds on the intraspecific level needs to be explored.

While the impact of climatic factors on xylem anatomy is well studied at the interspecific level (Maherali *et al.,* 2004; Hacke *et al.,* 2006; Pfautsch *et al.,* 2016), fewer studies have investigated differences in xylem anatomical traits between different populations or individuals of the same species (Schreiber *et al.,* 2015; Schuldt *et al.,* 2016; Petit *et al.,* 2018; Liang *et al.,* 2019). Pot experiments with drought-exposed tree saplings demonstrate that the extent of xylem anatomical adjustment to drier conditions varies among temperate broadleaf species, with a shift to on average smaller conduits observed in five (*Populus tremula x P. alba, Fagus sylvatica, Tilia cordata, Quercus robur, Q. petraea, Q. pubescens*) out of eight tested species (Awad *et al.,* 2010; Fonti *et al.,* 2013; Lübbe *et al.,* 2017). Comparative branch xylem anatomical studies in mature stands along climatic gradients showed reduced conduit diameters in response to lower precipitation in *P. tremula, F. sylvatica* and *Castanopsis fargesii*, while vessel density was unrelated to the precipitation level in *F. sylvatica, C. fargesii* and *Pinus sylvestris* (Martínez-Vilalta *et al.,* 2009; Schreiber *et al.,* 2015; Schuldt *et*

al., 2016; Liang *et al.,* 2019). In most cases, these studies along climatic gradients did not control for tree height and thus cannot exclude an underlying height effect.

Plant height and flow path length have been identified as other major factors influencing conduit dimensions (Anfodillo *et al.,* 2006; Petit *et al.,* 2010; Olson *et al.,* 2021). Hydraulic optimality theory as expressed in the WBE model (West *et al.,* 1999) predicts a conduit widening from the plant top to the base at a scaling exponent somewhat greater than 0.2 (Anfodillo *et al.,* 2013). Vessel widening in the more basal parts of the plant counteracts the increase in flow resistance with increasing flow path length, as conduit widening reduces the friction against conduit walls per unit flowing water volume. The existing empirical evidence closely agrees with vessel tapering predicted by theory (Anfodillo *et al.,* 2013; Olson *et al.,* 2014; Gleason *et al.,* 2018). Taller trees should therefore produce wider conduits at the stem base than shorter trees, regardless of climate. Within-species variation in mean vessel diameter (*D*) across aridity gradients may thus be the consequence of either increasing water deficiency, which impairs cambial activity and leads to smaller conduits, or caused by reduction in tree size, as tree height is usually negatively correlated with aridity (Liu *et al.,* 2019). It is intensively debated which of the two drivers is more important for the observed reduction in conduit diameters upon increasing aridity (Olson *et al.,* 2018; Lechthaler *et al.,* 2019).

The few studies on intraspecific variation in *D* that controlled for tree height produced contradicting evidence with respect to the importance of tree height or climate. While in the genus *Eucalyptus,* climate was the dominant factor influencing vessel diameter, and tree height had only a minor effect (Pfautsch *et al.,* 2016), a study with the small-statured (<10 m) tree species *Embothrium coccineum* and *Nothofagus antarctica* demonstrated that flow path length, and not climate, is the main driver of a reduction in *D* at the stem base (Fajardo *et al.,* 2020). Sampling different species across climatic zones demonstrated that not only conduit diameters at the stem base, but also vessel diameters of terminal branches at the canopy top, increased with tree height (Olson *et al.,* 2014; Rosell *et al.,* 2017; Olson *et al.,* 2018, 2020). A possible explanation is a height-dependent greater conduit widening in the leaf veins of tall trees, resulting in larger vessels at the petiole base and in terminal twigs as well (Rosell *et al.,* 2017). To our knowledge, the phenomenon of a putative increase in conduit size with increasing precipitation and/or tree height in terminal upper-canopy branches has not been studied at the intraspecific level so far. An unpublished study on mature *F. sylvatica* trees differing in height revealed the opposite relation, i.e. decreasing conduit diameters in terminal tree top twigs with increasing tree height (Mazzocco *et al.,*

unpublished). Thus, intraspecific xylem anatomical studies with tree top twigs of mature trees along climate gradients are needed that consider tree height as a variable in order to distinguish between height, climate and possible age (ontogenetic) effects.

Besides tree height and climate, cambial age may also be a factor influencing conduit size and distribution in the xylem (Li *et al.,* 2019; Rodriguez-Zaccaro *et al.,* 2019). Studies in various broadleaf tree species have shown that conduit size increases linearly with cambial age during the first ten to 20 years of a tree's lifetime, but tend to remain more or less constant after this age threshold (Gartner *et al.,* 1997; Leal *et al.,* 2007; Fan *et al.,* 2009; Zhao, 2015). Similarly, a close linear positive relation between root diameter, and thus age, and mean vessel diameter was observed in *F. sylvatica* small-diameter roots (Kirfel *et al.,* 2017). Various hypotheses have been formulated to explain radial patterns in xylem anatomy in tree trunks and branches, which address the changing hydraulic and mechanical demands of the growing tree during its ontogeny (Lachenbruch *et al.,* 2011). An important fact to be considered is that cambial age is closely linked to the position on the flow path, with age decreasing towards the tree tip. The increase in tree height with ontogenetic development could thus possibly be a more influential driver of changes in conduit size than cambial age itself (Carrer *et al.,* 2015).

The consistent change of vessel properties with cambial age and flow path length is most plausibly explained by concentration gradients of auxin and other plant hormones, notably gibberellins, cytokinins and ethylene (Aloni, 2015; Hacke *et al.,* 2017). Auxin is a chemical signal, which is produced primarily in young leaves and transported through the vascular system, with concentrations generally decreasing from the apex to the stem base (Aloni & Zimmermann, 1983; Aloni, 2001). Plant cell expansion is a turgor-driven process, in which cell wall extensibility is controlled by auxin and other agents, and cambial cell turgor is closely related to overall plant water status. Therefore, conduit size in the xylem is to a certain extent regulated by water availability during the period of cell expansion as shown for *Pinus sylvestris* (Cabon *et al.,* 2020) and *Fagus sylvatica* (Sass & Eckstein 1995; Zimmermann *et al.,* 2021). In correspondence, height-dependent variation in cell expansion in tall Douglas-fir trees was shown to match the vertical turgor gradient, which results from friction and gravity forces (Woodruff *et al.,* 2004).

Xylem anatomy, which is determined by various abiotic and biotic factors, exerts a major control over the conductance of the flow path. Hydraulic efficiency has frequently been suggested to relate negatively to hydraulic safety, but this assumption is mostly based on evidence from interspecific comparisons, and it may not be generalizable (Hacke *et al.,*

2017). Intraspecific studies found wide conduits to be more susceptible to cavitation-related drought stress in *Populus* (Awad *et al.,* 2010; Hajek *et al.,* 2014), but a dependence of vulnerability on conduit diameter has not been confirmed in other intraspecific studies (Burgess *et al.,* 2006; Martínez-Vilalta *et al.,* 2009; Fichot *et al.,* 2010, Schumann *et al.,* 2019) including cross-population studies in *F. sylvatica* (Schuldt *et al.,* 2016; Hajek *et al.,* 2016). While vessel density seems not to be associated with hydraulic safety in most studies (Lens *et al.,* 2011; Ogasa *et al.,* 2013; Hajek *et al.,* 2014; but see Schuldt *et al.,* 2016), a higher vessel grouping index has been found to be tightly linked to greater embolism resistance in *Acer* (Lens *et al.,* 2011) and *Populus* species (Lemaire *et al.,* 2020). Contradicting results were obtained by Loepfe *et al.* (2007) who demonstrated higher vulnerability to embolism with increasing connectivity of the xylem network. Recently, Kaack *et al.* (2021) demonstrated that embolism resistance seems primarily determined by the size of pore constrictions in pit membranes, which is related to pit membrane thickness and to a lesser extent to the number of pits per vessel, suggesting that embolism resistance may be largely uncoupled from hydraulic efficiency.

To fill the knowledge gap with respect to intraspecific variation in the anatomy of tree-top branch xylem, we conducted a comparative study in 30 mature *F. sylvatica* forests across a precipitation gradient, examining the influence of climatic and edaphic aridity, tree height, and branch age on xylem anatomy. We expected that the anatomical traits vessel diameter, vessel density, vessel grouping index, vessel lumen fraction and related potential hydraulic conductivity are sensitive to increasing climatic and/or edaphic aridity, i.e. reduced precipitation and lower soil water storage capacity. As water availability may also depend on competition with neighbours, we further included a measure of competition intensity in the neighbourhood of the target tree in our analysis. We hypothesized that (i) water availability (characterized by climatic water balance, soil water storage capacity and competition intensity), (ii) tree height and thus flow path length, and (iii) branch age are jointly affecting the studied xylem anatomical traits of uppermost canopy branches. We further assumed that (iv) vessel properties with association to the number of pits per xylem cross-sectional area, such as lumen-to-sapwood area ratio and vessel grouping index, are linked to observed differences in embolism resistance. To test the last hypothesis, the results of this study were related to the findings of an accompanying investigation on the embolism resistance of the studied trees (Weithmann *et al.,* 2022).

3.3 Methods

3.3.1 Study sites and water availability

The study was conducted on mature beech (*Fagus sylvatica*) trees in 30 stands located in the lowlands of northern Germany between the Dutch border in the west and the Polish border in the east (Figure S3.1). The climate is cool temperate with mean annual temperatures between 9.0 and 10.0 °C and with a west-east gradient in precipitation and climate continentality (Table 3.1). Long-term mean annual precipitation (MAP) ranges from 522 mm yr^{-1} in the south-east (site 4) to 886 mm yr^{-1} in the north-west (site 12). All beech stands are stocking on deep, mostly nutrient-poor sandy soils on deposits of the penultimate (Saalian) and last glacial (Weichselian) at 19 m to 159 m a.s.l. Mean tree height of the stands ranged from 21 m to 34 m.

Climate data were extracted for the period 1991–2018 from the Climate Data Centre (CDC) of the German Weather Service (DWD, Deutscher Wetterdienst, Offenbach, https://opendata.dwd.de/, accessed 2019-11-14) using the R package rdwd v. 1.2.0 (Boessenkool, 2020). From extrapolated 1 km-gridded data, precipitation and potential evapotranspiration data (calculated after Penman-Monteith and with a hydraulic soil water balance model) were extracted and then used to calculate the monthly cumulative water balance (CWB, mm month^{-1}) as the difference between precipitation and potential evapotranspiration. As MAP and CWB were closely related to mean summer and mean growing season precipitation, we decided to use the whole-year data for our analyses.

In addition to precipitation and CWB, an estimate of soil water availability as an important determinant of drought stress exposure (Piedallu *et al.*, 2013) was assessed, using the soil storage capacity for plant-available water (AWC, mm) of the soil profiles as a measure. AWC was calculated as the water content hold in the soil between -60 hPa (field capacity) and the conventional permanent wilting point (-1.5 MPa). Soil samples were collected at the three walls of one pit per stand at 0–10 cm, 10–30 cm and 30–60 cm depth, resulting in three samples per stand. With a PARIO Soil Particle Size Analyser (METER group, Munich, Germany), the contents of sand, silt and clay were determined through sieving and differential sedimentation. From the measured particle size distribution and soil bulk density, soil hydraulic properties (the so-called van Genuchten (1980) parameters) were estimated by applying pedotransfer functions according to Schaap *et al.,* (2001). The calculations were conducted with the module "Rosetta light", implemented in the Software RETC (version 6.02, van Genuchten *et al.,* 1991). The volumetric water contents at -1.5 MPa (pF 4.2) and -

60 hPa (pF 1.8) were then retrieved from the estimated retention curves. Soil AWC was then calculated for the three depth layers to 60 cm and extrapolated to a standard depth of 100 cm, assuming a homogenous soil particle composition in the 30–100 cm layer.

Soil depth was in all profiles >120 cm and soil cores taken at greater depth showed no obvious differences in soil texture in the 30–100 cm depth range. In addition, we determined soil pH, the C_{org}/N_{total} ratio and the total nitrogen and total phosphorus contents of the soil through gas chromatography (CN elemental analyzer) and ICP-OES (P) of six samples per site.

Table 3.1: Stand characteristics of the 30 investigated European beech forests. Given are the site number, locality (latitude and longitude), elevation (m a.s.l.), mean annual precipitation (MAP; mm yr-1), mean spring precipitation (April-June, MSP; mm), mean climatic water balance (CWB, mm month-1), and mean annual temperature (MAT; °C) for the period 1991–2018, plant-available water capacity of the soil (AWC, mm), diameter at breast height (DBH; cm), tree height (Height, m), tree age, and Hegyi-competition-index (CI). Climate data were extracted from the Climate Data Centre of the German Weather Service (DWD, Offenbach). Data on tree level show means per site ± SE.

Site	Lat	Lon	Elev	MAP	MSP	CWB	MAT	AWC	DBH	Height	Tree age	CI
1	52.572	9.315	85	720.7	162.1	10.19	9.9	301	44.9 ± 1.0	26.6 ± 0.6	88.5 ± 4.7	0.49 ± 0.04
2	54.429	9.653	99	878.3	179	25.56	9	226.8	45.6 ± 2.3	27.1 ± 0.5	110.5 ± 1.4	0.59 ± 0.08
3	54.155	10.559	77	752.8	165.4	14.93	9.1	252.5	58.2 ± 2.8	30.0 ± 0.4	108.0 ± 3.7	0.44 ± 0.05
4	51.5	11.917	124	522	137.6	-10.82	10	286.4	45.1 ± 0.5	25.2 ± 0.7	87.0 ± 1.7	0.49 ± 0.03
5	51.75	12.21	80	565.8	142.9	-7.31	10	177.8	44.5 ± 1.2	28.1 ± 0.5	93.6 ± 0.8	0.53 ± 0.05
6	51.681	12.586	159	673.3	157.4	3.12	9.5	90.7	42.0 ± 2.2	26.8 ± 0.5	86.2 ± 1.9	0.64 ± 0.08
7	52.042	12.379	142	653.1	154.8	1.87	9.5	126	47.9 ± 2.5	28.8 ± 0.5	95.3 ± 2.1	0.54 ± 0.04
8	52.332	13.585	47	575.7	145.8	-7.32	9.7	169.4	40.2 ± 0.8	28.1 ± 0.6	80.5 ± 1.1	0.60 ± 0.06
9	52.446	13.075	45	582.3	144.3	-6.14	9.9	197.6	35.7 ± 1.1	21.1 ± 0.3	94.5 ± 2.3	0.58 ± 0.08
10	53.413	7.778	19	819.7	172.5	19.01	9.7	57.7	43.2 ± 1.6	27.1 ± 0.4	84.3 ± 2.4	0.51 ± 0.03
11	53.6	8.767	30	858.4	181.3	22.59	9.6	203	53.7 ± 2.7	34.4 ± 0.8	98.9 ± 2.2	0.44 ± 0.04
12	53.783	8.622	33	886.2	185.7	25.23	9.6	103.7	44.5 ± 1.4	30.6 ± 0.3	84.7 ± 1.8	0.51 ± 0.09
13	53.853	8.612	23	849	177.7	22.23	9.7	75.7	42.3 ± 1.9	26.1 ± 0.6	91.9 ± 1.3	0.57 ± 0.06
14	52.896	13.854	64	571.4	142.1	-6.02	9.6	118.6	49.6 ± 2.4	30.9 ± 0.6	91.4 ± 2.8	0.46 ± 0.04
15	53.113	12.854	81	610.7	149.5	-0.6	9.2	146.6	46.2 ± 1.6	29.2 ± 0.5	139.9 ± 6.2	0.44 ± 0.05
16	53.2	12.737	109	627.8	153	2.19	9	188.7	40.5 ± 1.4	28.8 ± 0.4	102.3 ± 4.4	0.41 ± 0.03
17	52.696	13.405	58	601.9	145.1	-3.49	9.8	43.4	45.1 ± 1.5	27.5 ± 0.4	89.9 ± 2.1	0.52 ± 0.05
18	53.675	11.734	70	655.3	156.2	5.64	9.2	78.9	45.4 ± 1.6	28.3 ± 0.7	94.7 ± 4.7	0.40 ± 0.03
19	53.715	14.138	32	584.5	149.4	-1.71	9.1	130.4	44.0 ± 1.5	27.2 ± 0.5	112.3 ± 5.3	0.39 ± 0.07
20	52.621	11.23	116	648.4	153	2.74	9.4	260.2	47.9 ± 1.5	33.9 ± 1.0	131.4 ± 4.4	0.61 ± 0.06
21	52.404	11.261	87	572.8	139.9	-4.65	9.7	159.5	42.0 ± 1.1	26.5 ± 0.4	106.8 ± 3.8	0.59 ± 0.06
22	53.123	10.82	94	718.7	164.2	10.48	9.2	172.1	46.1 ± 2.5	26.7 ± 0.6	164.6 ± 10.2	0.49 ± 0.03
23	53.172	9.953	144	863.2	192.3	24.32	9	161.3	43.0 ± 1.1	30.1 ± 0.7	121.0 ± 4.9	0.62 ± 0.04
24	52.831	10.317	141	804.7	174.5	17.93	9.1	127.1	46.3 ± 1.5	28.9 ± 0.6	110.6 ± 3.4	0.43 ± 0.04
25	54.417	13.555	37	646.3	152.4	5.87	9.1	218.3	48.1 ± 1.9	28.0 ± 0.4	122.1 ± 5.7	0.56 ± 0.05
26	54.02	12.48	49	663.3	158.8	6.4	9	166.2	43.3 ± 1.4	30.7 ± 0.5	85.1 ± 1.5	0.62 ± 0.05
27	53.461	9.908	72	798	179.3	17.45	9.7	88.4	47.1 ± 2.0	28.4 ± 0.6	153.7 ± 6.6	0.59 ± 0.06
28	53.623	9.768	34	799	175.3	17.48	9.6	158.2	46.5 ± 1.5	31.1 ± 0.6	119.0 ± 2.7	0.46 ± 0.01
29	54.055	10.723	51	707.8	157.3	10.81	9.2	256.4	42.2 ± 1.9	27.9 ± 0.6	62.4 ± 1.4	0.48 ± 0.05
30	53.962	10.126	68	851.5	179.8	22.69	9.2	164.2	44.3 ± 1.3	27.5 ± 0.5	138.2 ± 5.4	0.73 ± 0.09

The water availability of a tree depends not only on the climatic water balance and soil hydrology but may also be determined by competition with neighbouring trees in the stand. For estimating the intensity of competition our target trees were exposed to, the competition index after Hegyi (CI, Hegyi, 1974) was calculated for each sampled tree i including diameter and distance of the three nearest neighbouring trees j as:

$$CI_i = \sum_{j=1}^{n} \frac{d_j/d_i}{Dist_{ij}}$$

where d_i is the diameter at breast height of the sampled tree i (cm), d_j the diameter at breast height of the competitor j (cm), $Dist_{ij}$ the distance between target tree and competitor (m), and n the number of measured neighbouring trees (= 3).

3.3.2 Plant material and sample processing

Branch samples of the uppermost sun-exposed crown of ten mature beech trees were collected by professional tree climbers in each of the 30 stands. Per tree, one main branch located at $1 - 2$ m distance to the outermost tree tip was selected (n = 300). The branch samples used for anatomical analysis (one per tree) were segments of 1st-order side branches of the detached main branch and had a diameter (D_{branch}) of $7 - 11$ mm. The distance to the side branch apex was estimated from branch diameter - distance-to-tip relationships established for 85 upper-canopy branches of European beech trees taken from Hajek *et al.* (2015). The 85 branches were divided into three equal-sized groups according to tapering rates along the segment. Linear regressions were calculated separately for branches with high, medium, or low tapering rates (Figure S3.2). Based on these regressions, distance to the tip was estimated for our branch samples from their diameter, after grouping the samples according to the tapering rate of the 30 cm-segment located distal to the segment used for anatomical analyses. Accordingly, the estimated distance to the tip ranged from 36.8 to 91.4 cm (average: 60.08 ± 0.5 cm) among our branch samples. Note that this value applies only to the flow path in the outermost (youngest) annual ring, while older, inner rings had shorter distances to the tip position in past years.

The segments used for anatomical analyses were stored in 70% (v/v) ethanol before anatomical analysis. Afterwards, thin transverse sections were cut with a sliding microtome (G.S.L.1; Schenkung Dapples, Zurich, Switzerland). Microslide cross-sections were digitalized at x100 magnification using a stereomicroscope attached to a digital camera (SteREOV20; Carl Zeiss MicroImaging GmbH, Göttingen, Germany). The images were processed using the software ROXAS for anatomical analyses (Arx & Carrer, 2014), that is

based on the image manipulation and registration capability of Image Pro Plus v7.0.0.591 (Media Cybernetics, Silver Spring, USA). We always selected a representative portion of the cross section (30 to 60%, typically about 40%, of the whole cross section) and if tension wood was present, we included a representative portion of the tension wood. All annual rings except the oldest innermost ring were included in the analyses (Figure S3.3).

3.3.3   Anatomical and hydraulic traits

The variables considered in our analyses were mean vessel diameter (D, µm; corrected for the effect of elliptical conduit shape on flow according to Lewis & Boose, 1995), vessel density (VD, no mm^{-2}), hydraulically-weighted vessel diameter (D_h, µm; calculated after Sperry et $al.$, (1994) as $D_h = (\Sigma\ D^5\ /\ \Sigma\ D^4)$), lumen-to-sapwood area ratio (A_L/A_X, %), potential hydraulic conductivity (K_p, kg m^{-1} MPa^{-1} s^{-1}; approximated by Hagen-Poiseuille's law and adjusted to elliptical tubes, as $K_p = (A_{lumen} * r^2) / (\eta * k)$, where A_{lumen} is the vessel lumen area, η the viscosity of water at 20 °C, r the mean hydraulic radius, and k the coefficient depending on the geometry of the cell, see Nonweiler (1975), vessel grouping index (VGI; mean group size including solitary vessels with a group of size one), and vessel solitary fraction, i.e. the fraction of solitary cells relative to total cell number (VSF, %). Furthermore, the abundances of vessels in the diameter classes $10 - 20$ µm ($D_{10\text{-}20}$), $20 - 30$ µm ($D_{20\text{-}30}$), $30 - 40$ µm ($D_{30\text{-}40}$), and $40 - 50$ µm ($D_{40\text{-}50}$) were determined. All variables were determined for the analysed xylem section, which represents about 40% of the cross-sectional area and includes all annual rings except the first (oldest) ring. The anatomical traits were not calculated separately for the different annual rings. Branch age at the analysed cross-section was determined by counting annual rings in the xylem, which were well developed in most branches.

Anatomical variables were related to embolism resistance, i.e. the pressure causing 50% loss of conductivity (P_{50}) determined by Cavitron measurement (Cochard et $al.$, 2005). The vulnerability measurements were conducted on the same branches from which the basipetal ends had previously been cut for anatomical analyses (for details see Weithmann et $al.$, 2022). Briefly, the twigs were re-saturated und recut under water, flushed, and xylem vulnerability curves constructed within two weeks after sample collection with the flow-centrifuge technique for branches of 27.5 cm length and a basipetal diameter of $5 - 10$ mm. A study on the influence of storage time on different branch segments of the same beech tree did not show an effect of storage time on P_{50} within 10 weeks (Herbette et $al.$, 2010). We thus assumed that this factor did not influence our hydraulic measurements.

3.3.4   Data analyses

All statistical analyses were performed with the software `R` version 3.6.2 (R. Core Team 2019) in the framework of the `tidyverse` package (Wickham *et al.,* 2019). For testing the effect of water availability-related variables (CWB, AWC and CI), tree height and branch age at the time of sample collection on different anatomical variables, different linear mixed effects models (LME) were fitted with CWB, AWC, CI, tree height and branch age as fixed effects and random intercept for the stands. Two additional models were fitted to test the effect of distance to the apex on D and D_h. As the distance to the tip was only estimated in our study and analyses were not conducted for each annual ring separately in all samples, we refrained from including distance to the tip in our models in the main results part. However, we present the results of two additional models with the estimated distance to the tip as additional fixed effect factor in Table S3.4 in the Supplementary. As the distance to the tip refers to the conduits of the outermost annual ring, we analysed mean vessel size of the outermost ring and measured distance to the tip in a subsample of our dataset that consisted of 30 branch samples from three sites, i.e. each one site with high, intermediate or low CWB. The effect of distance to the tip on vessel size of the outermost ring was tested with simple linear regression analyses using the `lm`-function. Another LME model was fitted to test the effect of water availability and tree height on branch age (with CWB, AWC, CI and tree height as fixed effects and random intercept for the stands). Numeric predictor variables were scaled by their standard deviations and centered around zero. LME-models base on the `R` package `lme4` v. 1.1-23 (Bates *et al.,* 2015) and were fitted using Restricted Maximum Likelihood. Inference was based on Wald *t*-tests with Satterthwaite's approximation to the degrees of freedom using R package `lmerTest` v. 3.1-2 (Kuznetsova *et al.,* 2017) and the marginal and conditional R^2 (Nakagawa *et al.,* 2017) was calculated using R package `MuMIn` v. 1.43.17 (Bartón, 2020). To depict the relations between the variables addressed in the hypotheses (water availability, tree height, branch age and P_{50} in relation to anatomical variables), simple linear regression analyses were conducted using the `lm`-function. To illustrate pairwise linear associations between variables included in the model and to show the effect of soil chemical variables on anatomical traits, Pearson correlation analyses were computed using the R package `corrmorant` v. 0.0.0.9007 (Link, 2020). No problematic level of multicollinearity was detected for the fixed effects variables (CWB, AWC, CI, tree height and branch age) of the LME models (Figure S3.4).

3.4 Results

3.4.1   Variability of anatomical and hydraulic traits

The investigated variables characterizing the anatomy of branch xylem approximately 37 –
91 cm distant from the terminal branch tip differed markedly across the 300 investigated
trees in the 30 stands (Figure S3.5, Table S3.1). According to the results of the linear mixed
effects models, the greatest proportion of variance in all variables was attributable to
unexplained differences between individual trees (ranging from 52% for mean vessel
diameter (D) to 71% for lumen-to-sapwood area ratio (A_L/A_X, Figure 3.1).

The variance explained by the fixed effects (climatic water balance (CWB), plant-available
water capacity (AWC), Hegyi competition index (CI), tree height and branch age) was
highest for vessel density (VD, 38%) and lowest for A_L/A_X (7%). In the case of VD, only
1.2% of the variance was related to unexplained differences between stands, i.e. the variance
between sites that was not explained by CWB or AWC, whereas 17 to 26% of the variance
was attributed to this component in the other variables.
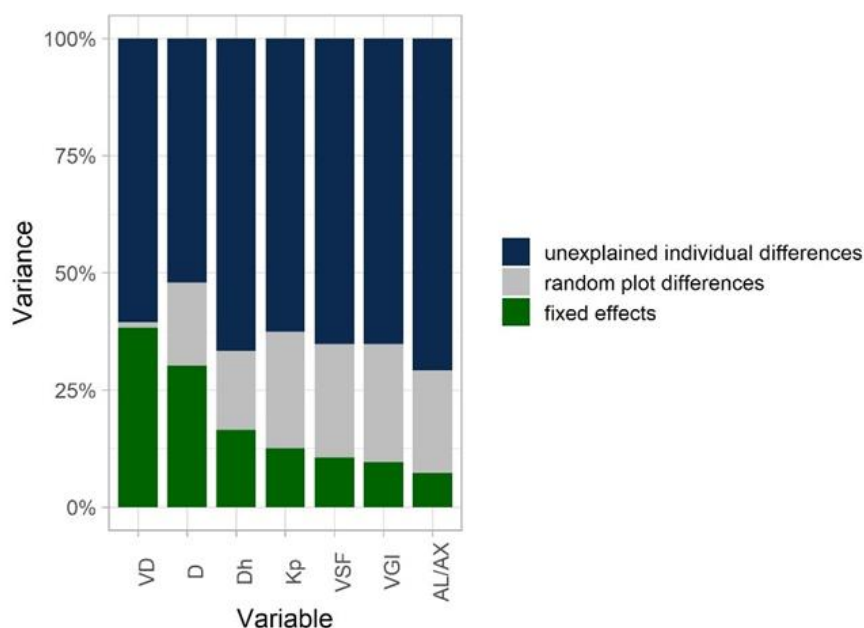
Figure 3.1: Variance components of the linear mixed effects models for the variables vessel
density (VD), mean vessel diameter (D), hydraulically-weighted vessel diameter (D_h),
potential hydraulic conductivity (K_p), vessel solitary fraction (VSF), vessel grouping index
(VGI) and lumen-to-sapwood area ratio (A_L/A_X) with climatic water balance (CWB), plant-
available soil water capacity (AWC), Hegyi competition index (CI, log-transformed), branch
age (log-transformed) and tree height as fixed variables and site as random variable, and
residual variability between individuals (see Table 3.2).

3.4.2   Effects of water availability and soil chemical properties on branch anatomy

For the water availability-related variables (i.e. CWB, AWC and CI), the LME model results showed significant positive effects of CWB on D, A_L/A_X and potential hydraulic conductivity (K_p), whereas AWC influenced only VD significantly. Hydraulically-weighted diameter (D_h), vessel grouping index (VGI) and vessel solitary fraction (VSF) were neither related to CWB nor AWC (Table 3.2, see Table S3.2 for standard errors, test statistics, and degrees of freedom, and Figure 3.2A for regression results). Competition intensity CI as a measure of assumed competition for water did not influence any of the studied traits. Similar to the effect of CWB, mean annual precipitation and mean spring precipitation correlated positively with D and A_L/A_X, but not with VD (Figure S3.6), reflecting the close inter-relation between these three precipitation-related variables. The relatedness of D, VD and A_L/A_X to mean annual temperature and soil chemical properties (pH value, carbon/nitrogen ratio, phosphor concentration and nitrogen content of mineral soil) was generally weak (Figure S3.6).

Table 3.2: Results of linear mixed effects models examining the influence of climatic water balance (CWB), plant-available water capacity (AWC), Hegyi competition index (CI, log-transformed), branch age (log-transformed), and tree height as fixed variables and site as random variable on mean vessel diameter (D), hydraulically weighted vessel diameter (Dh), vessel density (VD), lumen to sapwood area ratio (AL/AX, log-transformed), potential hydraulic conductivity (Kp, log-transformed), vessel grouping index (VGI, log-transformed) and vessel solitary fraction (VSF). n = 296. See Table S2 for standard errors, test statistics, and degrees of freedom.

| Fixed parts	D Est.	D p	D_h Est.	D_h p	VD Est.	VD p	$\log(A_L/A_X)$ Est.	$\log(A_L/A_X)$ p	$\log(K_p)$ Est.	$\log(K_p)$ p	$\log(VGI)$ Est.	$\log(VGI)$ p	VSF Est.	VSF p
Intercept	20,473	<0.001	28,203	<0.001	460,034	<0.001	2,857	<0.001	1,197	<0.001	0,393	<0.001	49,136	<0.001
CWB	0,385	0,017	0,437	0,059	1,846	0,560	0,041	0,013	0,076	0,021	0,013	0,160	-1,088	0,152
AWC	0,226	0,140	0,116	0,600	-6,665	0,037	0,006	0,713	0,019	0,540	-0,008	0,409	0,578	0,434
log (CI)	-0,025	0,755	-0,045	0,727	3,692	0,203	0,004	0,662	0,000	0,981	-0,002	0,745	0,038	0,921
log (Br. age)	-0,810	<0.001	-0,859	<0.001	37,578	<0.001	0,002	0,783	-0,068	<0.001	0,022	<0.001	-2,001	<0.001
Tree height	-0,147	0,185	-0,165	0,341	0,073	0,982	-0,019	0,105	-0,032	0,137	-0,011	0,103	0,764	0,148
Random part														
SD (Intercept)	0,707		0,999		6,583		0,071		0,147		0,043		3,500	
SD (Obs.)	1,213		1,978		47,141		0,128		0,234		0,070		5,730	
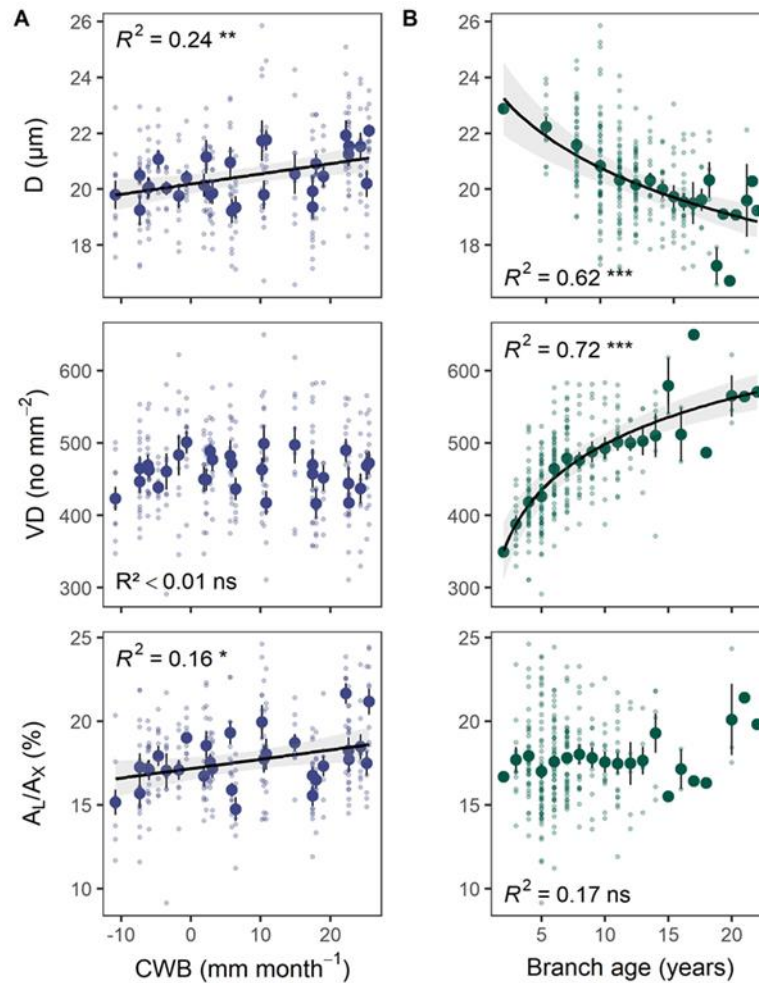
Figure 3.2: Linear regression analyses showing the effect of climatic water balance (panel A) and branch age (panel B, log-function) on mean vessel diameter (D, top), mean vessel density (VD, middle) and mean lumen-to-sapwood area ratio (A_L/A_X, bottom). Given are the means per site $\pm$ standard error (A, n = 30) and the means per branch age class $\pm$ standard error (B, n = 20). Linear regressions refer to the mean values and raw data are depicted in the background. For significant relationships, the linear regression line with its 95% confidence intervals is shown. Asterisks indicate the level of significance (***, $p < 0.001$; **, $p < 0.01$; *, $p < 0.05$; ns, non-significant relationship).

3.4.3 Effect of tree height on branch anatomy

None of the measured anatomical or hydraulic variables was related to tree height, that varied between 21 and 34 m in the 30 stands (Table 3.2, Figure 3.3). The relation of the three variables associated with site water availability (CWB, AWC, CI) to tree height was weak (Figure S3.4), and mean tree height of the sites was not significantly related to MAP.
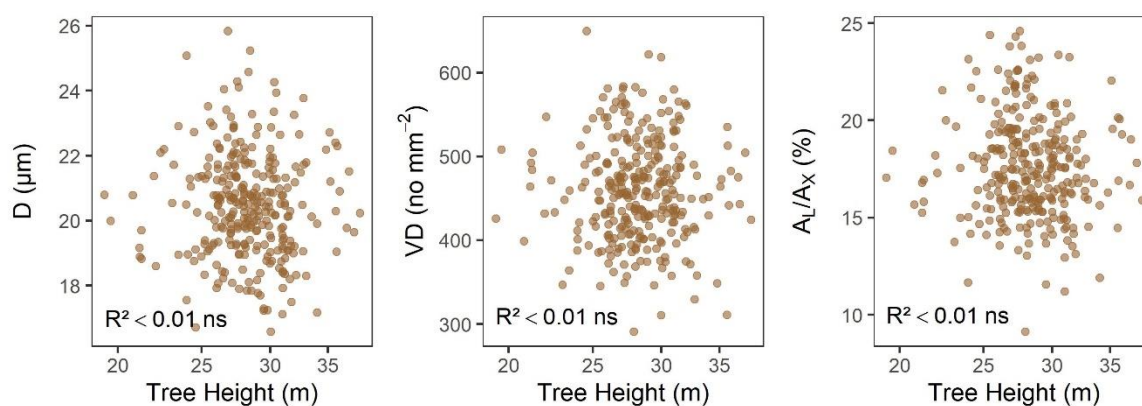
Figure 3.3: Relationship of antaomical traits (D, VD, A_L/A_X) to tree height. Given are the results of linear regression analyses (n = 298). Level of significance is shown (ns, p > 0.05, non-significant relationship).

3.4.4 Influence of branch age on anatomical traits

The linear mixed effects models showed a highly significant negative effect of branch age on D and a positive one on VD of the upper-canopy branches (Table 3.2). Branch age was further significantly related to D_h, K_p, VGI and VSF, but not to A_L/A_X. Linear regression analyses also showed a significant relationship of branch age to D and VD (Figure 3.2B). The decrease in D with increasing branch age is depicted in the cross-sections and vessel diameter frequency distributions in Figure 3.4. Results of a separate linear mixed effects model revealed that branch age was not related to CWB, AWC, CI or tree height; only 1.6% of the variance was explained by these effects, and 77% of the variance was attributed to unexplained within-population differences (Table S3.3).

3.4.5 Effect of branch age and CWB on the abundance of different vessel diameter classes

Linear regression analysis for different vessel size classes showed that the observed increase in D with increasing CWB is driven by an increase in the abundance of vessels >20 µm (D_{20-30}, D_{30-40}, D_{40-50}) and a decrease in the abundance of vessels of 10 – 20 µm (D_{10-20}, Figure 3.5). The opposite trend was observed for branch age, where a significant increase in the abundance of D_{10-20} vessels and a significant decrease of vessels > 20 µm with increasing branch age was found.
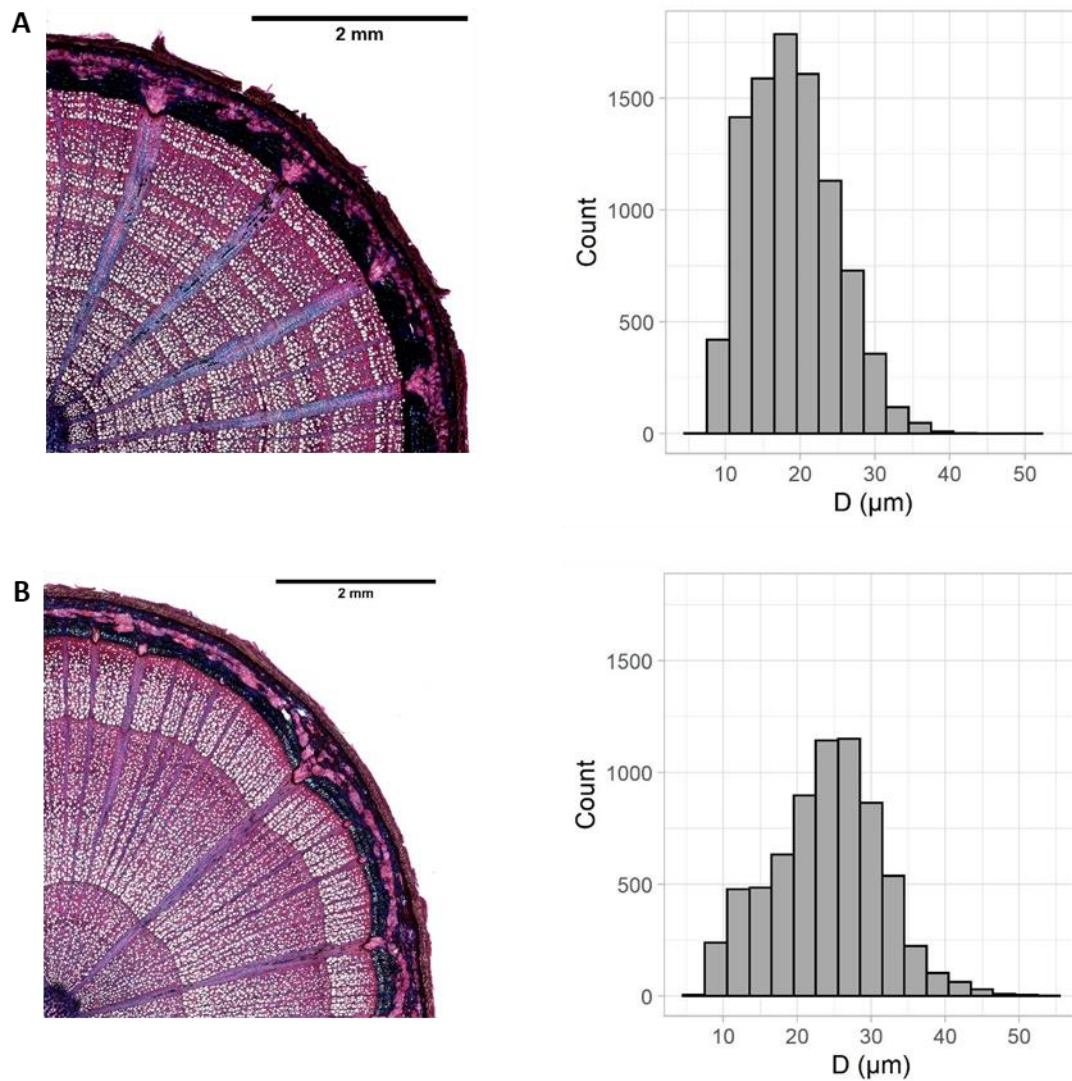
Figure 3.4: Anatomical sections of branches sampled in the uppermost canopy with branch age of 20 years, potential conductivity of 2.76 kg m^{-1} s^{-1} MPa^{-1} and diameter of 7.7 mm (A, left) or branch age of three years, potential conductivity of 5.79 kg m^{-1} s^{-1} MPa^{-1} and diameter of 10.2 mm (B, left), and histograms showing the vessel diameter distribution of the corresponding samples (A and B, right).
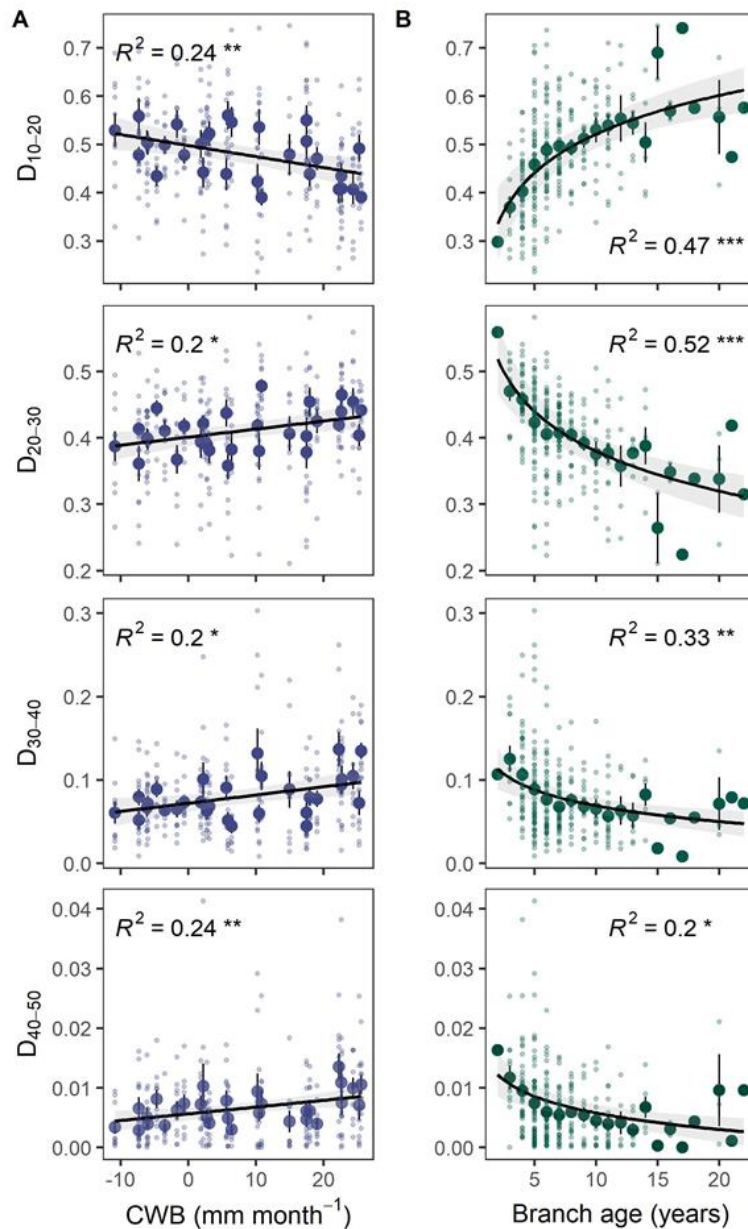
Figure 3.5: Linear regression analyses showing the effect of climatic water balance (panel A) and branch age (panel B, log-function) on the average abundance of different vessel diameter classes (D_{10-20}, D_{20-30}, D_{30-40}, D_{40-50}). Given are the means per site ± standard error (A) and means per branch age class ± standard error (B) and raw data are depicted in the background. For significant relationships, the linear regression line with its 95% confidence intervals is shown. Asterisks indicate the level of significance (***, $p < 0.001$; **, $p < 0.01$; *, $p < 0.05$; ns, non-significant relationship).

3.4.6   Relation of anatomical traits to embolism resistance

According to linear regression analyses, embolism resistance in terms of the xylem pressure causing 50% loss of hydraulic conductivity (P_{50}) was not related to D or D_h, while a weak but highly significant effect of A_L/A_X, and VGI on P_{50} was observed (Figure 3.6).
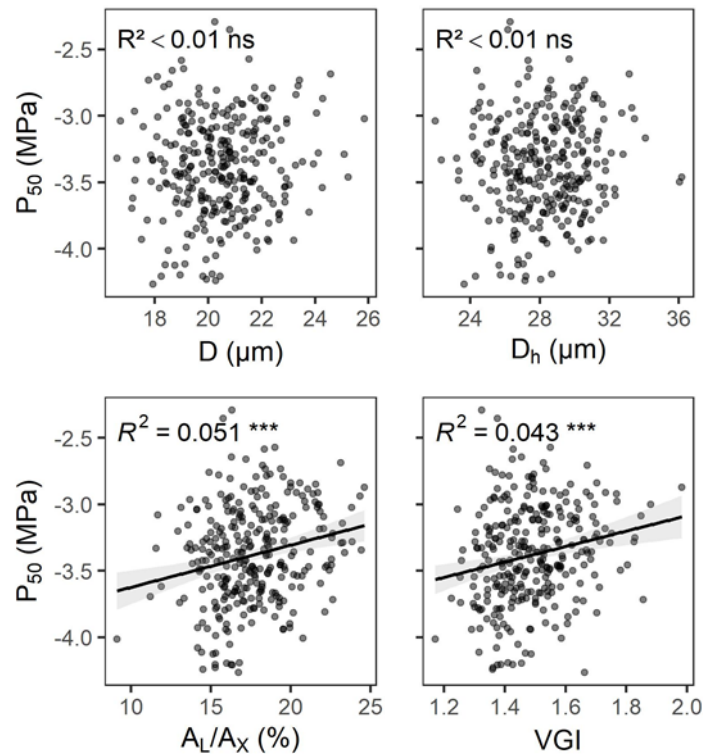
Figure 3.6: Linear regression analyses showing the effect of mean vessel diameter (D), hydraulically weighted vessel diameter (D_h) lumen-to-sapwood area ratio (A_L/A_X) and vessel grouping index (VGI) on embolism resistance in terms of pressure causing 50% loss of hydraulic conductance (P_{50}). The linear regression line with its 95% confidence intervals is shown. Asterisks indicate the level of significance (***, $p < 0.001$; ns, non-significant relationship).

3.5 Discussion

3.5.1 Within- and between-population variability in xylem anatomy

For all anatomical and derived hydraulic traits, the greatest part of observed variance was attributed to unexplained differences between tree individuals in a population. This high intra-population trait variability is consistent with results on hydraulic properties obtained from earlier studies in European beech forests (Wortemann *et al.,* 2011, Schuldt *et al.,* 2016, Stojnic *et al.,* 2017). Both genetic differences between individuals and phenotypic plasticity might be responsible for this variability (Aranda *et al.,* 2017).

The unexplained variance between populations, i.e. differences between sites not explicable by variation in water availability, tree height or branch age, was especially low for vessel density (1.2% of the variance) and ranged from 17% to 26% in the other variables. As genetic differences between beech populations are usually small at the regional level (Jump & Peñuelas, 2007), these random between-population differences might well represent acclimative responses to the local climatic conditions deviating from long-term trends or to

differences in soil moisture availability among the stands. Stem anatomical time-series analysis has demonstrated that beech is capable of rapid acclimation in vessel diameter (D) and vessel density (VD) to climatic variation between years (Zimmermann *et al.,* 2021).

3.5.2 Influence of water availability on xylem anatomy

The observed positive relationship between climatic water balance (CWB) and D of tree-top branches in mature beech trees supports our first hypothesis and matches the results of other studies on intraspecific variation in branch and stem xylem anatomy of temperate, subtropical and tropical broadleaf trees (Schreiber *et al.,* 2015; Schuldt *et al.,* 2016; Pfautsch *et al.,* 2016; Liang *et al.,* 2019). In *Populus tremula*, it appears that mainly the formation of earlywood vessels is affected by environmental conditions (Schreiber *et al.,* 2015). This contrasts with *Fagus sylvatica,* where cambial activity is more sensitive to environmental factors at the end of the growing season than at the beginning, when predominantly internal factors are controlling activity (Sass & Eckstein, 1995). A study combining dendrochronological time-series analysis with radial vessel features in the stem of mature beech trees demonstrated a highly significant positive effect of current-summer CWB, and also previous-summer CWB, on hydraulically-weighted vessel diameter (D_h; Zimmermann *et al.,* 2021). This matches the results of a xylem micro-coring study in *Pinus sylvestris* that found a close relation between final tracheid diameter and water availability during tracheid enlargement (Cabon *et al.,* 2020). In our data set, CWB affected not only D (and the related potential hydraulic conductivity, K_p) but also lumen-to-sapwood area ratio (A_L/A_X), while the relation to D_h was only marginally significant and none existed to VD. The lack of an effect of climatic water availability on VD corresponds with results of a gradient study on terminal branches of *F. sylvatica* by Schuldt *et al.* (2016). Also in agreement with the latter study, we found the decrease in mean D with deterioration of the climatic water balance being caused by an increase in the number of vessels in the 10 – 20 µm size class at the expense of vessels in the >20 µm size class.

VD was the only anatomical variable that was significantly affected by the soil storage capacity for plant-available water (AWC). As expected, VD increased with decreasing AWC, reflecting the fact that the likelihood of summer drought stress increases with a reduction in soil water storage. In correspondence, the reduction in the climatic water balance since the 1980s has led to an increasing VD in the stem xylem of beech (Zimmermann *et al.,* 2021).

We had expected that competition with neighbour trees expressed by the competition index (CI) after Hegyi (1974) could be a factor that deteriorates the tree water balance with consequences for cambial activity and xylem anatomy. Such an effect of asymmetric competition for water on xylem anatomy has been demonstrated for beech saplings grown in mixture with water spending neighbours, where beech tended to form vessels with smaller diameter in the stem and thus reduced hydraulic efficiency (Lübbe *et al.,* 2017). In our study with mature trees, we could not confirm such a competition-driven effect, which might be due to the fact that we investigated intraspecific instead of interspecific competition, and stands were fairly homogeneous in stem diameters and height, indicating rather symmetric than asymmetric competition for water. It is also possible that stem density has approached sort of an ecohydrological equilibrium, where competition for water is minimized under conditions of ample supply (Hatton *et al.,* 1997). It should also be considered that we selected the stands at sites without high groundwater levels and in level terrain in order to minimize the lateral inflow of water and strengthen the effect of precipitation. Yet, we cannot fully exclude the existence of sub-surface flow at some of the sites.

3.5.3   No tree height effect on xylem anatomy

Contrary to our expectations, no effect of tree height on the xylem anatomy of tree-top branches was observed in our beech tree sample. Clearly, the range of canopy heights was with 13 m only moderate in the 30 stands (21.1 – 34.4 m), and canopy height was not dependent on climatic or edaphic variables related to water availability, or, in other words, drought stress intensity did not influence tree height in our stands. Yet, the result of our analysis is trustworthy, as the sample with 30 stands is large and the model clearly excludes a tree height effect, while confirming a highly significant influence of CWB and branch age on the anatomical variables in question. In our study, light conditions and evaporative demand in the tree top were comparable across sites and only mature trees were sampled. These factors may represent important boundary conditions in some other studies, as height growth varies with growth stage and in dependence on environmental conditions, with the consequence that branch segments at a given distance to the terminal tip are generally the older, the more restricted height growth is, when light, water or nutrients are limiting. This can influence vessel dimensions as shown by our results. Given that we always collected samples from the uppermost sun-exposed branches, a relevant increase in tree height during the lifetime of our branch samples is unlikely. As mean tree height was not related to MAP in our study, we can exclude that a tree height effect was mistaken for a climate effect on *D*.

Clearly, it is a limitation of our study that the sample distance to the tip was not directly measured in the field. However, we always sampled similar-sized branches from the sun-exposed canopy and the estimated distance to the branch apex was unrelated to tree height in our sample (Figure S3.7). Our results highlight the importance of additional field studies on intraspecific variation in xylem properties with consideration of branch and tree age as covariates to reach at more general conclusions on the drivers of vascular differentiation in upper canopy branches.

3.5.4 Effect of branch age on xylem anatomical and hydraulic properties

We observed a strong branch age effect on the xylem anatomical and hydraulic properties of tree-top branches. The age of branch samples of $7 - 11$ mm diameter with an estimated distance to the apex of $37 - 91$ cm varied between 2 and 22 years and was not affected by other possibly explaining variables, notably CWB, AWC and CI, and also tree height (Table S3.3). Linear mixed effects models revealed a significant influence of branch age on all investigated anatomical traits, except for A_L/A_X. D, D_h, K_p, and vessel solitary fraction (VSF) significantly decreased with increasing branch age in our sample of 298 branches, whereas VD and vessel grouping index (VGI) increased with age. The age effect on xylem anatomy is a logical, yet unexpected, consequence of the sampling design, which sought to collect branches of similar diameter and at similar distance to the tree top. When branch age is so variable in the upper sun crown as found here and sampling is done for similar branch diameters, then older branches must have narrower annual rings and are likely to have smaller vessels at higher density. Zimmermann *et al.* (2021) also found higher conduit densities in narrower annual rings of beech stem wood. Two aspects of this finding are interesting. First, variation in branch annual ring width and VD is high among different trees and stands, despite similar position of the sampled segments in the flow path. This heterogeneity cannot be explained by variation in tree height (Table S3.3) and it was unrelated to the distance to the branch tip (Figure S3.7). Instead, it rather relates to differences in length growth patterns over time and between sites, that may relate to the local microclimatic and hydrologic constraints experienced by the canopy. Second, theory predicts an increase, and not decrease, in mean D with increasing cambial age (Gartner *et al.,* 1997; Leal *et al.,* 2007; Fan *et al.,* 2009; Zhao, 2015). Our results also contrast with an earlier study on intraspecific variation in beech xylem anatomy that did not find an age dependency of branch anatomy (Schuldt *et al.,* 2016), even though the sampling design was comparable, albeit with much smaller sample size. It is unlikely that the observed branch

age effect on conduit dimensions is caused by differences in the distance to the tip among the samples, since including distance to the tip as an additional fixed effect factor in our models did not shift the variables that significantly affect D and D_h (Table S3.4). According to this model, distance to the tip had no significant effect on D_h; yet, a marginally significant influence on D was observed. It must be kept in mind that distance to the tip considers only the flow path length in the outermost annual ring, while the anatomical properties were determined in our branch sample for the entire branch xylem with several annual rings (excluding the first, oldest ring). The enormous labour amount required for a focused analysis of the anatomy of only the youngest, outermost ring forced us to restrict such an investigation on a subset of branch samples that were selected from three sites with either a high, intermediate or low climatic water balance. This detailed side-analysis confirmed our earlier finding that vessel diameter was not influenced by distance to the tip in our sample (see Figure S3.8). Nevertheless, other studies have found a significant effect of distance to the tip on vessel size (Anfodillo *et al.,* 2006; Petit *et al.,* 2010; Olson *et al.,* 2021), which calls for considering this factor in future hydraulic and anatomical studies.

We speculate that the observed pattern in branch age is partly a consequence of the crown architectural type realized in beech (type 'Troll' after Hallé *et al.,* 1978), in which the dominance of the main axis is abandoned early in life for an oligo- to polycormic branching pattern in the canopy. Branching is mostly dichotomous with different side branches taking over lead growth in the top during the lifetime of the tree. Decreased growth rates of older branches could then be caused by small-scale differences in microclimatic conditions in the uppermost canopy, when they are over-topped by other branches. We speculate that this flexible crown architecture without a single main axis may cause some deviation from the basic architectural model that assumes continuous conduit widening with increasing cambial age when the tissue is young (Gartner *et al.,* 1997; Zhao, 2015). Finally, it cannot be ruled out that increasing atmospheric saturation deficits and a decreasing CWB with climate warming in the last decades have contributed to the formation of smaller conduits in recent time. A corresponding highly significant trend toward smaller D_h with increasing summer CWB (by -2.35% per decade) was detected in the stem wood of Central German beech stands (Zimmermann *et al.,* 2021). Further studies on within-crown xylem anatomy variation in canopies of different architectural types would improve our understanding of age and height effects on conduit dimensions.

3.5.5 Relation between branch xylem anatomy and embolism resistance

Regressing vessel properties on the pressure causing 50% loss of conductance (P_{50}) revealed no significant relations for D or D_h, but for the properties with association to the number of pits per xylem cross-sectional area, i.e. A_L/A_X and VGI. Wider conduits have been shown to be more susceptible to freezing-induced embolism, while this relation is less clear for drought-induced embolism (Hacke *et al.,* 2017). In beech, no dependence of resistance against drought-induced embolism on D or hydraulic efficiency was found (Schuldt *et al.,* 2016; Hajek *et al.,* 2016). From these findings, we did not expect a safety-efficiency trade-off. Instead, we expected anatomical traits associated with the fraction of inter-vessel cell walls and the number of pits, A_L/A_X and VGI to be associated with P_{50}. Indeed, we found for both variables a weak, but highly significant positive relationship with P_{50}. The vulnerability of vessels to embolism is related to structural and chemical properties of the pits (Jansen *et al.,* 2009; Lens *et al.,* 2011; Li *et al.,* 2016) as well as to quantitative pit properties (Christman *et al.,* 2009). A study on poplar showed that, on the intraspecific level, embolism resistance depends more on pit properties such as pit area and vessel grouping than on pit structure itself, and that embolism resistance increased with an increase in vessel connectivity and grouping (Lemaire *et al.,* 2020). In contrast, our data showed a decrease of embolism resistance with increasing connectivity, supporting the results of a modelling approach by Loepfe *et al.,* (2007). However, it is possible that the large variation in branch age is masking a clearer relationship between vessel grouping and embolism resistance in our sample, as is suggested by the significant branch age effect on P_{50}, with older branches being less embolism resistant (Weithmann *et al.*, 2022).

3.5.6 Conclusion

European beech as a main tree species of Central Europe's natural forest vegetation and a major timber species is increasingly threatened by climate warming-related heat and drought events (Schuldt *et al.,* 2020; Leuschner, 2020; Walthert *et al.,* 2021). Tree physiologists and foresters are interested in the species' adaptive and acclimative potential to a deteriorating climatic water balance in order to define more precisely the drought limit of the species and to support silvicultural decisions on the choice of drought-hardier provenances (Leuschner 2020). This study provides a large dataset on xylem anatomical traits of the most distal tree-top branches of mature trees, which are growing across a steep precipitation and (weaker) temperature gradient. By additionally investigating soil hydrological variation across the sites, we provide a comprehensive picture of the plasticity in anatomical traits and in the

adaptive response potential of the branch xylem for beech forests in the entire northern German lowland region. In line with previous studies on *F. sylvatica*, the greatest part of variance was attributable to between-tree differences within populations. Despite this variation, *D* was found to significantly decrease with a decrease of the climatic water balance, whereas VD was negatively related to the soil capacity for plant-available water. While tree height was unrelated to vascular modifications in top-canopy branches, we found significant effects of water availability on *D* and VD. The absence of an effect of distance to the tip on vessel diameter matches the results of anatomical time-series analyses in beech, where tree height is definitely not a factor (Zimmermann *et al.,* 2021). The observed great variation in branch age and the highly significant age effect on anatomy demand for a more detailed investigation of branch anatomical variation across tree canopies and its causes, which also compares different tree architectural types, before more general conclusions on the relative importance of environmental vs. size-related drivers of xylem anatomy can be drawn. Combining our anatomical results with a study on variation in embolism resistance in the same trees allows the conclusion that European beech modifies its xylem anatomy in branches and also in the stem sensitively to variation in water availability, but this response has only a minor effect on embolism resistance in the upper canopy. This may suggest that the observed anatomical changes are primarily a consequence of drought-induced reductions in cell enlargement of the xylem primordia, leading to smaller annual rings, rather than active acclimative responses to increase the hydraulic safety of the conduit system.

Acknowledgements

3.6 Supplementary information

Table S3.1: Summary of explored variables. These are the mean vessel diameter (D, µm), hydraulically weighted vessel diameter (D_h, µm), vessel density (VD, no mm^{-2}), lumen to sapwood area ratio (A_L/A_X, %), potential hydraulic conductivity (K_p, kg m^{-1} s^{-1} MPa^{-1}), vessel grouping index (VGI) and vessel solitary fraction (VSF, %). Furthermore, the pressure at 50% loss of hydraulic conductance (P_{50}, MPa) of the sampled branches is shown (Weithmann et al. 2022). Given values are means ± SE per site.

Site	D	D_h	VD	A_L/A_X	K_p	VGI	VSF	P_{50}
1	21.73 ± 0.73	29.28 ± 0.88	462.9 ± 17.0	19.95 ± 1.01	4.38 ± 0.48	1.61 ± 0.05	43.09 ± 1.83	-3.09 ± 0.07
2	22.08 ± 0.23	30.63 ± 0.41	472.3 ± 16.3	21.17 ± 0.78	4.86 ± 0.27	1.57 ± 0.04	44.23 ± 1.86	-3.27 ± 0.07
3	20.54 ± 0.71	27.37 ± 0.89	497.4 ± 25.7	18.71 ± 0.53	3.56 ± 0.30	1.52 ± 0.03	46.42 ± 1.54	-3.18 ± 0.09
4	19.80 ± 0.51	26.69 ± 0.69	423 .0± 16.7	15.16 ± 0.76	2.67 ± 0.25	1.39 ± 0.03	54.71 ± 2.00	-3.16 ± 0.07
5	20.49 ± 0.29	28.37 ± 0.64	446.5 ± 16.0	17.26 ± 0.82	3.39 ± 0.28	1.47 ± 0.04	50.20 ± 2.24	-3.45 ± 0.09
6	19.85 ± 0.38	27.64 ± 0.44	477.2 ± 16.0	17.17 ± 0.53	3.16 ± 0.19	1.47 ± 0.02	49.74 ± 1.26	-3.43 ± 0.08
7	20.14 ± 0.41	28.65 ± 0.47	449.7 ± 17.4	16.72 ± 0.60	3.25 ± 0.21	1.47 ± 0.03	49.86 ± 1.67	-3.74 ± 0.11
8	19.25 ± 0.53	26.37 ± 0.69	464.5 ± 17.1	15.67 ± 0.89	2.69 ± 0.30	1.43 ± 0.04	52.57 ± 2.16	-3.19 ± 0.08
9	20.04 ± 0.38	27.55 ± 0.68	469.2 ± 14.6	17.15 ± 0.46	3.18 ± 0.21	1.55 ± 0.03	46.05 ± 1.25	-3.36 ± 0.09
10	20.47 ± 0.39	27.72 ± 0.44	451.7 ± 17.9	17.31 ± 0.62	3.28 ± 0.21	1.46 ± 0.03	50.48 ± 1.80	-3.24 ± 0.08
11	21.25 ± 0.42	29.31 ± 0.89	443.7 ± 24.3	18.24 ± 0.78	3.81 ± 0.26	1.53 ± 0.04	47.27 ± 2.24	-3.39 ± 0.08
12	20.20 ± 0.48	27.84 ± 0.82	468.3 ± 18.4	17.47 ± 0.74	3.34 ± 0.30	1.52 ± 0.03	46.84 ± 1.69	-3.33 ± 0.06
13	21.92 ± 0.54	30.57 ± 0.59	489.8 ± 16.1	21.65 ± 0.63	4.96 ± 0.32	1.71 ± 0.04	38.73 ± 1.61	-3.25 ± 0.06
14	20.07 ± 0.35	27.72 ± 0.51	462.5 ± 11.3	17.08 ± 0.61	3.21 ± 0.21	1.52 ± 0.04	47.19 ± 1.99	-3.20 ± 0.12
15	20.41 ± 0.26	28.60 ± 0.47	501.0 ± 15.6	18.99 ± 0.31	3.69 ± 0.11	1.59 ± 0.03	43.16 ± 1.24	-3.33 ± 0.07
16	21.16 ± 0.60	29.77 ± 1.20	449.2 ± 15.4	18.53 ± 0.89	4.02 ± 0.46	1.54 ± 0.03	45.93 ± 1.72	-3.57 ± 0.08
17	20.03 ± 0.25	27.44 ± 0.45	460.5 ± 25.0	17.04 ± 1.04	3.13 ± 0.23	1.50 ± 0.05	49.07 ± 3.17	-3.34 ± 0.10
18	20.96 ± 0.54	28.87 ± 0.59	482.2 ± 21.3	19.31 ± 0.69	3.93 ± 0.27	1.59 ± 0.04	43.83 ± 1.85	-3.66 ± 0.08
19	19.76 ± 0.44	28.02 ± 0.77	483.3 ± 28.2	17.08 ± 0.60	3.15 ± 0.17	1.46 ± 0.04	50.03 ± 2.29	-3.19 ± 0.10
20	19.81 ± 0.31	27.73 ± 0.60	489.0 ± 8.8	17.55 ± 0.46	3.26 ± 0.21	1.51 ± 0.04	47.66 ± 1.81	-3.07 ± 0.10
21	21.06 ± 0.34	29.05 ± 0.51	438.8 ± 8.6	17.92 ± 0.60	3.68 ± 0.24	1.44 ± 0.03	51.69 ± 1.58	-3.64 ± 0.07
22	19.80 ± 0.51	27.53 ± 0.93	498.8 ± 26.0	17.74 ± 0.82	3.23 ± 0.28	1.51 ± 0.05	47.83 ± 2.55	-3.23 ± 0.14
23	21.53 ± 0.50	29.69 ± 0.55	437.1 ± 20.9	18.46 ± 0.75	3.96 ± 0.27	1.53 ± 0.04	46.51 ± 1.93	-3.64 ± 0.07
24	20.90 ± 0.36	28.36 ± 0.52	416.0 ± 20.3	16.49 ± 0.52	3.24 ± 0.17	1.38 ± 0.04	55.55 ± 2.18	-3.57 ± 0.06
25	19.22 ± 0.44	27.00 ± 0.78	471.5 ± 13.4	15.89 ± 0.41	2.78 ± 0.21	1.38 ± 0.02	54.94 ± 1.08	-3.63 ± 0.09
26	19.35 ± 0.40	26.30 ± 0.51	436.4 ± 15.6	14.74 ± 0.70	2.49 ± 0.20	1.38 ± 0.02	55.30 ± 1.27	-3.66 ± 0.15
27	19.92 ± 0.54	27.83 ± 0.64	469.3 ± 22.9	16.75 ± 0.52	3.09 ± 0.21	1.47 ± 0.04	49.92 ± 2.26	-3.84 ± 0.10
28	19.35 ± 0.42	26.80 ± 0.61	457.4 ± 18.9	15.54 ± 0.61	2.66 ± 0.18	1.38 ± 0.02	55.42 ± 1.61	-3.84 ± 0.09
29	21.75 ± 0.37	28.84 ± 0.72	417.2 ± 16.5	18.02 ± 0.93	3.80 ± 0.35	1.39 ± 0.03	54.84 ± 2.19	-2.82 ± 0.10
30	21.54 ± 0.51	28.73 ± 0.77	417.0 ± 6.6	17.72 ± 0.75	3.69 ± 0.34	1.41 ± 0.02	53.03 ± 1.46	-3.14 ± 0.13

Table S3.2: Standard errors, test statistics, and degrees of freedom of linear mixed effects models examining the influence of climatic water balance (CWB), plant available water capacity (AWC), Hegyi competition index (CI, log-transformed), branch age (log-transformed) and tree height as fixed effect variables and site as random effect on mean vessel diameter (D), hydraulically weighted vessel diameter (D_h), vessel density (VD), lumen to sapwood area ratio (A_L/A_X, log-transformed), potential hydraulic conductivity (K_p, log-transformed), vessel grouping index (VGI) and vessel solitary fraction (VSF); n = 296. See Table 3.2 for estimates and *p*-values.

|		Intercept	CWB	AWC	log (CI)	log (**Br. age**)	**Tree height**
D	*SE*	0.147	0.151	0.149	0.08	0.08	0.11
	t - val.	139.222	2.549	1.522	-0.313	-10.117	-1.331
	df	25.226	26.591	25.272	288.789	289.633	168.366
D$_h$	*SE*	0.216	0.222	0.218	0.13	0.129	0.173
	t - val.	130.836	1.968	0.531	-0.349	-6.638	-0.955
	df	25.312	26.77	25.355	289.888	289.817	142.239
VD	*SE*	2.992	3.131	3.026	2.895	2.832	3.138
	t - val.	153.735	0.59	-2.203	1.275	13.271	0.023
	df	26.242	27.733	26.171	265.09	232.667	63.919
log (A_L/A_X)	*SE*	0.015	0.015	0.015	0.008	0.008	0.011
	t - val.	190.87	2.669	0.372	0.438	0.276	-1.63
	df	25.751	27.175	25.797	289.288	289.926	160.791
log (K_p)	*SE*	0.03	0.031	0.031	0.016	0.016	0.022
	t - val.	39.69	2.435	0.617	0.163	-4.403	-1.438
	df	25.738	27.065	25.784	287.788	288.741	186.223
VGI	*SE*	0.009	0.009	0.009	0.005	0.005	0.006
	t - val.	44.045	1.442	-0.839	-0.326	4.802	-1.637
	df	26.694	28.076	26.742	288.056	288.965	186.138
VSF	*SE*	0.721	0.74	0.729	0.381	0.38	0.527
	t - val.	68.182	-1.472	0.794	0.099	-5.273	1.451
	df	26.632	28.028	26.68	288.306	289.198	181.994

Table S3.3: Results of a linear mixed effects model examining the influence of climatic water balance (CWB), plant available water capacity (AWC), Hegyi competition index (CI, log-transformed) and tree height as fixed effect variables and site as random effect on branch age (log-transformed); n = 296.

	Branch age (log)				
Fixed parts	*Est.*	*Std. error.*	*Test statistic*	*df*	*p*
(Intercept)	1.876	0.042	44.214	25.991	**>0.001**
CWB	-0.041	0.044	-0.952	27.331	0.350
AWC	0.031	0.043	0.728	25.948	0.473
log (CI)	0.005	0.025	0.213	290.528	0.831
Tree height	0.006	0.033	0.171	154.935	0.865
Random part					
Sd (Intercept)	0.200				
Sd (Obs.)	0.373				
Variance components (%)					
Fixed effects	1.6				
Random effects	21.9				
Residual	76.5				

Table S3.4: Results of linear mixed effects models examining the influence of climatic water balance (CWB), plant-available water capacity (AWC), Hegyi competition index (CI, log-transformed), branch age (log-transformed), tree height and distance to the branch tip (Dist. To tip) as fixed variables and site as random variable on mean vessel diameter (D) and hydraulically weighted vessel diameter (D_h). n = 296.

	D					D_h				
Fixed parts	*Est.*	*SE*	*t - val.*	*df*	*p*	*Est.*	*SE*	*t - val.*	*df*	*p*
(Intercept)	20.472	0.144	141.835	24.960	**<0.001**	28.203	0.216	130.783	25.281	**<0.001**
CWB	0.386	0.148	2.603	26.327	**0.015**	0.437	0.222	1.968	26.737	0.059
AWC	0.219	0.146	1.500	25.045	0.146	0.112	0.218	0.512	25.371	0.613
log (CI)	-0.033	0.080	-0.405	288.060	0.686	-0.049	0.130	-0.374	288.910	0.709
log(Br. age)	-0.821	0.080	-10.239	288.878	**<0.001**	-0.865	0.130	-6.656	288.689	**<0.001**
Tree height	-0.154	0.109	-1.407	163.071	0.161	-0.168	0.173	-0.971	141.877	0.831
Dist. to tip	0.136	0.079	1.718	288.083	0.087	0.076	0.128	0.591	288.989	0.865
Random part										
SD (Intercept)	0.690					0.999				
SD (Obs.)	1.211					1.980				
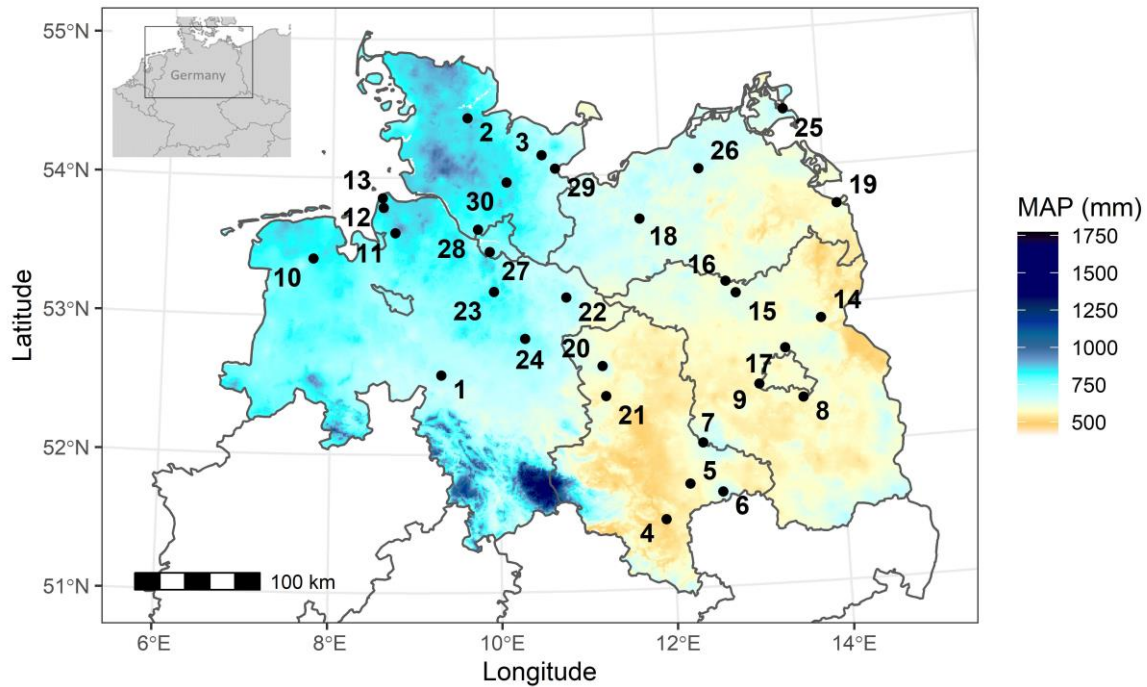
Figure S3.1: Map of the northern part of Germany with federal states and the location of the 30investigated beech stands. Colours indicate mean annual precipitation (MAP, 1991-2018, data provided by DWD). See Table 1 for site codes.
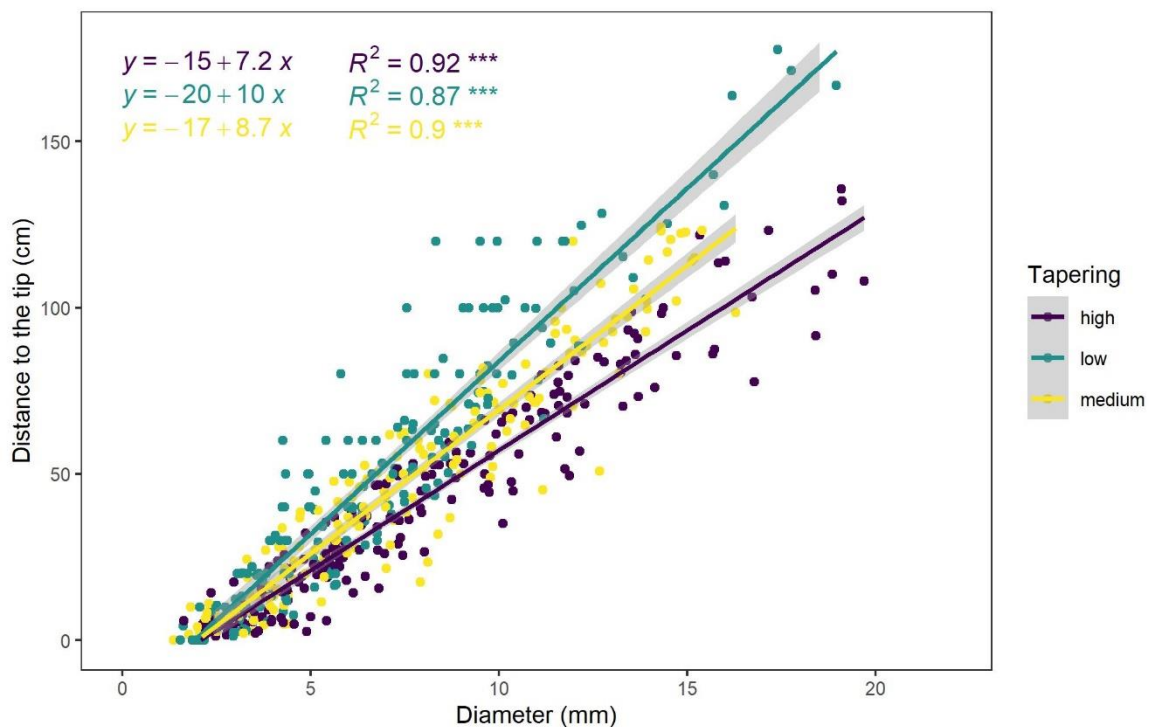
Figure S3.2: Linear regression analyses showing the relationship between branch diameter and the distance to the branch tip for 85 additional upper-canopy beech branches analyzed (data source: Hajek et al. 2015). Branches were divided into three equal-sized groups according to their tapering rates (high: >0.11 mm cm^{-1}, medium: 0.89 - 0.11 mm cm^{-1}, low: < 0.89 mm cm^{-1}). Asterisks indicate the level of significance (***, $p < 0.001$).
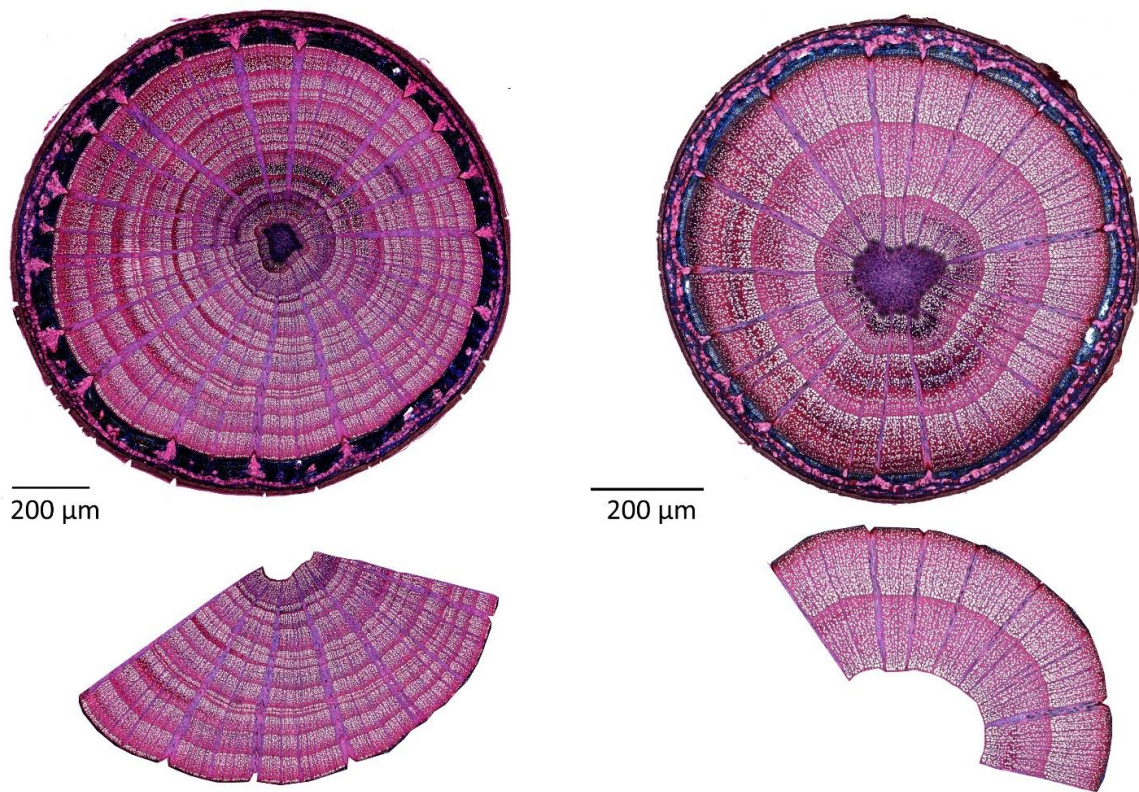
Figure S3.3: Cross sections of two branch samples (top) and the corresponding section that was used for the analyses.
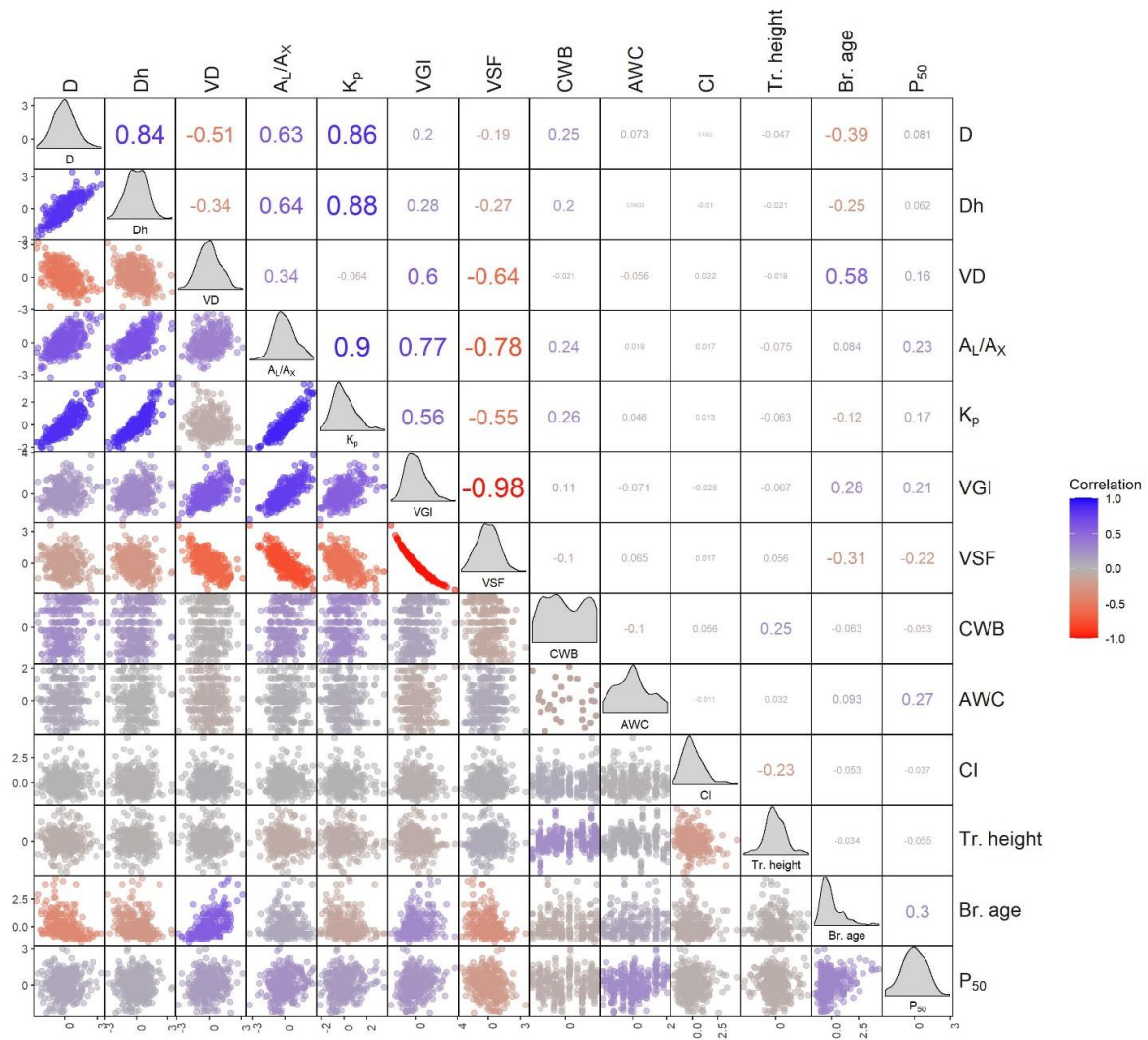
Figure S3.4: Correlation matrix of mean vessel diameter (*D*), hydraulically weighted vessel diameter (D_h), vessel density (VD), lumen to sapwood area ratio (A_L/A_X), potential hydraulic conductivity (K_p), vessel grouping index (VGI), vessel solitary fraction (VSF), climatic water balance (CWB), plant available water capacity (AWC), Hegyi competition index (CI), tree height and branch age. The lower triangle depicts the variables from x- and y-axis in relation, the upper triangle shows the correlation strength (Pearson's *r*) and the plot diagonal shows density plots of the corresponding variables.
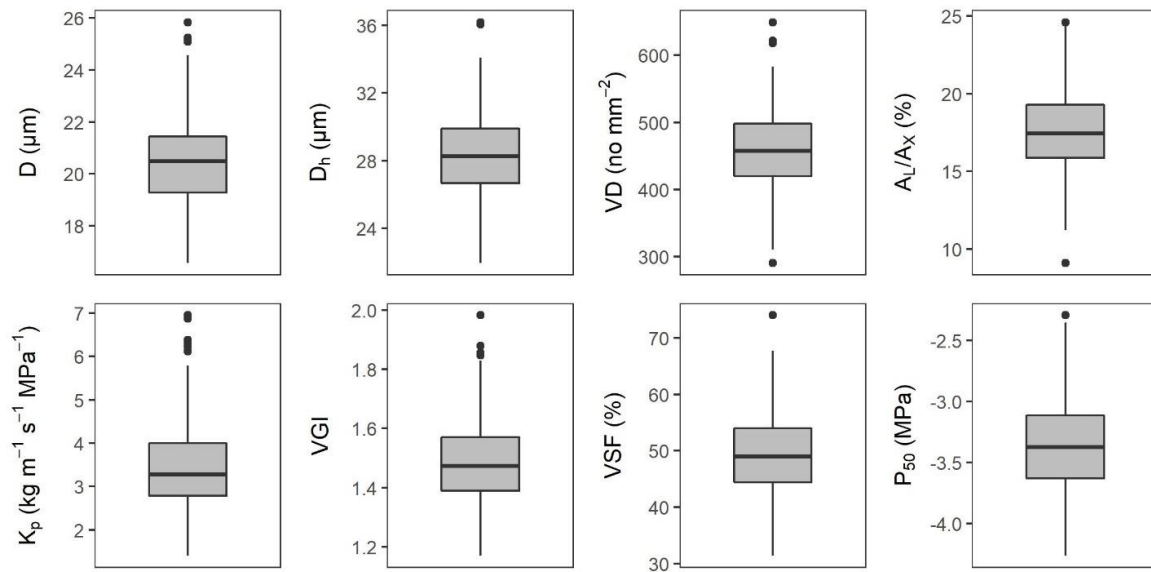
Figure S3.5: Boxplots showing median, 25- and 75-percentiles, minimum, maximum and outliers of mean vessel diameter (D), hydraulically-weighted vessel diamter (D_h), vessel density (VD), lumen-to-sapwood area ratio (A_L/A_X), potential hydraulic conductivity (K_p), vessel grouping index (VGI), vessel solitary fraction (VSF), and pressure causing 50% loss of hydraulic conductance (P_{50}) for the whole sample consisting of each 10 trees of 30 stands.
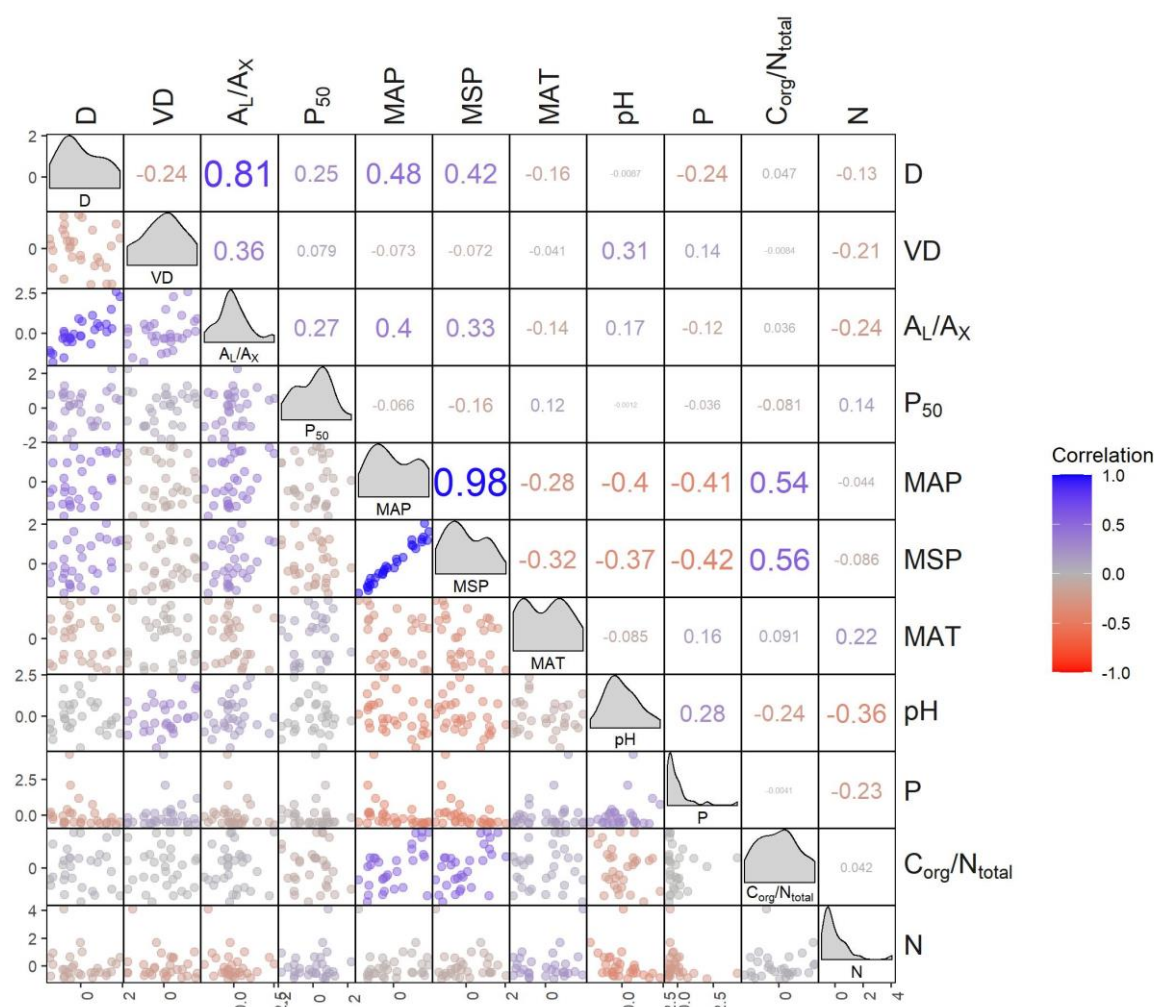
Figure S3.6: Correlation matrix of mean branch anatomical variables (vessel diameter (D), vessel density (VD), lumen to sapwood area ratio (A_L/A_X)), climatic variables (mean annual precipitation (MAP), mean spring precipitation (MSP), mean annual temperature (MAT)), and chemical properties of mineral soil (pH value, organic carbon to total nitrogen ratio (C_{org}/N_{total}), phosphor content (P) and nitrogen content (N)). Anatomical variables were averaged by site (n = 30), mean climatic variables of the 30 sites refer to the period from 1991-2018 and soil variables are means of three depth layers (up to 60cm, n = 6 per site). Values are scaled by the standard deviation and centered around zero. The lower triangle depicts the variables from x- and y-axis in relation, the upper triangle shows the correlation strength (Pearson's r) and the plot diagonal shows density plots of the corresponding variables
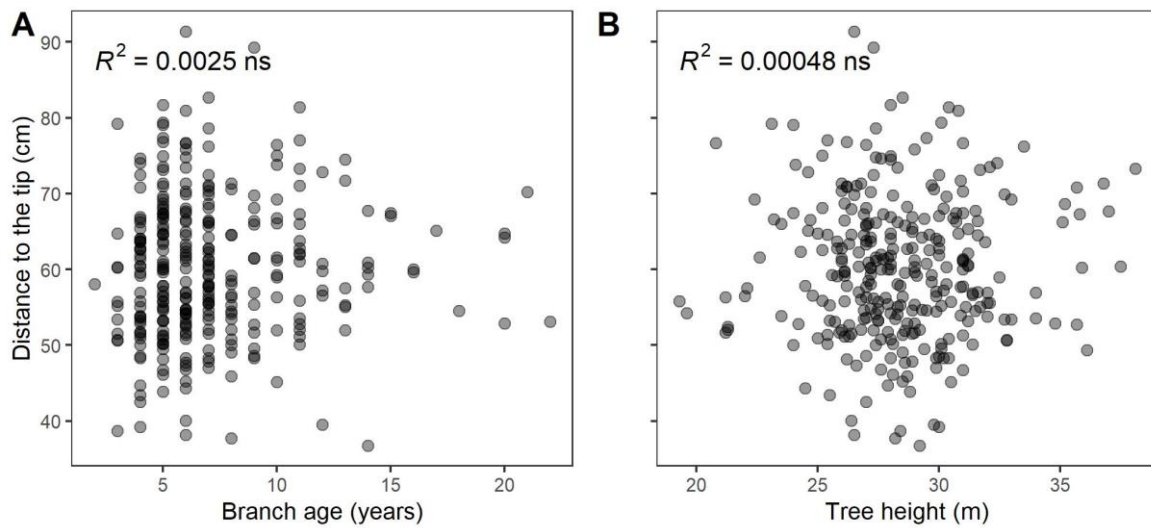
Figure S7: Relationship between (A) branch age and (B) tree height and estimated distance to the branch tip (ns: non-significant relation).
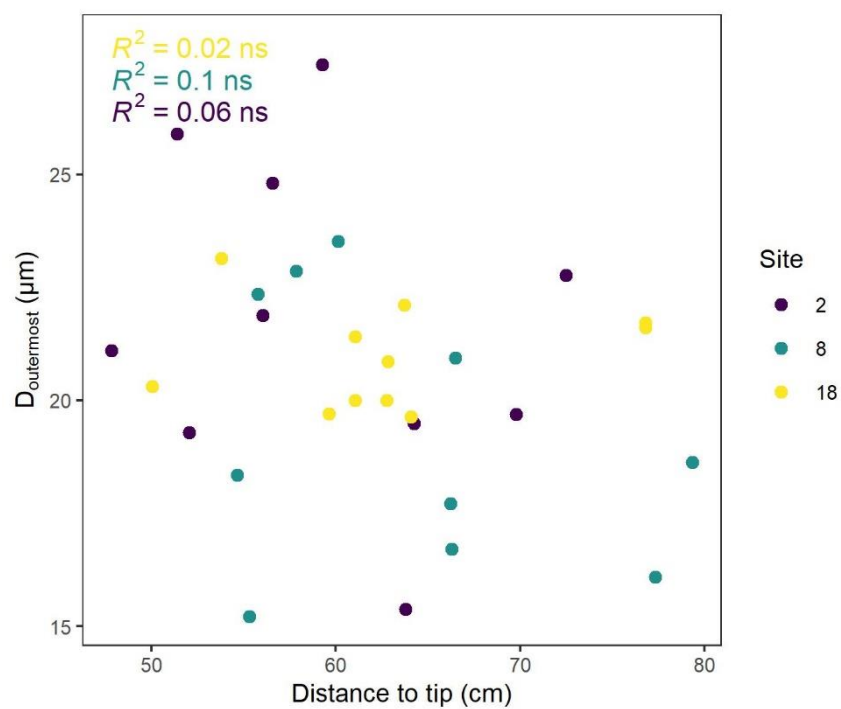
Figure S3.8: Linear regression analyses showing the effect of the distance to the branch tip on mean vessel diameter of the outermost annual ring for 30 samples from three sites with high (site 2: 25.6mm) intermediate (site 18: 5.6mm) and low (site 8: -7.3mm) climatic water balance.

References

Aloni R. 2001. Foliar and axial aspects of vascular differentiation: hypotheses and evidence. *Journal of Plant Growth Regulation* **20**: 22–34.

Aloni R. 2015. Ecophysiological implications of vascular differentiation and plant evolution. *Trees* **29**: 1–16.

Aloni R, Zimmermann MH. 1983. The control of vessel size and density along the plant axis. *Differentiation* **24**: 203–208.

Anfodillo T, Petit G, Crivellaro A. 2013. Axial conduit widening in woody species: a still neglected anatomical pattern. In: Baas P, ed. *Wood Structure in Plant Biology and Ecology.* Leiden: Brill, 24–36.

Anfodillo T, Carraro V, Carrer M, Fior C, Rossi S. 2006. Convergent tapering of xylem conduits in different woody species. *New Phytologist* **169**: 279–290.

Aranda I, Bahamonde HA, Sánchez-Gómez D. 2017. Intra-population variability in the drought response of a beech (*Fagus sylvatica* L.) population in the southwest of Europe. *Tree Physiology* **37**: 938–949.

Arx G von, Carrer M. 2014. ROXAS – A new tool to build centuries-long tracheid-lumen chronologies in conifers. *Dendrochronologia* **32**: 290–293.

Awad H, Barigah T, Badel E, Cochard H, Herbette S. 2010. Poplar vulnerability to xylem cavitation acclimates to drier soil conditions. *Physiologia Plantarum* **139**: 280–288.

Baas P, Werker E, Fahn A. 1983. Some ecological trends in vessel characters. *IAWA Journal* **4**: 141–159.

Bartón K. 2020. MuMIn: Multi-Model Inference. https://CRAN.R-project.org/package=MuMIn.

Bates D, Mächler M, Bolker B, Walker S. 2015. Fitting linear mixed-effects models using lme4. *Journal of Statistical Software* **67**: 1–48.

Boessenkool B. 2020. rdwd: Select and download climate data from 'DWD' (German Weather Service). https://CRAN.R-project.org/package=rdwd.

Borghetti M, Gentilesca T, Leonardi S, van Noije T, Rita A, Mencuccini M. 2017. Long-term temporal relationships between environmental conditions and xylem functional traits: a meta-analysis across a range of woody species along climatic and nitrogen deposition gradients. *Tree Physiology* **37**: 4–17.

Burgess SSO, Pittermann J, Dawson TE. 2006. Hydraulic efficiency and safety of branch xylem increases with height in *Sequoia sempervirens* (D. Don) crowns. *Plant, Cell & Environment* **29**: 229–239.

Cabon A, Fernández-de-Uña L, Gea-Izquierdo G, Meinzer FC, Woodruff DR, Martínez-Vilalta J, Cáceres M. 2020. Water potential control of turgor-driven tracheid enlargement in Scots pine at its xeric distribution edge. *New Phytologist* **225**: 209–221.

Carlquist S. 1977. Wood anatomy of Onagraceae: additional species and concepts. *Annals of the Missouri Botanical Garden* **64**: 627.

Carrer M, von Arx G, Castagneri D, Petit G. 2015. Distilling allometric and environmental information from time series of conduit size: the standardization issue and its relationship to tree hydraulic architecture. *Tree Physiology* **35**: 27–33.

Chenlemuge T, Schuldt B, Dulamsuren C, Hertel D, Leuschner C, Hauck M. 2015. Stem increment and hydraulic architecture of a boreal conifer (*Larix sibirica*) under contrasting macroclimates. *Trees* **29**: 623–636.

Christman MA, Sperry JS, Adler FR. 2009. Testing the 'rare pit' hypothesis for xylem cavitation resistance in three species of *Acer*. *New Phytologist* **182**: 664–674.

Cochard H, Damour G, Bodet C, Tharwat I, Poirier M, Améglio T. 2005. Evaluation of a new centrifuge technique for rapid generation of xylem vulnerability curves. *Physiologia plantarum* **124**: 410–418.

Fajardo A, Martínez-Pérez C, Cervantes-Alcayde MA, Olson ME. 2020. Stem length, not climate, controls vessel diameter in two trees species across a sharp precipitation gradient. *New Phytologist* **225**: 2347–2355.

Fan Z-X, Cao K-F, Becker P. 2009. Axial and radial variations in xylem anatomy of angiosperm and conifer trees in Yunnan, China. *IAWA Journal* **30**: 1–13.

Fichot R, Barigah TS, Chamaillard S, Le Thiec D, Laurans F, Cochard H, Brignolas F. 2010. Common trade-offs between xylem resistance to cavitation and other physiological traits do not hold among unrelated *Populus deltoides* x *Populus nigra* hybrids. *Plant, Cell & Environment* **33**: 1553–1568.

Fonti P, Heller O, Cherubini P, Rigling A, Arend M. 2013. Wood anatomical responses of oak saplings exposed to air warming and soil drought. *Plant Biology* **15:** 210–219.

Gartner BL, Lei H, Milota MR. 1997. Variation in the anatomy and specific gravity of wood within and between trees of red alder (*Alnus rubra* Bong.). *Wood and Fiber Science* **29**: 10–20.

van Genuchten MT. 1980. A closed-form equation for predicting the hydraulic conductivity of unsaturated soils. *Soil Science Society of America Journal* **44**: 892–898.

van Genuchten MT, Leij FJ, Yates SR. 1991. The RETC code for quantifying the hydraulic functions of unsaturated soils. Washington, D.C.: Environmental Protection Agency EPA/600/2-91/065.

Gleason SM, Blackman CJ, Gleason ST, McCulloh KA, Ocheltree TW, Westoby M. 2018. Vessel scaling in evergreen angiosperm leaves conforms with Murray's law and area-filling assumptions: implications for plant size, leaf size and cold tolerance. *New Phytologist* **218**: 1360–1370.

Hacke UG, Spicer R, Schreiber SG, Plavcová L. 2017. An ecophysiological and developmental perspective on variation in vessel diameter. *Plant, Cell & Environment* **40**: 831–845.

Hacke UG, Sperry JS, Wheeler JK, Castro L. 2006. Scaling of angiosperm xylem structure with safety and efficiency. *Tree Physiology* **26**: 689–701.

Hajek P, Leuschner C, Hertel D, Delzon S, Schuldt B. 2014. Trade-offs between xylem hydraulic properties, wood anatomy and yield in *Populus*. *Tree Physiology* **34**: 744–756.

Hajek P, Kurjak D, Wühlisch G von, Delzon S, Schuldt B. 2016. Intraspecific variation in wood anatomical, hydraulic, and foliar traits in ten European beech provenances differing in growth yield. *Frontiers in Plant Science* **7**: 791.

Hajek P, Seidel D, Leuschner C. 2015. Mechanical abrasion, and not competition for light, is the dominant canopy interaction in a temperate mixed forest. *Forest Ecology and Management* **348**: 108–116.

Hallé F, Oldeman RAA, Tomlinson PB. 1978. Tropical trees and forests: An architectural analysis. Berlin, Heidelberg: Springer.

Hatton TJ, Salvucci GD, Wu HI. 1997. Eagleson's Optimality Theory of an ecohydrological equilibrium: Quo vadis? *Functional Ecology* **11**: 665-674.

Hegyi F. 1974. A simulation model for managing jack pine stands: In: Fries J, ed. *Growth models for tree and stand simulation*. Stockholm: Royal College of Forestry, 74–90.

Herbette S, Wortemann R, Awad H, Huc R, Cochard H, Barigah TS. 2010. Insights into xylem vulnerability to cavitation in *Fagus sylvatica* L.: phenotypic and environmental sources of variability. *Tree Physiology* **30**: 1448-1455.

Jansen S, Choat B, Pletsers A. 2009. Morphological variation of intervessel pit membranes and implications to xylem function in angiosperms. *American Journal of Botany* **96**: 409–419.

Jump AS, Peñuelas J. 2007. Extensive spatial genetic structure revealed by AFLP but not SSR molecular markers in the wind-pollinated tree, *Fagus sylvatica*. *Molecular Ecology* **16**: 925–936.

Kaack L, Weber M, Isasa E, Karimi Z, Li S, Pereira L, Trabi CL, Zhang Y, Schenk HJ, Schuldt B *et al.* 2021. Pore constrictions in intervessel pit membranes provide a mechanistic explanation for xylem embolism resistance in angiosperms. *New Phytologist* **230**: 1829–1843.

Kirfel K, Leuschner C, Hertel D, Schuldt B. 2017. Influence of root diameter and soil depth on the xylem anatomy of fine- to medium-sized roots of mature beech trees in the top- and subsoil. *Frontiers in Plant Science* **8**: 1194.

Kuznetsova A, Brockhoff PB, Christensen RHB. 2017. lmerTest package: tests in linear mixed effects models. *Journal of Statistical Software* **82**: 1–26.

Lachenbruch B, Moore JR, Evans R. 2011. Radial variation in wood structure and function in woody plants, and hypotheses for its occurrence. In: Meinzer FC, Lachenbruch B, Dawson TE eds. *Size- and age-related changes in tree structure and function*. Dordrecht, Netherlands: Springer, 121–164.

Lambers H, Oliveira RS. 2019. *Plant physiological ecology*, Third edition. Cham: Springer Nature Switzerland AG.

Leal S, Sousa VB, Pereira H. 2007. Radial variation of vessel size and distribution in cork oak wood (*Quercus suber* L.). *Wood Science and Technology* **41**: 339–350.

Lechthaler S, Turnbull TL, Gelmini Y, Pirotti F, Anfodillo T, Adams MA, Petit G. 2019. A standardization method to disentangle environmental information from axial trends of xylem anatomical traits. *Tree Physiology* **39**: 495–502.

Lemaire C, Quilichini Y, Brunel-Michac N, Santini J, Berti L, Cartailler J, Conchon P, Badel É, Herbette S. 2020. Plasticity of the xylem vulnerability to embolism in poplar relies on quantitative pit properties rather than on pit structure. *bioRxiv*. doi: 05.14.096222.

Lens F, Sperry JS, Christman MA, Choat B, Rabaey D, Jansen S. 2011. Testing hypotheses that link wood anatomy to cavitation resistance and hydraulic conductivity in the genus *Acer*. *New Phytologist* **190**: 709–723.

Leuschner C. 2020. Drought response of European beech (*Fagus sylvatica* L.) - A review. *Perspectives in Plant Ecology, Evolution and Systematics* **47**: 125576.

Lewis AM, Boose ER. 1995. Estimating volume flow rates through xylem conduits. *American Journal of Botany* **82**: 1112–1116.

Li S, Lens F, Espino S, Karimi Z, Klepsch M, Schenk HJ, Schmitt M, Schuldt B, Jansen S. 2016. Intervessel pit membrane thickness as a key determinant of embolism resistance in angiosperm xylem. *IAWA Journal* **37**: 152–171.

Li S, Li X, Link R, Li R, Deng L, Schuldt B, Jiang X, Zhao R, Zheng J, Li S, Yin Y. 2019. Influence of cambial age and axial height on the spatial patterns of xylem traits in *Catalpa bungei*, a ring-porous tree species native to China. *Forests* **10**: 662.

Liang X, He P, Liu H, Zhu S, Uyehara IK, Hou H, Wu G, Zhang H, You Z, Xiao Y, Ye Q. 2019. Precipitation has dominant influences on the variation of plant hydraulics of the

native *Castanopsis fargesii* (Fagaceae) in subtropical China. *Agricultural and Forest Meteorology* **271**: 83–91.

Link RM. 2020. corrmorant: Flexible correlation matrices based on 'ggplot2'. R package version 0.0.0.9007. http://github.com/r-link/corrmorant.

Liu H, Gleason SM, Hao G, Hua L, He P, Goldstein G, Ye Q. 2019. Hydraulic traits are coordinated with maximum plant height at the global scale. *Science Advances* **5**: eaav1332.

Loepfe L, Martinez-Vilalta J, Piñol J, Mencuccini M. 2007. The relevance of xylem network structure for plant hydraulic efficiency and safety. *Journal of Theoretical Biology* **247**: 788–803.

Lübbe T, Schuldt B, Leuschner C. 2017. Acclimation of leaf water status and stem hydraulics to drought and tree neighbourhood: alternative strategies among the saplings of five temperate deciduous tree species. *Tree Physiology* **37**: 456–468.

Maherali H, Pockman WT, Jackson RB. 2004. Adaptive variation in the vulnerability of woody plants to xylem cavitation. *Ecology* **85**: 2184–2199.

Martínez-Vilalta J, Cochard H, Mencuccini M, Sterck F, Herrero A, Korhonen JFJ, Llorens P, Nikinmaa E, Nolè A, Poyatos R *et al.* 2009. Hydraulic adjustment of Scots pine across Europe. *New Phytologist* **184**: 353–364.

Nakagawa S, Johnson PCD, Schielzeth H. 2017. The coefficient of determination R^2 and intra-class correlation coefficient from generalized linear mixed-effects models revisited and expanded. *Journal of the Royal Society, Interface* **14**. doi: 10.1098/rsif.2017.0213.

Nonweiler T. 1975. Flow of biological fluids through non-ideal capillaries. In: Zimmermann MH, Milburn JA eds. *Encyclopedia of plant physiology. New series. 1: Transport in plants. 1: Phloem transport, Appendix 1.* Berlin: Springer, 474-477.

Ogasa M, Miki NH, Murakami Y, Yoshikawa K. 2013. Recovery performance in xylem hydraulic conductivity is correlated with cavitation resistance for temperate deciduous tree species. *Tree Physiology* **33**: 335–344.

Olson M, Rosell JA, Martínez-Pérez C, León-Gómez C, Fajardo A, Isnard S, Cervantes-Alcayde MA, Echeverría A, Figueroa-Abundiz VA, Segovia-Rivas A et al. 2020. Xylem vessel-diameter–shoot-length scaling: ecological significance of porosity types and other traits. *Ecological Monographs*: **90**. doi: 10.1002/ecm.1410.

Olson ME, Anfodillo T, Rosell JA, Petit G, Crivellaro A, Isnard S, León-Gómez C, Alvarado-Cárdenas LO, Castorena M. 2014. Universal hydraulics of the flowering plants: vessel diameter scales with stem length across angiosperm lineages, habits and climates. *Ecology Letters* **17**: 988–997.

Olson ME, Soriano D, Rosell JA, Anfodillo T, Donoghue MJ, Edwards EJ, León-Gómez C, Dawson T, Camarero Martínez JJ, Castorena M, Echeverría A *et al.* 2018. Plant height and hydraulic vulnerability to drought and cold. *PNAS* **115**: 7551–7556.

Olson ME, Anfodillo T, Gleason SM, McCulloh KA. 2021. Tip-to-base xylem conduit widening as an adaptation: causes, consequences, and empirical priorities. *New Phytologist* **229**: 1877–1893.

Petit G, von Arx G, Kiorapostolou N, Lechthaler S, Prendin AS, Anfodillo T, Caldeira MC, Cochard H, Copini P, Crivellaro A, Delzon S, Gebauer R, Gričar J, Grönholm L, Hölttä T, Jyske T, Lavrič M, Lintunen A, Lobo-do-Vale R, Peltoniemi M, Peters RL, Robert EMR, Roig Juan S, Senfeldr M, Steppe K, Urban J, Van Camp J, Sterck F. 2018. Tree differences in primary and secondary growth drive convergent scaling in leaf area to sapwood area across Europe. *New Phytologist* **218**:1383–1392.

Petit G, Pfautsch S, Anfodillo T, Adams MA. 2010. The challenge of tree height in Eucalyptus regnans: when xylem tapering overcomes hydraulic resistance. *New Phytologist* **187**: 1146–1153.

Pfautsch S, Harbusch M, Wesolowski A, Smith R, Macfarlane C, Tjoelker MG, Reich PB, Adams MA. 2016. Climate determines vascular traits in the ecologically diverse genus *Eucalyptus*. *Ecology letters* **19**: 240–248.

Piedallu C, Gégout J-C, Perez V, Lebourgeois F. 2013. Soil water balance performs better than climatic water variables in tree species distribution modelling. *Global Ecology and Biogeography* **22**: 470–482.

R Core Team. 2020. R: a language and environment for statistical computing. R Foundation for Statistical Computing. Vienna, Austria. https://www.R-project.org/.

Rosell JA, Olson ME, Anfodillo T. 2017. Scaling of xylem vessel diameter with plant size: causes, predictions, and outstanding questions. *Current Forestry Reports* 3:46–59.

Sass U, Eckstein D. 1995. The variability of vessel size in beech (*Fagus sylvatica* L.) and its ecophysiological interpretation. *Trees* **9**: 247–252.

Schaap MG, Leij FJ, van Genuchten MT. 2001. rosetta: a computer program for estimating soil hydraulic parameters with hierarchical pedotransfer functions. *Journal of Hydrology* **251**: 163–176.

Schreiber SG, Hacke UG, Hamann A. 2015. Variation of xylem vessel diameters across a climate gradient: insight from a reciprocal transplant experiment with a widespread boreal tree. *Functional Ecology* **29**: 1392–1401.

Schuldt B, Buras A, Arend M, Vitasse Y, Beierkuhnlein C, Damm A, Gharun M, Grams TEE, Hauck M, Hajek P *et al.* 2020. A first assessment of the impact of the extreme 2018 summer drought on Central European forests. *Basic and Applied Ecology* **45**: 86–103.

Schuldt B, Knutzen F, Delzon S, Jansen S, Müller-Haubold H, Burlett R, Clough Y, Leuschner C. 2016. How adaptable is the hydraulic system of European beech in the face of climate change-related precipitation reduction? *New Phytologist* **210**: 443–458.

Schumann K, Leuschner C, Schuldt B. 2019. Xylem hydraulic safety and efficiency in relation to leaf and wood traits in three temperate *Acer* species differing in habitat preferences. *Trees* **33**: 1475–1490.

Sperry JS, Nichols KL, Sullivan JEM, Eastlack SE. 1994. Xylem embolism in ring-porous, diffuse-porous, and coniferous trees of northern Utah and interior Alaska. *Ecology* **75**:1736–1752.

Stojnic S, Suchocka M, Benito-Garzón M, Torres-Ruiz JM, Cochard H, Bolte A, Cocozza C, Cvjetkovic B, Luis M de, Martinez-Vilalta J *et al.* 2018. Variation in xylem vulnerability to embolism in European beech from geographically marginal populations. *Tree Physiology* **38**: 173–185.

Walthert L, Ganthaler A, Mayr S, Saurer M, Waldner P, Walser M, Zweifel R, Arx G von. 2021. From the comfort zone to crown dieback: sequence of physiological stress thresholds in mature European beech trees across progressive drought. *Science of the Total Environment* **753**: 141792.

Weithmann G, Link R, Banzragch B-E, Würzberg L, Leuschner C, Schuldt B. 2022. Soil water availability and branch age explain variability in xylem safety of European beech in Central Europe. *Oecologia* **198**: 629–644.

West GB, Brown JH, Enquist BJ. 1999. A general model for the structure and allometry of plant vascular systems. *Nature* **400**: 664–667.

Wheeler EA, Baas P. 1993. The potentials and limitations of dicotyledonous wood anatomy for climatic reconstructions. *Paleobiology* **19**: 487–498.

Wickham H, Averick M, Bryan J, Chang W, McGowan LD'A, François R, Grolemund G, Hayes A, Henry L, Hester J *et al.* 2019. Welcome to the tidyverse. *Journal of Open Source Software* **4**: 1686.

Wiemann MC, Wheeler EA, Manchester SR, Portier KM. 1998. Dicotyledonous wood anatomical characters as predictors of climate. *Palaeogeography, Palaeoclimatology, Palaeoecology* **139**: 83–100.

Woodruff DR, Bond BJ, Meinzer FC. 2004. Does turgor limit growth in tall trees? *Plant, Cell & Environment* **27**: 229-236.

Wortemann R, Herbette S, Barigah TS, Fumanal B, Alia R, Ducousso A, Gomory D, Roeckel-Drevet P, Cochard H. 2011. Genotypic variability and phenotypic plasticity of cavitation resistance in *Fagus sylvatica* L. across Europe. *Tree Physiology* **31**: 1175–1182.

Zhao X. 2015. Effects of cambial age and flow path-length on vessel characteristics in birch. *Journal of Forestry Research* **20**: 175–185.

Zimmermann J, Link RM, Hauck M, Leuschner C, Schuldt B. **2021**. 60-year record of stem xylem anatomy and related hydraulic modification under increased summer drought in ring- and diffuse-porous temperate broad-leaved tree species. *Trees* **35**: 919–937.

Zimmermann MH. 1983. Xylem structure and the ascent of sap. Berlin, Heidelberg: Springer.

CHAPTER 4

Leaf trait modification in European beech trees in response to climatic and edaphic drought

Greta Weithmann, Bernhard Schuldt, Roman M. Link, Dorothea Heil,
Stefanie Hoeber, Hanna John, Hilmar Müller-Haubold, Lisa-Marie Schüller,
Katja Schumann, Christoph Leuschner

4.1 Abstract

Leaf morphological and physiological traits control the carbon and water relations of mature trees and are determinants of drought tolerance, but it is not well understood how they are modified in response to water deficits.

We analysed five sun-canopy leaf traits (mean leaf size (LS), specific leaf area (SLA), Huber value (HV), water potential at turgor loss point (Ψ_{tlp}) and foliar carbon isotope signature ($\delta^{13}C$)) in European beech (*Fagus sylvatica* L.) across three precipitation gradients sampled in moist (2010), dry (2019) and very dry summers (2018), and tested their response to short-term water deficits (climatic water balance (CWB) preceding the sample collection) and long-term water availability (including the effects of mean annual precipitation (MAP), plant-available soil water capacity (AWC) and neighbourhood competition).

Across the 34 sites, mean LS varied nearly sevenfold ($3.9 - 27.0$ cm^2), SLA fourfold ($77.1 - 306.9$ cm² g^{-1}) and HV sixfold ($1.0 - 6.65$ cm^2 m^{-2}). In the 2018 dataset, LS showed a negative and HV a positive relation to MAP, which is opposite to the relations found in multi-species samples. Average Ψ_{tlp} ranged from -1.90 to -2.62 MPa and decreased significantly across the sites with decreasing CWB in the month prior to measurement, as well as with decreasing MAP and AWC in 2019. Studied leaf traits varied considerably between years suggesting that mast fruiting and the severe 2018 drought caused the formation of smaller leaves.

We conclude that sun-canopy leaf traits of European beech exhibit considerable plasticity in response to climatic and edaphic aridity, and that osmotic adjustment may be an important element in the drought response strategy of this anisohydric tree species.

Keywords: Drought adaptation, Huber value, leaf size, leaf morphology, precipitation gradient, sapwood-to-leaf-area ratio, specific leaf area, water potential at turgor loss point.

4.2 Introduction

European beech *(Fagus sylvatica* L.) is Europe's most important temperate tree species, which dominates the natural forest vegetation of Central Europe and represents an important timber species (Leuschner & Ellenberg, 2017). Both experimental evidence with saplings and observations in adult trees indicate that beech is moderately sensitive to drought (Geβler *et al.*, 2004; Leuschner, 2020; Braun *et al.* 2021). Yet, the species follows an anisohydric water potential regulation strategy, encountering considerable drops in leaf water potential (Leuschner *et al.*, 2021). Thus, European beech is dependent on sufficient water supply during summer and likely also high atmospheric humidity, while sensitivity to frost and summer heat are limiting the species to mesic cool-temperate regions (Walthert & Meier, 2017; Leuschner, 2020). These limitations suggest that the species may in large parts of its distribution range be threatened by future increases in the frequency of "hotter droughts", i.e. a combination of drought and high temperatures (Buras *et al.*, 2020). The high mortality of European beech across Central Europe in consequence of the extreme 2018/2019 drought event suggests indeed a high vulnerability to climate warming (Braun *et al.*, 2020; Schuldt *et al.*, 2020; Walthert *et al.*, 2021). Apart from dieback especially on shallow soils and exposed ridges, many beech forests were left with visible foliar loss and crown damage, with only 11 % of Germany's beech forests being assessed as vital in the federal forest health assessment (BMEL 2020, 2021). On the other hand, beech is capable of recovering from moderate drought, if water deficits are not too extreme (van der Werf *et al.*, 2007; Pflug *et al.*, 2018; Dietrich *et al.*, 2019).

Increasing evidence suggests that hydraulic failure is a main mechanism leading to tree death in the context of recent climate warming-related forest dieback (Choat *et al.*, 2012; 2018; Anderegg *et al.*, 2016; Adams *et al.*, 2017; Brodribb *et al.*, 2020). Consequently, several studies have investigated the acclimative and adaptive potential of the hydraulic system of mature beech trees, pointing at only limited adjustment of branch xylem embolism resistance to increasing climatic aridity when comparing different populations (Herbette *et al.*, 2010; Wortemann *et al.*, 2011; Schuldt *et al.*, 2016; Weithmann *et al.,* unpubl.). Further, variability in embolism resistance within populations was usually higher than between populations (Aranda *et al.*, 2015; Hajek *et al.*, 2016; Stojnic *et al.*, 2018). Thus, it remains questionable whether acclimation or adaptation of embolism resistance is an important element in the drought adaptation of European beech, and leaf-level responses might give relevant insights into the species' performance under drought.

Adaptive responses of leaf morphological and functional traits to increasing aridity have mostly been investigated at the interspecific level, i.e. across species and at higher taxonomic levels, while much less is known about the acclimative and adaptive potential of leaf traits of mature trees to increasing water deficits at the intraspecific level. Adjustment to water deficits at the leaf morphological and physiological levels has been demonstrated in numerous interspecific studies, notably through a decrease in leaf size (LS) and specific leaf area (SLA), alteration of sapwood-to-leaf area ratio (Huber value, HV) and shifts in leaf tissue osmotic and elastic properties (Bussotti, 2008; Bartlett *et al.*, 2016; Powell *et al.*, 2017; McGregor *et al.*, 2020). However, linkages detected between leaf traits across species on the global scale may not hold at the intraspecific level (Niinemets, 2015; Anderegg *et al.*, 2018). This is demonstrated by the traits mean LS and SLA, which are typically lower in arid than in wet environments in global or continent-wide species samples (Wright *et al.*, 2002; Wright *et al.*, 2017), while the opposite was found at the intraspecific level in European beech: Meier & Leuschner (2008) and Salehi *et al.* (2020) observed increases in LS and SLA of sun-canopy leaves with decreasing mean annual precipitation along two precipitation gradients in Central European mature beech forests that were explained by higher temperatures at the drier sites, that still were moist during leaf enfolding in early summer. Similarly, a study on changes in HV with increasing climatic aridity found an increase in a global multi-species data set (Mencuccini *et al.*, 2019), but no relation appeared at the intraspecific level for beech populations along a precipitation gradient (Schuldt *et al.*, 2016).

A reduction in stomatal conductance is not only a short-term response to atmospheric and soil water deficits, but may also represent a longer lasting acclimative response of beech to reduced precipitation levels, reflected in elevated levels of leaf tissue $\delta^{13}C$ values (Meier & Leuschner, 2008; but see Schuldt *et al.*, 2016). It is possible that populations differ in the extent of stomatal closure, but evidence for mature trees seems to be lacking.

Widespread leaf shedding after extreme droughts in beech is thought to result from xylem embolism, as none of the trees with leaf loss and crown damage studied by Walthert *et al.* (2021) showed recovery in the subsequent year. This was also observed by Wohlgemuth *et al.* (2020), suggesting that leaf shedding must be considered as a symptom of vulnerability rather than protection against excessive water loss. In correspondence, a lower HV is usually linked to significantly higher embolism rates in mature beech trees (Schuldt *et al.*, 2020). This is in line with results of long-term canopy monitoring, which showed that beeches usually respond to hot summers with elevated defoliation in the following year (Seidling, 2007).

The water potential at turgor loss point (Ψ_{tlp}) was identified in a global data set as the single most influential leaf functional trait determining the drought tolerance of plants, with Ψ_{tlp} generally decreasing from mesic to xeric habitats (Bartlett *et al.*, 2012b). Ψ_{tlp} may also vary at the intraspecific level among populations along gradients of climatic aridity, as observed e.g. in *Eucalyptus obliqua* (Pritzkow *et al.*, 2020) and *Castanopsis fargesii* (Liang *et al.*, 2019). In contrast, a comparison of growing-season Ψ_{tlp} means among four mature European beech stands covering a reduction in mean annual precipitation (MAP) by 520 mm yr^{-1} showed no Ψ_{tlp} decrease with increasing climatic aridity (Schipka, 2002), while others observed osmotic adjustment during the summer period in this important Central European tree species (Backes & Leuschner, 2000; Leuschner *et al.*, 2021). This matches the reduction of Ψ_{tlp} after drought exposure found for saplings and adult beech trees by Tomasella *et al.* (2018; 2019), whereas others did not observe any osmotic adjustment in saplings (Knutzen *et al.*, 2015; Lübbe *et al.*, 2017). Overall, leaf osmotic adjustment in European beech might be less pronounced than in other tree species and may only be important under dry conditions (Leuschner, 2020). It is possible that anisohydric trees such as European beech are conducting significant active osmotic adjustment only upon pronounced drops in leaf water potential (Hartmann *et al.*, 2021, Leuschner *et al.*, 2021).

Apart from precipitation, soil water storage capacity is an important determinant of plant water relations, the importance of which increases with drought and heat intensities in the course of climate warming. As expected, beech trees on deep soils with a higher capacity of plant-available water (AWC) were less affected by the severe 2018/2019 drought (Walthert *et al.*, 2021). While soil physical properties have been considered less often in tree dieback studies than climatic variables, it is obvious that including soil parameters in models dealing with the distribution, vitality or mortality of woody species always improved the predictions (Tai *et al.*, 2017; Walthert & Meier, 2017; Renne *et al.*, 2019). This highlights the importance of including local data on soil water storage capacity, when investigating effects of water availability on tree performance. Another factor, which may influence water availability and thus tree vitality and mortality, is competition with neighbouring trees (Lübbe *et al.*, 2017; Hajek *et al.*, 2020), which has rarely been considered yet.

In the face of changing climatic conditions, phenotypic variation in combination with intraspecific genetic diversity can improve the acclimative and adaptive potential of a plant species (Aubin *et al.*, 2016). Despite the wide distribution range of *F. sylvatica*, this important tree species appears to be vulnerable to global change-type drought events, which demands for a better understanding of the acclimative and adaptive potential of the species

to drought and heat. In this study, we analyse the variation in LS, SLA, HV, the foliar δ^{13}C signature and Ψ_{tlp} in foliage from upper sun-canopy branches of 34 mature European beech forests on mostly sandy soil across three extended mean annual precipitation (MAP) gradients (866 – 497 mm yr^{-1}) in oceanic to sub-continental temperate climates. All sampled branches were collected during mid-summer in the upper sun canopy at similar distance to the tree tip. Sampling was conducted in three years with contrasting spring and early-summer moisture conditions, when leaf out of beech happens, i.e. moist (2010, 4 stands, MAP reduction: 229 mm yr^{-1}), extremely dry (2018, 11 stands, MAP reduction: 353 mm yr^{-1}), and dry conditions (2019, 19 stands, MAP reduction: 301 mm yr^{-1}). Besides precipitation and climatic aridity, we additionally investigated the influence of local soil water storage capacity and competition intensity in the stand on the five leaf traits to assess the influence of site water availability in a more comprehensive way. Sampling 10 (or 4) trees per stand and 3 – 5 branches per tree allowed to partition the observed leaf trait variation to within-tree, within-population and between-population components. We hypothesised, in accordance with the existing evidence on climatic effects on leaf morphological and hydraulic traits, that site water availability (including climatic, edaphic and competition-related effects) will affect leaf traits across the gradients of the 2018- and 2019-sampling campaigns. Across the study years and with decreasing climatic water balance in the period preceding sample collection, we expected mean leaf size (LS), specific leaf area (SLA), and the water potential at turgor loss point (Ψ_{tlp}) to decrease, while foliar carbon isotope signature (δ^{13}C) and Huber value (HV) were thought to increase.

4.3 Materials and Methods

4.3.1 Study sites and climatic conditions

The 34 monospecific mature beech (*Fagus sylvatica* L.) stands are located in the Pleistocene lowlands of northern Germany at elevations between 19 and 159 m a.s.l. (Figure 4.1A). Across the gradient, the climate is cool-temperate with mean annual temperature (MAT, sites 1 – 30: 1958 – 2017, sites 31 – 34: 1950 – 2009) increasing from 8.3 to 9.6°C from West to East and mean annual precipitation (MAP) decreasing from 866 to 497 mm yr^{-1}, reflecting a gradient from an oceanic to a sub-continental cool-temperate climate (Figure 4.1B, Table 4.1). The data for monthly precipitation, air temperature and potential evapotranspiration were extracted for the different sites for the period 1950 – 2019 from 1km-gridded data retrieved from the Climate Data Centre (CDC) of the German Weather Service (DWD,

Deutscher Wetterdienst, Offenbach, https://opendata.dwd.de/, accessed 2021-04-02) using the R package `rdwd` v. 1.2.0 (Boessenkool, 2020). The climatic water balance of the spring months (March to May) of the three sampling years 2010, 2018 and 2019 (CWBS current year), the climatic water balance of the month preceding the sample collection (CWB$_{pre}$), and the full-year climatic water balance for the three sampling years (CWB) was calculated for each site as the difference between precipitation and potential evapotranspiration of the respective months (see Table S4.2 in the Supplement for climatic data of two selected study sites, one in the west and one in the east of the study region).

4.3.2   Edaphic conditions

The sandy soils of the 34 sites developed from glacial deposits of the last (Weichselian) or penultimate (Saalian) Ice Age and were predominantly nutrient-poor with profile depths exceeding 120 cm. None of the soils was influenced by groundwater. For sites $1-30$, details on soil chemical and physical properties are given below, for sites $31-34$ (Calvörde, Göhrde, Sellhorn and Unterlüss with sandy soil texture) see information in Müller-Haubold *et al.* (2013). For analysing soil chemical properties, soil samples were taken in soil pits dug at two randomly placed locations per site, and for estimation of the plant-available soil water capacity (AWC, mm), volume samples from one soil pit each were taken from three different depth layers ($0-10$ cm, $10-30$ cm, $30-60$ cm). Furthermore, the stone content (particles >2 mm) was determined at one pit per site by sieving a volume of 45,000 cm^3. In the laboratory, pH in water was determined in the fresh soil, while soil nitrogen content and soil organic carbon and C/N ratio were determined through gas chromatographic analysis of the dried soil (70 °C, 48 h) (see Table S4.1).

For estimating AWC, particle size distribution, i.e. the relative proportion of sandy ($63-2000$ µm), silty ($2.0-63$ µm), and clay-sized (< 2.0 µm) particles, and soil bulk density were determined. The sand fraction was measured by sieving, and the silt and clay fractions by differential sedimentation in a PARIO Soil Particle Analyser (METER Group AG, Munich, Germany). To estimate soil hydraulic properties (the van Genuchten (1980) parameters), we then employed pedotransfer functions according to Schaap *et al.* (2001), using the module `ROSETTA light` implemented in the software RETC (version 6.02; van Genuchten *et al.*, 1991). From the modelled water retention curves, volumetric water content at permanent wilting point (at a water potential of -1.5 MPa; pF 4.2) and water content at field capacity (at a water potential of -60 hPa; pF 1.8) were extracted and AWC was calculated as the difference between these two water contents for the three depth layers to

60 cm and extrapolated to a standard depth of 100 cm, assuming a homogenous soil particle composition in the $30 - 100$ cm layer.
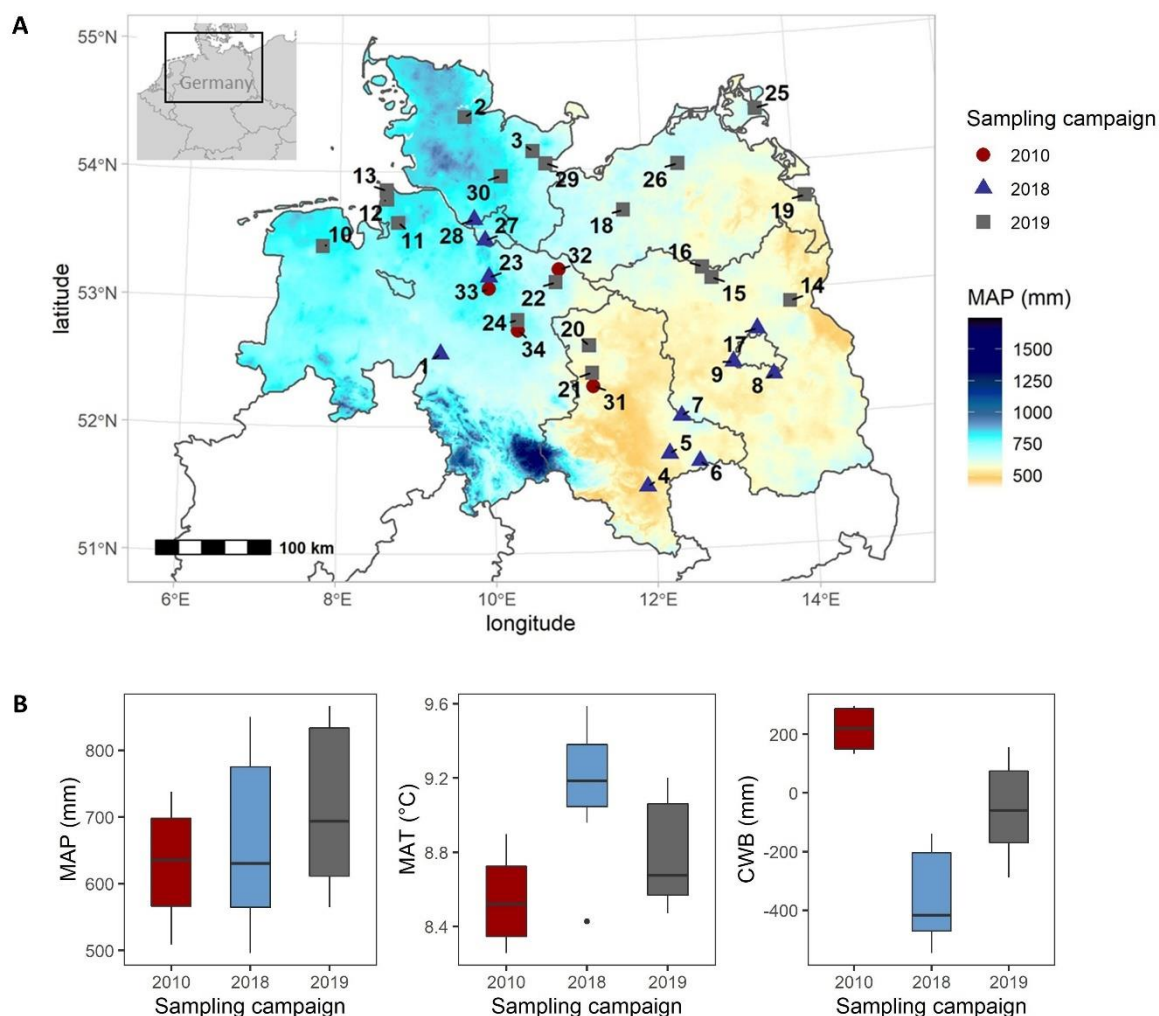
Figure 4.1: A: Map of the northern part of Germany with federal states and the location of the 34 investigated beech stands sampled in three different years. Colours and shape of the stand symbols show the sampling campaign (2010, 2018 or 2019) and mean annual precipitation (MAP, 1958 –2017, data provided by DWD) is indicated by colours. For site codes and more information on stands, see Table 4.1 and Table S4.1. B: 60-year mean annual precipitation (MAP, left), mean annual temperature (MAT, middle) and climatic water balance of the current year (CWB, right) of the sites, where sample collection took place in 2010 (n = 4), 2018 (n = 11) or 2019 (n = 19). 60-year mean values refer to the period 1950-2009 for the sites sampled in 2010 and to the period 1958-2017 for the 2018 and 2019 sites.

Table 4.1: Stand characteristics of the 34 investigated European beech (*Fagus sylvatica*) stands. Given are site number (see Figure 4.1), locality, sampling year, 60-year mean annual precipitation (MAP, mm yr^{-1}), and mean annual temperature (MAT, °C) for the period 1958 − 2017 (sites 1 − 30) or 1950 − 2009 (sites 31 − 34), mean potential evapotranspiration (pot. E, mm yr^{-1}) for the period 1991 – 2017 (sites 1 − 30) or 1991 – 2009 (sites 31 − 34), plant-available water capacity (AWC, mm; sites 31 – 34: source Müller-Haubold *et al.* (2013), adjusted to 100 cm), diameter at breast height (DBH, cm; sites 31 – 34: source Schuldt *et al.* (2016)), tree height (Height, m; sites 31 – 34: source Schuldt *et al.* (2016)), Hegyi competition index (CI), and the number of sampled trees (n_{tree}) and samples (n_{sample}) per site. Climate data were retrieved from the Climate Data Centre of the German Weather Service (DWD, Offenbach). For data on tree level, means per site ± SE are given.

Site	Name	Year	MAP	MAT	pot. E	AWC	DBH	Height	CI	n_{tree}	n_{sample}
1	Grinderwald	2018	720	9.30	592	301	44.9 ± 1.0	26.6 ± 0.6	0.49 ± 0.04	10	30
2	Brekendorf	2019	866	8.46	567	227	45.6 ± 2.3	27.1 ± 0.5	0.59 ± 0.08	10	30
3	Malente	2019	740	8.59	569	253	58.2 ± 2.8	30.0 ± 0.4	0.44 ± 0.05	10	30
4	Halle	2018	497	9.52	645	286	45.1 ± 0.5	25.2 ± 0.7	0.49 ± 0.03	10	30
5	Mosigkauer Heide	2018	550	9.58	647	178	44.5 ± 1.2	28.1 ± 0.5	0.53 ± 0.05	10	30
6	Dübener Heide	2018	656	9.11	629	91	42.0 ± 2.2	26.8 ± 0.5	0.64 ± 0.08	10	30
7	Medewitz	2018	631	8.95	624	126	47.9 ± 2.5	28.8 ± 0.5	0.54 ± 0.04	10	30
8	Zeuthen	2018	565	9.23	657	169	40.2 ± 0.8	28.1 ± 0.6	0.60 ± 0.06	10	30
9	Potsdam	2018	578	9.37	650	198	35.7 ± 1.1	21.1 ± 0.3	0.58 ± 0.08	10	30
10	Wiesmoor	2019	808	9.05	586	58	43.2 ± 1.6	27.1 ± 0.4	0.51 ± 0.03	10	30
11	Drangstedt	2019	847	9.03	582	203	53.7 ± 2.7	34.4 ± 0.8	0.44 ± 0.04	10	30
12	Nordholz	2019	859	9.11	578	104	44.5 ± 1.4	30.6 ± 0.3	0.51 ± 0.09	10	30
13	Sahlenburg	2019	832	9.19	577	76	42.3 ± 1.9	26.1 ± 0.6	0.57 ± 0.06	10	30
14	Chorin	2019	581	8.93	638	119	49.6 ± 2.4	30.9 ± 0.6	0.46 ± 0.04	10	30
15	Warenthin	2019	586	8.67	612	147	46.2 ± 1.6	29.2 ± 0.5	0.44 ± 0.05	10	30
16	Zempow	2019	599	8.54	596	189	40.5 ± 1.4	28.8 ± 0.4	0.41 ± 0.03	10	30
17	Summt	2018	592	9.17	638	43	45.1 ± 1.5	27.5 ± 0.4	0.52 ± 0.05	10	30
18	Kaarzer Holz	2019	639	8.64	582	79	45.4 ± 1.6	28.3 ± 0.7	0.40 ± 0.03	10	30
19	Eggesiner Forst	2019	578	8.56	600	130	44.0 ± 1.5	27.2 ± 0.5	0.39 ± 0.07	10	30
20	Klötze	2019	636	8.86	609	260	47.9 ± 1.5	33.9 ± 1.0	0.61 ± 0.06	10	30
21	Calvörde	2019	566	9.12	622	160	42.0 ± 1.1	26.5 ± 0.4	0.59 ± 0.06	10	30
22	Göhrde	2019	704	8.65	587	172	46.1 ± 2.5	26.7 ± 0.6	0.49 ± 0.03	10	30
23	Sellhorn	2018	850	8.42	566	161	43.0 ± 1.1	30.1 ± 0.7	0.62 ± 0.04	10	30
24	Unterlüss	2019	791	8.53	583	127	46.3 ± 1.5	28.9 ± 0.6	0.43 ± 0.04	10	30
25	Prora	2019	623	8.56	572	218	48.1 ± 1.9	28.0 ± 0.4	0.56 ± 0.05	10	30
26	Tessin	2019	653	8.51	582	166	43.3 ± 1.4	30.7 ± 0.5	0.62 ± 0.05	10	30
27	Haake	2018	776	9.11	583	88	47.1 ± 2.0	28.4 ± 0.6	0.59 ± 0.06	10	30
28	Klövensteen	2018	782	9.04	584	158	46.5 ± 1.5	31.1 ± 0.6	0.46 ± 0.01	10	30
29	Haffkrug	2019	693	8.72	573	256	42.2 ± 1.9	27.9 ± 0.6	0.48 ± 0.05	10	30
30	Heidmühlen	2019	833	8.66	574	164	44.3 ± 1.3	27.5 ± 0.5	0.73 ± 0.09	10	30
31	Calvörde	2010	509	8.90	604	38	37.4 ± 2.5	25.8 ± 0.2	–	4	12-24
32	Göhrde	2010	586	8.67	587	89	40.1 ± 2.0	24.2 ± 1.1	–	4	12-24
33	Sellhorn	2010	738	8.26	558	92	39.8 ± 2.4	28.9 ± 1.0	–	4	12-24
34	Unterlüss	2010	685	8.38	574	66	40.8 ± 3.1	22.3 ± 1.1	–	4	12-24

4.3.3 Tree size and competition intensity in the canopy

Mean tree height of the study sites ranged from 21.1 to 34.4 m and diameter at breast height (DBH) from 36 to 58 cm (Table 4.1). Because we assumed that soil water availability to the

tree individual may depend on the intensity of competition of the target tree with their direct neighbours, we calculated the Hegyi competition index (CI; Hegyi, 1974) for the sites 1 – 30 for each sampled tree i (10 per site) from the distance and height of the three nearest neighbouring trees j as:

$$CI_i = \sum_{j=1}^{n} \frac{d_j/d_i}{Dist_{ij}},$$

where d_i is the diameter at breast height of the sampled tree i (cm), d_j the diameter at breast height of the competitor j (cm), $Dist_{ij}$ the distance between target tree and competitor (m), and n the number of directly neighbouring trees considered (= 3).

4.3.4 Leaf sampling and analysis of foliar traits

Sample collection took place between June and August of 2010 (sites 31 – 34), and of 2018 and 2019 (sites 1 – 30). All three sampling campaigns covered sites from a broad range of MAP levels, each representing a precipitation gradient, but the moisture conditions during leaf formation in spring/early summer differed between the 2010 (moist), 2018 (extremely dry) and 2019 data sets (dry) (Table S4.2). At all sites, branches were cut from the uppermost sun-exposed crowns by professional tree climbers. Fully expanded intact leaves were sampled from first-order side branches of the collected main branch at a uniform distance of 1 – 2 m below the tree tip. Per site, we sampled leaves of four to five branch segments each of four trees at the sites 31 – 34 and leaves of three branches of ten trees each at the sites 1 – 30. For all leaf samples, average leaf size (LS, cm^2), specific leaf area (SLA, cm^2 g^{-1}), sapwood-to-leaf area ratio (Huber value, HV, cm^2 m^{-2}) and the carbon isotope signature of leaf dry mass (δ^{13}C, ‰; not available for samples of sites 31 – 34) were determined. Additionally, three small distal twigs per tree with fully intact leaves were cut to determine turgor loss point (Ψ_{tlp}; see Table 4.2 for a list of all variables).

From the samples of sites 1 – 30, all leaves distal to the basipetal end of the sample (50 – 100 cm from the apex, branch diameter between 5.5 and 14.6 mm) were detached and stored at about 6 °C. Per branch sample, a sub-sample of the leaves was scanned for leaf area determination (two scans per branch with an average of 58 leaves) using a flat-bed scanner and the software WinFOLIA Reg 2014a (Régent Instruments, Quebec City, Canada). At the sites 31 – 34, leaves of four to five branch segments per tree of 5 – 6 cm length with diameters of 6.0 – 8.0 mm were scanned.

LS was calculated by dividing the total area of the scanned leaves by the number of leaves, and SLA by dividing the total area of scanned leaves by their dry weight (oven-dried at 70

°C for 48 h). The total leaf area per branch was approximated by multiplying the total leaf dry mass per branch with SLA. For determination of HV, the xylem cross-sectional area without pith and bark (A_{xylem}), which was estimated from the branch cross-sectional area (A_{cross}) as $A_{xylem} = -3.715 + 0.770 * A_{cross}$ (Schuldt *et al.*, 2016), was divided by the total leaf area per branch. Afterwards, the dried leaf samples were ground and leaf N content (see Table S4.3) and the carbon isotope signature of the dry mass ($\delta^{13}C$) were analysed by mass-ratio spectroscopy (Delta Plus; Thermo Finnigan, Bremen, Germany) at the Centre for Stable Isotope Research and Analysis (KOSI) of the University of Göttingen.

The twigs collected for determination of Ψ_{tlp} at sites 1 – 30 were recut under water and transported to the laboratory in a cooling box at 6 °C under high air humidity with the cut surface placed under water. Ψ_{tlp} was determined within 72 h after sampling with the osmometer method, where Ψ_{tlp} is estimated based on the leaf osmotic potential at full hydration (Ψ_0, Bartlett *et al.*, 2012a). The leaf osmotic potential was measured in a vapor pressure osmometer (VAPRO 5600, Wescor, Logan, UT, USA) on leaf discs of fully rehydrated leaves after a 2 min-submersion in liquid nitrogen, following the protocol of Bartlett *et al.* (2012a). Ψ_{tlp} was estimated as $\Psi_{tlp} = 0.832\ \Psi_0 - 0.631$ (Bartlett *et al.*, 2012a). Although the osmometric method since then has shown to deliver valid results for several growth forms including grasses, herbaceous and woody plants (Arndt *et al.*, 2015; Griffin-Nolan *et al.*, 2019; Majekova *et al.*, 2019), it should be kept in mind that differences in the apoplastic fraction and leaf modulus of elasticity across populations and environmental conditions might affect the estimated Ψ_{tlp} values.

For sites 31 – 34, Ψ_{tlp} and Ψ_0 were estimated from pressure-volume curves established with the over-pressurization technique in a Scholander pressure chamber (Koide *et al.*, 2000). In July 2010, shoots with 4 – 6 leaves were collected in the lower sun canopy, cut under water, transported to the laboratory in a humidified plastic bag and rehydrated overnight at room temperature. Leaves were then weighed to obtain initial mass, inserted to the pressure chamber to determine the initial water potential, and subsequently subjected to a series of increasing pressures ranging from 0.4 to 3.1 MPa. The extruded water was collected in Eppendorf cups filled with cellulose pads and weighed immediately. After each step, the leaves were allowed to equilibrate for about 10 min before measuring the equilibrium pressure. After measurement, the leaves were oven-dried to determine dry mass and initial relative water content. Ψ_{tlp} was determined from the intersection between the nonlinear and linear branch of the plot of inverse water potential against cumulative expressed water fraction.

Additionally, data of three trees (three samples per tree) from a stand in Unterlüss (close to sites 24 and 34) were used to test for significant differences in LS, SLA and HV of upper canopy branches collected in 2018 and 2019.

Table 4.2: List of variables included in the study with abbreviations and units.

Abbreviaton	Unit	Definition
Foliar traits		
LS	cm^2	Mean leaf size
SLA	$cm^2\,g^{-1}$	Specific leaf area
HV	$cm^2\,m^{-2}$	Sapwood-to-leaf area ratio (Huber value)
$\delta^{13}C$	‰	Carbon isotope signature
Ψ_{tlp}	MPa	Water potential at turgor loss point
Climatic variables		
MAP	$mm\,yr^{-1}$	Mean annual precipitation
MAT	°C	Mean annual temperature
CWB	$mm\,yr^{-1}$	Climatic water balance (precipitation – pot. evapotranspiration)
CWBS	mm	Cumulative climatic water balance of March, April and May
CWB_{pre}	mm	CWB of the month preceding sample collection
Other variables		
AWC	mm	Plant-available water capacity of the soil (referring to 1m depth)
CI		Hegyi competition index
Height	m	Tree height

4.3.5   Statistical analyses

All statistical analyses were carried out with the software `R`, version 4.0.3. (R Core Team, 2020) using the `tidyverse` package, version 1.3.0 (Wickham *et al.*, 2019).

In our dataset, the effect of the sampling year (2010, 2018, 2019) on the leaf traits cannot reliably be separated from site and climate effects, as testing for this effect was not planned in the design stage of the study, and sampling could not be repeated on the same sites in consecutive years. We therefore refrain from formally testing for year differences, and only present visual comparisons of leaf traits on the tree level (average of three samples per tree) sampled at different sites in the summers 2010, 2018 and 2019. Only at one site (Unterlüss), data from repeated sampling in 2018 and 2019 on the same trees is available, with differences in LS, SLA and HV between 2018 and 2019 being tested with an unpaired two-samples Wilcoxon test.

Linear regression analyses were conducted to test for the effect of sampling year's climatic water balance in spring (CWBS, March to May) on the site means of LS, SLA, HV and $\delta^{13}C$.

In case of Ψ_{tlp} with higher seasonal variation than in the other traits, the climatic water balance of the month prior the sampling (CWB_{pre}) instead of CWBS was analysed.

To test for the effect of long-term water availability (combined effects of MAP (1958 – 2017), AWC and CI) on leaf traits, linear mixed effects models were fitted with the `R` package `lme4`, version 1.1.26 (Bates *et al.*, 2015) for leaves collected in 2018 and 2019 and for each trait separately. LS, SLA and HV were natural log-transformed and the five leaf traits were modelled as a function of MAP, AWC and CI (centred, scaled and, in case of CI, log-transformed) as fixed effects, and with random intercepts for tree nested in site. Due to convergence issues, the site-wise random intercept had to be omitted in the model for HV in 2018. The variance in the traits was then decomposed into variance components for the fixed effects, the random effects (between-sites and between-trees) and the residual variance (within-tree). The marginal and conditional R² (Nakagawa *et al.*, 2017) were computed based on R package `MuMIn` v. 1.43.17 (Bartón, 2020).

4.4 Results

4.4.1 Climatic conditions and soil water availability across the sites

The range of climatic conditions covered by the three data sets (2010, 2018, 2019) was not identical, but relatively similar. Sixty-year mean annual precipitation (MAP) was slightly higher at the sites sampled in 2019 (566 – 866 mm yr^{-1}, 1958 – 2017, n = 19) than at the sites of 2010 (509 – 738 mm yr^{-1}; 1950 – 2009, n = 4) and 2018 (497 – 850 mm yr^{-1}, 1958 – 2017, n = 11; Figure 4.1), while 60-year mean annual temperature (MAT) was slightly lower in the 2010 data set (8.3 – 8.9 °C) than in the 2018 (8.4 – 9.6 °C) and 2019 data sets (8.5 – 9.2 °C). As the mid- and late-summer of 2018 was extremely dry, the climatic water balance (CWB) of the full year at the sites sampled in 2018 was the lowest (between -564 and -138 mm yr^{-1}) compared to -287 – 156 mm yr^{-1} in the 2019 sample and to 133 – 297 mm yr^{-1} in the 2010 sample.

In the 60-year record of climate data of the study sites, early-growing season (MSP, April to June) and growing season precipitation (MGSP, April to October) were tightly correlated with full-year MAP, while early-growing season temperature (MST, April to June) and growing season temperature (MGST) showed a weaker relation to full-year MAT (Figure S4.1). CWBS was deviating from the 60-year MAP most in 2019, intermediate in 2018 and least in 2010. The relation between MAP and CWB_{pre} was strongest for the 2018 data set, the year with the most negative climatic water balance (Figure 4.1B).

4.4.2   Leaf traits in the 2010, 2018 and 2019 data sets

Across the 34 sites, mean leaf size (LS) of sun-canopy foliage varied nearly sevenfold between 3.9 ± 0.2 and 27.0 ± 1.8 cm^2, specific leaf area (SLA) fourfold between 77.1 ± 1.0 and 306.9 ± 18.2 cm² g^{-1}, and Huber value (HV) sixfold between 1.0 ± 0.1 and 6.65 ± 1.3 cm^2 m^{-2} (averaged over a tree, n = 3 – 5 samples per tree; Figure 4.2A). Average LS in the 2018 data set (17.3 ± 0.3, n = 110 trees) was clearly higher than in the 2010 data (13.8 ± 0.4, n = 16 trees) and the 2019 data (12.5 ± 0.3, n = 190 trees). Compared to LS, SLA varied much less between the three data sets, with the 2019 data having a slightly higher mean (144.4 ± 3.0 cm² g^{-1}) than the 2010 and the 2018 data (111.9 ± 3.5 and 128.9 ± 2.0, respectively). Yet, the range of average SLA values per tree spanned 229.8 cm² g^{-1} in the 2019 data set and was remarkably large. HV showed the inverse pattern of LS, with mean HV being higher in the 2019 data (2.7 ± 0.1) than in the 2018 and 2010 data sets (2.2 ± 0.1 and 2.3 ± 0.1, respectively).

The average leaf mass δ^{13}C value was higher in the 2018 data set (-27.8 ± 0.1 ‰) than in the 2019 data (-28.8 ± 0.1 ‰), indicating a generally lower stomatal conductance in the former data set (Figure 4.2B). Ψ_{tlp} was lower in the 2018 data set (-2.48 ± 0.01 MPa) compared to the 2019 data (-2.30 ± 0.02 MPa) and the 2010 data (-2.19 ± 0.02 MPa). The inter-relationships between the studied leaf traits differed between the three data sets (Figure S4.2).

Comparison of leaf traits in the same trees between 2018 and 2019 revealed significant differences in LS, SLA and HV, with a 50% reduction in LS (from 14.5 ± 0.9 to 7.1 ± 0.5 cm^2) and doubling in HV (from 1.8 ± 0.5 to 3.6 ± 1.1 cm^2 m^{-2}), while SLA decreased by 15% from 150 ± 16 to 128 ± 8 cm^2 g^{-1} (stand Unterlüss close to sites 24 and 34; Figure 4.3).
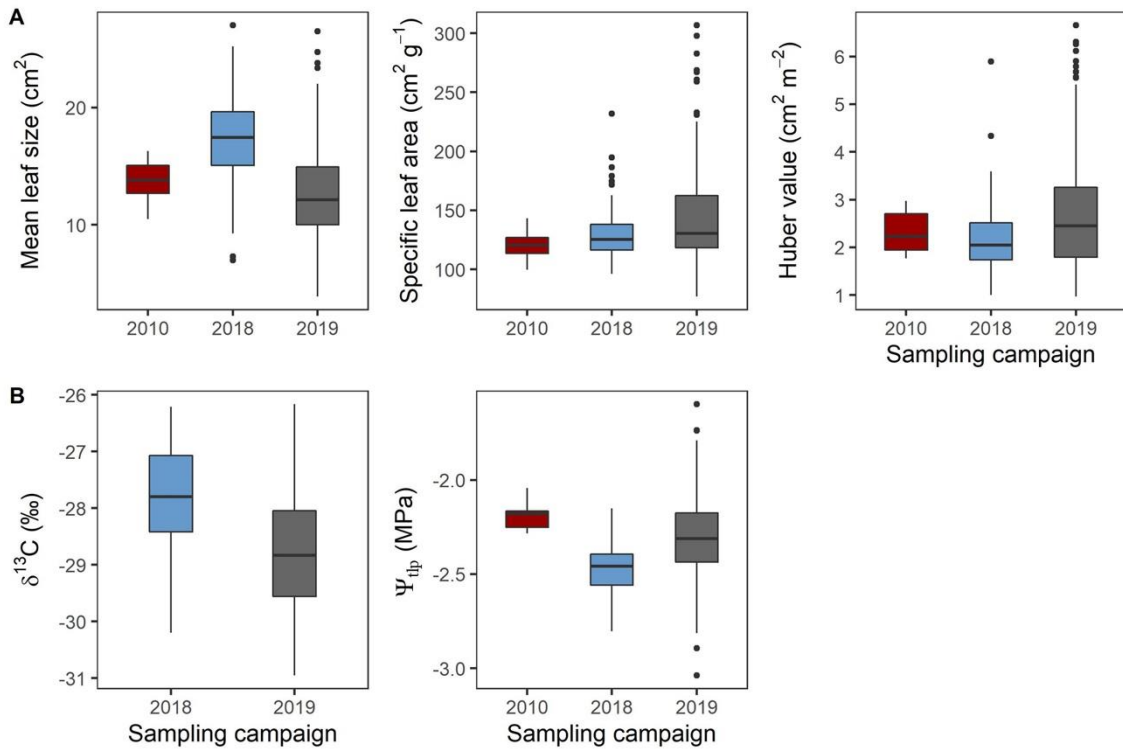
Figure 4.2: Mean leaf morphological (A) and physiological (B) traits on the tree level. Average leaf size (LS), specific leaf area (SLA), Huber value (HV), carbon isotope signature ($\delta^{13}C$) and water potential at turgor loss point (Ψ_{tlp}) for the three sampling campaigns (2010: n_{tree} = 16, 2018: n_{tree} = 110, 2019: n_{tree} = 190). Box-whisker plots depict median and interquartile ranges (Q1 – Q3); whiskers extend to max. 1.5 times the interquartile range.
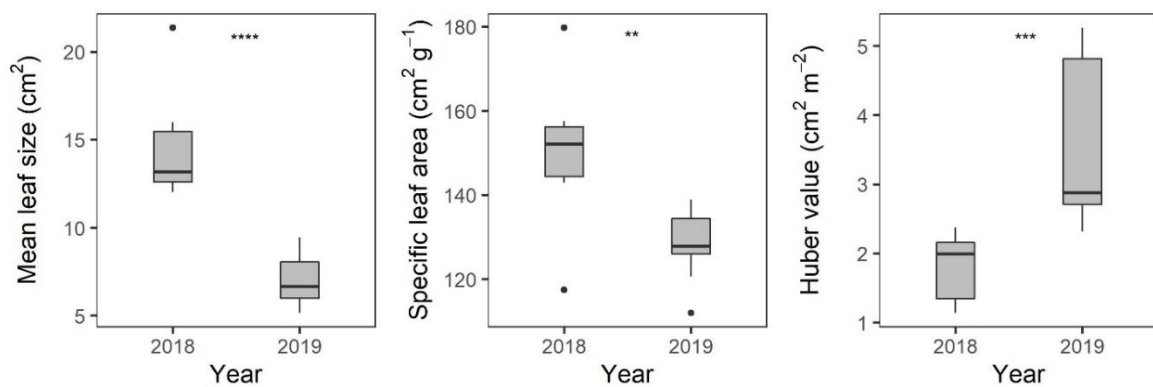
Figure 4.3: Mean leaf size, specific leaf area and Huber value of nine samples from three trees collected in Unterlüss (close to stands 24 and 34) in 2018 and again in 2019. Asteriscs indicate significant differences between the years (***, $p < 0.001$; **, $p < 0.01$). Box-whisker plots depict median and interquartile ranges (Q1 – Q3); whiskers extend to max. 1.5 times the interquartile range.

4.4.3   Effects of long-term water availability

The effects of mean annual precipitation (MAP, 1958 – 2017), plant-available soil water capacity (AWC) and Hegyi competition index (CI) on leaf traits were tested with linear mixed effects (LME) models for the 2018 and 2019 data sets (Table 4.3). LS was significantly affected only by MAP in 2018 (negative effect), while no significant influence was detectable in the 2019 data set. SLA was significantly positively influenced by CI in 2018, and by AWC in the 2019 data. MAP had a significant positive effect on HV in the 2018 data set, while CI influenced HV negatively. In the 2019 data set, HV was significantly related neither to MAP nor to AWC or CI. Foliar δ^{13}C was significantly influenced by competition intensity only in the 2018 data set with a positive effect of CI. Ψ_{tlp} significantly increased with MAP and AWC in the 2019 data set, but the effects of MAP, AWC and CI were not significant in the 2018 data set. In both data sets, a substantial fraction of the between-stand variance was not explained by MAP, AWC or CI, ranging from 33% in P_{tlp} to 45% in SLA in the 2019 data, and from 21% in LS and SLA to 32% in P_{tlp} in the 2018 data. The proportion of within-population variance not explained by competition intensity was high, ranging from 24% in case of SLA to 52% in δ^{13}C in the 2018 data set, and from 19% in SLA to 47% in LS in the 2019 data. Variance attributed to within-tree differences was high for SLA and HV in the 2018 data set (50 and 59%), but much lower in case of foliar δ^{13}C in both data sets (12 and 13% in the 2018 and 2019 data).

4.4.4   Relations between leaf traits and short-term water availability

Linear regression analyses between the climatic water balance one month before bud burst and during leaf expansion (March to May of the sampling year, CWBS) and average LS, SLA, HV and δ^{13}C of a site revealed significant decreases in LS and the δ^{13}C signature with increasing CWBS, i.e. larger leaves, under higher climatic aridity (Figure 4.4A and B), while SLA and HV were not significantly influenced. Ψ_{tlp} significantly decreased with diminishing CWB$_{pre}$. The correlation between δ^{13}C signature and leaf N content was very weak (Figure S4.2) indicating that discrimination against ^{13}C during photosynthesis was not dependent on foliar N.

Table 4.3: Results from linear mixed effects models examining the influence of 60-year mean annual precipitation (MAP), plant-available water capacity (AWC) and Hegyi competition index (CI, log-transformed) as fixed variables and random intercept for tree nested in site on the mean leaf size (LS), specific leaf area (SLA), Huber value (HV), carbon isotope signature (δ^{13}C) and pressure at turgor loss point (P_{tlp}) sampled in 2018 or 2019. Given are the scaled estimates (*est.*), standard errors (*std. error*), test statistics (*t-val.*), degrees of freedom (*df*) and *p*-values (fixed parts), the standard deviation of the random intercepts and the residual standard deviation (random parts) and the number of observations (Obs.) for each model.

Variable	Year		Fixed parts				Random parts			Obs.
			Intercept	MAP	AWC	CI (log)	tree:site	site	residual	
LS (log)	2018	est.	2.82	-0.10	-0.06	0.01	0.17	0.11	0.10	330
		std. error	0.04	0.04	0.04	0.02				
		t-val	73.01	-2.59	-1.62	0.42				
		df	7.96	7.97	8.01	101.15				
		p	**<0.001**	**0.03**	0.14	0.67				
	2019	est.	2.47	-0.01	0.06	-0.01	0.26	0.23	0.13	564
		std. error	0.06	0.06	0.06	0.02				
		t-val	44.57	-0.13	1.07	-0.40				
		df	15.91	15.93	15.96	176.32				
		p	**<0.001**	0.90	0.30	0.69				
SLA (log)	2018	est.	4.84	-0.02	0.02	0.03	0.09	0.08	0.13	330
		std. error	0.03	0.03	0.03	0.01				
		t-val	173.08	-0.78	0.63	2.56				
		df	8.00	8.01	8.04	100.74				
		p	**<0.001**	0.46	0.55	**0.01**				
	2019	est.	4.93	0.00	0.13	0.00	0.12	0.19	0.11	564
		std. error	0.04	0.04	0.04	0.01				
		t-val	110.75	-0.08	2.88	-0.28				
		df	15.98	15.98	15.99	171.79				
		p	**<0.001**	0.93	**0.01**	0.78				
HV (log)	2018	est.	0.70	0.10	-0.01	-0.08	0.20		0.28	330
		std. error	0.02	0.03	0.03	0.02				
		t-val	28.58	3.84	-0.22	-3.10				
		df	106.00	106.00	106.00	106.00				
		p	**<0.001**	**<0.001**	0.83	**<0.01**				
	2019	est.	0.88	-0.01	-0.08	0.02	0.25	0.30	0.32	564
		std. error	0.07	0.07	0.07	0.02				
		t-val	12.31	-0.17	-1.06	0.87				
		df	15.89	15.90	15.92	174.77				
		p	**<0.001**	0.87	0.30	0.38				
δ^{13}C	2018	est.	-27.82	-0.20	-0.09	-0.18	0.68	0.49	0.33	330
		std. error	0.16	0.17	0.17	0.07				
		t-val	-170.87	-1.20	-0.53	-2.49				
		df	7.99	8.00	8.03	100.83				
		p	**<0.001**	0.27	0.61	**0.01**				
	2019	est.	-28.78	-0.27	0.01	-0.05	0.72	0.68	0.39	564
		std. error	0.17	0.17	0.17	0.06				
		t-val	-174.37	-1.62	0.06	-0.85				
		df	15.67	15.64	15.79	171.95				
		p	**<0.001**	0.12	0.96	0.39				
P_{tlp}	2018	est.	-2.48	0.00	0.01	0.02	0.09	0.09	0.10	330
		std. error	0.03	0.03	0.03	0.01				
		t-val	-84.25	-0.03	0.34	1.55				
		df	7.97	7.97	7.99	99.96				
		p	**<0.001**	0.98	0.74	0.12				
	2019	est.	-2.30	0.09	0.08	-0.01	0.11	0.14	0.12	564
		std. error	0.03	0.03	0.03	0.01				
		t-val	-67.99	2.73	2.34	-0.55				
		df	15.98	16.00	16.01	173.82				
		p	**<0.001**	**0.01**	**0.03**	0.58				
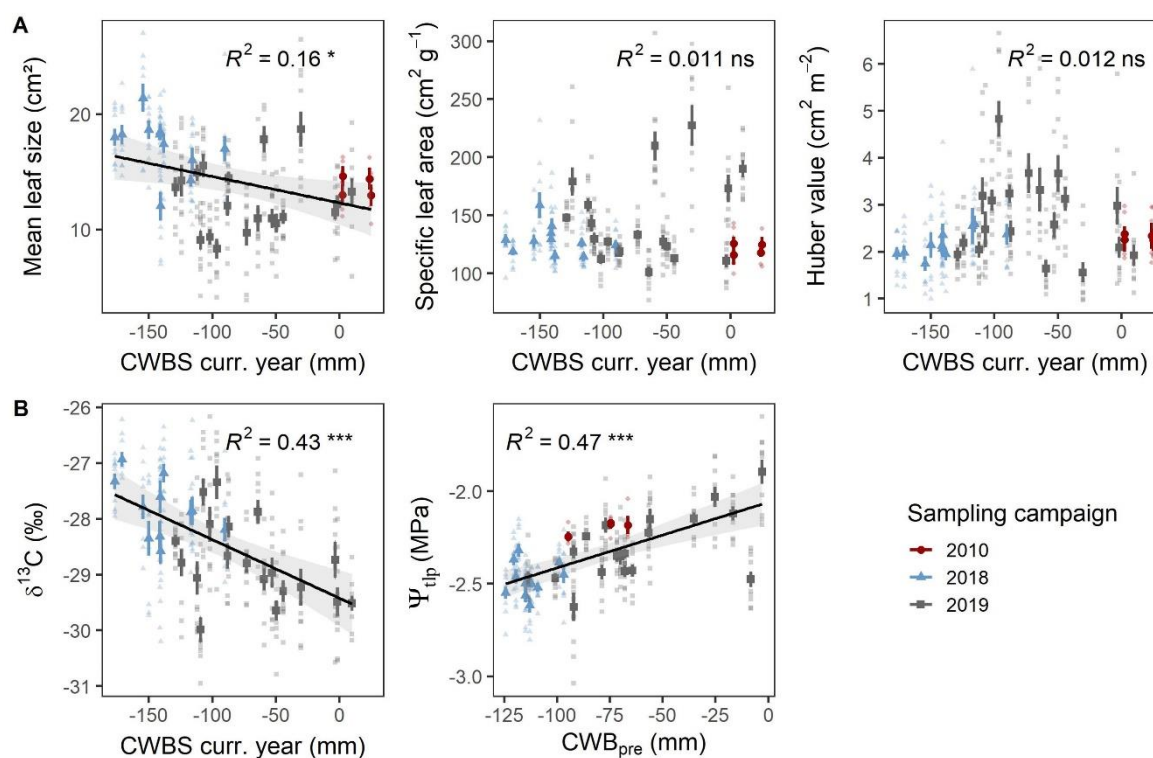
Figure 4.4: Linear regressions showing the effect of the cumulative water balance of different spring months of the current year (CWBS, March to May) or of the climatic water balance of the month before sample collection (CWB$_{pre}$, only for Ψ_{tlp}) on average leaf traits per site (mean ± SE). Colours and shape of the symbols indicate the sampling years, and raw data are depicted in the backround. Asteriscs indicate the level of significance (***, p < 0.001; **, p < 0.01; *, p < 0.05; ns, non-significant relationship). For significant relationships, the linear regression line with its 95% confidence interval is shown.

4.4.5   Variance components

Variance decomposition for the LME models in Table 4.3 revealed that site water availability as expressed by the combined effects of MAP, AWC and CI explained a rather small fraction of the variance of Ψ_{tlp} in the 2018 data set (1 %), while ranging from 5 % (SLA) to 18 % (LS) for the other traits (Figure 4.5). This was different in the 2019 data set with a relatively high proportion of variance explained by MAP, AWC and CI in case of Ψ_{tlp} (23 %) and SLA (21 %), while this proportion was lowest in case of LS (3 %). In both data sets, a substantial fraction of the between-stand variance was not explained by MAP, AWC or CI, ranging from 33 % in Ψ_{tlp} to 45 % in SLA in the 2019 data, and from 21 % in LS and SLA to 32 % in Ψ_{tlp} in the 2018 data. The proportion of within-population variance not explained by competition intensity was high, ranging from 24 % in case of SLA to 52 % in δ^{13}C in the 2018 data set, and from 19 % in SLA to 47 % in LS in the 2019 data. Variance attributed to within-tree differences was high for SLA and HV in the 2018 data set (50 and

59 %), but much lower in case of foliar $\delta^{13}C$ in both data sets (12 and 13 % in the 2018 and 2019 data).
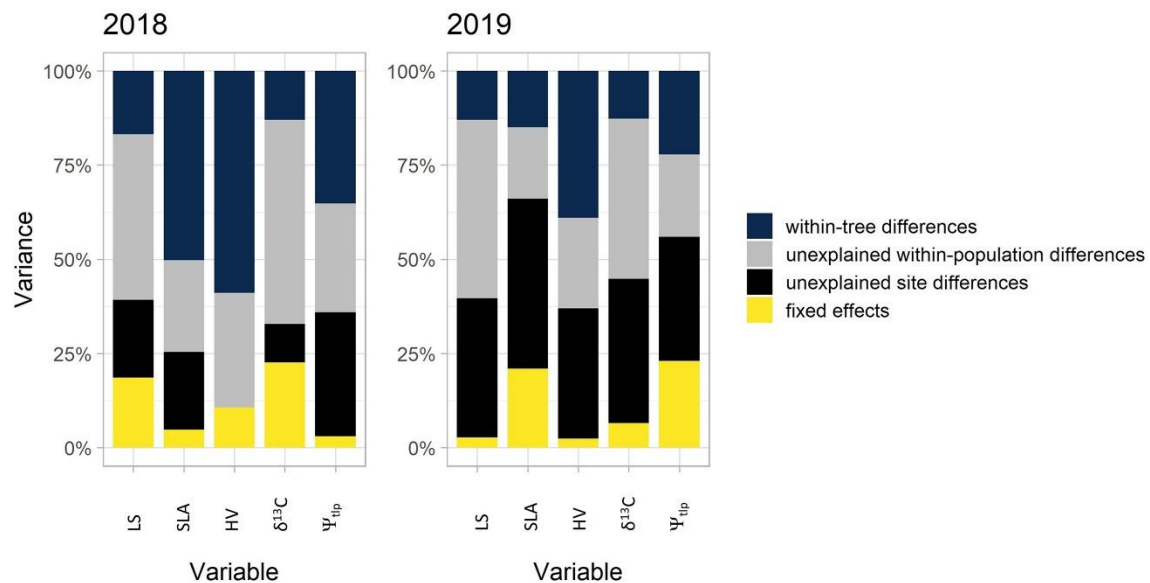
Figure 4.5: Variance components of the linear mixed effects models for average leaf size (LS), specific leaf area (SLA), Huber value (HV), carbon isotope signature ($\delta^{13}C$) and water potential at turgor loss point (Ψ_{tlp}) with MAP, AWC, and CI as fixed effects and with random intercepts for tree nested in site and residual variability between individuals for the samples collected in 2018 (left) and 2019 (right, see Table 4.3). Due to convergence issues, the site-wise random intercept had to be omitted in the model for HV in 2018.

4.5 Discussion

4.5.1 Leaf traits in the three sampling campaigns 2010, 2018 and 2019

Our study of leaf trait variation in beech forests across three climatic aridity gradients covers a large part of the species' habitat range in Central Europe and thus allows conclusions on the acclimative and adaptive potential of mature beech in response to climate warming. Average leaf size (LS) in the upper sun canopy of the 34 stands (12.6 – 17.3 cm²) was similar to LS determined in 2005 and 2006 across a comparable precipitation gradient (520 – 970 mm yr⁻¹) in Central Germany, though on different soil (Meier & Leuschner, 2008). It was clearly higher than LS of sun leaves collected in 2011 (8.22 – 11.48 cm²) in the stands 31 – 34 (Schuldt *et al.*, 2016), probably due to a strong masting event in 2011 (Müller-Haubold *et al.*, 2013). However, fructification also happened in 2019 in many beech forests of northern Germany (Scharnweber *et al.*, 2020), probably induced by the warm and dry summer in 2018, as mass fruiting in *F. sylvatica* was found to be stimulated by high

temperatures and high solar radiation in June and July of the year preceding a mast year (Müller-Haubold *et al.*, 2015). Hence, the on average nearly 40% greater mean LS in the 2018 data set as compared to the 2019 data was probably, at least partly, caused by mast fruiting, which reduces carbohydrate allocation to leaves. As LS was found to increase in beech with autumn temperature of the previous year (Zhu *et al.* 2021), the greater LS in the 2018 data set could partly also be the result of the somewhat higher mean annual temperatures recorded at the sites sampled in 2018. However, repeated sampling of the same trees in 2018 and 2019 at the Unterlüss site also revealed significantly smaller leaves in 2019 than in 2018, and cross-regional surveys after the severe 2018 drought showed for many Central European beech forests particularly small leaves in 2019 as an after-effect (Schuldt *et al.*, 2020; Walthert *et al.*, 2021; Zhu *et al.*, 2021). From their analysis of a 25-year record of leaf morphological trait data from Swiss beech forests, Zhu *et al.* (2021) conclude that higher vapour pressure deficit (VPD) results in reduced specific leaf area (SLA) in the subsequent year, as does a higher fruiting intensity. Therefore, a combined effect of masting and atmospheric drought on leaf morphology in 2019 is likely. Yet, our study design does not allow for a more thorough analysis of inter-annual leaf trait variation. As LS rapidly increases from the tree top downward in the crown of beech (Hagemeier & Leuschner, 2019), a standardized sampling of twigs in the uppermost crown as done here is important for recognizing spatial and temporal variation in leaf morphology.

Mean SLA of upper sun-crown leaves was less variable across the three sampling campaigns than LS, which might relate to the fact that cell expansion, the main determinant of leaf size, is more drought-susceptible than cell division (Hsiao *et al.*, 1976). Generally, SLA has been found to decrease with higher radiation and increasing nutrient deficiency, but also with decreasing water availability in soil and atmosphere (Wright *et al.*, 2002; 2004; Poorter *et al.*, 2009; Zhu *et al.*, 2021). In fact, the SLA of European beech trees has been found to be highly dependent on the light intensity in the crown (Curt *et al.*, 2005; Čater & Diaci, 2017; Chelli *et al.*, 2021). The large between-population variation in SLA in 2019 might by caused by differences in soil water availability and VPD along the climate gradient, or by local differences in masting intensity, which influences both carbohydrate and nutrient availability.

Average Huber values (HV) varied inversely to LS across the three sampling years, with higher HV being negatively related to LS (Figure S4.2). This suggests that inter-annual changes in HV are mainly driven by variation in LS and not by variable leaf numbers per twig. The 100% increase in HV after the severe 2018 drought at one central site is likely to

be driven by reduced water transport capacity of the branches due to drought legacy effects (Schuldt *et al.*, 2020).

As expected, leaf δ^{13}C was on average by about 1 ‰ higher in the drier and hotter summer 2018 as compared to 2019, indicating reduced stomatal conductance and a higher intrinsic water use efficiency in this summer (Farquhar *et al.*, 1989). This was associated with an on average lower water potential at turgor loss point (Ψ_{tlp}) in 2018 than in 2019, and the highest Ψ_{tlp} in the moist summer 2010, suggesting mean osmotic adjustment by about 0.2 – 0.3 MPa in response to inter-annual climatic differences. Seasonal osmotic adjustment in the leaves of adult beech trees has been observed in several studies in Central Europe, but its extent seems to depend on the drought intensity experienced in the growing season, as it was usually smaller than 0.4 MPa (Leuschner, 2020). In the foliage of drought-stressed beech saplings, amino acids accumulated together with mono- and disaccharides, and especially the trisaccharide raffinose, pointing at increased conversion of starch to non-structural carbohydrates under drought (Aranda *et al.*, 2018). It is therefore possible that the less negative Ψ_{tlp} values in the 2019 data set compared to 2018 are a consequence of carbohydrate depletion due to mast fruiting in that year, as higher concentrations of osmotic substances come along with elevated carbohydrate costs (Villagra *et al.*, 2013; Martinez-Vilalta *et al.*, 2016). The significant influence of the climatic water balance of the month preceding sample collection (CWB_{pre}) on Ψ_{tlp} over the three sampling years and the significant effect of mean annual precipitation (MAP) and plant-available water capacity (AWC) in 2019 confirms that Ψ_{tlp} is largely under the influence of water availability, at least under dry conditions (cf. Sjöman *et al.*, 2018; Aranda *et al.*, 2021).

4.5.2   Effects of lasting water deficits on leaf traits

As expected, site water availability impacted on the studied leaf traits across the gradients in the 2018- and 2019-sampling campaigns. In our study, site water availability was described by mean annual precipitation (MAP), available water capacitiy (AWC) of the soil, and competition intensity (CI) between neighbouring trees. A striking result of this precipitation gradient study is the highly significant positive relation of LS to MAP in the 2018 data set, i.e. larger sun-canopy leaves at the drier sites, contradicting the general assumption that plants produce smaller leaves in more xeric environments (Parkhurst & Loucks, 1972). Our finding does also contrast with the results from an Italian gradient, where leaves of *F. sylvatica* were smaller at the southernmost sites with a drier climate (Bussotti *et al.*, 2005). However, our finding is in line with other precipitation gradient studies in beech forests in

Germany and Switzerland (Meier & Leuschner, 2008; Schuldt *et al.*, 2016; Salehi *et al.*, 2020), which also found an LS increase with decreasing precipitation level. A likely explanation is that soil water availability is usually non-limiting in April and May even at the drier sites, which experience drought later in summer, so that higher temperatures stimulate the formation of large leaves in spring (Leuschner, 2020). As soil water reserves were not sufficiently refilled in winter 2018/19 after the very dry 2018 summer (Scharnweber *et al.*, 2020), leaf expansion in 2019 could not profit from ample moisture in spring, which can explain the missing correlation between LS and MAP in the 2019 data set. These results support the assumed mismatch between evaporative demand and transpiring leaf area, confronting beech with drought stress and often leading to pre-senescent leaf shedding, as the species is unable to produce a second, better-adapted leaf generation (Leuschner, 2020; Schuldt *et al.*, 2020; Wohlgemuth *et al.*, 2020; Walthert *et al.*, 2021).

The Huber value (HV), i.e. the sapwood-to-leaf area ratio, of sun-canopy branches decreased with a MAP decrease in the 2018 data set, which is opposite to earlier findings in intraspecific studies with trees, as e.g. in Scots pine (Mencuccini & Grace, 1995; Martínez-Vilalta *et al.*, 2009; Sterck *et al.*, 2012). This indicates that adult beech trees do not improve the water supply of their sun foliage under reduced precipitation through a reduction in the amount of leaf area supplied per unit hydraulic conductance, as would have been expected (Choat et al., 2018). This seems to relate to the finding that LS (Meier & Leuschner, 2008; Salehi *et al.,* 2020) and also stand leaf area index (Meier & Leuschner, 2008) increase in beech stands with decreasing MAP, while the branch and stem hydraulic system responds to increased climatic aridity with a reduction in mean vessel diameter and thus reduced specific conductance (Schuldt *et al.*, 2016; Zimmermann *et al.*, 2021; Weithmann *et al.,* unpubl.). It appears that foliar and xylem responses to increasing climatic aridity are poorly coordinated in mature beech trees, which must expose the foliage to increased drought stress in summers with water deficits.

Our results further demonstrate effects of the local soil moisture regime (AWC) on certain leaf morphological and physiological traits. While LS was unaffected, SLA decreased in the 2019 data set with a reduction in soil water storage capacity, suggesting that water deficits constrain leaf development in beech primarily through the soil water pool and less through the amount of rainfall. In correspondence, Ψ_{tlp} decreased with a reduction in AWC in the 2019 data set, indicating that osmotic adjustment at the leaf level was driven by both rainfall deficiency and a reduced soil water storage capacity. Walthert *et al.* (2021) and Obladen *et al.* (2021) observed after the 2018/19 drought more pronounced drought stress symptoms in

Central Europeans beech stands on soils with limited water storage capacity, which underpins the importance of soil physical properties for drought intensity.

4.5.3   Influence of short-term water deficits on leaf traits

Regressing LS, SLA, HV and the foliar carbon isotope signature (δ^{13}C) on the climatic water balance in the three months before and during leaf expansion (March to May, CWBS) across the 34 sites revealed significant positive effects of instantaneous water deficits on LS and δ^{13}C, while SLA and HV were unaffected. The observed promotion of leaf expansion by higher climatic aridity in spring is in line with the discussed negative MAP effect on LS, probably driven by the stimulation of leaf expansion by higher temperatures. The observed negative CWBS-LS relation contradicts our hypothesis that leaf size would decrease with decreasing CWBS. The δ^{13}C decrease with increasing CWBS, on the other hand, is in agreement with our assumption and suggests that leaf expansion at the sites with higher climatic aridity is closely linked to a reduction in stomatal conductance, relative to sites with lower aridity. Stomatal regulation in beech has been found to be relatively sensitive to atmospheric saturation deficits (Oren *et al.*, 1999; Aranda *et al.*, 2000; Leuschner *et al.,* 2021), which enables beech to reduce stand transpiration to moderate levels under high evaporative demand, even when high leaf area indexes (LAIs) >7 are developed at the drier sites (Meier & Leuschner, 2008).

For Ψ_{tlp}, a significant negative effect of CWB$_{pre}$ was demonstrated, supporting our hypothesis and matching the MAP and AWC effects. Our observation confirms the capacity of mature beech trees for active osmotic adjustment to maintain their cell turgor under drought stress conditions. Among the studied leaf properties and other hydraulic traits investigated earlier (Weithmann *et al.,* unpubl.), the water potential at turgor loss point appears as the trait with closest relatedness to local climatic aridity and thus atmospheric drought stress exposure of the studied beech forests in northern Germany. This supports the conclusion of previous studies on the high indicative value of Ψ_{tlp} for the drought exposure of plants (e.g. Turner, 1986; Abrams, 1988; Bartlett *et al.* 2012b).

4.5.4   Leaf trait variance partitioning and the role of within-population variability

In correspondence with earlier studies, the portion of leaf trait variance attributed to unexplained within-population as well as within-tree differences was high in the studied leaf traits (Leonardi *et al.*, 2006; Bresson *et al.*, 2011; Hajek *et al.*, 2016; Schuldt *et al.*, 2016). Within-crown variability in leaf morphology and physiology as caused by gradients in light

intensity, atmospheric water vapour deficit, and leaf water status is large especially in late-successional tree species as European beech (Reiter *et al.*, 2005; Niinemets, 2007; Oldham *et al.*, 2010; Hagemeier & Leuschner, 2019; Leuschner & Hagemeier, 2020). Therefore, intraspecific comparison of leaf traits is only feasible for samples taken at equivalent crown positions, as was realized in our study by collecting leaves from sun-exposed canopy branches uniformly at $1 - 2$ m distance to the tree tip.

Considerable phenotypic plasticity and high genetic variance within populations are the basis of considerable leaf trait variation among neighbouring trees in a stand (Carsjens *et al.*, 2014; Aranda *et al.*, 2017; Frank *et al.*, 2017). This is demonstrated by a proportion of >50% of within-tree or within-population variance (not explained by CI) in the total variance in most of the studied leaf traits in our study. The high intra-specific variance, be it phenotypic or genetic, represents the basis for successful adaptation of beech populations to drier environments (Aranda *et al.*, 2018). We assume that the high small-scale variation in soil water deficits that developed in consequence of the severe 2018 drought caused the observed higher portion of unexplained site differences in the 2019 data set. These water deficits were not represented by our AWC data that only consider water storage capacity but not actual water reserves. Moreover, including the atmospheric saturation deficit as an explanatory variable has the potential to increase the explained variance, as Zhu *et al.* (2021) could demonstrate a VPD effect on SLA in beech.

4.5.5   Conclusion

Even though our analysis includes only a limited data set on inter-annual leaf trait variation in a given stand, the broad variation in climatic and soil physical conditions covered by the three climatic aridity gradients and in the three years' weather conditions allows some conclusions on leaf trait plasticity and their adaptive modification in response to increasing climatic aridity. Despite sampling at equal positions in the crown, the spatial and inter-annual variation in sun-canopy mean leaf size (LS) and Huber value (HV), i.e. sapwood-to-leaf area ratio, is substantial across the study region, while specific leaf area (SLA) and the water potential at turgor loss point (Ψ_{tlp}) vary less. Reduced precipitation in more continental climates stimulates in beech the production of larger (and thinner) sun leaves, as long as water availability in spring is favourable, which prompts the trees to reduce stomatal conductance later in summer to reduce excessive water loss and to conduct active osmotic adjustment to maintain cell turgor during periods of water deficits. In contrast to findings in other tree species, sapwood-to-leaf area ratio did not increase with decreasing precipitation

level, which must increase the drought stress exposure of beech sun foliage at drier sites, and can be judged as a bottleneck in the drought response strategy of this species.

In contrast to the effect of reduced MAP, inter-annual differences indicate that the severe 2018 drought event triggered the formation of smaller leaves with reduced SLA, increased HV and higher water use efficiency. Thus, European beech exhibits considerable plasticity in sun-canopy leaf traits, which may well exceed the variation in hydraulic traits as demonstrated by climate gradient studies, but the degree of plasticity still awaits comparison with other tree species. As data from the mid crown and shade crown are missing, it is unclear, whether these modifications are restricted to the top crown or occur in the lower crown as well. Continuous monitoring of inter-annual variation in leaf and hydraulic traits in response to climate fluctuation is needed for a better understanding of the drivers and functional consequences of foliage dynamics in trees.

Acknowledgements

4.6 Supplementary information

Table S4.1: Additional stand characteristics of the 34 investigated European beech (*Fagus sylvatica*) stands. Given are site number (see Figure 4.1), name, sampling year, location (latitude and longitude), elevation (m a.s.l.), pH value (H_2O) of mineral soil, carbon/nitrogen ratio of the mineral soil (C/N, g g^{-1}), and the nitrogen content of the mineral soil (N, g kg^{-1}). Source for soil characteristics of sites 31 – 34: Müller-Haubold *et al.* (2013).

Site	Name	Year	Latitude	Longitude	Elevation	soil pH	soil C/N	soil N
1	Grinderwald	2018	52.5723	9.3145	85	4.2	21.0	0.43
2	Brekendorf	2019	54.4287	9.6530	99	4.1	14.4	0.86
3	Malente	2019	54.1547	10.5594	77	4.3	16.7	1.03
4	Halle	2018	51.4997	11.9165	124	4.3	18.8	2.33
5	Mosigkauer Heide	2018	51.7496	12.2095	80	4.6	12.8	0.34
6	Dübener Heide	2018	51.6811	12.5857	159	4.3	20.1	0.49
7	Medewitz	2018	52.0416	12.3792	142	4.2	19.2	0.57
8	Zeuthen	2018	52.3322	13.5853	47	4.2	17.3	0.31
9	Potsdam	2018	52.4461	13.0745	45	4.2	24.8	0.88
10	Wiesmoor	2019	53.4128	7.7775	19	3.9	31.5	1.32
11	Drangstedt	2019	53.5998	8.7668	30	4.1	25.7	0.42
12	Nordholz	2019	53.7829	8.6215	33	4.5	31.6	0.64
13	Sahlenburg	2019	53.8530	8.6120	23	4.3	31.9	0.67
14	Chorin	2019	52.8964	13.8539	64	4.4	22.3	0.21
15	Warenthin	2019	53.1133	12.8536	81	4.7	24.6	0.38
16	Zempow	2019	53.1996	12.7374	109	4.5	23.5	0.53
17	Summt	2018	52.6960	13.4046	58	4.5	24.8	0.38
18	Kaarzer Holz	2019	53.6747	11.7339	70	4.8	15.6	0.25
19	Eggesiner Forst	2019	53.7150	14.1382	32	4.5	22.8	0.50
20	Klötze	2019	52.6207	11.2298	116	4.3	14.7	0.30
21	Calvörde	2019	52.4039	11.2606	87	4.4	14.5	0.42
22	Göhrde	2019	53.1226	10.8196	94	4.7	24.0	0.25
23	Sellhorn	2018	53.1722	9.9528	144	4.2	25.1	0.32
24	Unterlüß	2019	52.8312	10.3170	141	4.5	24.0	0.40
25	Prora	2019	54.4167	13.5552	37	4.2	19.0	0.85
26	Tessin	2019	54.0201	12.4801	49	4.1	19.5	0.65
27	Haake	2018	53.4612	9.9075	72	4.2	27.2	0.42
28	Klövensteen	2018	53.6233	9.7681	34	4.0	28.5	0.99
29	Haffkrug	2019	54.0554	10.7229	51	4.3	16.3	0.73
30	Heidmühlen	2019	53.9619	10.1255	68	4.1	30.3	0.40
31	Calvörde	2010	52.3667	11.2667	105	4.1	19.0	0.33
32	Göhrde	2010	53.1500	10.8667	85	4.3	25.5	0.51
33	Sellhorn	2010	53.1667	9.9500	117	4.3	24.1	0.47
34	Unterlüß	2010	52.8333	10.3167	130	4.2	24.2	0.46

Table S4.2: Climatic variables from two selected sites; one located in the west (Sellhorn, site 23) and one in the east (Potsdam, site 9) of the study region. Given are the data for the study years 2010 (moist), 2018 (extremely dry) and 2019 (dry) and the 60-yr mean (1958 − 2017) for annual precipitation (AP), growing season precipitation (GSP, April − October), annual temperature (AT), growing season temperature (GST), climatic water balance (CWB) and spring climatic water balance (CWBS, March-May). In case of CWB, the long-term mean refers to the period 1991 − 2017.

Variable	Year	Sellhorn	Potsdam
(M)AP (mm yr^{-1})	1958-2017	849.9	576.7
	2010	831.5	625.7
	2018	586.3	358.1
	2019	750.0	503.1
(M)GSP (mm)	1958-2017	434.5	326.0
	2010	447.4	358.9
	2018	229.1	171.8
	2019	360.6	273.1
MAT (°C)	1958-2017	8.4	9.4
	2010	7.5	8.5
	2018	10.0	11.3
	2019	10.5	12.1
MGST (°C)	1958-2017	13.5	15.2
	2010	13.7	15.6
	2018	16.2	18.4
	2019	14.7	17.1
CWB (mm yr^{-1})	1991-2017	307.7	-59.0
	2010	297.2	26.2
	2018	-137.8	-471.0
	2019	86.6	-290.1
CWBS (mm)	1991-2017	-2.3	-81.4
	2010	24.8	-38.6
	2018	-90.3	-154.6
	2019	-47.2	-127.3

Table S4.3: Summary of all leaf variables explored. Given are means ± SE per site of mean leaf size (LS, cm²), specific leaf area (SLA, cm² g^{-1}), Huber value (HV, cm² m^{-1}), carbon isotope signature of leaf dry mass (δ^{13}C, ‰), water potential at turgor loss point (P_{tlp}, MPa) and leaf nitrogen content (N, %).

Site	LS	SLA	HV	δ^{13}C	P_{tlp}	N
1	12.04 ± 1.24	140.53 ± 6.76	2.35 ± 0.25	-28.58 ± 0.23	-2.50 ± 0.03	2.52 ± 0.06
2	13.28 ± 1.15	190.00 ± 7.40	1.92 ± 0.22	-29.51 ± 0.13	-1.90 ± 0.07	2.83 ± 0.07
3	18.71 ± 1.54	227.43 ± 17.52	1.56 ± 0.22	-29.23 ± 0.33	-2.03 ± 0.05	2.65 ± 0.06
4	18.00 ± 0.72	128.85 ± 4.77	1.96 ± 0.13	-27.33 ± 0.14	-2.37 ± 0.03	2.68 ± 0.05
5	18.24 ± 0.85	118.73 ± 3.09	1.98 ± 0.16	-26.93 ± 0.13	-2.62 ± 0.04	2.20 ± 0.03
6	17.42 ± 0.80	114.99 ± 5.14	1.95 ± 0.13	-27.18 ± 0.17	-2.50 ± 0.02	2.38 ± 0.07
7	18.48 ± 0.65	129.38 ± 2.67	2.06 ± 0.15	-27.60 ± 0.30	-2.52 ± 0.03	2.26 ± 0.06
8	18.65 ± 0.81	158.69 ± 11.18	2.14 ± 0.27	-28.35 ± 0.31	-2.32 ± 0.03	2.52 ± 0.06
9	21.41 ± 1.23	127.66 ± 5.62	1.75 ± 0.15	-27.78 ± 0.22	-2.55 ± 0.03	1.94 ± 0.05
10	11.49 ± 0.62	110.64 ± 5.59	2.98 ± 0.40	-28.74 ± 0.32	-2.33 ± 0.04	2.44 ± 0.08
11	11.09 ± 0.61	113.03 ± 3.11	3.13 ± 0.26	-29.29 ± 0.20	-2.35 ± 0.03	2.39 ± 0.05
12	10.96 ± 0.85	127.32 ± 6.09	2.58 ± 0.27	-28.97 ± 0.27	-2.44 ± 0.04	1.94 ± 0.03
13	10.55 ± 0.82	123.17 ± 3.85	3.67 ± 0.39	-29.64 ± 0.18	-2.18 ± 0.04	2.18 ± 0.05
14	14.93 ± 0.70	158.79 ± 5.75	2.05 ± 0.17	-29.06 ± 0.30	-2.47 ± 0.02	2.26 ± 0.04
15	13.68 ± 0.83	147.92 ± 3.68	1.94 ± 0.15	-28.40 ± 0.11	-2.48 ± 0.04	2.11 ± 0.05
16	14.25 ± 1.37	179.06 ± 12.08	2.19 ± 0.17	-28.79 ± 0.24	-2.43 ± 0.03	2.47 ± 0.03
17	18.24 ± 0.51	134.55 ± 5.94	2.12 ± 0.17	-28.31 ± 0.28	-2.46 ± 0.04	2.31 ± 0.06
18	9.35 ± 0.66	112.30 ± 4.39	3.09 ± 0.23	-28.10 ± 0.32	-2.35 ± 0.05	2.31 ± 0.04
19	9.09 ± 0.84	143.11 ± 7.22	3.19 ± 0.40	-29.98 ± 0.22	-2.47 ± 0.03	1.82 ± 0.03
20	8.33 ± 0.87	127.12 ± 3.87	4.83 ± 0.38	-27.34 ± 0.30	-2.15 ± 0.06	2.76 ± 0.07
21	15.53 ± 1.00	129.62 ± 5.32	2.48 ± 0.38	-27.52 ± 0.24	-2.24 ± 0.02	1.87 ± 0.06
22	12.07 ± 0.89	117.43 ± 1.49	3.24 ± 0.19	-28.66 ± 0.23	-2.22 ± 0.03	1.91 ± 0.08
23	17.00 ± 1.09	124.23 ± 3.99	2.37 ± 0.22	-28.19 ± 0.21	-2.38 ± 0.02	2.54 ± 0.04
24	10.96 ± 1.14	101.30 ± 4.39	3.32 ± 0.47	-27.87 ± 0.22	-2.34 ± 0.03	2.11 ± 0.07
25	9.72 ± 1.13	133.24 ± 3.84	3.67 ± 0.43	-28.79 ± 0.18	-2.62 ± 0.08	2.45 ± 0.05
26	14.44 ± 0.59	118.87 ± 2.50	2.43 ± 0.23	-28.14 ± 0.19	-2.43 ± 0.03	2.29 ± 0.05
27	14.25 ± 0.52	126.18 ± 4.25	2.55 ± 0.39	-27.88 ± 0.21	-2.45 ± 0.05	2.40 ± 0.05
28	16.03 ± 1.06	114.34 ± 3.84	2.59 ± 0.18	-27.86 ± 0.25	-2.56 ± 0.04	2.47 ± 0.05
29	17.84 ± 1.15	209.75 ± 12.46	1.64 ± 0.18	-29.08 ± 0.20	-2.15 ± 0.03	2.75 ± 0.07
30	12.18 ± 0.80	173.14 ± 11.95	2.09 ± 0.22	-29.49 ± 0.26	-2.12 ± 0.04	2.48 ± 0.05
31	14.61 ± 0.87	120.83 ± 11.55	2.38 ± 0.16	-	-2.24 ± 0.03	-
32	13.00 ± 0.92	114.27 ± 4.70	2.34 ± 0.29	-	-2.18 ± 0.03	-
33	12.97 ± 0.92	110.56 ± 3.87	2.27 ± 0.23	-	-2.18 ± 0.05	-
34	14.41 ± 0.41	102.00 ± 3.47	2.31 ± 0.29	-	-2.17 ± 0.00	-
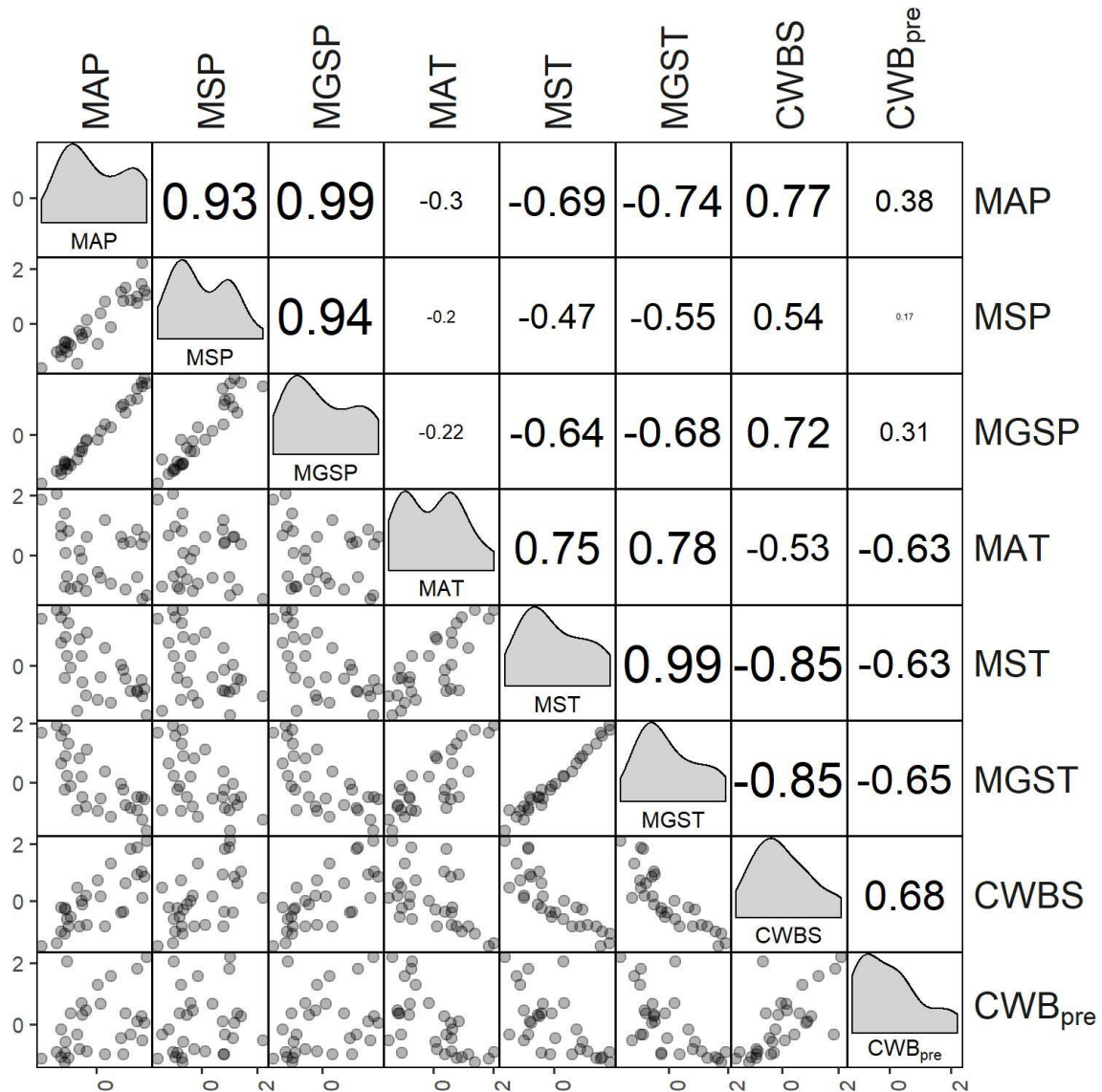
Figure S4.1: Correlation matrix on the site level of climatic variables (sites $1 - 30$). Mean annual precipitation (MAP), mean spring precipitation (April – June, MSP), mean growing season precipitation (April − September, MGSP), mean annual temperature (MAT), mean spring temperature (April – June, MST), mean growing season temperature (April − October, MGST) for the period 1958 – 2017, each, the spring climatic water balance (CWBS, March to May) of the sampling year and the climatic water balance of the month preceding sample collection (CWB$_{pre}$). Data were provided by DWD. The lower triangle depicts the variables on the x- and y-axis in relation, the upper triangle shows the correlation strength (Pearson's *r*) and the plot diagonal shows density plots of the corresponding variables.
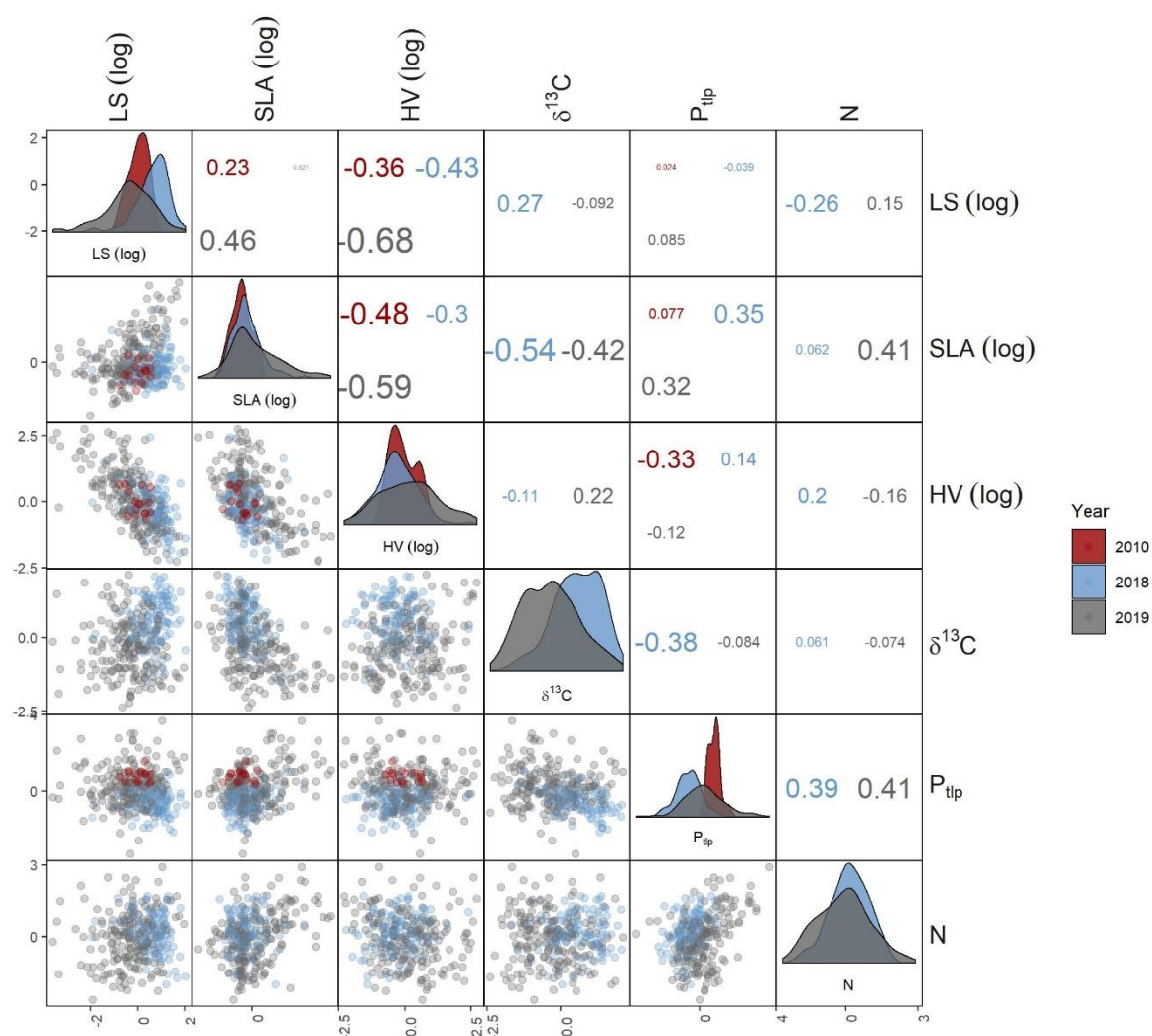
Figure S4.2: Pearson correlation matrix of the investigated leaf traits. Given are the Pearson correlation coefficients per sampling year (upper triangle), the variables on the x- and y-axis in relation (lower triangle), and the plot diagonal shows density plots of the corresponding variables. LS = mean leaf size; SLA = specific leaf area; HV = Huber value; $\delta^{13}C$ = carbon isotope signature, P_{tlp} = leaf water potential at turgor loss point, N = leaf nitrogen content. All variables are means per tree, scaled by their standard deviation, and centred around zero. LS, SLA and HV are log-transformed.

References

Abrams MD. 1988. Sources of variation in osmotic potentials with special reference to North American tree species. *Forest Science*, **34**, 1030–1046.

Adams HD, Zeppel MJB, Anderegg WRL, Hartmann H, Landhäusser SM, Tissue DT, Huxman TE, Hudson PJ, Franz TE, Allen CD *et al.* 2017. A multi-species synthesis of physiological mechanisms in drought-induced tree mortality. *Nature Ecology & Evolution* **1**: 1285–1291.

Anderegg LDL, Berner LT, Badgley G, Sethi ML, Law BE, HilleRisLambers J. 2018. Within-species patterns challenge our understanding of the leaf economics spectrum. *Ecology Letters* **21**: 734–744.

Anderegg WRL, Klein T, Bartlett M, Sack L, Pellegrini AFA, Choat B, Jansen S. 2016. Meta-analysis reveals that hydraulic traits explain cross-species patterns of drought-induced tree mortality across the globe. *PNAS* **113**: 5024–5029.

Aranda I, Bahamonde HA, Sánchez-Gómez D. 2017. Intra-population variability in the drought response of a beech (*Fagus sylvatica* L.) population in the southwest of Europe. *Tree Physiology* **37**: 938–949.

Aranda I, Cadahía E, Fernández de Simón B. 2021. Specific leaf metabolic changes that underlie adjustment of osmotic potential in response to drought by four *Quercus* species. *Tree Physiology*, **41**, 728–743.

Aranda I, Cano FJ, Gascó A, Cochard H, Nardini A, Mancha JA, López R, Sánchez-Gómez D. 2015. Variation in photosynthetic performance and hydraulic architecture across European beech (*Fagus sylvatica* L.) populations supports the case for local adaptation to water stress. *Tree Physiology*, **35**, 34–46.

Aranda I, Gil L, Pardos JA. 2000. Water relations and gas exchange in *Fagus sylvatica* L. and *Quercus petraea* (Mattuschka) Liebl. in a mixed stand at their southern limit of distribution in Europe. *Trees*, **14**, 344–352.

Aranda I, Sánchez-Gómez D, Cadahía E, Simón BF de. **2018.** Ecophysiological and metabolic response patterns to drought under controlled condition in open-pollinated maternal families from a *Fagus sylvatica* L. population. *Environmental and Experimental Botany* **150**: 209–221.

Arndt SK, Irawan A, Sanders GJ. 2015. Apoplastic water fraction and rehydration techniques introduce significant errors in measurements of relative water content and osmotic potential in plant leaves. *Physiologia Plantarum*, **155**, 355–368.

Aubin I, Munson AD, Cardou F, Burton PJ, Isabel N, Pedlar JH, Paquette A, Taylor AR, Delagrange S, Kebli H *et al.* 2016. Traits to stay, traits to move: a review of functional traits to assess sensitivity and adaptive capacity of temperate and boreal trees to climate change. *Environmental Reviews* **24**: 164–186.

Backes K, Leuschner C. 2000. Leaf water relations of competitive *Fagus sylvatica* and *Quercus petraea* trees during 4 years differing in soil drought. *Canadian Journal of Forest Research*, **30**, 335–346.

Bartlett MK, Klein T, Jansen S, Choat B, Sack L. 2016. The correlations and sequence of plant stomatal, hydraulic, and wilting responses to drought. *PNAS* **113**: 13098–13103.

Bartlett MK, Scoffoni C, Ardy R, Zhang Y, Sun S, Cao K, Sack L. 2012a. Rapid determination of comparative drought tolerance traits: using an osmometer to predict turgor loss point. *Methods in Ecology and Evolution* **3**: 880–888.

Bartlett MK, Scoffoni C, Sack L. 2012b. The determinants of leaf turgor loss point and prediction of drought tolerance of species and biomes: a global meta-analysis. *Ecology Letters* **15**: 393–405.

Bartón K. 2020. MuMIn: Multi-Model Inference. https://CRAN.R-project.org/package=MuMIn.

Bates D, Mächler M, Bolker B, Walker S. 2015. Fitting linear mixed-effects models using lme4. *Journal of Statistical Software* **67**: 1–48.

BMEL (Bundesministerium für Ernährung und Landwirtschaft) 2020. Ergebnisse der Waldzustandserhebung 2019.

www.bmel.de/SharedDocs/Downloads/DE/Broschueren/ergebnisse-waldzustandserhebung-2019.html.

BMEL (Bundesministerium für Ernährung und Landwirtschaft) 2021. Ergebnisse der Waldzustandserhebung 2020. www.bmel.de/SharedDocs/Downloads/DE/Broschueren/ergebnisse-waldzustandserhebung-2020.html.

Boessenkool B. 2020. rdwd: select and download climate data from 'DWD' (German Weather Service). https://CRAN.R-project.org/package=rdwd.

Braun S, Witte LC de, **Hopf SE. 2020.** Auswirkungen des Trockensommers 2018 auf Flächen der Interkantonalen Walddauerbeobachtung. *Schweizerische Zeitschrift für Forstwesen* **171**: 270–280.

Braun S, Hopf S-E, Tresch S, Remund J, Schindler C. 2021. 37 years of forest monitoring in Switzerland: Drought effects on Fagus sylvatica. *Frontiers Forests and Global Change* (in press).

Bresson CC, Vitasse Y, Kremer A, Delzon S. 2011. To what extent is altitudinal variation of functional traits driven by genetic adaptation in European oak and beech? *Tree Physiology* **31**: 1164–1174.

Brodribb TJ, Powers J, Cochard H, Choat B. 2020. Hanging by a thread? Forests and drought. *Science* **368**: 261–266.

Buras A, Rammig A, Zang CS. 2020. Quantifying impacts of the 2018 drought on European ecosystems in comparison to 2003. *Biogeosciences* **17**: 1655–1672.

Bussotti F. 2008. Functional leaf traits, plant communities and acclimation processes in relation to oxidative stress in trees: a critical overview. *Global Change Biology* **14**: 2727–2739.

Bussotti F, Prancrazi M, Matteucci G, Gerosa G. 2005. Leaf morphology and chemistry in *Fagus sylvatica* (beech) trees as affected by site factors and ozone: results from CONECOFOR permanent monitoring plots in Italy. *Tree Physiology* **25**: 211–219.

Carsjens C, Nguyen Ngoc Q, Guzy J, Knutzen F, Meier IC, Müller M, Finkeldey R, Leuschner C, Polle A. 2014. Intra-specific variations in expression of stress-related genes in beech progenies are stronger than drought-induced responses. *Tree Physiology* **34**: 1348–1361.

Čater M, Diaci J. 2017. Divergent response of European beech, silver fir and Norway spruce advance regeneration to increased light levels following natural disturbance. *Forest Ecology and Management*, **399**, 206–212.

Chelli S, Ottaviani G, Simonetti E, Campetella G, Wellstein C, Bartha S, Cervellini M, Canullo R. 2021. Intraspecific variability of specific leaf area fosters the persistence of understorey specialists across a light availability gradient. Plant biology (Stuttgart, Germany), **23**, 212–216.

Choat B, Brodribb TJ, Brodersen CR, Duursma RA, López R, Medlyn BE. 2018. Triggers of tree mortality under drought. *Nature* **558:** 531–539.

Choat B, Jansen S, Brodribb TJ, Cochard H, Delzon S, Bhaskar R, Bucci SJ, Feild TS, Gleason SM, Hacke UG *et al.* **2012.** Global convergence in the vulnerability of forests to drought. *Nature* **491:** 752–755.

Curt T, Coll L, Prvosto B, Balandier P, Kunstler G. 2005. Plasticity in growth, biomass allocation and root morphology in beech seedlings as induced by irradiance and herbaceous competition. *Annals of Forest Science*, **62**, 51–60.

Dietrich L, Delzon S, Hoch G, Kahmen A. 2019. No role for xylem embolism or carbohydrate shortage in temperate trees during the severe 2015 drought. *Journal of Ecology* **107**: 334–349.

Farquhar GD, Ehleringer JR, Hubick KT. 1989. Carbon isotope discrimination and photosynthesis. *Annual Review of Plant Physiology and Plant Molecular Biology* **40**: 503–537.

Frank A, Pluess AR, Howe GT, Sperisen C, Heiri C. 2017. Quantitative genetic differentiation and phenotypic plasticity of European beech in a heterogeneous landscape: Indications for past climate adaptation. *Perspectives in Plant Ecology, Evolution and Systematics* **26**: 1–13.

Geβler A, Keitel C, Nahm M, Rennenberg H. 2004. Water shortage affects the water and nitrogen balance in central European beech forests. *Plant Biology* **6**: 289–298.

Hagemeier M, Leuschner C. 2019. Functional crown architecture of five temperate broadleaf tree species: vertical gradients in leaf morphology, leaf angle, and leaf area density. *Forests* **10**: 265.

Hajek P, Kurjak D, Wühlisch G von, Delzon S, Schuldt B. 2016. Intraspecific variation in wood anatomical, hydraulic, and foliar traits in ten European beech provenances differing in growth yield. *Frontiers in Plant Science* **7**: 791.

Hajek P, Link RM, Nock C, Bauhus J, Gebauer T, Gessler A, Kovach K, Messier C, Paquette A, Saurer M et al. 2020. Mutually inclusive mechanisms of drought-induced tree mortality. *bioRxiv*: 2020.12.17.423038.

Hartmann H, Link RM, Schuldt B. 2021. A whole-plant perspective of isohydry: stem-level support for leaf-level plant water regulation. *Tree Physiology*, **41**, 901–905.

Hegyi F. 1974. A simulation model for managing jack pine stands. In: Fries J ed. *Growth models for tree and stand simulation.* Royal College of Forestry, Stockholm: 74–90.

Herbette S, Wortemann R, Awad H, Huc R, Cochard H, Barigah TS. 2010. Insights into xylem vulnerability to cavitation in *Fagus sylvatica* L.: phenotypic and environmental sources of variability. *Tree Physiology* **30**: 1448–1455.

Hsiao TC, Acevedo E, Fereres E, Henderson DW. 1976. Water stress, growth and osmotic adjustment. *Philosophical Transactions of the Royal Society of London* **273**: 479–500.

Knutzen F, Meier IC, Leuschner C. 2015. Does reduced precipitation trigger physiological and morphological drought adaptations in European beech (*Fagus sylvatica* L.)? Comparing provenances across a precipitation gradient. *Tree Physiology*, **35**, 949–963.

Koide RT, Robichaux RH, Morse RH, Smith CM. 2000. Plant water status, hydraulic resistance and capacitance. In: Pearcy RW, Ehleringer JR, Mooney HA, Rundel PW eds. *Plant physiological ecology: field methods and instrumentation.* Dordrecht: Kluwer: 161–183.

Leonardi S, Piovani P, Magnani F, Menozzi P. 2006. A simple general method to evaluate intra-specific transpiration parameters within and among seedling families. *Oecologia* **149**: 185–193.

Leuschner C. 2020. Drought response of European beech (*Fagus sylvatica* L.) - A review. *Perspectives in Plant Ecology, Evolution and Systematics* **47**: 125576.

Leuschner C, Ellenberg H. 2017. Ecology of Central European Forests. Cham: Springer International Publishing AG.

Leuschner C, Hagemeier M. 2020. The economy of canopy space occupation and shade production in early- to late-successional temperate tree species and their relation to productivity. *Forests* **11**: 317.

Leuschner C, Schipka F, Backes K. 2021. Stomatal regulation and water potential variation in European beech: Challenging the iso/anisohydry concept. *Tree Physiology*.

Leuschner C, Wedde P, Lübbe T. 2019. The relation between pressure–volume curve traits and stomatal regulation of water potential in five temperate broadleaf tree species. *Annals of Forest Science*, **76**, 1–14.

Liang X, He P, Liu H, Zhu S, Uyehara IK, Hou H, Wu G, Zhang H, You Z, Xiao Y *et al.* 2019. Precipitation has dominant influences on the variation of plant hydraulics of the native *Castanopsis fargesii* (Fagaceae) in subtropical China. *Agricultural and Forest Meteorology* **271**: 83–91.

Lübbe T, Schuldt B, Leuschner C. 2017. Acclimation of leaf water status and stem hydraulics to drought and tree neighbourhood: alternative strategies among the saplings of five temperate deciduous tree species. *Tree Physiology* **37**: 456–468.

Májeková M, Martínková J, Hájek T. 2019. Grassland plants show no relationship between leaf drought tolerance and soil moisture affinity, but rapidly adjust to changes in soil moisture. *Functional Ecology*, **33**, 774–785.

Martínez-Vilalta J, Cochard H, Mencuccini M, Sterck F, Herrero A, Korhonen JFJ, Llorens P, Nikinmaa E, Nolè A, Poyatos R *et al.* 2009. Hydraulic adjustment of Scots pine across Europe. *New Phytologist* **184:** 353–364.

McGregor IR, Helcoski R, Kunert N, Tepley AJ, Gonzalez-Akre EB, Herrmann V, Zailaa J, Stovall AEL, Bourg NA, McShea WJ *et al.* 2020. Tree height and leaf drought tolerance traits shape growth responses across droughts in a temperate broadleaf forest. *New Phytologist*. doi: 10.1111/nph.16996.

Meier IC, Leuschner C. 2008. Leaf size and leaf area index in *Fagus sylvatica* forests: competing effects of precipitation, temperature, and nitrogen availability. *Ecosystems* **11**: 655–669.

Mencuccini M, Grace J. 1995. Climate influences the leaf area/sapwood area ratio in Scots pine. *Tree Physiology* **15**: 1–10.

Mencuccini M, Rosas T, Rowland L, Choat B, Cornelissen H, Jansen S, Kramer K, Lapenis A, Manzoni S, Niinemets Ü *et al.* 2019. Leaf economics and plant hydraulics drive leaf wood area ratios. *New Phytologist* **224:** 1544–1556.

Müller-Haubold H, Hertel D, Leuschner C. 2015. Climatic drivers of mast fruiting in European beech and resulting C and N allocation shifts. *Ecosystems* **18**: 1083–1100.

Müller-Haubold H, Hertel D, Seidel D, Knutzen F, Leuschner C. 2013. Climate responses of aboveground productivity and allocation in *Fagus sylvatica*: a transect study in mature forests. *Ecosystems* **16**: 1498–1516.

Nakagawa S, Johnson PCD, Schielzeth H. 2017. The coefficient of determination R^2 and intra-class correlation coefficient from generalized linear mixed-effects models revisited and expanded. *Journal of the Royal Society, Interface* **14**. doi: 10.1002/ecm.1410.

Niinemets U. 2007. Photosynthesis and resource distribution through plant canopies. *Plant, Cell & Environment* **30**: 1052–1071.

Niinemets U. 2015. Is there a species spectrum within the world-wide leaf economics spectrum? Major variations in leaf functional traits in the Mediterranean sclerophyll *Quercus ilex*. *New Phytologist* **205**: 79–96.

Obladen N, Dechering P, Skiadaresis G, Tegel W, Keßler J, Höllerl S, Kaps S, Hertel M, Dulamsuren C, Seifert T, Hirsch M, Seim A. 2021. Tree mortality of European beech and Norway spruce induced by 2018-2019 hot droughts in central Germany. *Agricultural and Forest Meteorology*, **307**, 104482.

Oldham AR, Sillett SC, Tomescu AMF, Koch GW. 2010. The hydrostatic gradient, not light availability, drives height-related variation in *Sequoia sempervirens* (Cupressaceae) leaf anatomy. *American Journal of Botany* **97**: 1087–1097.

Oren R, Sperry JS, Katul GG, Pataki DE, Ewers BE, Phillips N, Schäfer KVR. 1999. Survey and synthesis of intra- and interspecific variation in stomatal sensitivity to vapour pressure deficit. *Plant, Cell & Environment* **22**: 1515–1526.

Parkhurst DF, Loucks OL. 1972. Optimal leaf size in relation to environment. *Journal of Ecology* **60**: 505.

Pflug EE, Buchmann N, Siegwolf RTW, Schaub M, Rigling A, Arend M. 2018. Resilient leaf physiological response of European beech (*Fagus sylvatica* L.) to summer drought and drought release. *Frontiers in Plant Science* **9**: 187.

Poorter H, Niinemets Ü, Poorter L, Wright IJ, Villar R. 2009. Causes and consequences of variation in leaf mass per area (LMA): a meta-analysis. *New Phytologist* **182**: 565–588.

Powell TL, Wheeler JK, Oliveira AAR de, **da Costa ACL, Saleska SR, Meir P, Moorcroft PR. 2017.** Differences in xylem and leaf hydraulic traits explain differences in drought tolerance among mature Amazon rainforest trees. *Global Change Biology* **23**: 4280–4293.

Pritzkow C, Williamson V, Szota C, Trouvé R, Arndt SK. 2020. Phenotypic plasticity and genetic adaptation of functional traits influences intra-specific variation in hydraulic efficiency and safety. *Tree Physiology* **40**: 215–229.

R Core Team. 2020. R: a language and environment for statistical computing. Vienna, Austria. https://www.R-project.org/.

Reiter IM, Häberle K-H, Nunn AJ, Heerdt C, Reitmayer H, Grote R, Matyssek R. 2005. Competitive strategies in adult beech and spruce: space-related foliar carbon investment versus carbon gain. *Oecologia* **146**: 337–349.

Renne RR, Schlaepfer DR, Palmquist KA, Bradford JB, Burke IC, Lauenroth WK. 2019. Soil and stand structure explain shrub mortality patterns following global change-type drought and extreme precipitation. *Ecology* **100**: e02889.

Salehi M, Walthert L, Zimmermann S, Waldner P, Schmitt M, Schleppi P, Liechti M, Amadi M., Zahedi Amiri G, Brunner I, Thimonier A. 2020. Leaf morphological traits and leaf nutrient concentrations of European beech across a water availability gradient in Switzerland. *Frontiers in Forests and Global Change*, **3**, article 19.

Schaap MG, Leij FJ, van Genuchten MT. 2001. rosetta: a computer program for estimating soil hydraulic parameters with hierarchical pedotransfer functions. *Journal of Hydrology* **251**: 163–176.

Scharnweber T, Smiljanic M, Cruz-García R, Manthey M, Wilmking M. 2020. Tree growth at the end of the 21st century - the extreme years 2018/19 as template for future growth conditions. *Environmental Research Letters* **15**: 74022.

Schipka F. 2002. Blattwasserzustand und Wasserumsatz von vier Buchenwäldern entlang eines Niederschlagsgradienten in Mitteldeutschland. PhD thesis. University of Göttingen, Germany.

Schuldt B, Buras A, Arend M, Vitasse Y, Beierkuhnlein C, Damm A, Gharun M, Grams TEE, Hauck M, Hajek P *et al.* **2020.** A first assessment of the impact of the extreme 2018 summer drought on Central European forests. *Basic and Applied Ecology* **45**: 86–103.

Schuldt B, Knutzen F, Delzon S, Jansen S, Müller-Haubold H, Burlett R, Clough Y, Leuschner C. 2016. How adaptable is the hydraulic system of European beech in the face of climate change-related precipitation reduction? *New Phytologist* **210**: 443–458.

Seidling W. 2007. Signals of summer drought in crown condition data from the German Level I network. *European Journal of Forest Research* **126**: 529–544.

Sjöman H, Hirons AD, Bassuk NL. 2018. Improving confidence in tree species selection for challenging urban sites: a role for leaf turgor loss. *Urban Ecosystems*, **21**, 1171–1188.

Sterck FJ, Martínez-Vilalta J, Mencuccini M, Cochard H, Gerrits P, Zweifel R, Herrero A, Korhonen JFJ, Llorens P, Nikinmaa E *et al.* **2012.** Understanding trait interactions and their impacts on growth in Scots pine branches across Europe. *Functional Ecology* **26:** 541–549.

Stojnic S, Suchocka M, Benito-Garzón M, Torres-Ruiz JM, Cochard H, Bolte A, Cocozza C, Cvjetkovic B, Luis M. de, Martinez-Vilalta J, Ræbild A, Tognetti R, Delzon S. 2018. Variation in xylem vulnerability to embolism in European beech from geographically marginal populations. *Tree Physiology*, **38**, 173–185.

Tai X, Mackay DS, Anderegg WRL, Sperry JS, Brooks PD. 2017. Plant hydraulics improves and topography mediates prediction of aspen mortality in southwestern USA. *New Phytologist* **213**: 113–127.

Tomasella M, Beikircher B, Häberle K-H, Hesse B, Kallenbach C, Matyssek R, Mayr S 2018. Acclimation of branch and leaf hydraulics in adult *Fagus sylvatica* and *Picea abies* in a forest through-fall exclusion experiment. *Tree Physiology*, **38**, 198–211.

Tomasella M, Nardini A, Hesse BD, Machlet A, Matyssek R, Häberle K-H. 2019. Close to the edge: effects of repeated severe drought on stem hydraulics and non-structural carbohydrates in European beech saplings. *Tree Physiology*, **39**, 717–728.

Turner NC. 1986. Adaptation to water deficits: a changing perspective. *Functional Plant Biology*, **13**, 175.

van der Werf GW, Sass-Klaassen UGW, Mohren GMJ. 2007. The impact of the 2003 summer drought on the intra-annual growth pattern of beech (*Fagus sylvatica* L.) and oak (*Quercus robur* L.) on a dry site in the Netherlands. *Dendrochronologia* **25**: 103–112.

van Genuchten MT. 1980. A closed-form equation for predicting the hydraulic conductivity of unsaturated soils. *Soil Science Society of America Journal* **44**: 892–898.

van Genuchten MT, Leij FJ, Yates SR. 1991. The RETC code for quantifying the hydraulic functions of unsaturated soils. Washington, D.C.: Environmental Protection Agency EPA/600/2-91/065.

Villagra M, Campanello PI, Bucci SJ, Goldstein G. 2013. Functional relationships between leaf hydraulics and leaf economic traits in response to nutrient addition in subtropical tree species. *Tree Physiology* **33**: 1308–1318.

Walthert L, Ganthaler A, Mayr S, Saurer M, Waldner P, Walser M, Zweifel R, Arx G von. 2021. From the comfort zone to crown dieback: Sequence of physiological stress thresholds in mature European beech trees across progressive drought. *Science of the Total Environment* **753**: 141792.

Walthert L, Meier ES. 2017. Tree species distribution in temperate forests is more influenced by soil than by climate. *Ecology and Evolution* **7**: 9473–9484.

Wickham H, Averick M, Bryan J, Chang W, McGowan LD'A, François R, Grolemund G, Hayes A, Henry L, Hester J *et al.* **2019.** Welcome to the tidyverse. *Journal of Open Source Software* **4:** 1686.

Wohlgemuth T, Kistler M, Aymon C, Hagedorn F, Gessler A, Gossner MM, Queloz V, Vögtli I, Wasem U, Vitasse Y *et al.* 2020. Früher Laubfall der Buche während der Sommertrockenheit 2018: Resistenz oder Schwächesymptom? *Schweizerische Zeitschrift für Forstwesen* **171**: 257–269.

Wortemann R, Herbette S, Barigah TS, Fumanal B, Alia R, Ducousso A, Gomory D, Roeckel-Drevet P, Cochard H. 2011. Genotypic variability and phenotypic plasticity of cavitation resistance in *Fagus sylvatica* L. across Europe. *Tree Physiology* **31**: 1175–1182.

Wright IJ, Dong N, Maire V, Prentice IC, Westoby M, Díaz S, Gallagher RV, Jacobs BF, Kooyman R, Law EA *et al.* 2017. Global climatic drivers of leaf size. *Science* 357: 917–921.

Wright IJ, Reich PB, Westoby M, Ackerly DD, Baruch Z, Bongers F, Cavender-Bares J, Chapin T, Cornelissen JHC, Diemer M, Flexas J, Garnier E, Groom PK, Gulias J, Hikosaka K, Lamont BB, Lee T, Lee W, Lusk C, Midgley JJ, Navas M-L, Niinemets U, Oleksyn J, Osada N, Poorter H, Poot P, Prior L, Pyankov VI, Roumet C, Thomas SC, Tjoelker MG, Veneklaas EJ, Villar R. 2004. The worldwide leaf economics spectrum. *Nature*, **428**, 821–827.

Wright IJ, Westoby M, Reich PB. 2002. Convergence towards higher leaf mass per area in dry and nutrient-poor habitats has different consequences for leaf life span. *Journal of Ecology* **90**: 534–543.

Zimmermann J, Link RM, Hauck M, Leuschner C, Schuldt B. 2021. 60-year record of stem xylem anatomy and related hydraulic modification under increased summer drought in ring- and diffuse-porous temperate broad-leaved tree species. *Trees* **35**: 919–937.

Zhu J, Thimonier A, Etzold S, Meusburger K, Waldner P, Schmitt M, Schleppi P, Schaub M, Thormann J-J, Lehmann MM. 2021. Variations in leaf morphological traits of European beech and Norway spruce over two decades in Switzerland. *Frontiers in Forests and Global Change* (in press).

CHAPTER
5

Synopsis

The present study provides one of the largest intra-specific datasets on xylem as well as leaf traits of upper canopy branches in European beech, a main tree species in Central Europe's deciduous forests and a major timber species. The investigated mature stands are growing across a steep precipitation gradient and on differing soil textures, yet Pleistocene unconsolidated substrate throughout the study. The focus of this work was to provide a comprehensive picture of the plasticity in the determined traits and their adjustments in response to water availability. Further, the effects of branch age and tree height on xylem traits were considered. The following chapter aims to summarize, relate, and discuss the results of the three presented studies.

5.1 Trait adjustments in relation to water availability

While most of the existing trait-based intra-specific gradient studies focus on climatic variables to explain changes in the investigated traits alongside precipitation gradients (e.g. Herbette *et al.*, 2010; Schuldt *et al.*, 2016; Liang *et al.*, 2019), we further included plant-available water capacity of the soils and competition between neighbouring trees to provide a more comprehensive approach describing the water availability across our gradient (see Jump *et al.*, 2017; Walthert & Meier, 2017; Hajek *et al.*, 2020). To provide an overview and to compare the effects of long-term water availability between the studied traits, linear mixed effects models were conducted on tree level with 60-year mean annual precipitation (MAP), plant available water capacity of the soils (AWC) and Hegyi competition index (CI) as fixed effects variables and random intercepts for site (Table 5.1).

The influence of the variables related to water availability on xylem traits was surprisingly small (Chapter 2 and 3). Embolism resistance (in terms of water potential inducing 50% loss of hydraulic conductance (P_{50})) was significantly related to AWC, but only 7% of the variance was explained by water availability referring to the model results presented in this Chapter (Table 5.1 and Figure 5.2). For xylem-specific hydraulic conductivity (K_s) 2% of the variance was attributed to these variables with no significant effect of water availability on K_s. The expected increase in embolism resistance towards drier conditions as found for *F. sylvatica* by Schuldt *et al.* (2016) supposing an intra-specific adaption or acclimation in this trait, could therefore only partly be confirmed. Besides the high variability within populations and the considerable effect of branch age on $P_{50,}$ that may hamper the identification of a clearer environmental signal (Chapter 2), a certain measurement inaccuracy may also play a role. A clogging of some vessels provoked by tiny particles within the measurement solution (used for the flushing procedure and the conductivity

measurements), that were released from the Xyl'em apparatus, may be possible. The mentioned measurement uncertainties might particularly be relevant concerning the results on K_s with additional uncertainties due to the formation of small air bubbles within the measurement solution during the measurement procedure. This might additionally impede the identification of intra-specific drivers of embolism resistance and hydraulic conductivity. Like for P_{50} and K_s, the variance explained by long-term water availability was small for the anatomical variables selected for the overview shown in the present Chapter (1%, 4% and 6% for vessel density (VD), hydraulically weighted vessel diameter (D_h) and lumen to sapwood area ratio (A_L/A_X), respectively). D_h and A_L/A_X were significantly affected by MAP as well as climatic water balance (CWB; Chapter 3), while VD was only significantly related to AWC when branch age was included in the model as fixed effect variable as in Chapter 3 (Table 3.2). The observed positive relationship between vessel diameter and MAP (Table 5.1) or climatic water balance (Chapter 3) is in line with our expectations, as final cell diameter is likely to depend on the water availability during cell enlargement, like it was observed for tracheid diameter in *Pinus sylvestris* L. (Cabon *et al.*, 2020).

In view of considering edaphic factors besides CWB, the rather low influence of long-term water availability on the investigated xylem traits was unexpected, but the lacking effect of climatic water availability on embolism resistance matches results of previous studies on *F. sylvatica* (Herbette *et al.*, 2010; Wortemann *et al.*, 2011; Rosas *et al.*, 2019; but see Schuldt *et al.*, 2016). Regarding the anatomical variables, annual ring-wise analyses might have revealed clearer relations, because long-term anatomical time series showed a strong influence of current and previous year's CWB on vessel diameter and vessel density in stem wood of *F. sylvatica*, while modifications in the hydraulic architecture across a precipitation gradient were less clear (Zimmermann *et al.*, 2021). As only a minor influence of xylem anatomy on embolism resistance was observed (Figure 3.6), the effects of water availability on the anatomical architecture are possibly rather a consequence of drought-induced reductions in cell enlargement than represent an active acclimative response to increase the hydraulic safety of the xylem (Chapter 3). The limited adaptive variation in embolism resistance was also observed in Scots pine, another species with a wide climatic envelope (Martínez-Vilalta *et al.*, 2009). Branch embolism resistance might therefore be a rather conserved trait, with only limited adjustments to drier conditions on the intra-specific level.

Table 5.1: Results of linear mixed effect models testing the relationship between water availability and investigated traits. Given are the scaled estimates and p-values for the intercept, mean annual precipitation (MAP), plant available soil water capacity (AWC) and competition between neighbouring trees (Hegyi competition index, CI, log-transformed), the standard deviation for random intercepts for site, the residual standard deviation and the number of observations. P_{50} = water potential inducing a 50% loss of hydraulic conductance, K_s = xylem-specific hydraulic conductivity, D_h = hydraulically weighted vessel diameter, VD = vessel density, A_L/A_X = lumen to sapwood area ratio (log-transformed), LS = mean leaf size (log-transformed), SLA = specific leaf area (log-transformed), HV = sapwood to leaf area ratio (Huber value, log-transformed), $\delta^{13}C$ = leaf carbon isotope signature, P_{tlp} = water potential at turgor loss point. Leaf traits are means per tree and were tested for the sampling years 2018 and 2019, separately. P-values < 0.05 for fixed effect variables are in bold.

Variable	Fixed parts								Random parts		Obs.
	Intercept		MAP		AWC		CI		Site	Res.	
	Est.	p	Est.	p	Est.	p	Est.	p	SD	SD	n
P_{50}	-3.39	<0.001	0.00	0.98	0.10	**0.03**	-0.01	0.44	0.22	0.29	298
K_s	1.53	<0.001	0.06	0.15	0.01	0.80	0.02	0.51	0.16	0.49	298
D_h	28.21	<0.001	0.48	**0.02**	0.06	0.77	-0.03	0.84	0.81	2.15	296
VD	460.37	<0.001	-2.26	0.63	-4.07	0.40	3.20	0.37	17.43	58.02	296
A_L/A_X	2.86	<0.001	0.04	**0.03**	0.01	0.70	0.01	0.33	0.07	0.13	296
LS 18	2.82	<0.001	-0.10	**0.03**	-0.06	0.15	0.01	0.68	0.12	0.18	110
LS 19	2.47	<0.001	-0.01	0.90	0.06	0.30	-0.01	0.67	0.23	0.27	190
SLA 18	4.85	<0.001	-0.02	0.42	0.02	0.53	0.03	**0.02**	0.08	0.12	110
SLA 19	4.94	<0.001	0.00	0.97	0.13	**0.01**	0.00	0.80	0.19	0.14	190
HV 18	0.73	<0.001	0.10	**<0.001**	0.00	0.89	-0.08	**<0.01**	0.00	0.27	110
HV 19	0.92	<0.001	-0.01	0.85	-0.07	0.32	0.02	0.42	0.29	0.32	190
$\delta^{13}C$ 18	-27.82	<0.001	-0.20	0.27	-0.09	0.61	-0.18	**0.01**	0.49	0.71	110
$\delta^{13}C$ 19	-28.78	<0.001	-0.27	0.13	0.01	0.95	-0.05	0.40	0.68	0.76	186
P_{tlp} 18	-2.48	<0.001	0.00	0.98	0.01	0.74	0.02	0.12	0.09	0.11	110
P_{tlp} 19	-2.30	<0.001	0.09	**0.01**	0.08	**0.03**	-0.01	0.58	0.14	0.13	190

In contrast to the studied xylem traits, leaf traits showed a high plasticity in response to water availability. As sample collection was conducted in the two consecutive summers of 2018 (11 sites) and 2019 (19 sites), and moreover 2018 was an exceptional dry year, the effects of long-term water availability on leaf traits were analysed separately for the two sampling years. Even though the study design does not allow for direct comparisons between the two sampling years, some conclusions on the possible impact of the 2018/19 drought were drawn in Chapter 4. Particularly mean leaf size (LS) and sapwood-to-leaf area ratio (Huber value, HV) varied between 2018 and 2019, possibly affected by both, dry conditions and mast fruiting. Results of other studies investigating the effects of the 2018/19 drought on European beech suggest that modifications in LS and leaf number are rather stress reaction than acclimative responses (Schuldt *et al.*, 2020; Wohlgemuth *et al.*, 2020; Walthert *et al.*, 2021).

Contrary to findings on *Pinus sylvestris* and *Eucalyptus obliqua,* where acclimative changes in HV in response to drought were described (Mencuccini & Grace, 1995; Martínez-Vilalta *et al.*, 2009; Sterck *et al.*, 2012; Pritzkow *et al.*, 2020), HV decreased towards drier sites and with decreasing neighbourhood competition (CI). This increase in leaf area per unit of conducting sapwood area with decreasing water availability was at least partly related to an increase in LS (see Figure S4.2), indicating that leaf number was not significantly modified in order to adjust HV. The observed increase in LS with decreasing MAP for the 2018 data set is in line with other studies (Meier & Leuschner, 2008; Schuldt *et al.*, 2016) and is assumable induced by higher temperatures during leaf expansion at drier sites under adequate water supply in spring. This assumption is supported by the lack of relation between LS and MAP for the 2019 data set, when water availability during leaf expansion was low. Moreover, the observed decrease of HV with MAP indicates that European beech does not improve the water supply to sun-canopy leaves towards drier conditions and therefore, drought stress exposure is increased during dry summers, what can be seen as a bottleneck in the species' drought tolerance strategy. However, leaf mass and leaf area index were found to decrease towards drier sites across a shorter gradient in the same region (Müller-Haubold, 2015), indicating that water demand is not increasing towards drier conditions despite greater LS. Furthermore, the water potential at turgor loss point (P_{tlp}) and specific leaf area were adjusted towards drier conditions in 2019, and P_{tlp} as well as δ^{13}C-signature were modified in response to short-term CWB, indicating an acclimative variation in response to drought in these traits.

Generally, one must keep in mind that the retrieved monthly grid-data on MAP and CWB are interpolated from DWD station data and therefore uncertainties originate from the interpolation method, and erroneous or missing observations. Furthermore, processes relevant for local climate which are not covered by measurements of the climate stations are missing. Therefore, including stand specific data on the vapour pressure deficit (VPD) referred from on-site measurements and additional information on soil water content might have revealed stronger effects of water availability on the investigated variables, as VPD was identified as an important factor affecting the drought intensity a tree is exposed to (Rawson *et al.*, 1977; Yuan *et al.*, 2019; Grossiord *et al.*, 2020;).

The overall low effect of neighbourhood competition on the investigated traits might be due to the structural similarity between the stands as indicated by values of CI ranging from 0.4 to 0.7.

5.2 Intra-specific trait variability

All investigated variables differed notably between trees and between sites (see Table 5.2 for summaries on tree level). To illustrate the variation of selected variables, the coefficient of quartile variation (CQV= (Q3-Q1)/(Q1+Q3)) was calculated (Figure 5.1) and the total variance in the traits included in the LME models (see Table 5.1) was decomposed into fixed (water availability) and random effects (unexplained site differences) as well as the residual variance (unexplained within-population variability; Figure 5.2).

The observed high intra-specific variability in the investigated traits matches the results of previous trait-based studies in *F. sylvatica* (Herbette *et al.*, 2010; ; Schuldt *et al.*, 2016; Lübbe *et al.*, 2017) and arises from a combination of genetic variation and phenotypic plasticity (Bresson *et al.*, 2011; Wortemann *et al.*, 2011; Knutzen *et al.*, 2015; Stojnic *et al.*, 2017).

Table 5.2: Means, standard errors (SE) and minimum and maximum values of selected traits on tree level (n = 300). P_{50} = water potential inducing a 50% loss of hydraulic conductance, K_s = xylem-specific hydraulic conductivity, D_h = hydraulically weighted vessel diameter, VD = vessel density, A_L/A_X = lumen to sapwood area ratio (log-transformed), LS = mean leaf size (log-transformed), SLA = specific leaf area (log-transformed), Hv = sapwood to leaf area ratio (Huber value, log-transformed), $\delta^{13}C$ = leaf carbon isotope signature, P_{tlp} = leaf water potential at turgor loss point. Leaf traits represent means of three samples per tree.

Variable	P_{50}	K_s	D_h	VD	A_L/A_X	LS	SLA	HV	$\delta^{13}C$	P_{tlp}
Mean	-3.38	1.53	28.21	460.33	17.63	14.27	138.71	2.53	-28.43	-2.36
SE	0.02	0.03	0.13	3.47	0.15	0.26	2.10	0.06	0.06	0.01
Min	-4.27	0.12	21.96	291.07	9.13	3.89	77.07	0.97	-30.95	-3.04
Max	-2.29	3.12	36.18	649.39	24.60	27.04	306.95	6.66	-26.17	-1.60

Corresponding to results of studies investigating similar traits on the inter-specific level, HV, K_s and SLA were the most variable traits, while P_{tlp} and $\delta^{13}C$ showed the least variability (Figure 5.1; Rosas *et al.*, 2019; Fuchs *et al.*, 2021). Remarkably, the intra-specific coefficient of quartile variation (CQV) in HV and K_s in the present study was higher than the inter-specific CQV in three broadleaved species (*Acer plataniodes* L., *Carpinus betulus* L. and *Tilia cordata* Mill.), corresponding with the finding that only a small portion of variation in these traits was attributed to differences between species (Fuchs *et al.*, 2021). In contrast, variance in P_{50} and P_{tlp} mainly occurred across species and was therefore higher on the inter-specific level (Rosas *et al.*, 2019; Fuchs *et al.*, 2021), but the ranges in site-averages of P_{50} and P_{tlp} were with 1.02 MPa and 0.73 MPa in *F. sylvatica* higher than for the three species

investigated by Fuchs *et al.* (2021) with 0.84 MPa and 0.36 MPa in *C. betulus*, 0.52 MPa and 0.26 MPa in *A. platanoides* and 0.31 MPa and 0.50 MPa in *T. cordata* for P_{50} and P_{tlp}, respectively. However, the number of sites differed considerably between the two studies and the higher intra-population than between-population variability weakens the informative value of comparing site averages.
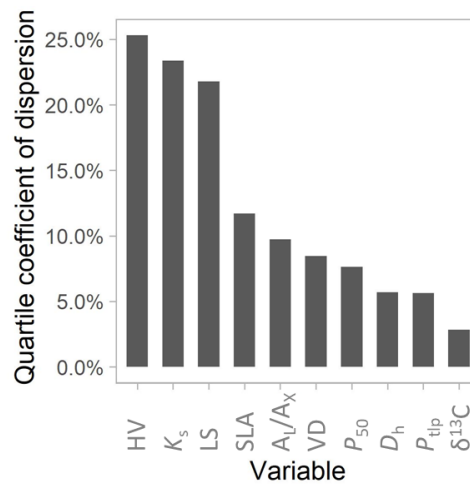
Figure 5.1: Coefficients of quartile variation (CQV) of the studied traits on tree level. See Table 5.2 for abbreviations.

The overall high portion of variance in the investigated traits attributed to differences between trees of a population (Figure 5.2) corresponds with findings of a higher intra-population genetic variance compared with the genetic variance between populations in European beech (Buiteveld *et al.*, 2007; Carsjens *et al.*, 2014). Even though intra-population differences might partly be genetically determined, the observed variation within single trees and between trees of a population demands further investigations of underlying factors. As forest management usually aims at concentrating growth to a limited number of trees, the investigated stands mostly were single layer stands with widely protruding crowns. This management practice could additionally influence the variability within crowns compared to natural or semi-natural beech forests with two to three canopy layers (Leuschner & Ellenberg, 2017).

The unexplained variance between populations was discussed to be attributable to either genetic differences between populations or more likely to non-determined environmental factors like short-term weather events deviating from long-term climatic averages. Differences in soil water availability might also play a role. Moreover, local differences in masting intensity, which influences carbohydrate and nutrient availability might have

affected the between-population variability, particularly in leaf morphology of the 2019 data set.

Overall, the identification of drought hardier populations referring to the investigated traits is hampered by the high unexplained intrapopulation variability (not explained by CI), combined with the considerable unexplained variance between populations (not explained by MAP and AWC). Generally, a high intra-specific variability is considered to improve the acclimation potential of a species to changing environmental conditions, but the rather small portion of variance explained by long-term water availability in xylem traits and the decrease of HV with decreasing MAP do not indicate a high acclimation capacity to drought in European beech. The high variability of the investigated traits highlights the importance of considering this intra-specific variability instead of using mean values at the species level when working with trait-based models.
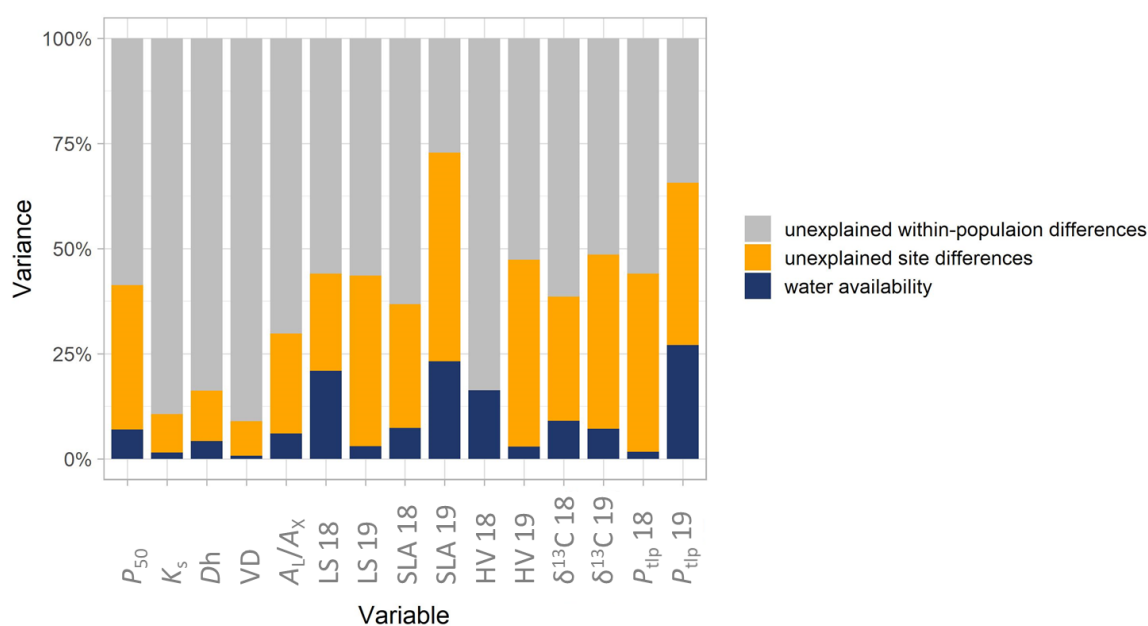
Figure 5.2: Variance components of the linear mixed effects models testing the effects of MAP, AWC, and CI (water availability), with random intercepts for sites on selected traits. Due to convergence issues, the site-wise random intercept had to be omitted in the model for HV in 2018. See Table 5.1 for details.

5.3 Effect of branch age on xylem traits

A striking finding of this study is the dominant effect of branch age on embolism resistance and the anatomical variables (except for A_L/A_X, Table 2.2 and Table 3.2). As branches of similar diameter (8.9 ± 0.1 mm) were selected for the vulnerability measurements, and anatomical analyses were conducted on a basipetal segment of these branches (with

diameters ranging from 7 – 11 mm), the range of branch age from 2 – 22 years at the basipetal end was surprisingly high. As discussed in Chapter 3, the differences in branch age could be partly due to the branching pattern in beech, which is mostly dichotomous with different side branches taking over lead growth in the top. Overtopping by other branches could lead to small-scale differences in microclimatic conditions in the uppermost canopy and induce reduced growth rates. Moreover, a study on lateral and vertical crown expansion revealed no dependence on light availability of lateral branch increment of canopy branches in the contact zone between trees, but more than 50 percent of the lateral branches were broken at least once within the six years preceding the investigations (Hajek *et al.*, 2015). Therefore, mechanical interactions with neighbouring trees could also have an impact on growth rates, at least in more lateral crown sections.

The observed decrease in vessel diameter and increase in vessel density with increasing branch age (Figure 3.2) seems obvious when comparing different-aged branches of similar diameter. However, the significant decrease in embolism resistance with branch age (Figure 2.4) was less foreseeable, as generally embolism resistance is predicted to increase with decreasing conduit size (see Hacke *et al.*, 2017 for review). Decreasing embolism resistance could be due to the so-called "cavitation fatigue", describing the reduction of embolism resistance after a cycle of embolism formation and refilling in some species while other species seem to be resistant to this phenomenon (Hacke *et al.*, 2001). There is evidence that some species are capable to refill embolised conduits after drought, but how frequently refilling occurs is not clear, while recovery during spring associated with positive xylem pressures after frost-induced losses of conductivity seems likely (Brodersen & McElrone, 2013; Cochard & Delzon, 2013; Schenk *et al.*, 2021). In the present study, branches were flushed with a standard measurement solution, imitating xylem sap characteristics, prior to the construction of vulnerability curves, to ensure that all conduits are included in the vulnerability measurements. Vulnerability curves obtained from flushed samples may therefore include weakened xylem (cavitation fatigue), that is not fully functional under natural conditions, but a comparison of vulnerability curves of flushed versus non-flushed samples from ten trees (site 20) did not show a significant difference in mean P_{50}-values (L. Würzberg, unpublished data). Nevertheless, frost-fatigue, i.e. reduced embolism resistance preceding frost-induced embolism and spring recovery, was discussed as possible explanation for the decreasing embolism resistance with increasing branch age (Chapter 2). The choice of the best sampling strategy to gain comparable values on the one hand and maintaining information about traits' variability on the other hand is an open issue in

functional trait ecology. As sun exposure is known to have a dominant effect on our studied traits, we decided to collected samples from the sun-exposed canopy, being aware that tree height will not be constant, as it is usually varying across climatic gradients. Furthermore, the selected second-order side branches must meet the criteria for the Cavitron measurements (diameter, length, straight shape), leading to a certain range in the distances to the tip of the collected main branch. Even though branch age was not related to any site- or tree-specific variable, the unexpected strong influence on xylem anatomy and embolism resistance might have impaired the identification of an effect of other variables. Therefore, it can be recommended for future studies investigating the influence of environmental variables on branch traits to keep branch age preferably constant, despite the higher expenditure of time. Overall, the results highlight the importance of further investigations on within-tree variability of xylem anatomical and hydraulic traits. This might especially be important for angiosperms, as in four Pinaceae species no variability in embolism resistance between branches within the crown was observed (Bouche *et al.*, 2016).

5.4 Xylem anatomy and tree height

Despite the non-existent relation between climatic variables and tree height across our study sites, tree height is linked to climate on a global scale (Moles *et al.*, 2009). Studies investigating the hydraulic architecture of trees did not always consider both factors, therefore the influence of plant height versus water availability on xylem anatomy remains controversial (Pfautsch *et al.*, 2016; Lechthaler *et al.*, 2019; Fajardo *et al.*, 2020; Chapter 3). Theory predicting vessel widening towards the basal parts of trees to maintain flow resistance constant with increasing path length (West *et al.*, 1999), widely agrees with empirical evidence (Anfodillo *et al.*, 2013; Olson *et al.*, 2014; Gleason *et al.*, 2018). Besides path-length resistance, the gravitational component of water potential induces vertical changes along the flow path resulting in an increase in xylem tension with tree height of about 0.01 MPa m^{-1} in trees, as was demonstrated at midday in tall *Sequoia sempervirens* trees (Koch *et al.*, 2004). These changes in xylem tension were found to result in vertical changes in leaf and xylem hydraulic characteristics (Woodruff *et al.*, 2004; 2007; 2008; Domec *et al.*, 2008). The predicted increase of apical vessel diameter with tree height across species (Rosell *et al.*, 2017) does not correspond with observed and predicted within-tree constraints of increasing xylem tension on branch elongation, leaf dimensions and leaf mass per area (Koch *et al.*, 2004; Woodruff *et al.*, 2007), demonstrating the complexity of the height effect. Moreover, the lacking effect of tree height on anatomical traits (Chapter 3) and

embolism resistance (results not shown), combined with the strong effect of branch age, point out that the effects of growth rate, which are often ignored despite the considerable ontogenetic variation along the main axis as well as within the crown, need particular emphasis when the effect of tree height on xylem characteristics is investigated.

5.5 Comparison to other species and general conclusions

Embolism resistance was identified as an important trait related to the survival success of tree species after droughts in various forest regions (Anderegg *et al.*, 2016; Brodribb *et al.*, 2020; Arend *et al.*, 2021). While most of the studies focus on inter-specific differences in hydraulic traits, the present study provides one of the largest datasets on intra-specific variability in xylem and leaf traits of upper canopy branches.

Compared to other broadleaf timber species, average P_{50} of the 300 investigated beech trees was with -3.38 ± 0.02 MPa less resistant than branch xylem of *A. platanoides* (-4.62 MPa), *C. betulus* (-4.25 MPa) and *Quercus petraea* Liebl. (-5.0 MPa), but more resistant than *T. cordata* (-3.06 MPa; data from Dietrich *et al.*, 2019 and Fuchs *et al.*, 2021). The rather low embolism resistance is in agreement with the known drought sensitivity of *F. sylvatica*, which is also reflected in continuous growth declines in many Central European beech forests from 2010 onwards (Leuschner, 2020). Even though embolism resistance was supposed to be assessed as an evolutionary canalized trait due to the relatively lower intra-specific than inter-specific variability (Fuchs *et al.*, 2021), the span of nearly 2 MPa in P_{50} between the 300 investigated beech trees points out that intra-specific variability should not be ignored in the context of trait-based models predicting tree mortality. The observed variability in P_{50}, which is mainly attributed to within-population variance (that can partly be explained by branch age, Chapter 2) demands further investigations on the drivers of this variability. Yet, the rather low portion of the variance in embolism resistance explained by long-term water availability, which matches results of previous studies on European beech and other tree species (e.g. Herbette *et al.*, 2010; Martínez-Vilalta *et al.*, 2009; Rosas *et al.*, 2019; Fuchs *et al.*, 2021; but see Schuldt *et al.*, 2016), suggests a low acclimative or adaptive response in this trait. Therefore, branch embolism resistance might not be a promising trait regarding the identification of drought-resistant populations but can be robust measure for species-comparisons. Furthermore, the results suggest a minor importance of this variability in embolism resistance for the capacity to acclimate to changing climatic conditions. However, P_{50} was significantly related to AWC of the soils, a driver that has not been

intensively studied so far and might be of importance particularly in respect of water supply during drought periods.

Embolism resistance has been found to increase with an increase in vessel connectivity and vessel grouping in poplar (Lemaire *et al.*, 2020). In contrast, our data showed a significant decrease with these anatomical parameters, but the relation was weak. As embolism resistance is significantly decreasing with increasing branch age (Chapter 2), while vessel grouping index is increasing (Chapter 3), a clearer relationship is possibly masked by the effect of branch age. However, the observed modifications in xylem anatomy in response to water availability suggest that anatomical changes are more a growth consequence of water shortage than active acclimative responses to increase embolism resistance. Accordingly, a sensitive drought-response of radial vessel properties in *F. sylvatica* was observed by Zimmermann *et al.* (2021), resulting in the largest long-term decrease in tree-ring width and the largest ring width reduction in and after dry years compared to *A. platanoides*, *A. pseudoplatanus*, *Fraxinus excelsio*r L. and *Q. petraea*, while adjustments in xylem hydraulic properties across a precipitation gradient were less clear for all species. Correspondingly, tree growth was not correlated to MAP for the European beech trees of this study, while summer drought was the most limiting factor, which was more pronounced at the drier and sandier sites (R. Weigel & E. Banzragch, personal communication).

The tissue-specific dehydration tolerance plays an important role in the survival of trees under limited water supply (Körner, 2019) and P_{tlp} was identified as an important leaf trait to characterize a plant's drought tolerance (Bartlett *et al.*, 2012; Zhu *et al.*, 2018; McGregor *et al.*, 2020). In contrast to xylem embolism resistance, studies on intra-specific adjustments in P_{tlp} with increasing aridity are rather consistent (Tomasella *et al.*, 2018; Liang *et al.*, 2019; Rosas *et al.*, 2019; Pritzkow *et al.*, 2020). Yet, Fuchs *et al.* (2021) observed a marginal significant relation between P_{tlp} and aridity only in *C. betulus*, but not in *A. campestre* or *T. cordata*. The suggestion of Leuschner (2020) that adjustments in P_{tlp} occur mostly under dry conditions in *F. sylvatica* was confirmed by the significant relation between P_{tlp} and MAP as well as AWC of the soils for the 2019 data set, while for the 2018 data set no relationship was found (Chapter 4). Indeed, influence of water availability was with 27% of explained variance highest for P_{tlp} of the 2019 data set compared to other studied traits (Figure 5.2). Furthermore, P_{tlp} was adjusted to CWB of the month preceding sample collection. With mean P_{tlp} of -2.36 ± 0.01 MPa, leaves of *F. sylvatica* reached higher tissue osmotic concentrations than *A. platanoides* (-2.02 MPa) and *T.cordata* (-2.23 MPa), but smaller concentrations than *C. betulus* (-2.66 MPa; data from Fuchs *et al.*, 2021). Despite the low

variability in P_{tlp} compared to the other variables, the intra-specific range of 1,44 MPa is high, considering the predicted restriction in variation of P_{tlp} to 2 MPa, excluding plants with sclerophyllous leaves or from perhumid ecosystems (Bartlett *et al.*, 2012). Besides P_{tlp}, SLA was adjusted towards drier sites in the drought-affected year 2019, while LS and HV were not (Chapter 4). In contrast, the increase in LS towards drier sites concomitant with a decrease in HV for the 2018 data set, suggests an increased drought stress exposure of sun foliage in summers with water deficits. Moreover, the drought stress exposure may be enhanced by the low coordination of foliar and xylem responses to reductions in water availability.

Overall, our results confirm the anticipated drought sensitivity of European beech. The findings suggest a stronger environmental influence on leaf traits than on xylem traits and that under dry conditions, osmotic adjustment is one of the main acclimative responses to water deficits in *F. sylvatica*. Furthermore, our results show that trait patterns interpreted as an adaption to climatic aridity on a global scale cannot simply be extrapolated to the intra-specific level.

References

Anderegg WRL, Klein T, Bartlett M, Sack L, Pellegrini AFA, Choat B, Jansen S. 2016. Meta-analysis reveals that hydraulic traits explain cross-species patterns of drought-induced tree mortality across the globe. *PNAS* **113**: 5024–5029.

Anfodillo T, Petit G, Crivellaro A. 2013. Axial conduit widening in woody species: a still neglected anatomical pattern. In: Baas P, ed. *Wood Structure in Plant Biology and Ecology*. Leiden: Brill, 24–36.

Arend M, Link RM, Patthey R, Hoch G, Schuldt B, Kahmen A. 2021. Rapid hydraulic collapse as cause of drought-induced mortality in conifers. *PNAS* **118**. doi: 10.1073/pnas.2025251118

Bartlett MK, Scoffoni C, Sack L. 2012. The determinants of leaf turgor loss point and prediction of drought tolerance of species and biomes: a global meta-analysis. *Ecology letters* **15**: 393–405.

Bouche PS, Jansen S, Sabalera JC, Cochard H, Burlett R, Delzon S. 2016. Low intra-tree variability in resistance to embolism in four Pinaceae species. *Annals of Forest Science* **73**: 681–689.

Bresson CC, Vitasse Y, Kremer A, Delzon S. 2011. To what extent is altitudinal variation of functional traits driven by genetic adaptation in European oak and beech? *Tree Physiology* **31**: 1164–1174.

Brodersen CR, McElrone AJ. 2013. Maintenance of xylem network transport capacity: a review of embolism repair in vascular plants. *Frontiers in Plant Science* **4**: 108.

Brodribb TJ, Powers J, Cochard H, Choat B. 2020. Hanging by a thread? Forests and drought. *Science* **368**: 261–266.

Buiteveld J, Vendramin GG, Leonardi S, Kamer K, Geburek T. 2007. Genetic diversity and differentiation in European beech (*Fagus sylvatica* L.) stands varying in management history. *Forest Ecology and Management* **247**: 98–106.

Cabon A, Fernández-de-Uña L, Gea-Izquierdo G, Meinzer FC, Woodruff DR, Martínez-Vilalta J, Cáceres M de. **2020.** Water potential control of turgor-driven tracheid enlargement in Scots pine at its xeric distribution edge. *New Phytologist* **225**: 209–221.

Carsjens C, Nguyen Ngoc Q, Guzy J, Knutzen F, Meier IC, Müller M, Finkeldey R, Leuschner C, Polle A. 2014. Intra-specific variations in expression of stress-related genes in beech progenies are stronger than drought-induced responses. *Tree Physiology* **34**: 1348–1361.

Choat B, Brodribb TJ, Brodersen CR, Duursma RA, López R, Medlyn BE. 2018. Triggers of tree mortality under drought. *Nature* **558**: 531–539.

Cochard H, Delzon S. 2013. Hydraulic failure and repair are not routine in trees. *Annals of Forest Science* **70**: 659–661.

Dietrich L, Delzon S, Hoch G, Kahmen A. 2019. No role for xylem embolism or carbohydrate shortage in temperate trees during the severe 2015 drought. *Journal of Ecology* **107**: 334–349.

Domec J-C, Lachenbruch B, Meinzer FC, Woodruff DR, Warren JM, McCulloh KA. 2008. Maximum height in a conifer is associated with conflicting requirements for xylem design. *PNAS* **105**: 12069–12074.

Fajardo A, Martínez-Pérez C, Cervantes-Alcayde MA, Olson ME. 2020. Stem length, not climate, controls vessel diameter in two trees species across a sharp precipitation gradient. *New Phytologist* **225**: 2347–2355.

Fuchs S, Leuschner C, Mathias Link R, Schuldt B. 2021. Hydraulic variability of three temperate broadleaf tree species along a water availability gradient in central Europe. *New Phytologist*. doi: 10.1111/NPH.17448.

Gleason SM, Blackman CJ, Gleason ST, McCulloh KA, Ocheltree TW, Westoby M. 2018. Vessel scaling in evergreen angiosperm leaves conforms with Murray's law and area-filling assumptions: implications for plant size, leaf size and cold tolerance. *New Phytologist* **218**: 1360–1370.

Grossiord C, Buckley TN, Cernusak LA, Novick KA, Poulter B, Siegwolf RTW, Sperry JS, McDowell NG. 2020. Plant responses to rising vapor pressure deficit. *New Phytologist* **226**: 1550–1566.

Hacke UG, Spicer R, Schreiber SG, Plavcová L. 2017. An ecophysiological and developmental perspective on variation in vessel diameter. *Plant, Cell & Environment* **40**: 831–845.

Hacke UG, Stiller V, Sperry JS, Pittermann J, McCulloh KA. 2001. Cavitation fatigue. Embolism and refilling cycles can weaken the cavitation resistance of xylem. *Plant Physiology* **125**: 779–786.

Hajek P, Link RM, Nock C, Bauhus J, Gebauer T, Gessler A, Kovach K, Messier C, Paquette A, Saurer M *et al.* **2020.** Mutually inclusive mechanisms of drought-induced tree mortality. *bioRxiv*. doi:12.17.423038.

Hajek P, Seidel D, Leuschner C. 2015. Mechanical abrasion, and not competition for light, is the dominant canopy interaction in a temperate mixed forest. *Forest Ecology and Management* **348**: 108–116.

Herbette S, Wortemann R, Awad H, Huc R, Cochard H, Barigah TS. 2010. Insights into xylem vulnerability to cavitation in *Fagus sylvatica* L.: phenotypic and environmental sources of variability. *Tree Physiology* **30**: 1448–1455.

Jump AS, Ruiz-Benito P, Greenwood S, Allen CD, Kitzberger T, Fensham R, Martínez-Vilalta J, Lloret F. 2017. Structural overshoot of tree growth with climate variability and the global spectrum of drought-induced forest dieback. *Global Change Biology* **23**: 3742–3757.

Knutzen F, Meier IC, Leuschner C. 2015. Does reduced precipitation trigger physiological and morphological drought adaptations in European beech (*Fagus sylvatica* L.)? Comparing provenances across a precipitation gradient. *Tree Physiology* **35**: 949–963.

Koch GW, Sillett SC, Jennings GM, Davis SD. 2004. The limits to tree height. *Nature* **428**: 851–854.

Körner C. 2019. No need for pipes when the well is dry-a comment on hydraulic failure in trees. *Tree Physiology* **39**: 695–700.

Lechthaler S, Turnbull TL, Gelmini Y, Pirotti F, Anfodillo T, Adams MA, Petit G. 2019. A standardization method to disentangle environmental information from axial trends of xylem anatomical traits. *Tree Physiology* **39**: 495–502.

Lemaire C, Quilichini Y, Brunel-Michac N, Santini J, Berti L, Cartailler J, Conchon P, Badel É, Herbette S. 2020. Plasticity of the xylem vulnerability to embolism in poplar relies on quantitative pit properties rather than on pit structure. *bioRxiv*. doi: 10.1101/2020.05.14.096222

Leuschner C. 2020. Drought response of European beech (*Fagus sylvatica* L.) - A review. *Perspectives in Plant Ecology, Evolution and Systematics* **47**: 125576.

Leuschner C, Ellenberg H. 2017. Ecology of central European forests. Cham: Springer.

Liang X, He P, Liu H, Zhu S, Uyehara IK, Hou H, Wu G, Zhang H, You Z, Xiao Y *et al.* 2019. Precipitation has dominant influences on the variation of plant hydraulics of the native *Castanopsis fargesii* (Fagaceae) in subtropical China. *Agricultural and Forest Meteorology* **271**: 83–91.

Lübbe T, Schuldt B, Leuschner C. 2017. Acclimation of leaf water status and stem hydraulics to drought and tree neighbourhood: alternative strategies among the saplings of five temperate deciduous tree species. *Tree Physiology* **37**: 456–468.

Martínez-Vilalta J, Cochard H, Mencuccini M, Sterck F, Herrero A, Korhonen JFJ, Llorens P, Nikinmaa E, Nolè A, Poyatos R *et al.* 2009. Hydraulic adjustment of Scots pine across Europe. *New Phytologist* **184**: 353–364.

McGregor IR, Helcoski R, Kunert N, Tepley AJ, Gonzalez-Akre EB, Herrmann V, Zailaa J, Stovall AEL, Bourg NA, McShea WJ *et al.* 2020. Tree height and leaf drought tolerance traits shape growth responses across droughts in a temperate broadleaf forest. *New Phytologist*. doi: 10.1111/nph.16996.

Meier IC, Leuschner C. 2008a. Belowground drought response of European beech: fine root biomass and carbon partitioning in 14 mature stands across a precipitation gradient. *Global Change Biology* **14**: 2081–2095.

Meier IC, Leuschner C. 2008b. Leaf size and leaf area index in *Fagus sylvatica* forests: competing effects of precipitation, temperature, and nitrogen availability. *Ecosystems* **11**: 655–669.

Mencuccini M, Grace J. 1995. Climate influences the leaf area/sapwood area ratio in Scots pine. *Tree Physiology* **15**: 1–10.

Moles AT, Warton DI, Warman L, Swenson NG, Laffan SW, Zanne AE, Pitman A, Hemmings FA, Leishman MR. 2009. Global patterns in plant height. *Journal of Ecology* **97**: 923–932.

Müller-Haubold H. 2015. Climate response of above- and belowground productivity and allocation in European beech. PhD thesis. University of Göttingen, Germany. http://hdl.handle.net/11858/00-1735-0000-0022-5FFB-6.

Olson ME, Anfodillo T, Rosell JA, Petit G, Crivellaro A, Isnard S, León-Gómez C, Alvarado-Cárdenas LO, Castorena M. 2014. Universal hydraulics of the flowering plants: vessel diameter scales with stem length across angiosperm lineages, habits and climates. *Ecology letters* **17**: 988–997.

Pfautsch S, Harbusch M, Wesolowski A, Smith R, Macfarlane C, Tjoelker MG, Reich PB, Adams MA. 2016. Climate determines vascular traits in the ecologically diverse genus *Eucalyptus*. *Ecology letters* **19**: 240–248.

Pritzkow C, Williamson V, Szota C, Trouvé R, Arndt SK. 2020. Phenotypic plasticity and genetic adaptation of functional traits influences intra-specific variation in hydraulic efficiency and safety. *Tree Physiology* **40**: 215–229.

Rawson HM, Begg JE, Woodward RG. 1977. The effect of atmospheric humidity on photosynthesis, transpiration and water use efficiency of leaves of several plant species. *Planta* **134**: 5–10.

Rosas T, Mencuccini M, Barba J, Cochard H, Saura-Mas S, Martínez-Vilalta J. 2019. Adjustments and coordination of hydraulic, leaf and stem traits along a water availability gradient. *New Phytologist* **223**: 632–646.

Rosell JA, Olson ME, Anfodillo T. 2017. Scaling of xylem vessel diameter with plant size: causes, predictions, and outstanding questions. *Current Forestry Reports* **3**: 46–59.

Schenk HJ, Jansen S, Hölttä T. 2021. Positive pressure in xylem and its role in hydraulic function. *New Phytologist* **230**: 27–45.

Schuldt B, Buras A, Arend M, Vitasse Y, Beierkuhnlein C, Damm A, Gharun M, Grams TEE, Hauck M, Hajek P *et al.* 2020. A first assessment of the impact of the extreme 2018 summer drought on Central European forests. *Basic and Applied Ecology* **45**: 86–103.

Schuldt B, Knutzen F, Delzon S, Jansen S, Müller-Haubold H, Burlett R, Clough Y, Leuschner C. 2016. How adaptable is the hydraulic system of European beech in the face of climate change-related precipitation reduction? *New Phytologist* **210**: 443–458.

Sterck FJ, Martínez-Vilalta J, Mencuccini M, Cochard H, Gerrits P, Zweifel R, Herrero A, Korhonen JFJ, Llorens P, Nikinmaa E *et al.* 2012. Understanding trait interactions and their impacts on growth in Scots pine branches across Europe. *Functional Ecology* **26**: 541–549.

Stojnic S, Suchocka M, Benito-Garzón M, Torres-Ruiz JM, Cochard H, Bolte A, Cocozza C, Cvjetkovic B, Luis M de, Martinez-Vilalta J *et al.* 2017. Variation in xylem vulnerability to embolism in European beech from geographically marginal populations. *Tree Physiology* **38**: 173–185.

Tomasella M, Beikircher B, Häberle K-H, Hesse B, Kallenbach C, Matyssek R, Mayr S. 2018. Acclimation of branch and leaf hydraulics in adult *Fagus sylvatica* and *Picea abies* in a forest through-fall exclusion experiment. *Tree Physiology* **38**: 198–211.

Walthert L, Ganthaler A, Mayr S, Saurer M, Waldner P, Walser M, Zweifel R, Arx G von. 2021. From the comfort zone to crown dieback: Sequence of physiological stress thresholds in mature European beech trees across progressive drought. *Science of the Total Environment* **753**: 141792.

Walthert L, Meier ES. 2017. Tree species distribution in temperate forests is more influenced by soil than by climate. *Ecology and evolution* **7**: 9473–9484.

West GB, Brown JH, Enquist BJ. 1999. A general model for the structure and allometry of plant vascular systems. *Nature* **400**: 664–667.

Wohlgemuth T, Kistler M, Aymon C, Hagedorn F, Gessler A, Gossner MM, Queloz V, Vögtli I, Wasem U, Vitasse Y *et al.* 2020. Früher Laubfall der Buche während der Sommertrockenheit 2018: Resistenz oder Schwächesymptom? *Schweizerische Zeitschrift für Forstwesen* **171**: 257–269.

Woodruff DR, Bond BJ, Meinzer FC. 2004. Does turgor limit growth in tall trees? *Plant, Cell & Environment* **27**: 229–236.

Woodruff DR, McCulloh KA, Warren JM, Meinzer FC, Lachenbruch B. 2007. Impacts of tree height on leaf hydraulic architecture and stomatal control in Douglas-fir. *Plant, Cell & Environment* **30**: 559–569.

Woodruff DR, Meinzer FC, Lachenbruch B. 2008. Height-related trends in leaf xylem anatomy and shoot hydraulic characteristics in a tall conifer: safety versus efficiency in water transport. *New Phytologist* **180**: 90–99.

Wortemann R, Herbette S, Barigah TS, Fumanal B, Alia R, Ducousso A, Gomory D, Roeckel-Drevet P, Cochard H. 2011. Genotypic variability and phenotypic plasticity of cavitation resistance in *Fagus sylvatica* L. across Europe. *Tree Physiology* **31**: 1175–1182.

Yuan W, Zheng Y, Piao S, Ciais P, Lombardozzi D, Wang Y, Ryu Y, Chen G, Dong W, Hu Z *et al.* 2019. Increased atmospheric vapor pressure deficit reduces global vegetation growth. *Science advances* **5**: eaax1396.

Zhu S-D, Chen Y-J, Ye Q, He P-C, Liu H, Li R-H, Fu P-L, Jiang G-F, Cao K-F. 2018. Leaf turgor loss point is correlated with drought tolerance and leaf carbon economics traits. *Tree Physiology* **38**: 658–663.

Zimmermann J, Link RM, Hauck M, Leuschner C, Schuldt B. 2021. 60-year record of stem xylem anatomy and related hydraulic modification under increased summer drought in ring- and diffuse-porous temperate broad-leaved tree species. *Trees* **35**: 919–937.

List of Tables

List of Figures

Acknowledgements